Informatics Control Measurement
in Economy and Environment Protection

4/2022

Informatyka Automatyka Pomiary

w gospodarce i ochronie środowiska

www.e-IAPGOS.pl

ISSN 2083-0157

Kwartalnik Naukowo-Techniczny

4/2022

październik – grudzień

Wydanie pod redakcją naukową
prof. dr hab. inż. Waldemara Wójcika

INFORMATYKA AUTOMATYKA POMIARY
W GOSPODARCE i OCHRONIE ŚRODOWISKA
Informatics Control Measurement in Economy and Environment Protection

p-ISSN 2083-0157, e-ISSN 2391-6761, www.e-iapgos.pl

PRINTING HOUSE – DRUKARNIA

Agencja Reklamowa TOP
https://www.agencjatop.pl

nakład: 100 egzemplarzy

OTHER INFORMATION – INNE INFORMACJE

Czasopismo jest indeksowane w bazach:

DOAJ	doaj.org
BazTech	baztech.icm.edu.pl
IC Journals Master List	www.journals.indexcopernicus.com
Google Scholar	scholar.google.pl
POL-index	pbn.nauka.gov.pl
Sherpa RoMEO	www.sherpa.ac.uk
OAJI	oaji.net
SCOPUS	www.scopus.com

Czasopismo *Informatyka, Automatyka, Pomiary w Gospodarce i Ochronie Środowiska* zostało objęte finansowaniem przez Ministerstwo Nauki i Szkolnictwa Wyższego w ramach programu *Wsparcie dla czasopism naukowych* w latach 2019-2020.

Czasopismo znajduje się w wykazie czasopism naukowych opublikowanym w Komunikacie Ministra Edukacji i Nauki z dnia 1 grudnia 2021 r., Unikatowy Identyfikator Czasopisma: 200167 – z przypisaną liczbą punktów przyznawanych za publikację artykułu równą 20.

Zasady publikowania artykułów, przygotowania tekstów, zasady etyczne, procedura recenzowania, wykazy recenzentów oraz pełne teksty artykułów dostępne są na stronie internetowej czasopisma:

www.e-iapgos.pl

W celu zwiększenia oddziaływania czasopisma w środowisku naukowym redakcja zaleca:

- w artykułach publikowanych w IAPGOS cytować artykuły z renomowanych czasopism międzynarodowych (szczególnie indeksowanych w bazach Web of Science oraz Scopus) używając oficjalnych skrótów nazw czasopism,
- w artykułach publikowanych w innych czasopismach (zwłaszcza indeksowanych w bazach Web of Science oraz Scopus) cytować prace publikowane w IAPGOS – zwłaszcza posługując się numerami DOI, np.:
  Kluszczyński K. *Modelowanie – umiejętność czy sztuka?* Informatyka, Automatyka, Pomiary w Gospodarce i Ochronie Środowiska – IAPGOS, 1/2016, 4–15, https://doi.org/10.5604/20830157.1193833.

CONTENTS – SPIS TREŚCI

http://doi.org/10.35784/iapgos.3376 *received: 16.05.2022 | revised: 02.09.2022 | accepted: 15.12.2022 | available online: 30.12.2022*

SCATTERING BY CIRCULAR VOIDS WITH RIGID BOUNDARY: DIRECT AND INVERSE PROBLEMS FOR OPEN AND CLOSE DOMAINS

Tomasz Rymarczyk[1,2], Jan Sikora[1,2]
[1]Research & Development Centre Netrix S.A., Lublin, Poland, [2]WSEI University, Faculty of Transport and Informatics, Lublin, Poland

Abstract*. Problems with the accuracy of calculations by the Boundary Element Method of acoustic and ultrasonic problems formulated in the frequency domain were presented in this paper. The inverse problem was formulated to identify the position and dimensions of the scattering object. A series of numerical experiments carried out with the help of the Boundary Elements Method proved the algorithm's robustness to noise and high precision in a wide frequency spectrum.*

Keywords: acoustics-ultrasound wave propagation, BEM simulation, inverse problems, optimization methods

ROZPRASZANIE PRZEZ PUSTE PRZESTRZENIE KOŁOWE ZE SZTYWNĄ GRANICĄ: PROSTE I ODWROTNE ZAGADNIENIA DLA OBSZARÓW OTWARTYCH I ZAMKNIĘTYCH

Streszczenie. *W pracy przedstawiono problemy z dokładnością obliczeń Metodą Elementów Brzegowych zagadnień akustycznych i ultradźwiękowych sformułowanych w dziedzinie częstotliwości. Sformułowano zagadnienie odwrotne dla identyfikacji położenia i wymiarów obiektu rozpraszającego. Seria eksperymentów numerycznych przeprowadzonych z pomocą Metody Elementów Brzegowych udowodniła odporność algorytmu na szum oraz wysoką precyzję w szerokim spektrum częstotliwości.*

Słowa kluczowe: propagacja fal akustycznych-ultradźwiękowych, symulacja Metodą Elementów Brzegowych (MEB), zadania odwrotne, metody optymalizacyjne

Introduction

The key problem of each inverse problem is the forward problem. This paper deals with the accuracy and effectiveness of calculating the acoustic and ultrasound forward problem. Very often, Ultrasound terminology is used interchangeably with Ultrasonic. What is the difference, then? In practice, ultrasound is used to reference clinical ultrasonic scanning and therapeutic ultrasound imagery, but Ultrasonic refers to technical imagining, for example, Non-Destructive Testing. We will use the acoustic waves in the acoustic and ultrasound ranges.

Briefly, we introduce two types of problems frequently occurring in practical applications. First, problems of wave propagation phenomena are usually classified as interior or exterior, depending on whether one is interested in the sound field in bounded or unbounded regions in space. In some cases, the third type of acoustic problem could also be defined when the domain of interest is not simply connected (see for example Fig. 5). The last one is often called the hybrid interior-exterior problem [4].

This paper focuses readers' attention on the BEM for hybrid interior-exterior problems formulated for the frequency domain.

Based on the Forward Problem, Dedicated iterative methods make it possible to formulate the inverse problems and solve the tomography tasks for acoustic [3, 4, 6]. The advantages of the acoustic or ultrasound approach for imaging, particularly in medicine, are obvious and do not demand further explanations.

Ultrasound tomography models, especially for the integral formulation, are difficult from a numerical point of view [4].

1. Point source

Why are we interested in problems related to point-generated wave fields? It has several reasons. The more important one is due to the variety of applications coming from the theory of composite materials and acoustic emission, from the theoretical analysis of biological studies at the cell level, from non-destructive testing and evaluation, from geophysics, and from modelling in medicine and health sciences. Furthermore, a point-source field is more easily realizable in a laboratory [2].

Suppose that our incoming wave is of point source form, with the source at r' illuminating the circular cylinder surface cross-section defined in terms of the incident angles (ψ_0,θ_0), as illustrated in Fig. 1a.

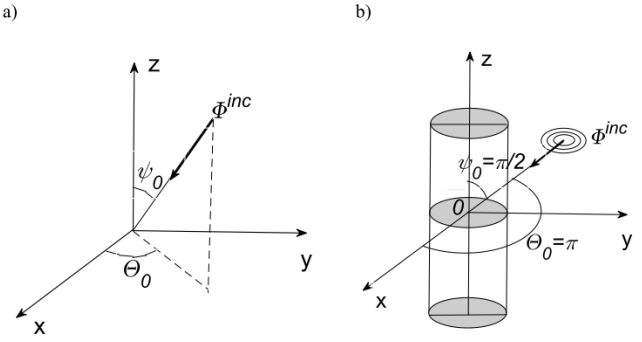

Fig. 1. Time-harmonic wave a) with an arbitrary incident angle (ψ_0,θ_0), b) scattering from a circular cylinder with an incident angle ($\theta_0 = \pi$)

Located the source point on the surface x0y (angle $\psi_0 = \pi/2$) and for angle $\theta_0 = \pi$ as is shown in Fig. 1b, the total field satisfies the Helmholtz equation (1).

The acoustic field is assumed to be present in the domain of a homogeneous isotropic fluid, and it is modelled by the linear wave equation [4]:

$$\nabla^2\psi(\mathbf{p},t) = \frac{1}{c^2}\frac{\partial^2}{\partial t^2}\psi(\mathbf{p},t) + Q \tag{1}$$

where $\psi(\mathbf{p},t)$ [m^2/s] is the scalar time-dependent velocity potential related to the time-dependent particle velocity $\mathbf{v}(\mathbf{p},t) = \nabla\psi(\mathbf{p},t)$ [m/s] and c [m/s] is the propagation velocity ($\mathbf{p}$ and t are the spatial and time variables in meters and seconds respectively). The time-dependent sound pressure is equal $p(\mathbf{p},t) = -\rho\frac{\partial}{\partial t}\psi(\mathbf{p},t)$ where ρ [kg/m^3] is the density of the acoustic medium.

Transferring from the time domain to the frequency domain, the velocity potential ψ can be expressed as follows:

$$\Psi(\mathbf{p},t) = \mathrm{Re}\{\varphi(\mathbf{p})\mathrm{e}^{-\mathrm{i}\omega t}\}, \tag{2}$$

where: $\omega = 2\pi f$ [1/s] and $\varphi(\mathbf{p})$ is the velocity potential amplitude. The substitution of the above expression into the wave equation reduces it to the Helmholtz equation of the form [4]:

$$\nabla^2\varphi(\mathbf{p}) + k^2\varphi(\mathbf{p}) = Q, \tag{3}$$

where $k^2 = \frac{\omega^2}{c^2}$ is the wave number and the wavelength is equal to $\lambda = c/f$. The right-hand side Q stands for the acoustic source. The complex-valued state function $\varphi(\mathbf{p})$ possess the magnitude and phase shift.

The problem is outlined by beginning with the time-harmonic reduction of the wave equation for the exterior-interior problem to the Helmholtz equation (Eq. 3) and finally to the Boundary Integral Equation formulation for the acoustic scattering problem.

The sound-hard scatterer is imposed on the interior and exterior boundary through a homogeneous Neumann boundary condition. Making use of Green's second identity, the Helmholtz equation can be expressed in an equivalent form of a Boundary Integral Equation (BIE) [4], i.e.

$$c(\boldsymbol{r})\varphi(\boldsymbol{r}) + \int_{\Gamma} \frac{\partial G(|\boldsymbol{r}-\boldsymbol{r}'|)}{\partial n}\varphi(\boldsymbol{r}')d\boldsymbol{\Gamma} = \\ = \int_{\Gamma} G(|\boldsymbol{r}-\boldsymbol{r}'|)\frac{\partial\varphi(\boldsymbol{r}')}{\partial n}d\boldsymbol{\Gamma} + \varphi^{inc}(\boldsymbol{r}), \quad \boldsymbol{r}\in\boldsymbol{\Gamma} \tag{4}$$

where φ^{inc} is the incident wave, and the vector $\boldsymbol{n}$ is the normal unit vector outward pointing from the considered domain.

Due to the homogeneous Neumann boundary conditions, the third term of Eq. (4) vanishes. So now the integral boundary equation (4) for constant boundary elements can be written in terms of local coordinate ξ as follows:

$$c(\boldsymbol{r})\varphi(\boldsymbol{r}) + \sum_{j=1}^{M}\varphi_j(\boldsymbol{r}')\int_{-1}^{+1}\frac{\partial G(|\boldsymbol{r}-\boldsymbol{r}'|)}{\partial n}J(\xi)d\xi = \varphi^{inc}(\boldsymbol{r}) \tag{5}$$

where: M – is the total number of constant elements and $J(\xi)$ – is the Jacobian of transformation $\left(J(\xi) = \frac{d\boldsymbol{\Gamma}}{d\xi} = \right.$ $\left. = \sqrt{\left(\frac{dx(\xi)}{d\xi}\right)^2 + \left(\frac{dy(\xi)}{d\xi}\right)^2} = \frac{L}{2}\right)$, where L is the length of the constant boundary element [7, 9].

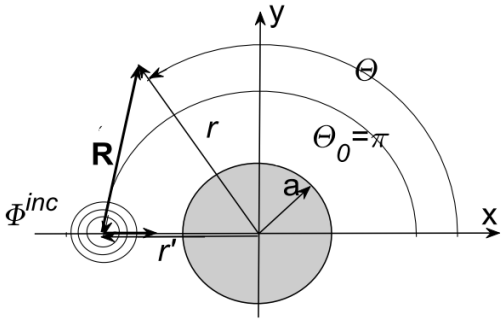

Fig. 2. Diagram showing the circular scatterer due to a point source located at r' at angle $\theta_0 = \pi$ calculated from the positive direction of x axis

Then, the fundamental solution for the field at **r** is given by:

$$\varphi^{inc}(r,\theta) = \frac{i}{4}H_0^{(1)}(kR) \tag{6}$$

where $R = |\mathbf{R}| = |\mathbf{r}-\mathbf{r}'|$, as seen in Fig. 2. The incoming wave described by Eq. (6) using the Graf's addition formula [5] can be expanded as follows:

$$\varphi^{inc}(r,\theta) = \frac{i}{4}H_0^{(1)}(kr')J_0(kr) + \\ + \frac{i}{4}\sum_{n=1}^{\infty}2\,(-1)^n H_n^{(1)}(kr')J_n(kr)\cos\big(n(\theta-\theta_0)\big) \tag{7}$$

Then, we can expand our scattered field in the following form:

$$\varphi^{scat}(r,\theta) = A_0H_0^{(1)}(kr) + \\ + \sum_{n=1}^{\infty}2\,(-1)^n A_nH_n^{(1)}(kr)\cos\big(n(\theta-\theta_0)\big) \tag{8}$$

The amplitude of the n-th mode for the Neumann boundary conditions will be:

$$A_n = -\frac{i}{4}\frac{H_n^{(1)}(kr')\,J_n'(ka)}{H_n^{(1)\prime}(ka)} \tag{9}$$

$$A_0 = -\frac{i}{4}\frac{H_0^{(1)}(kr')\,J_0'(ka)}{H_0^{(1)\prime}(ka)} \tag{10}$$

where the prime sign denotes derivatives concerning the argument ka and a is the radius of the circular void (see Fig. 2). The first derivatives are calculated according to [1], and we will have:

$$J_0'(ka) = -J_1(ka) \tag{11}$$

$$J_n'(ka) = \frac{1}{2}\big(J_{n-1}(ka) - J_{n+1}(ka)\big) \tag{12}$$

and similarly, for the Hankel functions, we have got:

$$H_0^{(1)\prime}(ka) = -H_1^{(1)}(ka) \tag{13}$$

$$H_n^{(1)\prime}(ka) = \frac{1}{2}\Big(H_{n-1}^{(1)}(ka) - H_{n+1}^{(1)}(ka)\Big) \tag{14}$$

So:

$$A_n = -\frac{i}{4}H_n^{(1)}(kr')\frac{J_{n-1}(ka)-J_{n+1}(ka)}{H_{n-1}^{(1)}(ka)-H_{n+1}^{(1)}(ka)} \tag{15}$$

and

$$A_0 = -\frac{i}{4}H_0^{(1)}(kr')\frac{J_1(ka)}{H_1^{(1)}(ka)} \tag{16}$$

2. Point wave and its asymptotic behaviour

When we do not have the analytic solution to check the BEM solution, we can add one more way of control. The point source generates a spherical wave. When the distance from the scatterer becomes infinitely long, the spherical wave could be treated as the plane wave. For this case exists, the analytic solution [8] so it is possible to compare the point source excitation results qualitatively. If the results are similar, we can get one more reason to ensure that the BEM calculations are correct. Let us consider the point source located in the position (2,0) outside the scatterer of radius a = 1 m (see Fig. 2).

In Fig. 3a and Fig. 3b, we can see that curve of potential distribution on the surface of the circular scatterer in the case of remote point source becomes, regarding the shape, identical to the plane wave shown in Fig. 3c.

Examples presented in figures 3 and 4 fulfil the demand concerning discretization that the number of boundary elements per wavelength should not be less than 10 [4, 9]. In this case, twelve boundary elements per wavelength should guarantee correct results. Additionally, we check the asymptotic behaviour of BEM calculation. The location of the source was moved far away from the scatterer, and the results closely approach the previous ones for the plane wave illumination. However, of course, we can make only a qualitative comparison.

Comparing results presented in Fig. 3b with results in Fig. 3c, the agreement concerning the shape is particularly good. However, the result magnitudes are different because, in both cases, the source amplitudes were equal, but the energy radiated due to the mathematical model was different. On this basis, we can state that the BEM model provides correct results.

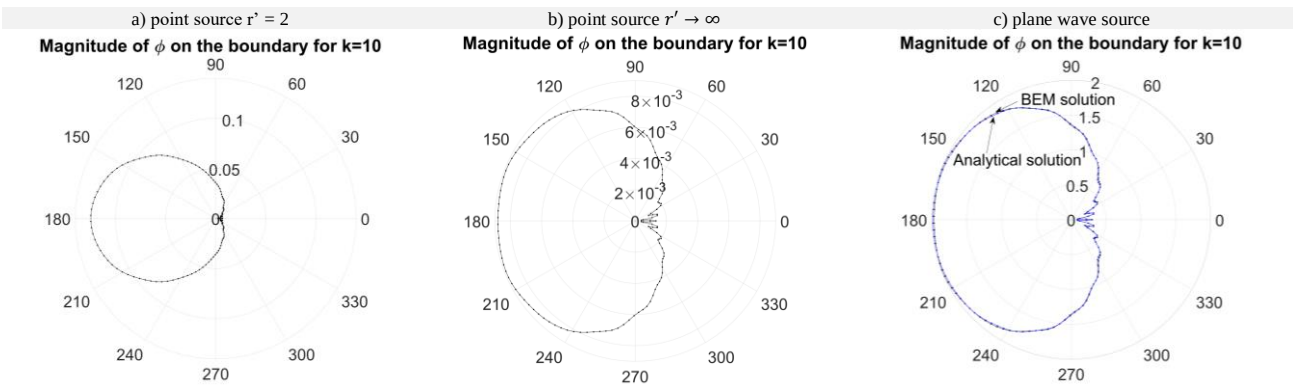

Fig. 3. The circular scatterer illuminated by: a) point source located close to the scatterer, b) source point located far away from the scatterer when the radius $r' \to \infty$, c) plane wave source

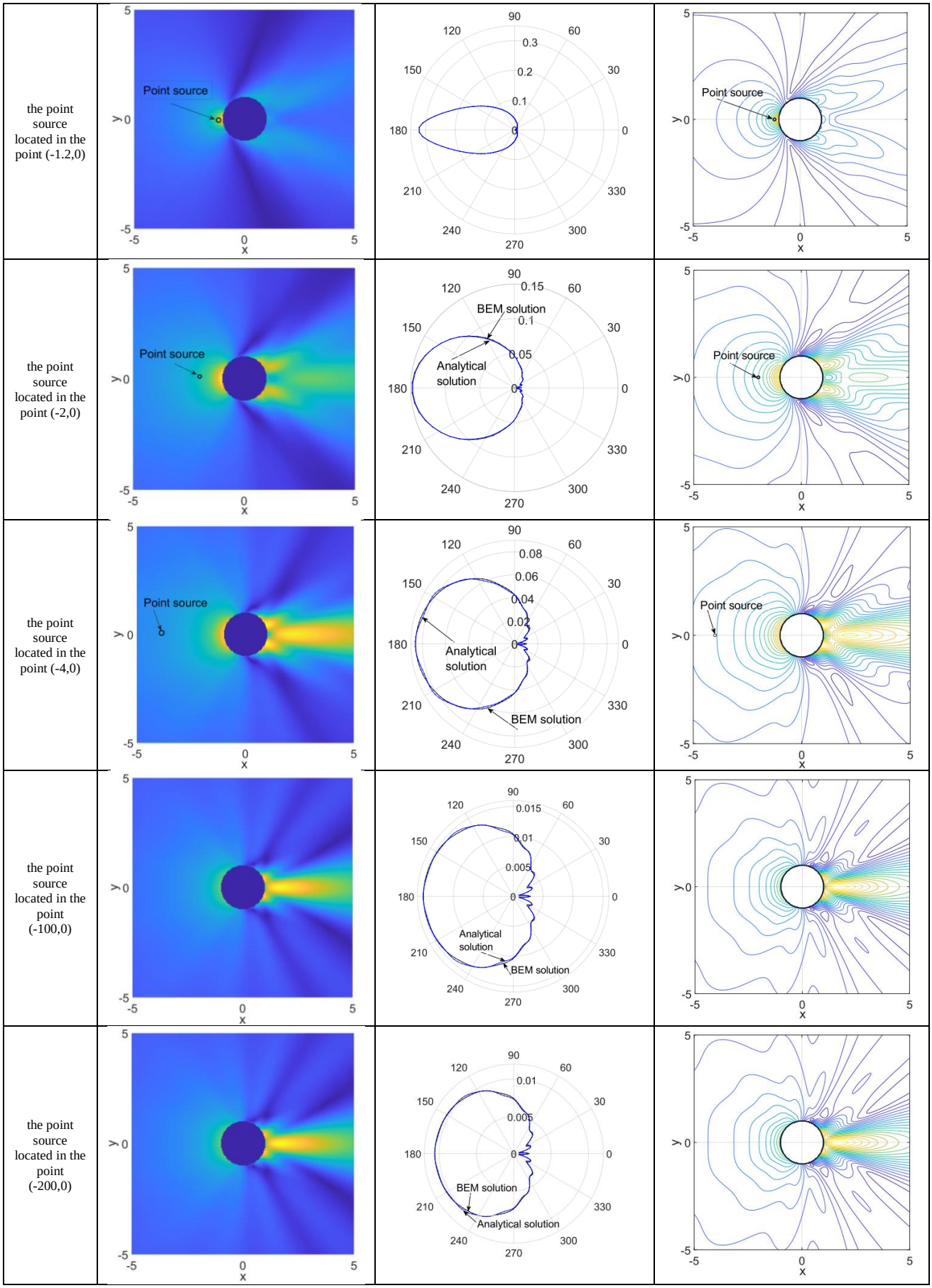

Fig. 4. Position of the point source (first column), the image of the acoustic field (second column), distribution of the acoustic velocity potential on the perimetry of the circular scatterer (third column) and equipotential lines of the velocity potential (fourth column), when the scatterer is illuminated by the point source placed in various locations

3. The inverse acoustic problem

The first part of the paper is devoted to precisely calculating the forward problems in acoustic or ultrasonic. Ultra-sound is a branch of acoustics with soundwave frequency above 20 kHz that utilize the mechanical pressure wave above the human hearing range.

This part could be treated as preparation and a benchmark for point sources used in the scattering acoustic/ultrasound problems. The BEM was selected as the most popular and effective for the open boundary problem so frequently encountered in Acoustic theory. The benchmark was needed due to a high argument of the Green functions (the Helmholtz function) and an integration of the singular integrands in BEM [4]. The first part of the paper proved that BEM could deal with both difficulties and provide a precise result. Moreover, some useful criteria for Inverse Problems in Acoustic or Ultrasound were formulated based on analytical results. In this paper, we would like to focus readers' attention on the BEM formulated for the frequency domain (see Eq. 3). Formally, the mathematical description would be almost identical as for Diffuse Optical Tomography [6–9], but the physical meaning of the state function, material coefficient and their units are different.

The idea of the inverse problem in the transmission mode is sketched in Fig. 5, where the signal is transmitted as a fan-shaped beam by the transducer and received by the opposite sensors acting as the receivers (see Fig. 5).

In the transmission mode of Acoustic/Ultrasonic Tomography (AT), we may compare the pulses' amplitudes measured on the external boundary's perimetry (see Fig. 6) to image the scatterer within the region.

The idea of the inverse problem in the transmission mode is sketched in Fig. 5, where the signal is transmitted as a fan-shaped beam by the transducer and received by the opposite sensors acting as the receivers (see Fig. 5).

In the transmission mode of Acoustic/Ultrasonic Tomography (AT) we may compare the amplitudes of the pulses measured on the perimetry of the external boundary (see Fig. 6) to image the scatterer within the region.

Application of the Boundary Element Method to solve the forward problem implies some simplified assumptions regarding imaging in AT. First, the BEM is designed for homogeneous region analysis only. So, in this case, imaging will be restricted to the dimensioning and location problem, a special case of the Optimal Shape Design problem. It means that the image would be parametrized. As a result, we will have only three parameters: namely, the scatterer's radius and two parameters (length and angle) for the position vector. For the scattering problems, such an approach is particularly justified [7].

4. The acoustic tomography

In tomography, we have only access to the external boundary to make the measurements. So, the number of measured data is strongly limited. To enlarge them successfully, the point source position is changed, illuminating the scatterer from different angles. The source positions are called the Projection Angles (PA). In that way, the number of measurements is multiplied by the number of Projection Angles (see Fig. 5).

The crucial point of an Inverse Problem is the Sensitivity Analysis, which is particularly difficult for BEM [4]. So, to avoid the Sensitivity Analysis for BEM being complicated and time-consuming, the **fmincon** function was selected [10, 11]. This function can effectively find a minimum of a constrained nonlinear multivariable function.

5. Definition of the objective function

To match the signal calculated in each iteration step to the measured one, the following objective function has been defined Eq. (17). The analysis was carried out in the frequency domain, which means that all signals are complex, having magnitude and phase shift.

This objective function will be subject to minimization with linear inequality constraints:

$$\hat{\Phi} = \sum_{j=1}^{j=p} \hat{\Phi}_j = \sum_{j=1}^{j=p} \left(\hat{f}_j - \hat{v}_{0j}\right) = \left(\hat{\mathbf{F}} - \hat{\boldsymbol{V}}_0\right) = \\ = \sum_{j=1}^{j=p} \mathrm{Re}\left(\hat{f}_j - \hat{v}_{0j}\right) + j \sum_{j=1}^{j=p} \mathrm{Im}\left(\hat{f}_j - \hat{v}_{0j}\right) \qquad (17)$$

where: hat means a complex quantity, $\hat{\Phi}$ – global auxiliary complex function calculated for all $p = 8$ or 16 positions of the points source (so-called projection angles), $j = 1, 2\,I\,, p$, $\hat{\Phi}_j$ – auxiliary complex function for the j-th position of the acoustic point source, $\hat{\mathbf{f}}_j$ a vector representing the calculated complex signal for the current iterative step (see, for example, Fig. 6), $\hat{\mathbf{v}}_{0j}$ – vector of measured signal for the j-th position of the point source. The complex matrices $\hat{\mathbf{F}}$ and $\hat{\boldsymbol{V}}_0$ are equal respectively:

$$\hat{\mathbf{F}} = \left[\hat{\mathbf{f}}_1, \hat{\mathbf{f}}_2, \ldots, \hat{\mathbf{f}}_{\boldsymbol{p}}\right]^{\boldsymbol{T}} \text{ and } \hat{\boldsymbol{V}}_0 = \left[\hat{\mathbf{v}}_{01}, \hat{\mathbf{v}}_{02}, \ldots, \hat{\mathbf{v}}_{0\boldsymbol{p}}\right]^{\boldsymbol{T}} \qquad (18)$$

Equation (17) could be shown in the following form:

$$\hat{\Phi} = \sum_{j=1}^{j=p} \hat{\phi}_j = \sum_{j=1}^{j=p} \mathrm{Re}\,\hat{\phi}_j + j \sum_{j=1}^{j=p} \mathrm{Im}\,\hat{\phi}_j. \qquad (19)$$

The objective function must be the real number, so it is defined in a following way:

$$F = \sum_{j=1}^{j=p} \left(\hat{\phi}_j \hat{\phi}_j^*\right) = \sum_{j=1}^{j=p} \left(\mathrm{Re}^2 \hat{\phi}_j + \mathrm{Im}^2 \hat{\phi}_j\right). \qquad (20)$$

where $\hat{\phi}_j^*$ means complex conjugate auxiliary function.

From the physical point of view, the objective function F is a distance in the complex plane between the measured and calculated signal. Minimizing distance means that both signals become as close to each other as possible.

Let us consider a set (array) of acoustic source points (sensors marked by yellow) to achieve the image, as shown in Fig. 5.

The reconstruction of the object (geometry only, without acoustical properties of the material) requires an accurate numerical model [4, 6]. Moreover, it allows us to solve the inverse scattering problem, i.e., determine the parameters of the scatterer based on measurements of the incident and scattered fields taken on the external circular boundary.

Inverse scattering problems are non-linear and ill-posed. Therefore, no single solution exists, and it is necessary to eliminate the solutions that do not correspond to reality.

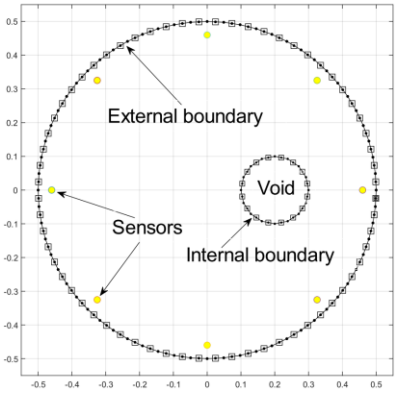

Fig. 5. Sketch of the transmission mode of AT

An example of state function distribution on the external boundary for all projection angles (PA) is shown in Fig. 6. Also, it is interesting to see the image of the acoustic field inside the region for different projection angles.

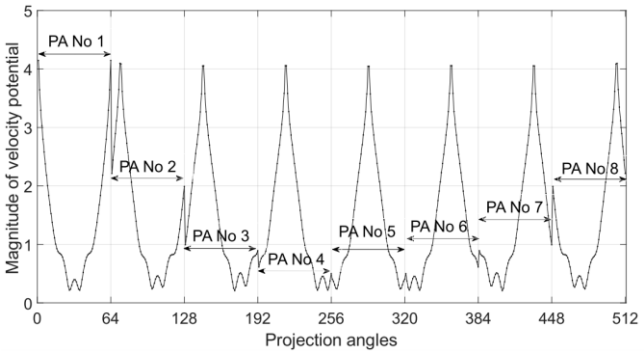

Fig. 6. State function (Velocity potential) distribution along the external boundary of the region for all Projection Angles

It demands of internal field calculations, which are numerically expensive because such numerical integration demands much more integration points compared to boundary integrals [9]. The images of the field are shown in Fig. 7.

6. Definition of inequality constrains

The imagining problem was turned into the optimization problem, which means parametrization of an image. following parameters could sufficiently describe the proposed image: internal radius of the circular void-scatterer r_1, and the position vector of the centre of the scattering object r_2.

During the optimization process, the internal object should not cross the external boundary of the region R_o. All radiuses should have a positive value.

Mathematically those constraints could be expressed as follows:

$$\begin{bmatrix} -1 & 0 \\ 0 & -1 \\ 1 & 1 \end{bmatrix} \begin{bmatrix} r_1 \\ r_2 \end{bmatrix} < \begin{bmatrix} -0.1R_0 \\ 0 \\ 0.9R_0 \end{bmatrix} \tag{21}$$

where: r_1 – radius of the scatterer, r_2 – length of the position vector, R_o – radius of the region to be imaged. The third parameter – an angle of position vector- remains without constraints.

7. Boundary conditions and material properties

The circular cross-section of the scatterer boundary and the boundary of the whole area is rigid. That is why the homogeneous Neumann boundary conditions on both edges were imposed. The air fills the area. The velocity of a sound wave is equal to 344 m/s [4, 6].

8. Result and discussion

The transmission mode and optimization algorithm with linear inequality constraints have been used to reconstruct the image which was parametrized. Transmission mode has the concept of transmitting the velocity potential and, as needed, the pressure signal from the transmitter when the other transducers act as receivers (see in Fig. 5). As shown in figure 5, where the transducer No one is transmitting a continuous sound wave signal and the other transducers are receiving. It is the first PA. Next, the second sensor starts playing the transmitter and sensor role. Then, no 1 becomes the receiver and so on. Such a change in the role of the sensors is named the projection angle. Results of the velocity potential distribution for all the projection angles is presented in Fig. 8. The signal is polluted by the 10% noise (the upper figure) and 20% noise (lower figure). The 20% pollution is really the big one.

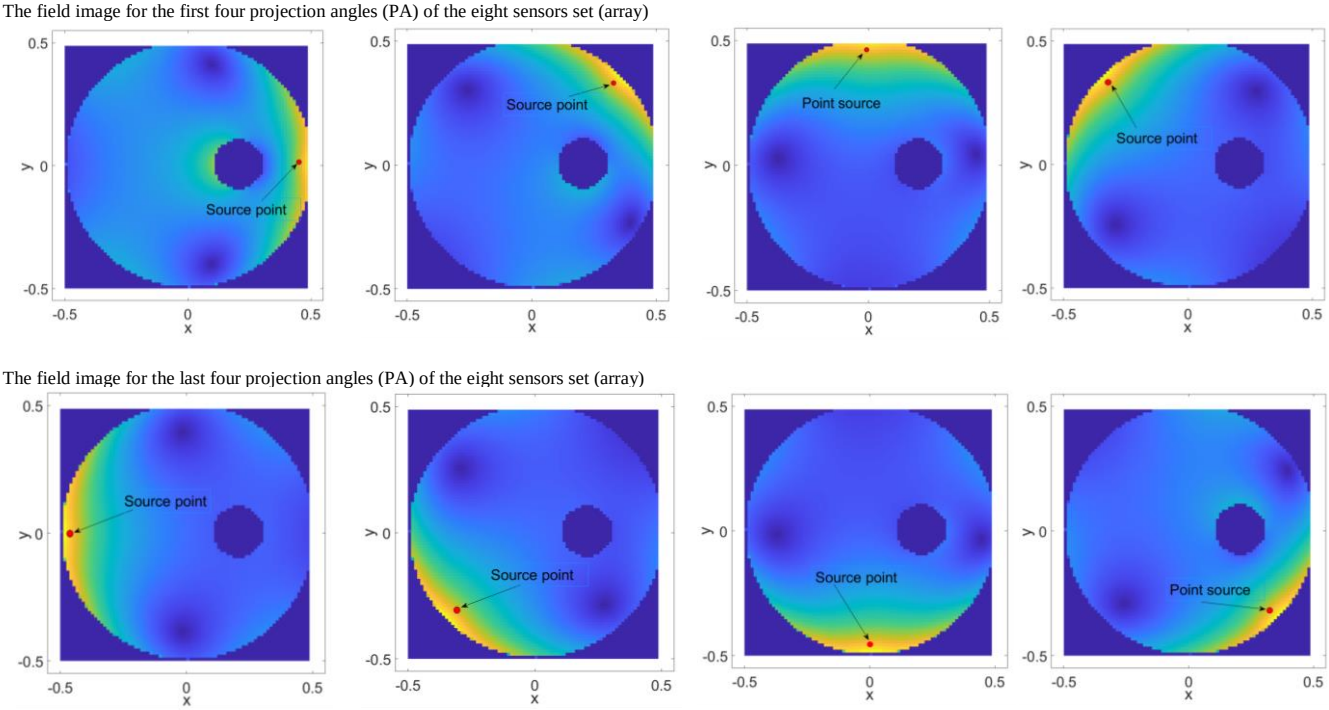

Fig. 7. Eight element array sensors: velocity absolute value distribution for the point source excitation

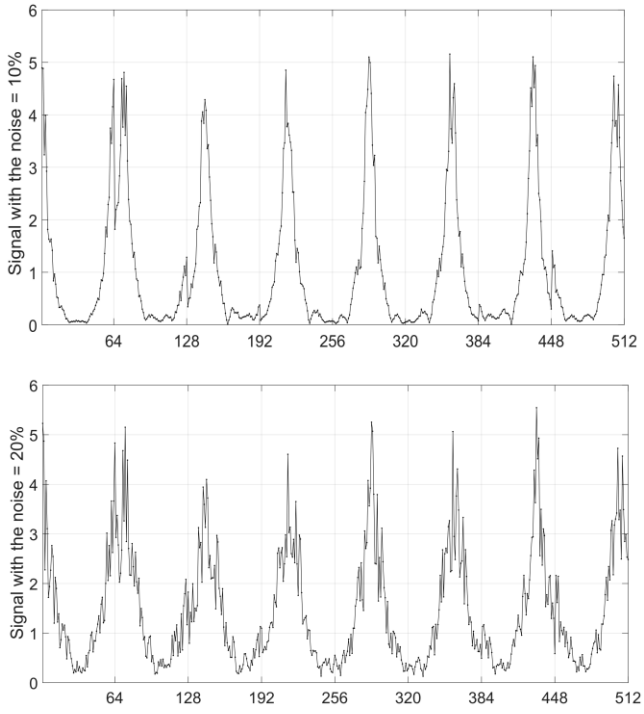

Fig. 8. Synthetic signal treated as the measured one with: a) 10% noise, b) 20% noise for eight projection angles

Numerical simulation was carried out for different geometrical parameters as well as for different frequency from acoustical range (Fig. 9) up to ultrasound range (Fig. 10).

The frequency is an impact factor when dealing with ultrasonic solutions in fluids and air. Therefore, a transducer with greater frequency can resolve objects with smaller dimensions. We can observe this phenomenon in the following figures.

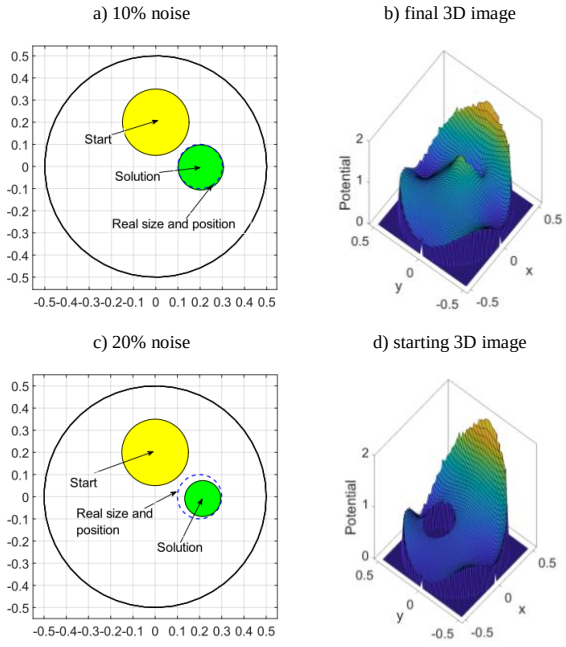

Fig. 9. Inverse problem solution of parametrized image when the measurements are polluted by: a) 10% noise, b) 3D image, c) 20% noise, d) 3D image for the starting point

Fig. 9 presents the inverse solution for the acoustic frequency equal to f = 5.47 kHz and for the wave number k = 1 [1/m].

For the outer boundary circle, the number of boundary elements per lambda wavelength = 128, and for the inner circle, the number of boundary elements per lambda wavelength = 160.

Those numbers are much higher than the discretisation criterion, stating that the number of boundary elements should be bigger than ten boundary elements per acoustic wavelength. Fig. 9 presents the results for 10% and 20% of pollution (left column). In the right column are shown the distribution of the acoustic fields inside the region for final and starting position.

For the 10% of pollution, the maximal error was 8.0% for the radius location and 2.5% for the radius of the scatterer. And for 20% of noise, 19%, and 7.0%, respectively. In the right column are pictures of the field distribution inside the area. In the upper row of this column, the image is for the real position of the scatterer, but the lower row is for the starting position of the optimization process.

The same numerical experiment was carried out for ultrasonic frequency equal to f = 38.30 kHz and the wave number k = 7 [1/m]. The images are presented in Fig. 10. Now, for the external boundary circle, the number of boundary elements per wavelength lambda = 18.3, and for the internal circle number of boundary elements per wavelength lambda = 22.9. This time the number of boundary elements per wavelength is closer to the precision criterion, which means that discretization is more economical from the tomography point of view.

For ultrasound tomography with 10% noise, the maximal error was less than 20% which is unacceptable (see Fig. 10 upper row). However, it is possible to reduce the significant error by enlarging the number of sensors (see Fig. 10, the lower row).

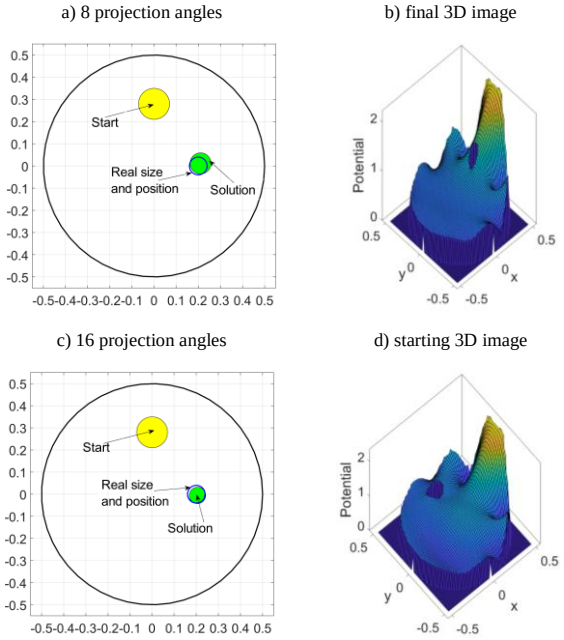

Fig. 10. Synthetic signal treated as the measured one with: a) 10% noise for 8PA, b) 3D field image c) 10% noise but for 16 PA d) 3D image for the starting point

The level of the maximal error for ultrasonic frequency is about twice as much as for the acoustical frequency, as shown in Fig. 11.

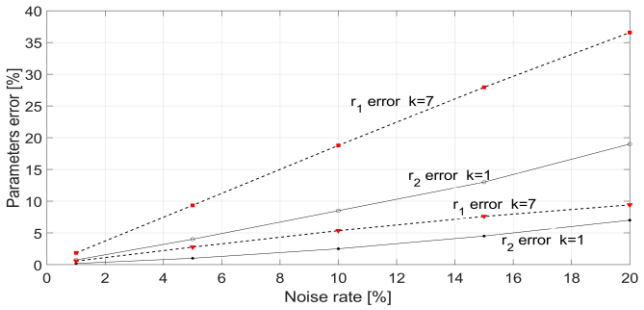

Fig. 11. Relative error as a function of the signal noise rate for two different wave numbers

As shown in figure 11, the error sometimes reaches more than 30%. So, the question is how to reduce the level of the maximal error?

There are at least two ways. One of them is presented in Fig. 10 (the lower row). Namely, the number of sensors doubled. For maximal error reduction, we must pay by the execution time, which is painful for the optimization process. However, it is possible to reach much better results, as seen in Fig. 10. The error was reduced to 7.1% for the radius location and 2.8% for the scatterer radius.

9. Conclusions

From a tomography point of view, the most important is a grid providing a minimum number of points per wavelength to resolve the acoustic or ultrasonic problem even for the highest frequencies. Our goal is ultrasound tomography, so we must consider frequency above 20 kHz. Unfortunately, the wavelength became noticeably short for such frequencies, even less than 0.017 m.

In tomography problems, we often deal with many sensors emitting and receiving signals closely located to the external boundary. For example, Diffuse Optical Tomography or Radio Tomography could be mentioned [5-7].

The literature [1-3] stresses that the acoustic wavelength should be much greater than the length scale of the region under consideration. That means that the ratio of the wavelength to the length of the boundary element should be at least equal to 8-10. Then, we trust that the precision of the calculation will be secured.

However, it might be difficult in tomography to fulfil such rigorous demands. For example, for the ultrasound frequency band, the length of the boundary elements should be extremely small if the error level should be kept at a low level. From the point of view of the Inverse Problem efficiency calculation, such a decision would be difficult to justify. Therefore, some compromise between the accuracy and the execution time must be preserved. In the author's opinion, coarse discretization might be sufficient in some cases.

References

[1] Abramowitz M., Stegun I. A.: Handbook of mathematical functions with formulas, graphs, and mathematical tables. John Wiley, New York 1973.
[2] Athanasiadis C.: Scattering relations for point sources: Acoustic and electromagnetic waves. Journal of mathematical physics 43(11), 2002, 5683.
[3] Harwood A. R. G.: Numerical Evaluation of Acoustic Green's Functions. PhD School of Mechanical, Aerospace & Civil Engineering, University of Manchester, Manchester 2014.
[4] Kirkup S.: The Boundary Element Method in Acoustics: A Survey. Applied Sciences 9(8), 2019, 1642 [http://doi.org/10.3390/app9081642].
[5] Lynott G. M.: Efficient numerical evaluation of the scattering of acoustic and elastic waves by arrays of cylinders of arbitrary cross section. Thesis of Doctor of Philosophy. School of Natural Sciences, Department of Mathematics, University of Manchester, Manchester 2020.
[6] Opieliński K. J., Pruchnicki P., Gudra T.: Ultrasonic Mammography with Circular Transducer Array. Archives of Acoustics 39(4), 2014, 559–568 [http://doi.org/10.2478/aoa-2014-0060].
[7] Rymarczyk T.: Tomographic Imaging in Environmental, Industrial and Medical Applications. Innovatio Press Publishing Hause, Lublin 2019.
[8] Rymarczyk T., Sikora J.: On precision acoustic wave calculation in a frequency domain. IAPGOS 2, 2022, 64–68 [http://doi.org/10.35784/iapgos.2966].
[9] Sikora J.: Boundary Element Method for Impedance and Optical Tomography. Warsaw University of Technology Publishing Hause, Warsaw 2007.
[10] https://www.comsol.com/acoustics-module
[11] https://reference.wolfram.com/language/PDEModels/tutorial/Acoustics/AcousticsFrequencyDomain.html

Prof. D.Sc. Ph.D. Eng. Tomasz Rymarczyk
e-mail: tomasz@rymarczyk.com

He is the director of the Research and Development Centre in Netrix S.A. and the Institute of Computer Science and Innovative Technologies at WSEI University, Lublin, Poland. He worked in many companies and instituted developing innovative projects and managing teams of employees. His research focuses on applying non-invasive imaging techniques, electrical tomography, image reconstruction, numerical modelling, image processing and analysis, process tomography, software engineering, knowledge engineering, artificial intelligence, and computer measurement systems.

http://orcid.org/0000-0002-3524-9151

Prof. D.Sc. Ph.D. Eng. Jan Sikora
e-mail: sik59@wp.pl

Prof. Jan Sikora (PhD. DSc. Eng.) graduated from Warsaw University of Technology Faculty of Electrical Engineering. During 44 years of professional work, he has obtained all grades, including the position of full professor at his alma mater. Since 1998 he has also worked for the Institute of Electrical Engineering in Warsaw. In 2008, he joined Electrical Engineering and Computer Science Faculty in Lublin University of Technology. During 2001-2004 he has worked as a Senior Research Fellow at University College London in the prof. S. Arridge's Group of Optical Tomography. His research interests are focused on numerical analysis application in field theory. He is the author of eight books and more than 180 papers published in international journals and conferences.

http://orcid.org/0000-0002-9492-5818

http://doi.org/10.35784/iapgos.3264 received: 9.11.2022 | revised: 8.12.2022 | accepted: 15.12.2022 | available online: 30.12.2022

FINITE ELEMENT MODEL FOR ANALYSIS OF CHARACTERISTICS OF SHROUDED ROTOR BLADE VIBRATIONS

Anatoliy Zinkovskii[1], Kyrylo Savchenko[1], Yevheniia Onyshchenko[1,2], Leonid Polishchuk[3], Abilkaiyr Nazerke[4], Bagashar Zhumazhanov[5]

[1]G.S. Pisarenko Institute for Problems of Strength of the National Academy of Sciences of Ukraine, Kyiv, Ukraine, [2]Department of Oscillations and Vibration Reliability, Kyiv, Ukraine, [3]Vinnytsia National Technical University, Vinnytsia, Ukraine, [4]Al-Farabi Kazakh National University, Almaty, Kazakhstan, [5]Institute of Information and Computing Technologies of the CS MES of RK, Almaty, Kazakhstan

Abstract. *The paper presents the approaches to FE modelling of blade airfoil, contact between the shrouds and operational damage. The regularities are established concerning the influence of the finite element type, finite element mesh and model of contact interaction on the spectrum of natural frequencies of blade assemblies. The use of the developed computational models is substantiated to determine the forced vibration characteristics of the selected objects of investigation. Based on the performed numerical experiments it was substantiated of finite element model selection for analysis of characteristics of shrouded rotor blade vibrations.*

Keywords: FE modeling, modal analysis, forced vibration analysis, shrouded blade, nonlinear vibrations

MODEL ELEMENTÓW SKOŃCZONYCH DO ANALIZY CHARAKTERYSTYK DRGAŃ ŁOPAT WIRNIKA OSŁONIĘTEGO

Streszczenie*: W artykule przedstawiono podejścia do modelowania elementów skończonych płata łopaty, styku osłon oraz uszkodzeń eksploatacyjnych. Ustalono prawidłowości dotyczące wpływu typu elementu skończonego, siatki elementów skończonych oraz modelu interakcji stykowej na widmo częstotliwości drgań własnych zespołów łopatek. Uzasadnione jest wykorzystanie opracowanych modeli obliczeniowych do wyznaczania charakterystyk drgań wymuszonych wybranych obiektów badań. Na podstawie przeprowadzonych eksperymentów numerycznych uzasadniono wybór modelu elementów skończonych do analizy charakterystyk drgań osłoniętych łopat wirnika.*

Słowa kluczowe: modelowanie MES, analiza modalna, analiza drgań wymuszonych, łopata osłonięta, drgania nieliniowe

Introduction

In the practice of modern aircraft engine design, determination of mechanisms of vibrations of compressor and turbine rotor blades is of current concern. To ensure high operational requirements for engines, their reliability, and functional serviceability, it is necessary to reduce the material consumption and improve technical and economic performance [3, 8].

Due to the significant increase in costs for the development of rotor blades, it is difficult to perform comprehensive laboratory and full-scale testing. Therefore, numerical experiment along with modern methods of computer modeling based on three-dimensional calculation models of blades and their assemblies is of great importance. It is one of the most common modes of discretization of the systems with the infinite number of degrees of freedom and developed procedures of their modeling. This method for the solution to the tasks of determination of the dynamic stress state of the specified objects is implemented in the majority of the modern software products.

Rotor blades with flange shrouding are the most critical and, at the same time, most heavily-loaded structural elements of gas-turbine engines. Finite element modeling (FEM) of rotor blades should consider the features of the airfoil geometry, contact interaction between the shrouds of adjacent blades, as well as their possible local damages in the engine operation [3, 5, 7].

However, the review of the scientific and technical manuscripts demonstrates that the accuracy of the obtained results depends (considerably) on the type of finite element (FE) and its dimensions, as well as the approaches to modeling of various types of interaction between the structural elements of the object under investigation. The goal of this paper is in the generalization of the methods and approaches used by the authors for FEM of such mechanical systems as assemblies of turbine engines with flange shrouding of blades in the determination of characteristics of their vibrations [1, 7, 8].

1. Object of investigation and general approaches to its finite element modeling

A turbine rotor wheel (Fig. 1a) with its blade assembly containing 136 (N = 136) shrouded blades made of heat-resistant alloy ZhS 26-VI is chosen to perform the numerical calculations. The physical and mechanical characteristics of the alloy are as follows: the elastic modulus E = 1.9·1011 Pa; density ρ = 8570 kg/m³; Poisson's ratio μ = 0.3.

Considering strict cyclic or rotational symmetry of the blade assembly its analysis is reduced to the consideration of certain cycle with the corresponding boundary conditions, which can involve one or several blades. The determining feature in FEM of the rotor wheel is the mesh of its blades, which should reflect (as possible) their geometry, properties of the material and acting loads. Noteworthy is that in practice it is impossible to consider these factors in full due to imperfections in the blade structure (and their materials) and different operation modes. Therefore, some idealization of the shape of blades, properties of the materials and conditions of external effects takes place in the development of FE models of rotor blades depending on the tasks assigned. Here the successful selection of the model's parameters defines the scope of calculations, validity, and accuracy of the obtained results.

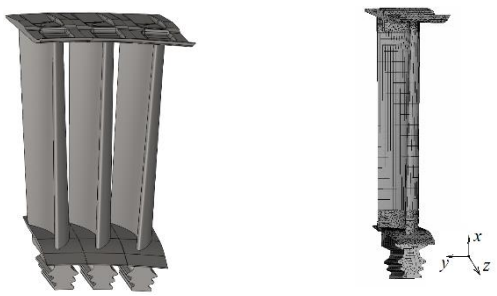

a) b)

Fig. 1. Fragment of the blade assembly under investigation (a) and FE model of isolated blade (b)

From the results of FEM calculations, it is apparent that regular mesh is the most preferred for any machine building structures. The only exceptions are those zones where irregular geometric shapes are observed, for instance, at the connections of the blades and the shrouds, as well as within areas containing different damages. Due to the specific geometric features, the model includes domains with different types of mesh [2, 6, 11].

To construct the FE models of the shrouded blades, three-dimensional 8-nodes and 20-nodes finite elements are used (Fig. 2). These types of elements were chosen in this investigation to solve the issue.

Figure 1b illustrates the FE model of the isolated blade using the approaches for it creating above.

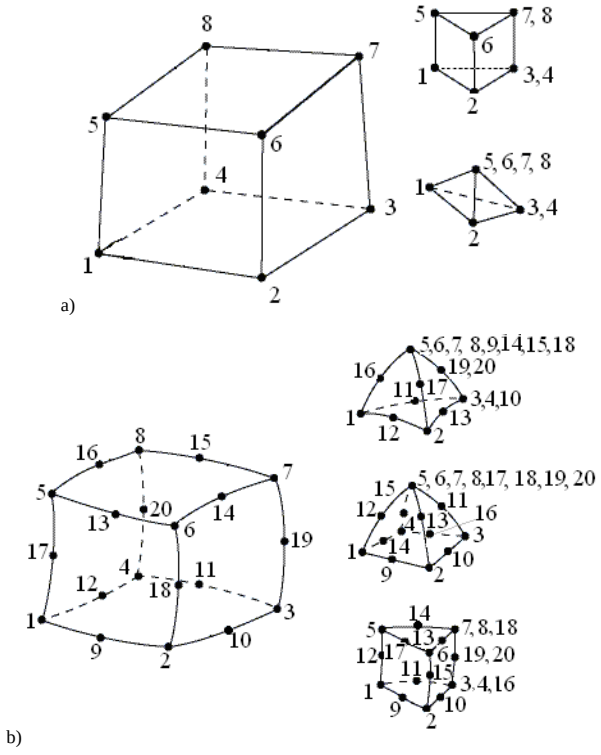

Fig. 2. Finite elements and their modifications: a – linear 8-nodes; b – quadratic 20-nodes

Let us consider the approaches to FEM of the shrouded blades and their assemblies in the solution to the issue aimed at the determination of characteristics of their vibrations [7, 9, 14].

2. Determination of the spectrum of natural vibration frequencies

Using the developed FE model of the rotor blade a set of numerical investigations was performed to determine the influence of the type and dimensions of FE, as well as contact interaction modeling, on the spectrum of the natural frequencies of vibrations of the blade assembly under investigation. The calculations were conducted employing various types of finite elements and the density of FE mesh, which is defined by the number of finite elements *k*, as well as procedures of linearization of the contact between the shrouds of the adjacent blades.

The structural cyclic symmetry of the blade assembly is assumed in this paper. As is known [4, 12], in this case, when performing the computational experiments, it is possible to confine ourselves to the consideration of the only one sector for a blade row, the number of which, in the presence of the annular shrouding, coincides with the number of blades. A mandatory requirement here is the fulfillment of the boundary conditions at the nodes of connecting the adjacent sectors along the contact surfaces of the shrouds and the disk.

For the purposes of simulating the shrouding of the blades, the procedure described earlier [5, 13, 15] was proposed, whose main thesis are as follows:

1. The shroud is cut in such a way that its parts are connected along the common surface, and the nodes lying on this surface coincide.
2. The cut-off part of the shroud with the FE mesh is displaced by the angle $\beta = 360^{\circ}/N$ (shown by the arrow in Fig. 3a) in the cylindrical system of coordinates, which makes it possible to simulate the tension along the contact surfaces of the shrouds.

Considering the cyclic symmetry of the assembly the conditions of coupling on the cut surfaces C1 and C2 of its sector are specified as shown in Fig. 3b.

It is also necessary to take into consideration the conditions of the blade-to-disk interaction along the contact surfaces of the root since this can influence the contacting character of the shrouds. Since the assembly process assumes that the contact surfaces of the fir-tree blade root fit closely to the corresponding surfaces of the disk, and also to avoid its influence on the investigation results, the rigid attachment of the blade root at the disk groove was adopted as the boundary conditions.

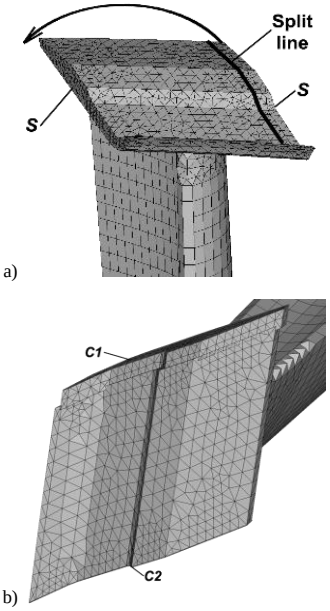

Fig. 3. Schemes of the three-dimensional cut of the shroud (a) and contact interaction modeling (b)

The procedure of substantiation of the developed FE model of the assembly was based on the solution to the issue in the absence of the shrouded coupling between the blades, i.e. individual or isolated blade. Figure 4 illustrates the diagrams of the first four natural frequencies of vibrations *pi* ($i = 1, \ldots, 4$) of the blade in the variation of its mesh density for the selected types of finite elements.

The analysis of the data indicates that the natural frequencies of vibrations of the considered blades are not affected by both the FE type and density of FE mesh. As is obvious does not exceed 2.22%. However, the calculation time is more efficient while using the models based on 8-node finite elements in comparison to 20-node elements.

Let us consider the determination of the influence of the FE type and FE mesh density on the spectrum of natural frequencies of the blade assembly under investigation providing its cyclic symmetry. Such numerical investigations imply exception of any nonlinear nature of deformation of the system under study. Thus, the modeling of contact interaction between the shrouds (it is generally of nonlinear nature) requires its linearization.

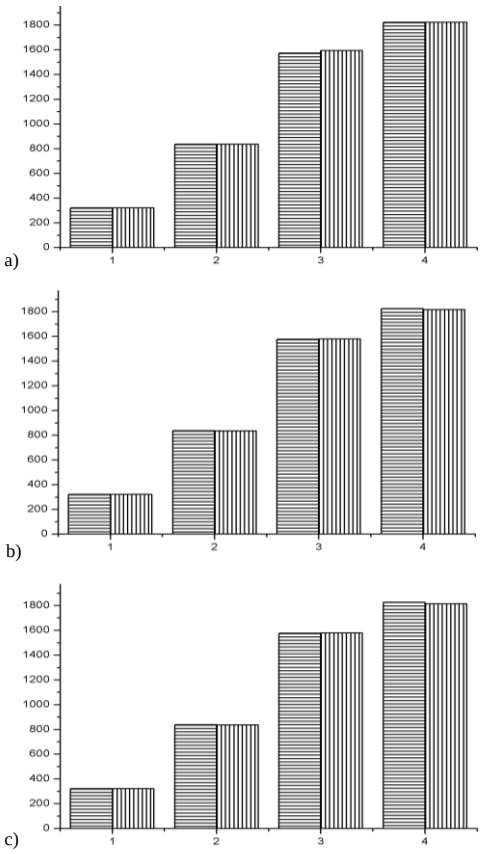

Fig. 4. Diagrams of the first four natural frequencies of the blade vibrations at k = 5000 (a), 7000 (b) and 12000 (c) of 8-nodes (horizontal lines) and 20-nodes (vertical lines) finite elements

There are different variants of modeling of the contact interaction between the shrouds, namely [2]:

1. The conditions of consistency of displacements are imposed on all the nodes of finite elements of the contact surfaces.
2. The conditions of consistency of displacements are imposed on all the nodes of finite elements of the contact surfaces with the non-zero values of contact pressure. Here the static contact issue was previously solved. The results of the solution are used to choose the nodes for the imposition of the corresponding conditions of consistency of displacements.
3. The elastic elements by two degrees of freedom (Ux and Uy) are added between the nodes of finite elements with the non-zero values of contact pressures. Moreover, the value of contact pressure (observed within the corresponding nodes) is specified for each such element. The conditions of consistency of displacements in the radial direction (along the blade airfoil) are imposed on the specified nodes within the region of the maximum values of contact pressure along the conjugated surfaces of the shrouds.

The values of contact pressure and its distribution over the planes of contact between the shrouds required to perform the numerical experiments are taken from [5, 10, 15]. Based on these calculation results, the natural frequencies of vibrations of the blade assembly under investigation were determined for the selected variants of the contact interaction between the shrouds. The obtained values of natural frequency were applied to plot the frequency functions (Fig. 5) as the dependencies of the vibration frequency on the number of nodal diameters m, where n is the number of nodal circles. The solution was made for the modes of the assembly vibrations $n = 0$.

It is seen that variant 1 is characterized by higher values of the natural frequencies of vibrations of the blade assembly as compared with variants 2 and 3. It is explained by the fact that variant 1 involves the blade assembly as a system with elastic coupling, which results in the considerable overestimation of the results of calculation of its natural vibration frequencies. Variant 2 describes the conditions of contact between the shrouds that are of identical character for all the nodes within its area, which also causes the stiffness increase for the system under consideration. Variant 3shows the calculation results that comply to the actual values of natural frequencies of the blade vibrations determined in full-scale testing. Also, the maximum difference ε in the values of natural frequencies of vibrations determined using the considered FE models of the blades is about 7% with the average density of the blade mesh.

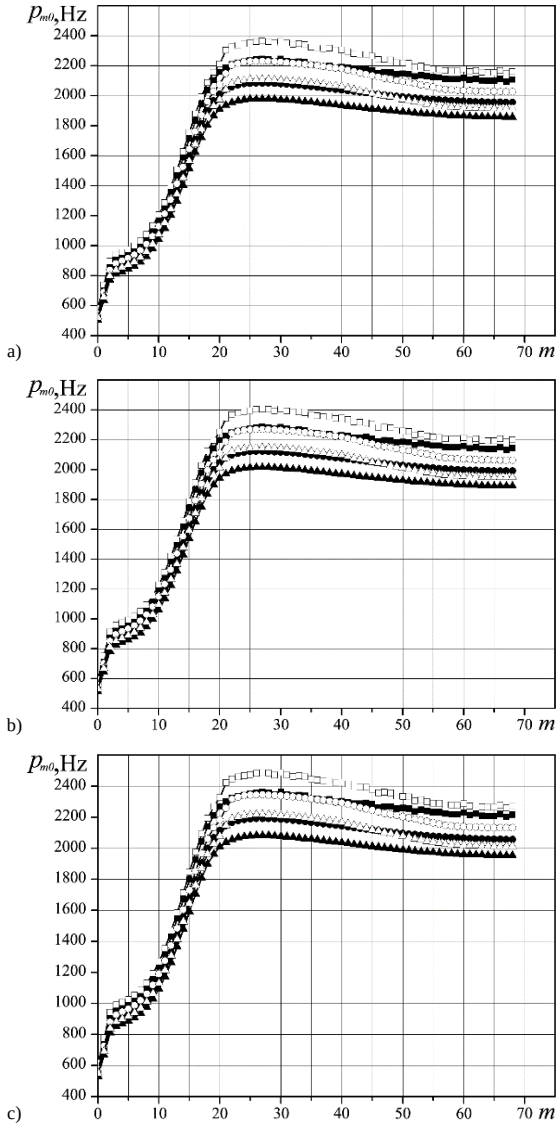

Fig. 5. Frequency functions of the blade assembly for variants 1 (■, □), 2 (●, ○) and 3 (▲, Δ) of the contact interaction k = 5000 (a), 7000 (b) and 12000 (c) 8-nodes (■, ●, ▲) and 20-nodes (□, ○, Δ) finite elements

3. Determination of characteristics of forced vibrations

The calculations on the determination of the influence of contact interaction modeling of the shrouds were made employing the assembly consisting of two blades, which is the simplest regular system as shown in [5, 15]. Here it is possible to fully investigate the influence of different factors on the vibrations of the studied structures.

Figure 6 illustrates the model of the selected assembly without the consideration of the root. Node A, where the characteristics of its forced vibrations were determined, is also shown here. There are two approaches to model the contact interaction between the shrouds. The first approach involves the solution of the contact issue using the Newton-Raphson procedure, while the second one – linearization of the contact interaction in compliance with variant 2 modeling considered in the analysis of the spectrum of natural vibration frequencies of the blade assembly. Later the equations of the forced vibrations were solved using the Newmark scheme.

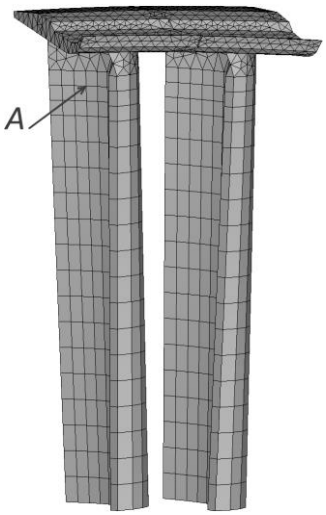

Fig. 6. FE model of the assembly consisting of two blades

The distribution of exciting forces Q acting on the blades due to the working body flow is of a complex nature. All the calculations were performed for two cases of harmonic excitation of vibrations of the blade assembly: in-phase $Q_1 = Q_2 = Q_0 \sin \nu t$ and anti-phase $Q_1 = -Q_2 = Q_0 \sin \nu t$. The frequency of the exciting force ν varied in the range of the spectrum of natural frequencies of the assembly vibrations.

From the results of the calculations, the amplitude-frequency characteristics (AFC) of the assembly were determined. They were used to build the dependencies of the amplitude of displacements within the chosen node A on the relations between the vibration frequencies ν/p_0, where p_0 is the resonance frequency of the assembly vibrations.

Figure 7 illustrates the examples of the AFC. Its detailed consideration and analysis allow one to draw the following conclusions:

1. The character of the AFC is almost identical during in-phase excitation using both nonlinear and linearized calculation models [5].
2. A significant nonlinearity of the system is evident only at anti-phase excitation of the blade assembly vibrations.
3. Depending on the calculation model used, the maximum stresses in the assembly will be observed at various frequencies of exciting force, their difference does not exceed 5%. When employing the linear model, the maximum stresses are observed at the lower frequency of exciting force in case of in-phase shape. For anti-phase shape, the maximum stresses are detected at the larger frequency of exciting force as compared with the results of calculations based on the nonlinear model. This is explained by the variation of the system stiffness.

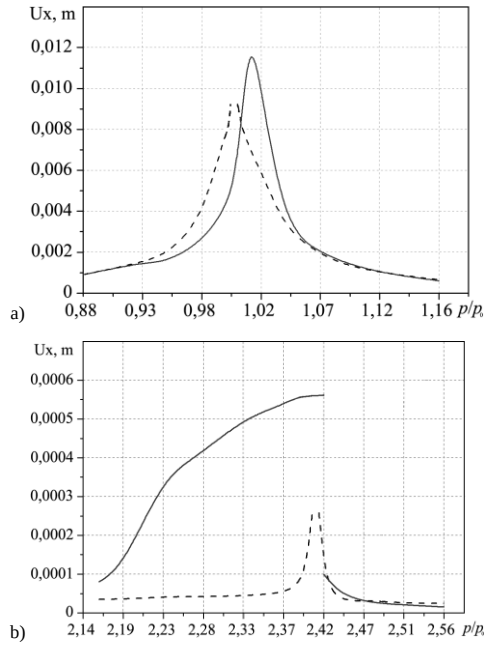

Fig. 7. Amplitude-frequency characteristics of displacements along axis 0x for nonlinear (solid lines) and linear (dashed lines) models during in-phase (a) and anti-phase (b) harmonic excitation of vibrations

4. Investigation of blade vibrations considering damages

Damage modeling in the investigation of its influence on the vibration characteristics of the structural elements is important. In the case of dents, erosion and other damages, it is possible to model the defect presented as a rectangular or wedge-shaped notch with fine FE mesh in its zone [15]. The mass of the system is maintained in the presence of a fatigue crack but its stiffness varies in the process of its cyclic deformation.

Based on the previous experience [3], a fatigue crack was modeled as the mathematical cut. In case of open crack, there is a mutual non-penetration of its faces. This is ensured by the introduction of the surface contact elements and solution of the contact issue along with modeling of contact interaction between the shrouds of rotor blades.

Considering that the calculation of forced vibrations for such complicated structural elements requires large computer resources, in the investigation of the blade airfoil the decision was made to consider only its less twisted part of the length $L = 0.086$ m (Fig. 8). The calculations on the influence of the crack presence on the vibration behavior of the chosen investigation objects were performed for the case where the crack is at the distance $x_T = 0.1L$ from the edge cross-section of the blade airfoil on the side of the blade root and rigid fixation of the beam as a cantilever.

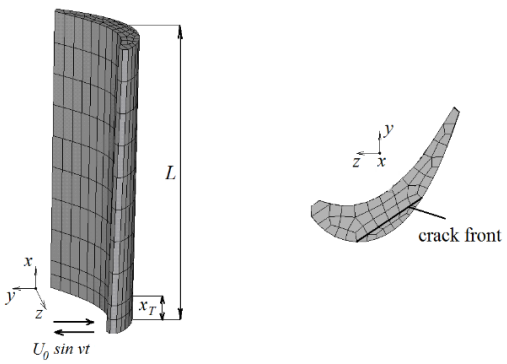

Fig. 8. FE model of the blade airfoil with damage and cross-section of the airfoil with a crack

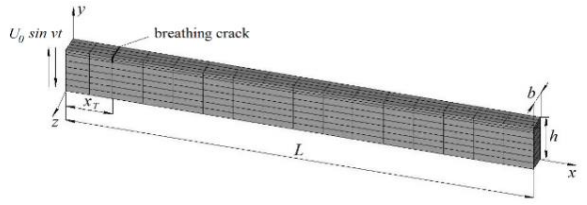

Fig. 9. FE model of the beam of the rectangular cross-section with breathing crack

To verify the accuracy of the proposed crack model, the results of calculation were compared with similar ones obtained for the beam of a rectangular cross-section of $b \times h = 0.004 \times 0.009$ m and $L = 0.086$ m (Fig. 9) [7] with identical dimensions in terms of area and crack location over the beam length.

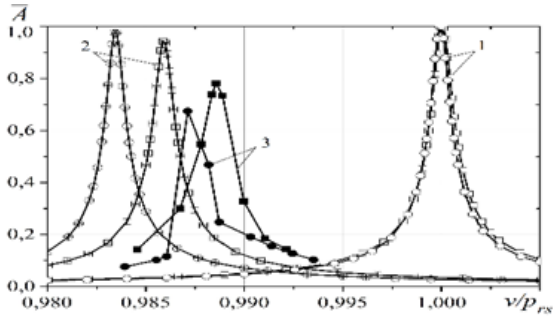

Fig. 10. Amplitude-frequency characteristics of the blade airfoil (○, ⊕, ●) and beam of the rectangular cross-section (□, ⊞, ■) without damage (1) and with open (2) and breathing

The forced vibrations were induced by means of harmonic displacement $U_0 \sin \nu t$ of edge sections of the chosen objects along the axis $0y$. Figure 10 displays the AFC of the selected objects of investigation without damage, as well as with open and breathing cracks, where p_{rs} is the resonance frequency of vibrations of the undamaged airfoil (beam), is the relation of the amplitude of forced vibrations and the maximum value of the amplitude of the undamaged airfoil (beam) at main resonance.

As it is seen AFC are practically identical for the undamaged blade airfoil and beam. AFC are different in the presence of open and breathing cracks of the airfoil and beam. This is due to the complex geometry of the blade airfoil and variation of the mode of its vibrations with damage.

Noteworthy is that the model of open crack (fatigue damage) exhibits the reduced value of the resonance frequency of vibrations and, as a rule, does not allow to evaluate the actual damage parameters.

During vibrations of the objects with a breathing crack on a frequency of the main resonance the vibration diagnostic parameters of its presence were determined, namely: variation of the resonance frequency of vibrations $\Delta\overline{\omega}_0$, as well as the relation between the amplitudes of the dominant harmonics of displacements $\overline{A}_2$ and accelerations $\overline{A}_2^a$ due to the stiffness system variation (table 1). They are in a good correlation between each other and can be used in the damage diagnostics.

Table 1. Vibration diagnostic parameters of the presence of breathing crack

Object of investigation	$\Delta\overline{\omega}_0$	$\overline{A}_2$	$\overline{A}_2^a$
Beam	0.011	0.0042	0.0168
Blade airfoil	0.0132	0.0055	0.022

Thus, the procedure of modeling of open and breathing cracks in turbine machine blades was proposed for further investigation of forced vibrations.

5. Conclusions

Based on the performed numerical experiments it was substantiated of finite element model selection for analysis of characteristics of shrouded rotor blade vibrations. Also, it was established the following:

- FE type and density of FE mesh do not practically affect the results of calculations of natural frequencies of the isolated blade vibrations. The results of determination of the spectrum of natural frequencies of the blade assembly vibrations depend significantly on the specified characteristics of FE mesh. For instance, the difference ε in the values of natural frequencies of vibrations (with the average density of FE meshes) obtained using the models based on 8 and 20-nodes finite elements is approximately 7%;
- modeling of the interaction between rotor blades using the imposition of the consistency of displacements between all the nodes of contact surfaces or those with non-zero contact pressures result in the increased values of natural frequencies of vibrations of the blade assembly as compared with those obtained using spring elements. This is explained by the maximum stiffness of the joint in comparison with the latter variant of modeling;
- for the in-phase mode of excitation of vibrations of the blades, the AFC's character obtained using non-linear and linear calculation models is practically identical. The considerable nonlinearity is observed only at the anti-phase mode of excitation. Here the difference between the frequencies, whereby the maximum stresses are observed, does not exceed 5% for the investigated models;
- breathing crack modeling with the contact elements allows one to determine the frequency and nonlinear characteristics of vibrations more accurately as compared with the open crack modeling, which enhances the efficiency of its use in the investigation of fatigue damages of rotor blades.

References

[1] Abdelrhman A. M. et al.: Condition monitoring of blade in turbomachinery: A review. Advances in Mechanical Engineering 6(1), 2014, 210717.
[2] Giannini O., Casini P., Vestroni F.: Nonlinear harmonic identification of breathing cracks in beams. Computers & Structures 129, 2013, 166–177.
[3] Larin O. O.: Forced vibrations of bladings with the random technological mistuning. Proceedings of the ASME Turbo Expo 2010, 6, 2010, 667–672.
[4] Oh Y., Yoo H. H.: Vibration analysis of a rotating pre-twisted blade considering the coupling effects of stretching, bending, and torsion. Journal of Sound and Vibration 431, 2018, 20–39.
[5] Onishchenko E. A., Zinkovskii A. P., Kruts V. A.: Determination of the Vibration Diagnostic Parameters Indicating the Presence of a Mode I Crack in a Blade Airfoil at the Main, Super-and Subharmonic Resonances. Strength of Materials 50(3), 2018, 369–375.
[6] Panigrahi B., Pohit G.: Effect of cracks on nonlinear flexural vibration of rotating Timoshenko functionally graded material beam having large amplitude motion. Proceedings of the Institution of Mechanical Engineers Part C. Journal of Mechanical Engineering Science, 2018.
[7] Polishchuk L., Bilyy O., Kharchenko Y.: Prediction of the propagation of crack-like defects in profile elements of the boom of stack discharge conveyor. Eastern-European Journal of Enterprise Technologies 6(1), 2016, 44–52.
[8] Polishchuk L., Mamyrbayev O., Gromaszek K.: Mechatronic Systems II. Applications in Material Handling Processes and Robotics. Taylor & Francis Group, CRC Press, Balkema book Boca Raton, 2021.
[9] Rafiee M., Nitzsche F., Labrosse M.: Dynamics, vibration and control of rotating composite beams and blades: A critical review. Thin-Walled Structures 119, 2017, 795–819.
[10] Saito A.: Nonlinear vibration analysis of cracked structures: Application to turbomachinery rotors with cracked blades. Dissertation for the Doctoral Degree. The University of Michigan, Michigan 2009.
[11] Savulyak V. et al.: Modification of surfaces of steel details using graphite electrode plasma. In: Polishchuk L. et al.: Mechatronic Systems II. Applications in Material Handling Processes and Robotics, Taylor & Francis Group, CRC Press, Balkema book, Boca Raton, London, New York, Leiden 2021, 141–150.
[12] Tang W., Epureanu B. I.: Nonlinear dynamics of mistuned bladed disks with ring dampers. International Journal of Non-linear Mechanics 97, 2017, 30–40.
[13] Wójcik W. et al.: Mechatronic Systems I. Applications in Transport, Logistics, Diagnostics and Control. Taylor & Francis Group, CRC Press, Balkema book, London, New York 2021.
[14] Yang L. et al.: Mechanism of fast time-varying vibration for rotor–stator contact system: With application to fault diagnosis. Journal of Vibration and Acoustics 140(1), 2018, 014501.
[15] Zinkovskii K. et al.: Influence of modeling of contact interaction conditions on spectrum of natural vibration frequencies of blade assembly. 23rd International Congress on Sound and Vibration – ICSV 23, 2016, 289–293.

D.Sc. Anatoliy Zinkovskii
e-mail: zinkovskii@ipp.kiev.ua

Corresponding member of the National Academy of Sciences of Ukraine, Doctor of Technical Sciences, professor, G.S. Pisarenko Institute for Problems of Strength of the National Academy of Sciences of Ukraine.
Methods of research and determination of regularities of coupled oscillations of regular non-conservative mechanical systems with broken symmetry, taking into account the peculiarities of elastic-dissipative and aerodynamic coupling and amplitude dependence of damping characteristics of the same type of elements, mechanical vibrations, finite element method, vibrodiagnostics of fatigue damage, breathing crack

http://orcid.org/0000-0003-0803-7054

Ph.D. Kyrylo Savchenko
e-mail: savchenko@ipp.kiev.ua

Ph.D., G.S. Pisarenko Institute for Problems of Strength of the National Academy of Sciences of Ukraine.
Research Interests: investigations of deformability and destruction of metals during plastic forming; evaluation of the deformability of metals during pressure treatment, mechanical vibrations, finite element method, vibrodiagnostics of fatigue damage, breathing crack

http://orcid.org/0000-0002-9690-9758

Ph.D. Yevheniia Onyshchenko
e-mail: onyshchenko@ipp.kiev.ua

Ph.D., G.S. Pisarenko Institute for Problems of Strength of the National Academy of Sciences of Ukraine. Department of Oscillations and Vibration Reliability, Kyiv, Ukraine.
The scientific focus is the dynamics of drive systems with devices and control systems with variable operating modes and diagnostics of metal structures of hoisting-and-transport and technological machines, mechanical vibrations, finite element method, vibrodiagnostics of fatigue damage, breathing crack.

http://orcid.org/0000-0001-7550-8544

D.Sc. Leonid Polishchuk
e-mail: leo.polishchuk@gmail.com

Doctor of technical sciences, professor, academician at the Ukraine Academy of Hoisting-and-Transport Sciences, Vinnytsia National Technical University.
Head of the Department of Industrial Engineering at Vinnytsia National Technical University.
The scientific focus is the dynamics of drive systems with devices and control systems with variable operating modes and diagnostics of metal structures of hoisting-and-transport and technological machines.

http://orcid.org/0000-0002-5916-2413

M.Sc. Abilkaiyr Nazerke
e-mail: abilkaiyr.nazerke@gmail.com

Abilkaiyr Nazerke is a graduate of the Faculty of General Medicine of Kazakh National medicine University. Currently works at the faculty of medicine and healthcare of Al-Farabi Kazakh National University. She is the author or co-author of several scientific publications in the field of public health, epidemiology primary healthcare and economics in public health. Currently, she conducts research related to CTTN Joint Regional Project “COVID – Induced Inequalities: Education, Health Services, Digital Access, and Female Labor Force Participation”. Case Studies from Azerbaijan, Kazakhstan, Pakistan, and Uzbekistan.

http://orcid.org/0000-0003-1603-5577

Ph.D. Bagashar Zhumazhanov
e-mail: bagasharj@mail.ru

Senior researcher of the Institute of Information and Computing Technologies of the CS MES RK, associate professor.
Graduated from the Faculty of Physics and Mathematics of the Abai Almaty State University with a degree in Computer Science and Mathematics. Master's degree in “Information Systems”.
In 2011 he defended his thesis for the degree of Candidate of technical sciences. associate professor of the OP “Digital Engineering and Data Analysis”.

http://orcid.org/0000-0002-5035-9076

http://doi.org/10.35784/iapgos.3058 received: 2.09.2022 | revised: 13.12.2022 | accepted: 15.12.2022 | available online: 30.12.2022

EFFICIENTLY PROCESSING DATA IN TABLE WITH BILLIONS OF RECORDS

Piotr Bednarczuk, Adam Borsuk
University of Economics and Innovation in Lublin, Institute of Computer Science, Lublin, Poland

Abstract: *Over time, systems connected to databases slow down. This is usually due to the increase in the amount of data stored in individual tables, counted even in the billions of records. Nevertheless, there are methods for making the speed of the system independent of the number of records in the database. One of these ways is table partitioning. When used correctly, the solution can ensure efficient operation of very large databases even after several years. However, not everything is predictable because of some undesirable phenomena become apparent only with a very large amount of data. The article presents a study of the execution time of the same queries with increasing number of records in a table. These studies reveal and present the timing and circumstances of the anomaly for a certain number of records.*

Keywords: systems aging, partitioning, efficiently data processing, billions of records

WYDAJNE PRZETWARZANIE DANYCH W TABELI Z MILIARDAMI REKORDÓW

Streszczenie: *Z biegiem czasu systemy podłączone do baz danych zwalniają. Wynika to zwykle ze wzrostu ilości danych przechowywanych w poszczególnych tabelach, liczonych nawet w miliardach rekordów. Niemniej jednak istnieją metody uniezależnienia szybkości systemu od liczby rekordów w bazie danych. Jednym z tych sposobów jest partycjonowanie tabel. Przy prawidłowym zastosowaniu rozwiązanie to może zapewnić wydajne przetwarzanie danych w bardzo dużych bazach danych nawet po kilku latach działania. Jednak nie wszystko jest tak przewidywalne ponieważ niektóre niepożądane zjawiska ujawniają się dopiero przy bardzo dużej ilości danych. W artykule przedstawiono badanie czasu wykonania tych samych zapytań przy rosnącej liczbie rekordów w tabeli. Badania te ujawniają i przedstawiają moment i okoliczności występowania anomalii dla pewnej liczby rekordów.*

Słowa kluczowe: starzenie się systemów, partycjonowanie, efektywne przetwarzanie danych, miliardy rekordów

Introduction

Billions of records in single tables are often found in data warehouses or BIG DATA databases. The administrators of such databases often face a optimalisation task of queries execution time. This is an important problem because it occurs in every large database. The ideal solution would allow, despite the increase of the number of records in the tables, to perform operations on the database as quickly as at the time of its implementation [2].

An example of such a solution that is implemented in most database engines is table partitioning [3].

The report presents a practical example of the use of partitioning on tables containing up to a billion records. The greatest advantage of partitioning was presented in the study which shows that the increase number of records in tables does not affect the query execution time.

The paper is an extension of publication [1] therefore appearing repetitions or similarities of the text in first four chapters result solely from the desire to present a coherent and complete the course of the research.

1. Table partitioning

Table partitioning is a division of tables into parts, physical files, constituting some separated ranges of data, e.g.: monthly, quarterly or annually. This division takes place in the database files, but the developer sees them as one object; one table. Although it is always possible to read the contents of each partition by using the appropriate tags, a standard queries e.g. SELECT, UPDATE and MERGE on the partitioned table will processing the data only from one or a few set of records, not all records.

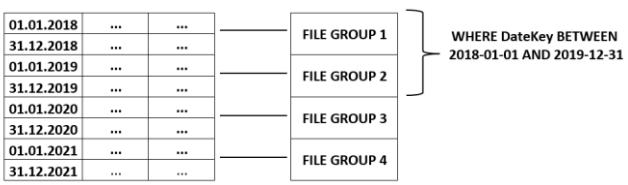

Fig. 1. Visualisation of table partitioning by yearly partitioning function

In this way, regardless of the increase in the number of records in the table, the number of records that the query will be performed on is almost always significantly smaller than the total size of the table. Then you will achieve the best performance and predictability of query execution times because it will usually relate only to a limited number of partitions, e.g. always 2 for data from the last 30 days. This is the main advantage and benefit of data partitioning.

2. Preparing for partitioning

The first step to start the implementation of partitioning in our database, is to first create a partitioning function. For this purpose, it is worth doing a short analysis of use cases to set the optimal period of partitioning. Based on my experience, there are three such most common periods: yearly, quarterly, and monthly, and in many of cases monthly is the best. This is why the monthly partitioning function was selected for the research, as can be seen in listing 1.

Listing 1. A monthly partitioning function

```
CREATE PARTITION FUNCTION PartitionFunctionByMonth (int)
AS RANGE RIGHT FOR VALUES(
            20150101
           ,20150201
           ,20150301
            :
            :
            :
           ,20201201
         );
```

Instead of date type, partitioning function is based on integer type and in this way monthly, quarterly or annual ranges are set. Using integer type can seems to be incorrect. This conscious optimization procedure used in data warehouses [5]. In queries of tables with billions of records, it matters what exactly data type the WHERE clauses will be based on. Queries will run much faster, with the integer type then date type. The next step is to create a partitioning scheme based on the partitioning function. The code responsible for creating the schema is shown in listing 2.

Listing 2. Partitioning scheme based on the monthly partitioning function

```
CREATE PARTITION SCHEME PartitionSchemaByMonth
AS PARTITION PartitionFunctionByMonth all to ([PRIMARY])
```

Having a function and a partitioning scheme the tables can be created where bilions of records will be generate. For this research there is created partitioned table was created FactResellerSalesPartitioned along with an identical table without

partitions FactResellerSales. Is worth to note that the integer type as a key has too small a range for a writing billion records, so the bigint type is selected.

To ensure the same measurement conditions of time executions for NSERT, SELECT, UPDATE, and MERGE queries, exactly the same data will be inserted into both tables. Measurements will be taken after added 100 million records added to both table each time. he structure of the partitioned table is presented in listing 3.

Listing 3. Partitioned table structure; the unpartitioned table will have the same structure

```
CREATE TABLE [dbo].[FactResellerSalesPartitioned](
             [SalesKey] [bigint] IDENTITY(1,1) NOT NULL,
             [DateKey] [int] NOT NULL,
             [EmployeeKey] [int] NOT NULL,
             [CustomerKey] [int] NOT NULL,
             [ProductKey] [int] NOT NULL,
             [SalesValue] dec(5,2) NOT NULL
          )
```

It is not without significance, is to use the partitioning scheme when creating a clustering index on a partitioned table (FactResellerSalesPartitioned).To perform this operation before importing data into the table because it may take a long time, especially on a table with a large amount of data. the code creating the index is presented in the listing 4.

Listing 4. Index using a partitioning scheme

```
CREATE UNIQUE CLUSTERED INDEX [PartitionedIndexReport] on
[dbo].[FactResellerSalesPartitioned]([SalesKey],[DateKey])
on PartitionSchemaByMonth ([DateKey])
```

Listing 5 shows the code responsible for creating an identical clustered index for a table without partitions (FactResellerSales). Except that we do not create this index in the partitioning scheme.

Listing 5. Definition of the Index on the table without partitioning

```
CREATE UNIQUE CLUSTERED INDEX [IndexReport]
on [dbo].[FactResellerSales]( [SalesKey],[DateKey])
```

Now we can consider that partitioning on (FactResellerSalesPartitioned) table has been enabled after created and executed function, schema and clustered index. You do not need to change of SELECT, UPDATE, and MERGE instruction to use partitioning. The only necessity is that the condition in the WHERE section is built on the DateKey column that was added to the partition key. The query optimizer reads data only from those partitions that are within the date range included in the WHERE clause [1, 4]. Listing 6 shows the use of partitioning in a SELECT query.

Listing 6. A SELECT query on a partitioned table is no different from a query on a table with no partitions

```
SELECT EmployeeKey, SUM(SalesValue)
FROM [dbo].[FactResellerSales] --unpartitioned table
WHERE DateKey between 20070925 and 20070927
GROUP BY EmployeeKey

SELECT EmployeeKey, SUM(SalesValue)
FROM [dbo].[FactResellerSalesPartitioned] -- partitioned table
WHERE DateKey between 20070925 and 20070927
GROUP BY EmployeeKey
```

As you can see in the example of SELECT query, it looks almost identical, only the name of the table changes. Therefore, only queries against partitioned tables will be presented for subsequent queries. Listing 7 shows the example use of partitions in the UPDATE query.

Listing 7. A UPDATE query on a partitioned table

```
UPDATE fs
SET SalesValue = t.SalesValue
FROM [dbo]. [FactResellerSalesPartitioned] fs
JOIN [dbo].[TMP] t on [fs].DateKey = [t].DateKey
AND [fs].[SalesKey] = [t].[SalesKey]
WHERE fs.DateKey between 20320421 and 20320520
```

The most complicated is use of partitioning on MERGE query – listing 8.

Listing 8. A MERGE query on a partitioned table

```
MERGE
    dbo.FactResellerSalesPartitioned AS [TargetTable]
             USING (
             SELECT
             [SalesKey]
           , [DateKey]
           , [EmployeeKey]
           , [CustomerKey]
           , [ProductKey]
           , [SalesValue]
             FROM [dbo].[TMP]
            ) [SourceTable]
           on [TargetTable].DateKey = [SourceTable].DateKey
           and [TargetTable].[SalesKey] = [SourceTable].[SalesKey]
           when matched and (
             [TargetTable].[SalesValue]!=[SourceTable].[SalesValue]
             )
           THEN UPDATE
           set [TargetTable].[SalesValue]=[SourceTable]. [SalesValue]
           WHEN NOT MATCHED BY TARGET
           THEN INSERT (
             [DateKey]
           , [EmployeeKey]
           , [CustomerKey]
           , [ProductKey]
           , [SalesValue]
           )
           VALUES (
             [SourceTable].[DateKey]
           , [SourceTable].[EmployeeKey]
           . [SourceTable].[CustomerKey]
           , [SourceTable].[ProductKey]
           , [SourceTable].[SalesValue]
    );
```

In the presented queries, the condition in the WHERE clause had to be based on the DateKey field. Because this is the field that was defined when creating the clustering index as the one after which partitioning will take place. This column must be of the same data type as that defined in the partitioning function. In this case it is an integer so dates are written as numbers, e.g., October 14, 2020 will be 20201014.

3. Method and conditions of research

The AdventureWorksDW 2017 database was used to carry out the measurements. This database is a training database that reflects data warehouses used in real systems. The test consisted in comparing the execution times of operations on a partitioned table and a table without a partition. Since the AdventureWorksDW 2017 database contained only tens of thousands of records, it was necessary to generate more data based on a combination of records from existing dimensions: product (DimProduct), sellers (DimEmploye) and customers (DimCustomer) and dates that already existed in the DimDate table. The generated data was then inserted in parallel into a partitioned (FactResellerSalesPartitioned) and non-partitioned (FactResellerSales) table.

One million records were inserted for each day in a random way that was a combination of data from the various dimensions:

- 1000 clients from DimCustomer with over 18,000 records,
- 10 sellers from DimEmployee dimension with 300 items,
- 100 products from the dimProduct dimension with over 600 items. Then the combinations of these data were inserted into the sales fact tables. This is how the daily data increase of one million records was created ($1000 \times 10 \times 100 = 1{,}000{,}000$).

The measurements were conducted beginning from 1 million records to 10 million and later every 100 million up to 1 billion records and every billion records to reach 10 billion. Like this for each significant number of records: 1, 10, 100, 200 ... 1000, 2000 … 10000 million, measurements were taken of the amount of time the SELECT, UPDATE, MERGE commands took to reading data from the last 30 days, i.e. 30 million records. A monthly partitioning function was used operations were performed on the last two partitions. The exception was when the table contained one million and 10 million records what means that was used only one partition.

4. Measurement of query execution times

The measurements concerned the execution times of the SELECT, UPDATE and MERGE queries from listing 6, 7 and 8 always for the last 30 million records added to the tables. The time was measured in simply way with a precision in milliseconds. The script of execution queries time calculated is shown in listing 9.

Listing 9. A script that measures the execution time of the SELECT, UPDATE and MERGE operation

```
DECLARE @start datetime
DECLARE @stop datetime
SELECT @start = getdate ();

    SELECT, UPDATE OR MERGE

@stop = getdate ()
SELECT DATEDIFF (ms, @start, @stop) /1000.00
```

It is worth noting that in this research, precision time measurement is not so important. It is mainly about checking whether the query execution time on a partitioned table will remain at the same level while the time of performing the same query on a table without a partition will increase. It does not matter if it is three seconds, five or ten seconds. It is only important that the query execution time on a partitioned table is independent of the data increment.

5. Results

The measurements times for the following SQL statements: INSERT, SELECT, UPDATE, MERGE are compare for a non-partitioned and partitioned table for configuration:

- hardware: Samsung 870 QVO drive, Intel Core i5-3210M processor, 2.5GHz, memory 8GB RAM,
- software: Microsoft SQL Server 2018 Standard Edition with recommended by Microsoft training database AdventureWorksDW 2017.

Always, for each SQL statements: SELECT, UPDATE, MERGE the same constant conditions were keeping for the table with and without partitions:

- the same table structures,
- identical structure of the cluster index, which included the fields SalesKey and DateKey,
- always the same number of partitions: 2,
- always the same number of records participating in the each operations – 30 millions – see chapter 3. Method and conditions of research
- exactly the same data in both tables.

The measurement results are presented in table 1.

For better readability, the comparing the execution times of INSERT, SELECT, UPDATE, MERGE queries are presented on separate graphs on a logarithmic scale (figure 2–5).

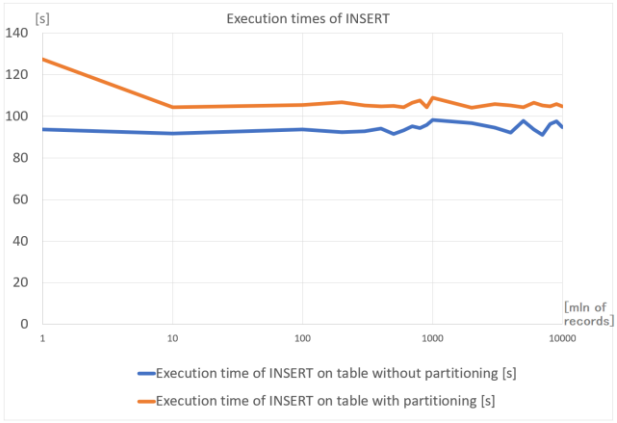

Fig. 2. Execution times of INSERT query on a table with and without partitioning, on a logarithmic scale

The execution time of the INSERT operation of the same number of records into a table with an increasing number of records is constant. For partitioning, it is only important that the INSERT execution time is also constant, and due to the use of the partitioning scheme and the partitioning function it is slightly longer.

Table 1. Execution times of INSERT, SELECT, UPDATE, MERGE query performed on tables with and without partitioning

Number of records	Execution time of							
	INSERT		SELECT		UPDATE		MERGE	
	on table without partitioning	on table with partitioning	on table without partitioning	on table with partitioning	on table without partitioning	on table with partitioning	on table without partitioning	on table with partitioning
[mln]	[s]	[s]	[s]	[s]	[s]	[s]	[s]	[s]
1	93.63	127.4	0.11	0.11	2.08	4.9	6.3	6.34
10	91.74	104.3	0.97	1	16.56	49.27	58.99	65.48
100	93.69	105.4	6.92	4.61	56.34	159.3	212.84	231.6
200	92.32	106.7	15.62	4.7	66.7	162.5	218.59	240.5
300	92.91	105.4	23.17	5.35	74.71	156.3	235.89	252.7
400	94.08	104.7	34.09	5.87	88.98	156.7	258.48	263
500	91.54	104.9	41.2	3.97	91.81	165.3	267.73	256.2
600	93.25	104.3	49.25	4.72	167.8	160.3	289.45	270.2
700	95.33	106.6	54.7	5.64	171.8	155.8	309.27	292.6
800	94.35	107.6	69.67	4.42	180.7	159.4	327.99	291.5
900	95.91	104.5	71.14	3.86	192.2	155.2	352.87	303.3
1000	98.22	108.9	81.57	5.54	197.6	159.9	374.99	337.8
2000	96.78	104.2	208.48	5.72	135.3	160.6	584.78	444.9
3000	94.56	105.8	307.11	5.45	137.3	154.5	776.89	547.8
4000	92.26	105.3	461.23	5.42	138.3	158.8	977.45	212.3
5000	97.88	104.4	513.26	5.73	138.8	156.3	1186.7	224.9
6000	93.78	106.5	644.78	5.12	139.2	156.8	1365.4	218.3
7000	91.11	105.4	724.59	5.33	143.8	158.9	1600.8	227.6
8000	96.27	104.7	852.17	5.53	140.8	163.6	1855	238.4
9000	97.54	105.9	1106.2	5.49	227.9	219.2	2062.7	297.5
10000	94.75	104.9	1160.7	5.88	289.2	348.3	2339.7	349.1

Fig. 3. Execution times of SELECT query on a table with and without partitioning, on a logarithmic scale

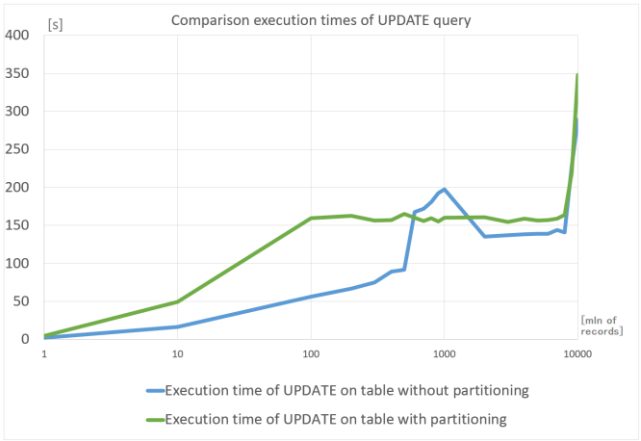

Fig. 4. Execution times of UPDATE query on a table with and without partitioning, on a logarithmic scale

As you can see in the figure 3, SELECT execution times for a partitioned table remain constant with exponentially increasing execution time of the same query on a table without partitioning.

UPDATE query times look similar for both partitioned and non-partitioned tables. Similarly, they also rise at the limit of 10 billion records. There is also a peak around three billions of records for a query on a table without partitioning (figure 4).

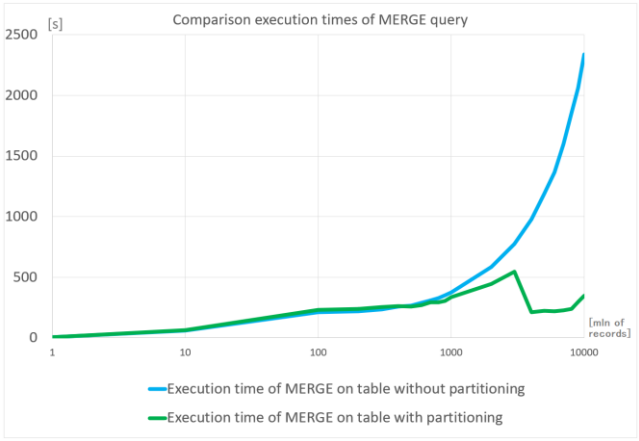

Fig. 5. Execution times of MERGE query on a table with and without partitioning, on a logarithmic scale

The results presented in table 1 and figure 3 clearly indicate that the SELECT query times from the partitioned table are relatively constant and fluctuate around 5-6 s. It is different for the table without partitioning, where this time always increases with the increase of data. The similar results is for the MERGE query where times from the partitioned table grows slightly to 350 s while the execution time on a non-partitioned table grows exponentially to 2340 s. I remind you that the tested SELECT query always operated on the same, invariable number of 30 million records.

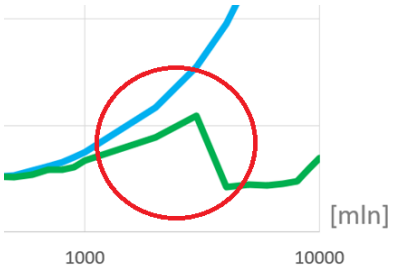

Fig. 6. The strange behavior of the MERGE query around three billions of records

That confirm that we do not lose much when arguing with tables without partitions on inserting and updating records, while we gain a lot from SELECT and MERGE queries on tables with partitions.

Noteworthy is the strange behavior of the MERGE query appearing from one billion of records, where a significant increase in processing time is visible, in the peak to over 500 s for three billions of records (figure 6). This may be due to the native optimization algorithm of the database engine or to hardware characteristic. This is what we will focus on in future research.

6. Conclusions

The research clearly indicate the partitioning table gives effectiveness of data processing in databases with billions of records. This is confirmed by the results of measurements of INSERT, SELECT, UPDATE, MERGE. We do not lose much with inserting and updating records, and we gain a lot from selecting and merging data on tables with partitions even on database with billions of records. The proposed solution solves the problem of "systems aging" with time when more and more records are added to the database. Thanks to partitioning, we can achieve the same system efficiency at the beginning, right after starting and after a few years of its implementation.

Additionally, when processing a large number, billions of records, an anomaly was noticed that to some extent deteriorates the SELECT and MERGE times on partitioned tables, it requires further investigation if the problems occur with a different hardware and software configuration.

References

[1] Bednarczuk P.: Optimization in very large databases by partitioning tables, Informatyka, Automatyka, Pomiary w Gospodarce i Ochronie Środowiska 10(3), 2020, 95–98.
[2] Bandle M., Giceva J., Neumann T.: To Partition, or Not to Partition, That is the Join Question in a Real System. International Conference on Management of Data, 2021.
[3] Kumar A., Jitendra Singh Y.: A Review on Partitioning Techniques in Database. International Journal of Computer Science and Mobile Computing 13(5), 2014, 342–347.
[4] Microsoft documentation, Data partitioning guidance, https://learn.microsoft.com/en-us/azure/architecture/best-practices/data-partitioning
[5] Qi W., Song J., Yu-bin B.: Near-uniform Range Partition Approach for Increased Partitioning in Large Database. 2nd IEEE International Conference on Information Management and Engineering, 2010, 101–106.
[6] Song J., Bao Y.: NPA: Increased Partitioning Approach for Massive Data in Real-time Data Warehouse. 2nd International Conference on Information Technology Convergence and Services, 2010, 1–6.
[7] Tanvi J., Shivani S.: Refreshing Datawarehouse in Near Real-Time. International Journal of Computer Applications 46(18), 2012, 24–29.
[8] Zheng K. et al.: Data storage optimization strategy in distributed column-oriented database by considering spatial adjacency. Cluster Computing 20, 2017.

Ph.D. Eng. Piotr Bednarczuk
e-mail: Piotr.Bednarczuk@wsei.lublin.pl

He is a doctor in the Institute of Computer Science at the University of Economics and Innovation in Lublin. Studied and defended his Ph.D. thesis at Lublin University of Technology. He supports his scientific knowledge with professional practice gained in a leading IT company, where he has been working for over 15 years, currently as the head of the database solutions department in the mobile systems department. His research area focuses on the software engineering web database systems, mobile-device systems and databases and data warehouses.

http://orcid.org/0000-0003-1933-7183

M.Sc. Adam Borsuk
e-mail: adam.max.borsuk@gmail.com

He is a master degree absolvent of the Institute of Computer Science at the University of Economics and Innovation in Lublin. Studied programming and data analysis and defended his master's thesis in 2021. He supports his scientific knowledge with professional practice gained in a leading IT company, where he has been working for over 4 years, currently as the database developer.

http://orcid.org/0000-0003-2316-1694

http://doi.org/10.35784/iapgos.3317 *received: 22.11.2022 | revised: 7.12.2022 | accepted: 15.12.2022 | available online: 30.12.2022*

GENERALIZED MODEL OF INFORMATION PROTECTION PROCESS IN AUDIOVISUAL CONTENT DISTRIBUTION NETWORKS

Heorhii Rozorinov[1], Oleksandr Hres[2], Volodymyr Rusyn[2]
[1]National Technical University of Ukraine "Igor Sikorsky Kyiv Politechnic Institute", Department of Acoustic Multimedia Electronic Systems, Kyiv, Ukraine, [2]Yuriy Fedkovych Chernivtsi National University, Department of Radio Engineering and Information Security, Chernivtsi, Ukraine

Abstract. *The most important indicators of the effectiveness of content protection systems are indicators of the achieved security level, i.e. functional properties of security. These indicators are: confidentiality, integrity, availability. Each of the indicators of the functional properties of content security is distributed according to the methods of ensuring and the degree of its achievement. A significant drawback of such indicators is that they are qualitative. This significantly narrows the scope of their use and makes it impossible to use them in mathematical expressions for optimizing the parameters of protection means, obtaining quantitative estimates of the performance quality of the protection system or its components, etc. The work offers a number of quantitative indicators, which, depending on the purpose, can be probabilistic and temporal. Calculation of such indicators makes it possible to assess the degree of ensuring the functional properties of information security or the possible degree of ensuring the functional properties of protected information.*

Keywords: security, content, communication network, model, indicator

UOGÓLNIONY MODEL PROCESU OCHRONY INFORMACJI W SIECIACH DYSTRYBUCJI TREŚCI AUDIOWIZUALNYCH

Streszczenie*. Najważniejszymi wskaźnikami skuteczności systemów ochrony treści są wskaźniki osiągniętego poziomu bezpieczeństwa – właściwości funkcjonalne zabezpieczeń. Takimi wskaźnikami są: poufność, integralność, dostępność. Każdy ze wskaźników właściwości funkcjonalnych bezpieczeństwa treści jest podzielony ze względu na metody zapewnienia i stopień ich osiągnięcia. Istotną wadą takich wskaźników jest to, że są one jakościowe. Zawęża to znacznie zakres ich stosowania i uniemożliwia wykorzystanie ich w wyrażeniach matematycznych do optymalizacji parametrów środków ochrony, uzyskania ilościowych ocen jakości działania systemu ochrony lub jego elementów itp. W pracy zaproponowano szereg wskaźników ilościowych, które w zależności od celu mogą mieć charakter probabilistyczny i czasowy. Obliczenie takich wskaźników pozwala ocenić stopień zapewnienia właściwości funkcjonalnych bezpieczeństwa informacji lub możliwy stopień zapewnienia właściwości użytkowych chronionych informacji.*

Słowa kluczowe: bezpieczeństwo, treść, sieć komunikacyjna, model, wskaźnik

Introduction

Computer facilities and infocommunication technologies are intensively implemented in all areas of human activity, the protection of information in audiovisual content distribution networks being of particular importance [4].

At the same time, significant contradictions arise: on the one hand, process automation significantly increases the capabilities of controls, and on the other hand, it leads to an increase in the dependence of control stability on the reliability of the operation of automation equipment and information protection from unauthorized access and interference [20].

Therefore, along with the requirements for efficiency, stability, continuity of operation, audiovisual content distribution networks are also subject to the requirements of such basic system security indicators as confidentiality, integrity, availability, and observability of processes related to the use of content.

This raises the classical problem of ensuring the maximum (or maximum possible) level of efficiency of the protection system by optimizing the parameters of its elements [17].

One of the main vectors of cyber threats to multimedia audiovisual content distributed in networks are cyber attacks. Today, these attacks can be seen simply as secondary threats creating "noise" in the network.

IoT are very common for protection of information in modern telecommunication networks [10, 22]. One of the most important functions of effective protection of the organization's information system is threat tracking and analysis and calculation of quantitative indicators of the functional properties of the security of content distributed in networks [1, 3, 5, 8, 9, 12, 19]. In [11] methods for ensuring data security in mobile standards are presented. Some methods can be used in programming level with biometric technical realization [16].

Today, the number of multimedia devices that use audiovisual content in networks continues to grow rapidly, therefore the issue of ensuring confidentiality and data security in networks is urgent, in particular, the development and improvement of information protection methods and data transmission methods (for example, based on pseudo-random sequences, chaos, etc.) [13, 14, 15].

The purpose of the work is to develop an effective system for the protection of audiovisual content with the formalization of the protection process in general, by developing its model.

1. Indicators of protection efficiency

Developing an effective content protection system is impossible without knowing what this efficiency is and how it is evaluated. The efficiency of the system means the degree of achievement of the goal set before it, and its assessment requires quantitative or qualitative characteristics, or a combination of them – the so-called performance indicators [2]. In so doing, the degree of achievement of the goal is determined by comparing the value of the achieved performance indicator with the desired or optimal value.

Quite often, it is difficult or even impossible to evaluate a complex system with a single efficiency indicator. In such cases, a system of indicators is introduced, and these indicators can be contradictory, that is, the improvement of the system according to some indicators leads to its deterioration according to others. In such cases, it is necessary to somehow combine these indicators into one, generalized, or define one of them as the main one, dominant, and the rest should be considered as certain peculiar restrictions. It is clear that such a problem is more or less well solved if these performance indicators have a numerical value and there are mathematical expressions for their calculation.

To build an effective audiovisual content protection system, it is necessary to:

1. formulate the purpose of the system functioning,
2. develop an objective function – an expression (expressions) for calculating an indicator or a set of system indicators,
3. find the optimal or acceptable value of the efficiency indicator and determine the conditions (values of the system parameters) under which this value is achieved,
4. determine the components of the system (subsystems or elements) that provide the necessary parameters.

There are system-wide and partial performance indicators, which can be qualitative or quantitative. Quantitative performance indicators are preferable, as they allow easier obtaining numerical values of the objective function and finding their optimal values.

The task of content protection can be formulated as:

1. achieving the necessary level of protection at the minimum cost of the permissible level of restrictions on types of information activities;
2. achieving the highest possible level of protection at acceptable costs and a given level of restrictions on types of information activities;
3. achieving the maximum level of protection at the necessary costs and the minimum level of restrictions on types of information activities.

Any of these options requires the presence of indicators that would allow evaluating the effectiveness of solving the problem of content protection.

The most important indicators of the effectiveness of content protection systems are indicators of the achieved level of security, which are called functional properties of security. These indicators of functional properties of content security are:

1. confidentiality (a feature of information that information cannot be obtained by an unauthorized user or process),
2. integrity (a feature of information that information cannot be modified by an unauthorized user or process),
3. availability (a property of information that a user (or process) with the appropriate authority can use the content in accordance with the rules established by the security policy without waiting longer than a specified (small) period of time).

Each of these indicators of the functional properties of content security is distributed according to the methods (mechanisms) of ensuring and the degree of its achievement and has certain levels [18].

A significant drawback of such indicators is that they are qualitative. This significantly narrows the scope of their use and makes it impossible to use them in mathematical expressions for optimizing the parameters of protective equipment, obtaining quantitative estimates of the quality of the functioning of the protection system or its components, etc.

Therefore, this work offers a number of quantitative indicators, which, depending on the goal, can be probabilistic and temporal, namely:

1. Quantitative characteristic of violation of the confidentiality of the content – the probability of meaningful (that is, with an understanding of the content) reading of the information, which, depending on the features of the construction of the protection system, is determined by:
   - the probability of unauthorized access when confidentiality is ensured only by means of access restriction, as well as in the absence or when the violator overcomes the means of cryptographic transformation of information,
   - cryptographic stability of the encrypted content (when confidentiality is ensured only by means of cryptographic transformation of information, as well as when the violator overcomes the means of restricting access to information).
2. Quantitative characteristics of violation of the integrity of the content, which, depending on the features of the construction of the protection system is determined by:
   - the probability of unauthorized access (when integrity is ensured only by means of access restriction, deliberate influence of authorized users, and also if the violator does not have or overcome the means of integrity control),
   - the probability of information distortion (during random user impacts, as well as direct impacts of natural factors on information resources).
3. Quantitative characteristics of violation of content availability, which, depending on the features of the construction of the protection system is determined by:
   - the probability of unauthorized access (when integrity is ensured only by means of restricting access and intentional user influences),
   - delay time in content access (or content delivery).

Calculation of the indicated quantitative characteristics of content security by means of technical protection makes it possible to assess the degree of ensuring the functional properties of information security or the possible degree of ensuring the functional properties of protected information with the aid of tools designed for implementation. In both cases, for such a definition, it is necessary to have either the actual structural diagrams of the tools used, or models of the tools being developed for implementation.

An extremely important type of indicators is the economic (cost) indicators of the effectiveness of the content protection system. This follows from the fact that cost indicators, regardless of their origin, can always be reduced to economic costs. In addition, if the task of protection is not fulfilled or appropriate tools of protecting the content are not applied, its owner suffers some damage, which is also often easily reduced to additional costs and, thus, to economic indicators. And, on the contrary, the fulfillment of the protection task with the use of appropriate tools reduces such possible costs and damage, that is, it allows preventing possible costs.

The amount of damage, including the amount of harm that can be prevented or the cost of spending a particular content, can be estimated using:

1. quantitative indicators of security,
2. time indicators of processes related to the organization and implementation of control,
3. the specific cost per time unit of the delay in the provision of relevant services for the use of content and the duration of such a delay,
4. the cost of spending this or that content – also due to the cost of the time unit of its use and the duration of its use,
5. the intensity of content security threat flows.
6. At the same time, the dependence of cost indicators of security on the listed variables can be considered as an objective function, and time and other characteristics can be used as parameters (in some cases, as restrictions) for optimizing economic (cost) performance indicators.

For the technical protection of content, which effectively provides the required level of functional services or functional security properties in the conditions of the influence of threats to these functional security properties, it is advisable to:

1. Formalize the process of technical protection of content in general, by developing its adequate model.
2. Formalize the processes of ensuring the functional properties of content security by developing models of such processes and introduce their quantitative characteristics.
3. Determine the composition and sufficiency (functional completeness) of the tools that should be used for the technical protection of content.

2. Generalized model of technical content protection

The general formulation of the task of formalizing the content protection process is as follows [6].

Let there be a protected audiovisual content distribution network, the information resources of which are the objects of influence of unauthorized users-infringers, who, by their unauthorized actions on the resources of this network, create i (i = 1, 2, 3) types of threats to these resources, namely: threats to privacy, threats to integrity and availability threats (Fig. 1). Let a successful attempt to implement each of these threats cause damage to the system (or its owner) (for example, in the form of monetary damage), the amount of which depends on the type of threat, the duration of its action and is equal to conventional units per unit of time on average. Let also this damage be of an additive nature, that is, it can accumulate depending on the number and duration of threats that have not been countered.

Obviously, the amount, nature and even the time of manifestation of damage depends on the type of the corresponding threat. For example, the implementation

of an availability threat leads to the blocking of the network and the termination of the service provision process. Realized threats to the integrity of part of the basic and application software are equivalent to threats to availability, and as threats to some information resources.

Realized privacy threats most likely will not affect the network performance in any way, but may manifest themselves in the area of damage due to loss of image, trust in the owner of the content (or relevant information), failure of contracts, loss of positions in the service market, etc. Therefore, the mechanisms of calculating or recalculating the possible damage into conventional units F_i per unit of time have different complexity, but these mechanisms are either known or can be developed quite simply.

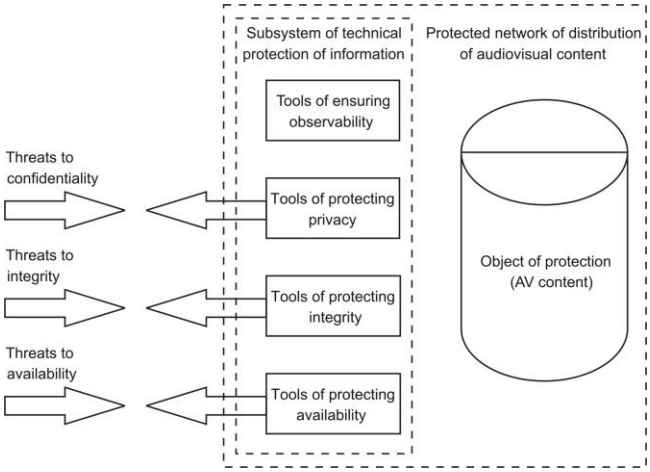

Fig. 1. Abstract model of technical content protection

Thus, there is a subsystem of technical protection of information, which provides protection against each of the types of specified threats with probability p_i, and includes tools of protecting confidentiality, tools of protecting integrity, and tools of protecting availability (Fig. 1) [6]. The subsystem performs its functions by periodically (with a period T_{ki}) monitoring the network's performance, which is formulated as its ability to provide its own functional service – observation, through the use of appropriate monitoring tools. We will assume that such control requires ΔT_{ki} time units. The frequency of control is determined by the owners of the protected resources, by any regulatory documents, or by the security administrator, and this control can be carried out at the start of the protection procedure. During the control, there is a check for violations of the network performance, its update, an audit of events related to information security, necessary reconfiguration of the parameters of the tools of ensuring the corresponding functional properties (for example, changing identifiers, passwords, key sets, with the help of which access control is ensured, necessary crypto- and impersonation resistance, etc.). The duration of control depends on the control methods implemented in the protection subsystem and the methods of their implementation [7, 20, 21]. Violations detected during control are eliminated. For this, it is possible to use various tools – the same backup copies, special fast-acting procedures (algorithms) for restoring integrity, etc. It is clear that the duration of the relevant procedures and the probability of correctly solving these problems depend on the quality of the applied methods and means of control and elimination of violations (resumption of working capacity).

In so doing, the overall goal of the functioning of the protection system is to minimize possible harm to the system or its owner by counteracting a variety of possible threats to the integrity, confidentiality and availability of network information resources.

In the mathematical formulation, this problem is reduced to the definition and optimization of the objective function, which describes the dependence of certain harm on the parameters of the protection system, the conditions for its application, and the characteristics of threats.

When determining the objective function, it should be assumed that the effects of these threats have certain frequency-time characteristics (for example, in the form of the probability of the occurrence of a threat during some average time interval). But for protection with information resources that are tempting for violators, it is appropriate to assume that such a probability is close to unity throughout the entire time of protection.

Each of the mentioned threats has as a consequence some damage to the content owner, if the corresponding protection system did not detect and counteract this damage. Let the probability of such an event be equal to $q_i = 1 - p_{di}$, where p_{di} is the probability of detection and subsequent countermeasures against the *i*-th type threat. It is clear that $p_{di} = p_{i1} p_{i2}$ is the probability for a threat of the *i*-th type, where p_{i2} is the probability of countering the same threat.

In this case, an undetected threat causes damage to the content $Q_i = F_i(1 - p_{di})$ owner per unit of time.

If we assume that the duration of the impact of the *i*-th threat is equal to T_{Di}, then the amount of damage can be determined as

$$Q_i = T_{Di} F_i (1 - p_{di}). \tag{1}$$

The duration of the impact of the threat T_{Di}, hence the duration of damage accumulation, is a random value in the time interval (0, $T_{ki} - \Delta T_{ki}$), where T_{ki} is the duration of time between two adjacent checks of the performance of the protection system against threats of the *i*-th type, and ΔT_{ki} is the duration of the *i*-th type of control and update of the functional properties of information security, for example, integrity (we believe that during control the system is inoperable and it is impossible to harm it by implementing any threats). It can be assumed that $T_{Di} = T_{ki} - \Delta T_{ki}$, if the violator managed to implement the threat immediately after the end of the corresponding control procedure, and $T_{Di} = 0$ in the case of an attempt to implement the threat immediately before its start. The worst conditions, in terms of the amount of possible damage, are created at $T_{Di} = T_{ki} - \Delta T_{ki}$, therefore, when developing a protection system, it is advisable to focus on this duration of the threat. At the same time, the maximum possible value of damage of the *i*-th type

$$Q_{i\max} = T_{Di}(T_{ki} - \Delta T_{ki}) F_i (1 - p_{di}) \tag{2}$$

Since the damage is additive in nature, the maximum amount of possible total damage (PTD) can be defined as

$$Q_{PTD1} = \sum_{i=1}^{i=n} Q_{i\max} = \sum_{i=1}^{i=n} (T_{ki} - \Delta T_{ki}) F_i (1 - p_{di}) \tag{3}$$

But (3) does not take into account the fact that during the performance control of the protection system for the duration ΔT_{ki} of time units, it is unable (especially in the case of detection of an attempt to influence with the probability of this event p_i) to perform its functions (at least in full), which is equivalent to damage, which occurs when the system is idle, since the implementation of the functional service "observability" and "maintenance" of attempts at such influence also requires spending a protection resource.

The amount of this damage can be defined as

$$Q_{PTD2} = \sum_{i=1}^{i=n} p_{di} \Delta T_{ki} C_i \tag{4}$$

where C_i is the damage due to downtime of the corresponding network resources during control, in conventional units per unit of time. Then

$$Q_{PTD} = Q_{PTD1} + Q_{PTD2} = \sum_{i=1}^{i=n} F_i (T_{ki} - \Delta T_{ki})(1 - p_{di}) + p_{di} C_i \Delta T_{ki} \tag{5}$$

It can be seen from expression (5) that it can be accepted as the target function of the protection system, since it reflects the dependence on the process and conditions of system operation. Indeed, the value of possible total damage (PTD) is the smaller, the smaller the number of threats *n*; the amount of damage C_i that can be caused by the successful implementation of each type of threat; control period T_{ki}; duration of the *i*-th type of control ΔT_{ki}; and the more is the probability of detecting and counteracting the threat of the *i*-th type p_{di}; size difference $T_{ki} - \Delta T_{ki}$.

Expression (5) is easily reduced to the form

$$Q_{PTD} = \sum_{i=1}^{i=n} F_i T_{ki} - \left\{ \sum_{i=1}^{i=n} F_i T_{ki} p_{di} - \sum_{i=1}^{i=n} \left[p_{di} C_i - F_i (1 - p_{di}) \right] \Delta T_{ki} \right\} \quad (6)$$

It is easy to make sure that the minuend, provided that the value of the frequency of control T_{ki} is not a control parameter, is equal to the maximum possible damage that can be caused to the network in the absence of counteraction to the impact of threats from the information security system.

Then it is clear that the value

$$Q_{PTDP} = \sum_{i=1}^{i=n} F_i T_{ki} p_{di} - \sum_{i=1}^{i=n} \left[p_{di} C_i - F_i (1 - p_{di}) \right] \Delta T_{ki} \quad (7)$$

is equal to the amount of damage that is eliminated (prevented) due to the protection of resources by the system. Therefore, this value can be applied as a separate objective function.

In expression (7), the value ΔT_{ki} consists of the duration of the control process (search for the fact of violation or non-violation of the corresponding functional property of information security) Δt_{ki} and the duration of the process of resuming the possibility of its provision.

For the sake of certainty, we will assume that now we are talking about ensuring the integrity of information. As already mentioned, control of the network's ability to provide the appropriate functional service, in this case – the integrity of information, can be carried out by applying some standard procedures (checking by tests, etc.). Let the characteristic of the control process be its duration Δt_{ki}. If a violation of integrity is detected during the control process, it is updated using, for example, backup copies of the relevant information. That is, the duration of the update is equal to zero, if a violation of the network's ability to provide one or the other of its functional properties, for example, integrity, is not detected during monitoring, or, if such a violation is detected, it is equal to the duration of the update process of the same functional property – Δt_{ni}. Characteristics of the update process – the duration of the update itself Δt_{ni} and the likelihood of its need p_{di} – the probability of detecting integrity violations. Then the expectation of the update duration is

$$\Delta t_{ni} p_{di} + 0 \cdot (1 - p_{di}) = \Delta t_{ni} p_{di} \quad (8)$$

That is, the duration of the entire control and update process is a random variable and is determined by the duration of the control process itself Δt_{ki} and the duration of the update Δt_{ni} with probability p_{di}. The average value of a quantity ΔT_{ki}, its mathematical expectation can be defined as

$$\Delta T_{ki} = \Delta t_{ki} + \Delta t_{ni} p_{di}. \quad (9)$$

Extending this to processes associated with threats of any type, the expression for calculating the value of harm to be prevented can be written as:

$$Q_{PTDPi} = F_i T_{ki} p_i - \left[p_i C_i - F_i (1 - p_i) \right] \left[\Delta t_{ki} + \Delta t_{ni} p_{ni} \right] \quad (10)$$

It is clear that the protection system is more effective the smaller the amount of damage (5) and the larger the amount of damage prevented (10). To do this, you should increase the value of the probability p_i and reduce the duration of the control procedure ΔT_{ki}. By the way, at $p_i = 1$ i.e. with a protection system that is absolutely reliable in terms of detecting and eliminating threats, the amount of damage that is prevented acquires a maximum value, which is equal to:

$$\max Q_{PTDP} = \sum_{i=1}^{i=n} F_i T_{ki} - \sum_{i=1}^{i=n} C_i \Delta T_{ki} \quad (11)$$

or

$$\max Q_{PTDP} = \sum_{i=1}^{i=n} F_i T_{ki} - \sum_{i=1}^{i=n} C_i \left[\Delta t_{ki} + \Delta t_{ni} p_{di} \right] \quad (12)$$

that is, it is equal to the maximum possible damage due to the successful implementation of threats, which is reduced by the amount of the maximum possible damage due to an idle network during control. It also follows from expressions (7), (10) that it is advisable to apply network protection against threats of any type only when the value of the damage to be prevented is not negative (is greater than zero). For threats of the *i*-th type, this means that

$$F_i T_{ki} p_i - \left[p_i C_i - F_i (1 - p_i) \right] \Delta T_{ki} > 0. \quad (13)$$

whence one can find the limit on the duration of control ΔT_{ki} (at a certain value p_i)

$$\Delta T_{ki} = \Delta t_{ki} + \Delta t_{ni} p_{di} < F_i T_{ki} p_{di} / \left[p_i C_i - F_i (1 - p_i) \right] \quad (14)$$

or on the probability p_{di} (taking into account that $\Delta T_{ki} < T_{ki}$)

$$p_{di} > \Delta T_{ki} / (T_{ki} - \Delta T_{ki}) - \Delta T_{ki} (C_i / F_i) \quad (15)$$

Since protection systems are used in practice, in which the value of the probability of detecting and further countering a threat of the *i*-th type approaches unity, expression (14) can be simplified.

$$\Delta T_{ki} = \Delta t_{ki} + \Delta t_{ni} p_{di} < T_{ki} (F_i / C_i) \quad (16)$$

It should be noted that the values ΔT_{ki} and p_{di} obtained from inequalities (10) – (16) are limited to those values when the application of control gives a gain that exceeds the losses of the network due to its downtime during control, that is, the system becomes efficient and its application is cost effective.

In other words, expressions (15), (16) are conditions for the expediency of using a system of protection against threats of this type.

3. Conclusions

1. The values of the probabilities should be chosen the greater, the more significant the losses in case of failure to detect the fact of a successful implementation of the threat compared to the losses due to network downtime during the control (the greater the value of the ratio F_i / C_i).

On the contrary, the more operative the control is (with a shorter duration of the control procedure Δt_{ki}, for example, integrity and a shorter duration of the further update procedure Δt_{ni}) the smaller this probability may be. Moreover, the more significant the losses due to failure to detect the fact of a successful implementation of the threat compared to the losses due to network downtime during monitoring (the greater the value of the ratio F_i / C_i) and the greater the values of the required or acceptable monitoring durations ΔT_{ki} and the probabilities of detecting and countering the threat of the *i*-th type p_{di}, the more perfect, and therefore, longer should be the control.

2. The considered generalized model makes it possible to obtain a number of conditions, restrictions and optimal values of the most general parameters of the protection system, which are most important for solving the problem of protecting audiovisual content, but do not allow formulating more specific requirements for the composition and parameters of the protection system or its components.

References

[1] Al-Mukaddim K. P., Rajkumar B.: A Taxonomy and Survey of Content Delivery Networks. Australia, 2007.
[2] Andreev V. I., Kozlov V. S., Horoshko V. A.: Kolychestvennaya otsenka zashishennosti tekhnicheskikh obektov s uchetom ikh funktsionirovaniya. Zakhyst informatsiyi 2, 2004, 47–51.
[3] Ayankoya F., Otushile O., Ohwo B.: A Review on Content Delivery Networks and Emerging Paradigms. International Journal of Scientific & Engineering Research 9, 2018, 211–217.
[4] Bohush V. M., Kudin A. M.: Monitorynh system informatsiinoi bezpeky. DUIKT, Kyiv 2006.
[5] Charles D. C. et al.: Enhanced Streaming Services in a Content Distribution Network. IEEE Computing Society, 2001, 66–75.
[6] Dmitrenko A. P., Sirchenko G. A., Horoshko V. A.: Modeli bezopasnogo soedineniya s udalennymi obektami. Zakhyst informatsiyi 1, 2010, 53–57.
[7] Dmitrenko A.P., Sirchenko G.A., Horoshko V.A.: Statisticheskoe modelirovanie dlya ocenki zashhishhennosti lokalnoj seti. Visnyk DUIKT 1, 2010, 62–67.
[8] Ingmar P. et al.: Improving Content Delivery with Provider-aided Distance Information System (PaDIS). IEEE Computer Society, 2012, 44–52.
[9] Jaeyeon J., Balachander K., Rabinovich M.: Flash crowds and denial of service attacks: Characterization and implications for CDNs and Web sites. 11th International World Wide Web Conference Hawaii: ACM, 2002, 293–304.
[10] Kirichek R., Kulik V., Koucheryavy A.: False clouds for Internet of Things and methods of protection. 18th International Conference on Advanced Communication Technology, Pyeongchang, South Korea 2016, 201–205.
[11] Moroz S. et al.: Methods for ensuring data security in mobile standards. Informatyka, Automatyka, Pomiary w Gospodarce i Ochronie Środowiska – IAPGOS, 1, 2022, 4–9 [http://doi.org/10.35784/iapgos.2877].
[12] Nikolaienko B., Vasylenko S.: Application of the threat intelligence platform to increase the security of government information resources. Informatyka, Automatyka, Pomiary w Gospodarce i Ochronie Środowiska – IAPGOS 4, 2021, 9–13 [http://doi.org/10.35784/iapgos.2822].
[13] Politanskyi R., Politanskyi L., Hres O., Lesinskyi V. Statistical estimation of pseudorandom number sequences. 14th International Conference on Advanced Trends in Radioelectronics, Telecommunications and Computer Engineering, TCSET 2018, 873–876.
[14] Rusyn V. et al.: Computer Modelling of the Information Properties of Hyper Chaotic Lorenz System and Its Application in Secure Communication System. Journal of Physics: Conference Series 1764, 2021, 012205 [http://doi.org/10.1088/1742-6596/1764/1/012205].
[15] Rusyn V., Sambas A., Mujiarto: Information security system based on chaotic signals. CEUR Workshop Proceedings 3039, 2021, 294–299.
[16] Rusyn V., Subbotin S., Sambas A.: Simple autonomous security system based on Arduino UNO platform and fingerprint scanner module: A study case. CEUR Workshop Proceedings 2864, 2021, 262–271.
[17] Shirochin V. P., Muhin V. E., Kramar D. I.: Analiz riskov v zadachah monitoringa bezopasnosti kompyuternyh sistem i setej. Zakhyst informatsii 1, 2003, 28–34.
[18] Shoroshev V. V., Ilnytskyi A. Yu.: Informatsiino-analitychna model bazovoho pervynnoho zakhystu PEOM vid zahroz NSD. Byznes y bezopasnost 3–5, 1999, 32–39.
[19] Shushura O. M. et al.: Simulation of information security risks of availability of project documents based on fuzzy logic. Informatyka, Automatyka, Pomiary w Gospodarce i Ochronie Środowiska – IAPGOS 3, 2022, 64–68 [http://doi.org/10.35784/iapgos.3033].
[20] Sirchenko H. A.: Zadachi zabezpechennia tsilisnosti ta dostupnosti informatsiinykh obiektiv v komunikatsiinykh merezhakh. Zakhyst informatsii 2, 2010, 49–54.
[21] Vasilenko V. S., Korolenko M. P.: Celostnost informacii v avtomatizirovannyh sistemah. Korporativnye sistemy 3, 1999, 52–58.
[22] Vyshnivskyi V. V., Sribna I. M., Zinchenko O. V.: Analysis of technical solutions for identification of internet things in modern communication networks. Electronics and Control Systems 1, 2021, 33–39 [http://doi.org/10.18372/1990-5548.67.15583].

D.Sc. Heorhii Rozorinov
e-mail: grozoryn@gmail.com

National Technical University of Ukraine "Igor Sikorsky Kyiv Politechnic Institute" Department of Acoustic Multimedia Electronic Systems. D.Sc. (Engineering Sciences) Professor of Department of Audiotechnic and Information Registration.
Research interests: pseudorandom sequence generators; encryption information, acoustics.
Author of nearly 135 publications.

http://orcid.org/0000-0002-6095-7539

Ph.D. Oleksandr Hres
e-mail: o.hres@chnu.edu.ua

Yuriy Fedkovych Chernivtsi National University Department of Radio Engineering and Information Security. Ph.D. (Engineering Sciences) Assistant Professor of Department of Radio Engineering and Information Security.
Research interests: pseudorandom sequence generators; encryption information. Author of nearly 42 publications.

http://orcid.org/0000-0002-8465-193X

Ph.D. Volodymyr Rusyn
e-mail: rusyn_v@ukr.net

Yuriy Fedkovych Chernivtsi National University Department of Radio Engineering and Information Security. Ph.D. (Engineering Sciences) Assistant Professor of Department of Radio Engineering and Information Security.
Research interests: modeling of nonlinear equations and chaotic generators; control of chaotic oscillations. Author of nearly 85 publications.

http://orcid.org/0000-0001-6219-1031

http://doi.org/10.35784/iapgos.3076 *received: 20.09.2022 | revised: 10.12.2022 | accepted: 15.12.2022 | available online: 30.12.2022*

MONITORING OF LINK-LEVEL CONGESTION IN TELECOMMUNICATION SYSTEMS USING INFORMATION CRITERIA

Natalia Yakymchuk, Yosyp Selepyna, Mykola Yevsiuk, Stanislav Prystupa, Serhii Moroz
Lutsk National Technical University, Faculty of Computer and Information Technologies/ Department of Electronics and Telecommunications, Lutsk, Ukraine

Abstract. *The successful functioning of telecommunication networks largely depends on the effectiveness of algorithms for detection and protection against overloads. The article describes the main differences that arise when forecasting, monitoring and managing congestion at the node level and at the channel level. An algorithm for detecting congestion by estimating the entropy of time distributions of traffic parameters is proposed. The entropy measures of data sets for various types of model distribution, in particular for the Pareto distribution, which optimally describes the behavior of self-similar random processes, were calculated and analyzed. The advantages of this approach include scalability, sensitivity to changes in distributions of traffic characteristics and ease of implementation and accessible interpretation*.

Keywords: telecommunication systems, self-similarity factor of network traffic, congestion detection

MONITOROWANIE PRZECIĄŻEŃ NA POZIOMIE ŁĄCZA W SYSTEMACH TELEKOMUNIKACYJNYCH Z WYKORZYSTANIEM KRYTERIÓW INFORMACYJNYCH

Streszczenie. *Pomyślne funkcjonowanie sieci telekomunikacyjnych w dużej mierze zależy od skuteczności algorytmów wykrywania i ochrony przed przeciążeniami. W artykule opisano główne różnice, jakie pojawiają się przy prognozowaniu, monitorowaniu i zarządzaniu przeciążeniami na poziomie węzła i na poziomie kanału. Zaproponowano algorytm wykrywania przeciążeń poprzez estymację entropii rozkładów czasowych parametrów ruchu. Obliczono i przeanalizowano miary entropii zbiorów danych dla różnych typów rozkładów modelowych, w szczególności dla rozkładu Pareto, który optymalnie opisuje zachowanie samopodobnych procesów losowych. Do zalet tego podejścia należy skalowalność, wrażliwość na zmiany rozkładów parametrów ruchu oraz łatwość implementacji i przystępnej interpretacji.*

Słowa kluczowe: systemy telekomunikacyjne, współczynnik samopodobieństwa ruchu sieciowego, wykrywanie przeciążeń

Introduction

In accordance with modern standards of network management systems and concepts of the development of the networks themselves, there is a need to determine the state of the system in its mode of operation. The most popular model provides that network components can accept only two states: „serviceable" (able to work) and „refuse" („disrepair"). The state of a network component is a random value that does not depend on the state of other components [20].

A crucial state of a network (computer, telecommunication, etc.) is the state of overloading of individual network nodes, data transmission routes, and autonomous network segments. Typical symptoms of congestion are packet loss, excessive packet delay, and reduced quality of service (QoS) in the network. This state can be taken by mistake for equipment refusal (and vice versa). Therefore, control and removal of overloads are important tasks of a statistical character [14].

Node-level congestion is detected by examining the buffer utilization and the interval between the consecutive data packets. Because a congestion condition usually occurs when the traffic load on a particular node exceeds the available buffer capacity of that node. If, when monitoring buffer occupancy, a load of 70% or higher was obtained, the interval between two consecutive packets is checked. Obviously, if the interval is small, the chances of buffer overflow will be high, which will increase the probability of packet loss. A large interval indicates that the node's bandwidth will be sufficient for the given traffic flow [10, 11].

Link-level congestion happens because of the unfair utilization of network resources. Link-level congestion is monitored through channel utilization. In this case, network flows are analyzed and not individual network packets (network flows are one-way meta-information about network packets that have the same source and destination IP address and ports, as well as the IP protocol type) [3, 4].

1. Literature review

The hidden disadvantage of overloads is that they reinforce themselves according to the principle of feedback [6]. If a collision occurs at a particular location on the network, if the client times out, the client will often resend requests. This increases the load on the system [22, 24]. If the call graph in a service-oriented architecture is deep enough (that is, a client calls a service that calls other services, and those call other services), and each level has several retries, then the load at the lower level will cause a cascading increase their number and the exponential increase in load [19].

Then, all the work already done by the server on this request will be wasted. And in the case of system overload, when resources are limited, it cannot afford to lose resources [8].

In order to monitor the risks of the occurrence of such situations, it is necessary to monitor the time parameters of the traffic flow constantly. However, the analysis of the averaged values of the traffic characteristics gives us a smoothed view of the process, in which it is not possible to track the appearance of load fluctuations, which are characteristic of heterogeneous traffic „Triple Play" (voice + video + data) or „Quadruple Play" (voice + video + data + mobile subscribers) [23].

The specific characteristics of such traffic are explained by the high degree of the grouping of packets at client sites, in routers, and in switching nodes of information communication networks. Even if the source generates a regular stream of packets, the data is delivered to the consumer in bursts interspersed with idle intervals. The reasons for this are the limited speed of network devices, insufficient volume of buffers, etc. To detect this kind of anomaly, an analysis at the level of total traffic is required, based on the use of statistical methods and information theory [21].

Entropy analysis is one of the types of behavioral methods for detecting anomalies, unlike wavelet analysis and spectral analysis; it is not characterized by the complexity of implementation and the requirements for big-time expenditures. Information analysis gives us a statistical criterion for determining anomalous traffic behavior. Today, methods for detecting DOS/DDoS attacks and some types of virus programs have been developed. The method of dividing traffic into unique network flows and calculating the entropy of a set of these flows by the IP address of the source has shown its effectiveness [2, 9].

By comparing the predicted entropy values with the real ones, a decision is made about whether the traffic belongs to a standard type, a DOS attack of a certain intensity, or peak values of legitimate traffic [1]. Estimating the entropy of the number of packets within a time window for network flows can be a tool for detecting „scanning" attacks [15].

2. Researches methodology

The main statistical characteristics of the random process of traffic transmission lead to gross errors in the assessment and prediction of system behavior. Options are possible when the average load values of network nodes over a long period are approximately the same, but the internal structure of the processes that take place is different [16, 17].

One type of traffic can change smoothly over time; the other can be characterized by significant bursts of activity, while the dependence on probabilities will be low. The choice of the distribution law for the characterization of random processes of information transmission is of great importance.

The numerical characteristic of the distribution, which can be a measure of its uncertainty, is the entropy of the distribution law. For the discrete distribution of the increase

$$H(m) = -\sum_{i=1}^{m} p_i \, log p_i \quad (1)$$

where p_i is the probability of the i state of the system, m is the number of all possible states of the system.

From the entropy properties, it can be seen that the entropy of the experiment with maximum uncertainty is maximum and minimum in the fully „determined" experiment. Entropy is in a certain sense additive: when uncertainty increases due to an increase in the number of outcomes, entropy increases, and the increase in entropy is proportional to the probability of additional outcomes. These properties show that the entropy defined by relation (1) is a reasonable measure of the uncertainty of a stochastic experiment with a finite number of outcomes.

Entropy does not depend on significance, which is a random value, but only on their probabilities, in fact, one is interested not in the absolute value of entropy, but in comparing the entropies of different laws. We will form a strategy for finding overloads based on the information criterion [5, 7].

To carry out the analysis procedure of congestion detection by estimating the entropy of time series, it is necessary to select the parameters of the assessment. To do this, consider the following criteria:

1) The length of the sliding window. This is the size of the interval in which point values of entropy time series are calculated. Small windows are very sensitive, and on the one hand, this will increase the detection rate, on the other hand, the frequency of false alarms will also increase. This will lead to the implementation of a traffic restriction policy, which will negatively affect the quality of the service. Large windows are relatively insensitive, which leads to the opposite effect. Windows of 5 to 10 minutes are used as a compromise.

2) The overlap size of sliding windows. Overlapping sliding windows results in a more detailed time series. We want to make our system respond as quickly as possible to sudden changes, so we chose a relative overlap of 80%.

3) The size of the sliding window for calculating variances. We decided to set the size of the sliding window to calculate the standard deviation up to 24 hours. Most often, such a sliding window covers the entire seasonal cycle. In other cases, we recommend choosing windows that are multiple 24 hours.

Each combination of parameters involves a trade-off: high detection rate at the expense of many false positives or vice versa.

To simulate traffic, we will use the distribution of traffic falling into a time window of fixed duration, using the ratio of transmission delay to the maximum permissible transmission interval or successful data transmission of one of the network nodes as a probability [18].

The main idea of the algorithm is to constantly make short-term predictions and determine the difference between the predictions and the actually observed entropy value. Entropy serves as an indicator of the equilibrium of the process. Thus, sharp changes in entropy indicate a qualitative change in the structure (through changes in the distributions of characteristics) of the system [12, 13].

The analysis of the time characteristics of the network is based on the model or geometric distribution of the probability of sending a packet by each terminal node of an autonomous network segment. In the case of a mixed (heterogeneous) network, each device is allocated an approximately equal time interval in traffic.

As emphasized above, entropy is the most general measure of evaluating the efficiency of information transmission for probability distributions belonging to at least one type (in this case – to the discrete type). Let us present the comparative entropy characteristics of model distributions.

1. The geometric distribution is inextricably linked with the binomial distribution. The difference is that the binomial random variable determines the probability m of success in trials n, while the geometric random variable determines the probability n of trials up to the first success (including the first success).

2. A random variable uniformly distributed on [$-a; a$] has the highest entropy among all random variables distributed on [$-a; a$].

3. The exponential distribution with the parameter λ has the largest entropy among all distributions defined on the semi-axis $[0; \infty]$ with mathematical expectation λ.

4. On the entire straight line, among all distributions with fixed mathematical expectation and variance, the normal distribution has the greatest entropy.

The entropy of a discrete source is always positive. Differential entropy $H(x)$, unlike the entropy of sources of discrete messages, can take positive, negative, and zero values. Differential entropy, in contrast to the usual entropy of a discrete source, is not a measure of its own information contained in an ensemble of values of a random variable. It depends on the scale X and can take negative values because the information meaning has not the absolute value of the differential entropy, but the difference between two differential entropies, which explains its name.

Differential entropy does not change when all possible values of a random variable are changed to a constant value. Indeed, the scale X does not change, and equality is fair:

$$h(x + C) = -\int_{-\infty}^{\infty} w(x + C) log_2 w(x + C) d(x + C) = \\ = -\int_{-\infty}^{\infty} w(x) log_2 w(x) d(x) \quad (2)$$

From this it follows that it does not depend on the mathematical expectation of a random variable, since changing all values $x+C$ to x, we thereby change its average to C, that is, the mathematical expectation.

Differential entropy is additive, i.e. for the union $x \cup y$ of independent random variables and the equality holds:

$$H(x \cup y) = H(x) + H(y) \quad (3)$$

For example, consider the subnet shown in Fig. 1. As a result of overlapping traffic flows, the bandwidth of the channel is not sufficient to ensure the required quality of service. Routers L, G, B, C, J are overloaded. Identifying these channels and removing them from the network will avoid information loss. For this purpose, a possible route of the virtual channel bypassing congested lines is established (shown by a dashed line).

At the same time, a compromise is reached between the host and the subnet during the establishment of a virtual channel, which determines the volume and form of traffic, the required quality of service and other parameters. As fulfillment of its part of the agreement, the subnet usually reserves resources in the path of the channel being created. These resources include memory for buffers and router tables and line bandwidth. With this approach, the occurrence of congestion in the new virtual channel is unlikely, since all the necessary resources have been reserved and their availability is guaranteed.

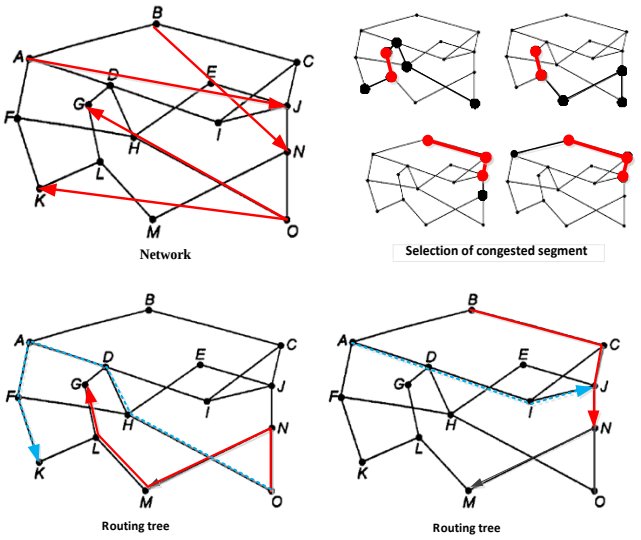

Fig. 1. Link-level congestion

In the case of the geometric distribution, we carry out independent transmissions of the test packet until „success" appears. To calculate entropy $H_G(x)$ let's make a state diagram with the probability of „success" $p < 1$ and „failure" $q < 1$. Obviously $p + q = 1$.

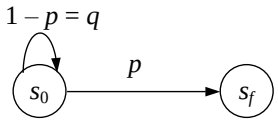

Fig. 2. System states

The system is in the initial state S_0. Having achieved success, it passes into an irreversible (absorbing) state S_f (Fig. 2). Thus, the random process is not transitive (not transitional to the previous state). The graph of transitions has the following form (Fig. 3). S_+ – transition state upon the success of the test; S_- – transition state in case of test failure; $H_{Gi}(x)$, $i = 1, 2, \ldots, n, \ldots$ is the entropy of the distribution upon success at the i step.

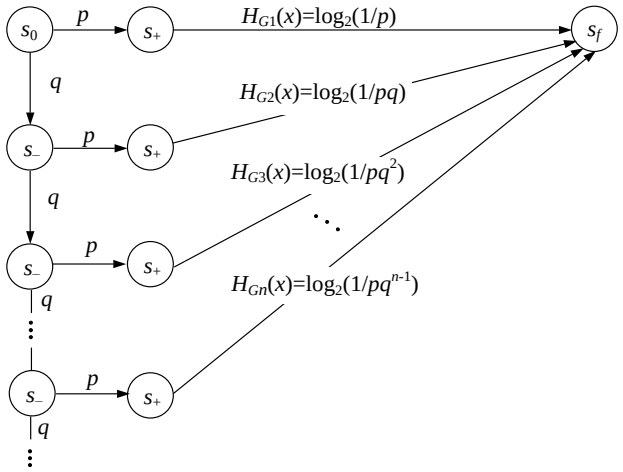

Fig. 3. The graph of transitions

Then the current entropy of the geometric distribution would be calculated using the following formulas:

$$\begin{gathered} H_G(x) = -plog_2p - pqlog_2(pq) - \cdots - pq^{n-1}log_2(pq^{n-1}) = \\ = -(1 + q + \cdots + q^{n-1} + \cdots)plog_2p - \\ -pq(1 + 2q + \cdots + +nq^{n-1})log_2q; \\ 1 + q + \cdots + q^{n-1} + \cdots = \frac{1}{1-q} \\ 1 + 2q + \cdots + nq^{n-1} + (n+1)q^n = \frac{1}{(1-q)^2} \\ H_G(x) = -log_2p - pq\frac{1}{(1-q)^2}log_2q = -log_2p - \frac{q}{p}log_2q \end{gathered} \tag{4}$$

In specialized networks, these assumptions are not fully fulfilled. As noted above, network traffic is usually heterogeneous (voice, video, data) and self-similar in nature. Its statistical characteristics can no longer be described by traditional. In this case, distributions with so-called „heavy tails" (Pareto, Weibull, gamma, and beta distributions) are used.

3. Results

Distributions with heavy tails are distributions in which large but rare events (outliers) cannot be neglected. All commonly used heavy-tailed distributions are subexponential.

Let us define the differential entropy for the exponential distribution. This distribution is widely used to determine the failure rate in electronic equipment.

$$\begin{gathered} f(x) = k \cdot e^{-kx}, x > 0 \\ h(x) = -\int_0^\infty k \cdot e^{-kx}(log_2k - k \cdot x \cdot log_2e)dx = \\ = -log_2k\int_0^\infty k \cdot e^{-kx}dx + log_2e\int_0^\infty x \cdot k \cdot e^{-kx}dx = \\ = -log_2k + log_2e = log_2\frac{e}{k} \end{gathered} \tag{5}$$

The total entropy for the exponential distribution is:

$$H(x) = h(x) - log_2\Delta x = log_2\frac{e}{k\Delta x} \tag{6}$$

The dependence of the entropy of the exponential distribution on the probability p of successful data transmission of one of the network nodes was calculated (Fig. 4). It can be seen that when the probability of success is set higher, the entropy of the distribution decreases, therefore, the required resource for data exchange decreases.

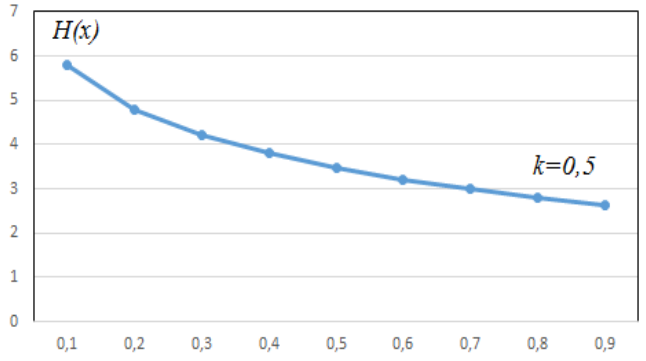

Fig. 4. Dependence of the entropy of the exponential distribution on the probability p of successful data transmission

To analyze the influence of the self-similarity factor of network traffic, an expression for the current entropy of the Pareto distribution as a typical distribution with „heavy tails" characteristic of self-similar traffic is derived:

$$H_p(x) = c\frac{log_2c}{ln2} \times \frac{x^{-c}}{-c-1} + (c-1)\left[x^{-c}log_2x - \frac{x^{-c}}{cln2}\right] \tag{7}$$

where c is a shape parameter.

At Fig. 5 shows graphs of the differential entropy of the Pareto distribution for the shape parameters 0.5 and 1. It can be seen that when the values x change, the entropy first decreases and then increases, which is explained by the influence of the „heavy tail" of the distribution. From the graphs presented in Fig. 5, it is seen that the total cost of Internet traffic increases when using the standard method, and when using the proposed method remains constant. This is due to the fact that when using the method described above, the flow of traffic occurs only when determining the correction factor on the first day of measurements. Further measurement of the bit rate of the Internet connection takes place without active data exchange, so traffic costs do not increase.

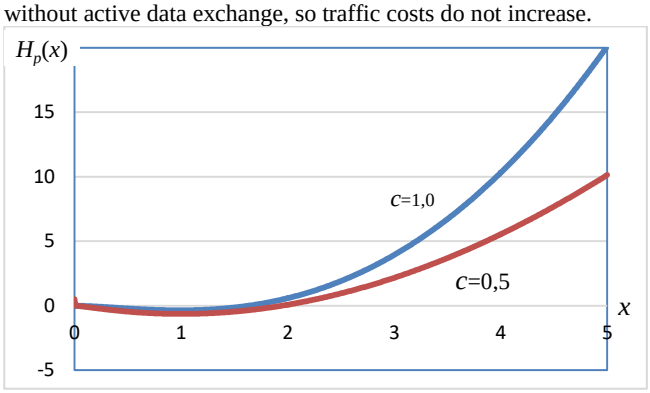

Fig. 5. Dependence of the entropy of the Pareto distribution for various parameters of the form

Note that when calculating entropy measures, you can use different parameters of model distributions. At the same time, comparative estimates based on entropy will be universal and clear.

The advantages of this approach include scalability (the proposed methods are able to use aggregated data, which makes it possible to use it in arbitrarily complex and highly loaded networks), sensitivity to changes in distributions of traffic characteristics and ease of implementation, and accessible interpretation (quickly ready to go, no need for training data).

In conclusion, it is necessary to note the main advantage of the described method: it allows you to effectively use the above methods in the study of networks operating at high load (with network utilization coefficients close to unity, i.e. on the verge of saturation), for their analytical modeling at arbitrary (in particular, small or normal) load.

In any case, congestion detection is the mechanism that usually initiates the procedure for launching management policies.

Congestion problems can be reduced by the fair distribution of resources in the network in identified areas. The composite routing metric is composed of the consumed energy (λ) of the sensor node, the participation level (η) of the sensor node, and the signal quality (Ω) between the sensor nodes. Amongst these three routing metrics, λ and η represent the characteristics of the sensor node, whereas, Ω represents the quality of the link between the sensor nodes. Each metric in the composite routing metric.

The mechanism must maintain routing entries in the routing table according to the least hops criterion to implement the shortest path to the receiver. Because there is a possibility that an inefficiently long route will be chosen to reduce congestion, which will increase the ETE delay. Due to the use of multiple paths, problems such as route coupling, contention, and channel access rate can occur, which can reduce network performance.

The goal of all congestion control methods is to limit the length of queues at nodes. Nevertheless, no method of dealing with the load provides a theoretical ideal. However, a good congestion control strategy avoids the collapse of bandwidth, bringing it closer to the ideal.

4. Conclusions

In the paper peculiarities of the occurrence of overloads in telecommunication networks at the node level and at the channel level are analyzed. The main causes and consequences of overloads are considered. A strategy for finding overloads based on the information criterion is proposed. The criteria for the selection of parameters for the evaluation of the congestion detection procedure by evaluating the entropy of time series have been determined. The entropy measures of data sets for various types of model distribution, in particular for the Pareto distribution, which optimally describes the behavior of self-similar random processes, were calculated and analyzed. The entropy of the Pareto distribution for the self-similarity coefficient of network traffic for various parameters of the form is presented.

In contrast to the methods of monitoring congestion in network nodes, the management of which consists in discarding redundant packets and limiting the speed of information transmission, which leads to a noticeable decrease in QOS parameters, the development of methods for detecting network congestion at the channel level will allow the application of a flow management policy based on the principle of „fair resources distribution". This will guarantee regulated quality indicators of consumer service. The estimation of the entropy of the proposed parameters of the time series will allow us to describe and predict the behavior of multimedia traffic data flows with higher quality, which belongs to the type of self-similar processes and is poorly described by traditional model distributions.

References

[1] Airehrour D., Gutierrez J. A., Ray S. K.: SecTrust-RPL: A secure trust-aware RPL routing protocol for Internet of Things. Future Generation Computer Systems 93, 2019, 860–876 [http://doi.org/10.1016/j.future.2018.03.021].

[2] Alashhab A. A., Zahid M. S. M., Azim M. A., Daha M. Y., Isyaku B., Ali S.: A Survey of Low Rate DDoS Detection Techniques Based on Machine Learning in Software-Defined Networks. Symmetry 14, 2022, 1563 [http://doi.org/10.3390/sym14081563].

[3] Bakhovskyy P. et al.: Stages of the Virtual Technical Functions Concept Networks Development. Cagáˇnová et al. (eds.): Advances in Industrial Internet of Things, Engineering and Management. EAI/Springer Innovations in Communication and Computing, 2021, 119–135 [http://doi.org/10.1007/978-3-030-69705-1_7].

[4] Bedin A., Chiariotti F., Kucera S., Zanella A.: Optimal Latency-Oriented Coding and Scheduling in Parallel Queuing Systems. IEEE Transactions on Communications 70(10), 2022, 6471–6488 [http://doi.org/10.1109/TCOMM.2022.3200105].

[5] Chughtai O., Badruddin N., Rehan M., Khan A.: Congestion Detection and Alleviation in Multihop Wireless Sensor Networks. Wireless Communications and Mobile Computing 2017, 9243019 [http://doi.org/10.1155/2017/9243019].

[6] Desai R. M., Patil B. P., Sharma D. P.: Learning based route management in mobile ad hoc networks. Indonesian Journal of Electrical Engineering and Computer Science 7(3), 2017, 718–723 [http://doi.org/10.11591/ijeecs.v7.i3.pp718-723].

[7] Desmoulins N., Fouque P.A., Onete C., Sanders O.: Pattern Matching on Encrypted Streams. ASIACRYPT 2018. Lecture Notes in Computer Science 11272, Springer, Cham. [http://doi.org/10.1007/978-3-030-03326-2_5].

[8] Divitskyi A., Salnyk S., Hol V., Sydorkin P., Storchak A.: Development of a model of a subsystem for forecasting changes in data transmission routes in special purpose mobile radio networks. Eastern-European Journal of Enterprise Technologies 3(9), 2021, 116–125 [http://doi.org/10.15587/1729-4061.2021.235609].

[9] Dobkach L.: Analysis of methods for recognizing computer attacks. Legal informatics 1, 2020, 67–75 [http://doi.org/10/21681/1944-1404-2020-1-67-75].

[10] Durairaj M., Hirudhaya Mary Asha J.: The Internet of Things (IoT) Routing Security – A Study. International Conference on Communication, Computing and Electronics Systems. Lecture Notes in Electrical Engineering 637. Springer, Singapore 2020 [http://doi.org/10.1007/978-981-15-2612-1_58].

[11] Hasan N., Mishra A, Ray A. K.: Fuzzy logic based cross-layer design to improve Quality of Service in Mobile ad-hoc networks for Next-gen Cyber Physical System. Engineering Science and Technology, an International Journal 35, 2022, 101099 [http://doi.org/10.1016/j.jestch.2022.101099].

[12] Hui W., Zijian C., Bo H.: A Network Intrusion Detection System Based on Convolutional Neural Network. Journal of Intelligent & Fuzzy Systems 38(6), 2020, 7623–7637 [http://doi.org/10.3233/JIFS-179833].

[13] Mangelkar S., Dhage S., Nimkar A.: A comparative study on RPL attacks and security solutions. International Conference on Intelligent Computing and Control (I2C2), 2017, 1–6 [http://doi.org/10.1109/I2C2.2017.8321851].

[14] Moroz S., Tkachuk A., Khvyshchun M., Prystupa S., Yevsiuk M.: Methods for Ensuring Data Security in Mobile Standards. Informatyka, Automatyka, Pomiary w Gospodarce i Ochronie Środowiska 12(1), 2022, 4–9 [http://doi.org/10.35784/iapgos.2877].
[15] Myneni S., Chowdhary A., Huang D., Alshamrani A.: A distributed deep defense against DDoS attacks with edge computing. Computer Networks 209, 2022, 108874 [http://doi.org/10.1016/j.comnet.2022.108874].
[16] Priyadarshini R., Rabindra K.: A deep learning based intelligent framework to mitigate DDoS attack in fog environment. Journal of King Saud University – Computer and Information Sciences 34(3), 2022, 825–831 [http://doi.org/10.1016/j.jksuci.2019.04.010].
[17] Rafe V., Mohammady S., Cuevas E.: Using Bayesian optimization algorithm for model-based integration testing. Soft Comput 26, 2022, 3503–3525 [http://doi.org/10.1007/s00500-021-06476-9].
[18] Showail A., Tahir R., Zaffar M. F., Noor M. H., Al-Khatib M.: An internet of secure and private things: A service-oriented architecture. Computers & Security 120, 2022, 102776 [http://doi.org/10.1016/j.cose.2022.102776].
[19] Tkachuk A. et al.: Basic Stations Work Optimization in Cellular Communication Network. Advances in Industrial Internet of Things, Engineering and Management, EAI. Springer Innovations in Communication and Computing, 2021, 1–19 [http://doi.org/10.1007/978-3-030-69705-1_1].
[20] Toroshanko Y., Selepyna Y., Yakymchuk N., Cherevyk V.: Control of traffic streams with the multi-rate token bucket, in International Conference on Advanced Information and Communications Technologies AICT 2019, 2019, 352–355 [http://doi.org/10.1109/AIACT.2019.8847860].
[21] Verma A., Ranga V.: Addressing Flooding Attacks in IPv6-based Low Power and Lossy Networks. TENCON 2019 - 2019 IEEE Region 10 Conference (TENCON), 2019, 552–557 [http://doi.org/10.1109/TENCON.2019.8929409].
[22] Yin C., Wang H., Yin X. et al.: Improved deep packet inspection in data stream detection. J Supercomput 75, 2019, 4295–4308 [http://doi.org/10.1007/s11227-018-2685-y].
[23] Yungaicela-Naula N., Vargas-Rosales C., Pérez-Díaz J., Carrera D.: A flexible SDN-based framework for slow-rate DDoS attack mitigation by using deep reinforcement learning. Journal of Network and Computer Applications 205, 2022, 103444 [http://doi.org/10.1016/j.jnca.2022.103444].
[24] Zheng C., Li X., Liu Q., Sun Y., Fang B.: Hashing Incomplete and Unordered Network Streams. Advances in Digital Forensics XIV. DigitalForensics 2018. IFIP Advances in Information and Communication Technology 532. Springer, Cham. 2018 [https://doi.org/10.1007/978-3-319-99277-8_12].

Ph.D. Natalia Yakymchuk
e-mail: n.yakymchuk@lntu.edu.ua

Research interests: diagnostics and control of the telecommunication networks state, end-to-end diagnostics, congestion management.

http://orcid.org/0000-0002-8173-449X

Ph.D. Stanislav Prystupa
e-mail: s.prystupa@lntu.edu.ua

Author of more than 60 scientific papers, 5 patents for utility models. Research interests: design of microelectronic intelligent sensors of physical quantities.

http://orcid.org/0000-0003-3705-1541

Ph.D. Yosyp Selepyna
e-mail: y.selepyna@lntu.edu.ua

Research interests: Modeling of electronic devices and systems. Digital signal processing and coding in telecommunication systems and networks.

http://orcid.org/0000-0002-2421-1844

Ph.D. Serhii Moroz
e-mail: s.moroz@lntu.edu.ua

Author of more than 100 scientific papers, 7 patents for utility models. Research interests: Methodological bases of construction of sensors of physical quantities and measuring modules, Research of info-communication systems in the context of the development of the concept of the Internet of Things.

http://orcid.org/0000-0003-4677-5170

Ph.D. Mykola Yevsiuk
e-mail: m.yevsiuk@lutsk-ntu.com.ua

Research interests: telecommunication networks, radio engineering devices, power supply systems of radio engineering devices and systems. Author and co-author of about 40 scientific articles, two textbooks, two monographs.

http://orcid.org/0000-0002-3768-8959

http://doi.org/10.35784/iapgos.3247 received: 6.11.2022 | revised: 11.12.2022 | accepted: 15.12.2022 | available online: 30.12.2022

POLARIZATION TOMOGRAPHY OF THE POLYCRYSTALINNE STRUCTURE OF HISTOLOGICAL SECTIONS OF HUMAN ORGANS IN DETERMINATION OF THE OLD DAMAGE

Olexandra Litvinenko[1], Victor Paliy[2], Olena Vysotska[3], Inna Vishtak[4], Saule Kumargazhanova[5]
[1]Higher State Educational Institution of Ukraine „Bukovynian State Medical University", Chernivtsi, Ukraine, [2]National Aerospace University H.E. Zhukovsky „Kharkiv Aviation Institute", Kharkiv, Ukraine, [3]National Pirogov Memorial University of Vinnytsia, Vinnytsia, Ukraine, [4]Vinnytsia National Technical University, Vinnytsia, Ukraine, [5]D. Serikbayev East Kazakhstan Technical University, Ust-Kamenogorsk, Kazakhstan

Abstract. *The results of algorithmic approbation of the technique of polarization tomography digital histological study of the age of damage to the myocardium and lung tissue based on the polarization reconstruction of linear birefringence maps are presented. Relationships between the temporal change in the magnitude of statistical moments of 1-4 orders characterizing the distribution of the magnitude of the degree of crystallization of histological sections of the myocardium and lung tissue and the duration of damage were determined. Established time intervals and accuracy of determining the prescription of damage to the myocardium and lung tissue.*

Keywords: polarization, tomography, optical anisotropy, biological tissues

TOMOGRAFIA POLARYZACYJNA STRUKTURY POLIKRYSTALICZNEJ WYCINKÓW HISTOLOGICZNYCH NARZĄDÓW CZŁOWIEKA W OKREŚLANIU DAWNYCH USZKODZEŃ

Streszczenie. *Przedstawiono wyniki algorytmicznej aprobaty techniki polaryzacyjnej tomografii cyfrowej histologicznego badania wieku uszkodzenia mięśnia sercowego i tkanki płucnej na podstawie rekonstrukcji polaryzacyjnej liniowych map dwójłomności. Określono zależności pomiędzy czasową zmianą wartości momentów statystycznych 1-4 rzędów, charakteryzujących rozkład stopnia krystalizacji skrawków histologicznych tkanki mięśnia sercowego i płuc, a czasem trwania uszkodzeń. Ustalono przedziały czasowe i dokładność określania predykcji uszkodzenia mięśnia sercowego i tkanki płucnej.*

Słowa kluczowe: polaryzacja, tomografia, anizotropia optyczna, tkanki biologiczne

Introduction

Histological study of microscopic images at different optical scales of the morphological structure of biological preparations is currently considered in the approximation of an objective (statistical) analysis of the distributions of photometric and polarization parameters [6, 12].

This approach makes it possible to determine a set of diagnostic relationships between a set of statistical moments of the 1st – 4th orders characterizing the distribution of structural anisotropy parameters of the morphological structure of the histological sections of biological tissues and two-dimensional distributions (polarization maps) of the magnitude of the azimuths and polarization ellipticity of their microscopic images [7, 14].

This work is aimed at further research and substantiation of new information possibilities of forensic digital histological examination using the method of polarization-phase tomography of birefringence distributions of histological sections of the myocardium and lung tissue in the problem of determining the age of damage [1, 8, 15].

1. Study design

The design of polarization tomography of the polycrystalline structure of histological sections of biological tissues of human internal organs is illustrated by the structural and logical scheme shown in table 1.

Table 1. Styles predefined in IAPGOS template

Structural-logical scheme of polarization tomography
Laser probe shaping unit
Block of multichannel formation of polarization probes
Block for placement of the studied histological section
Block for designing microscopic images of different scales
Block of multichannel polarization filtering of microscopic images
Block for digital registration of polarization filtered microscopic images
Block of algorithmic calculation of maps of linear and circular birefringence

2. Short theory and method

The structural and logical scheme of the Mueller-matrix tomography of histological sections of biological tissues contains:

I – optical sounding unit containing a source of coherent radiation – He-Ne laser [9, 11, 12];

II – block for forming an optical probe with a flat wavefront – two confocality located microobjectives with a vignette diaphragm.;

III – block for forming discrete states of polarization of the optical probe – phase-shifting plates 0.25λ and a linear polarizer that provide the formation of three types of linear polarization ($\alpha_0 = 0°;\ 90°;\ 45°$), as well as right circularly ($\otimes$) polarized laser radiation;

IV – object block – a microscopic table with a mount, adjustment and rotation of a biological sample;

V – projection unit – a polarizing microlens that provides the formation of a microscopic image of a biological preparation in the plane of a digital camera;

VI – polarization analysis block - phase-shifting plates 0.25λ and a linear polarizer, providing polarization analysis of the microscopic image of the biological layer 8 according to the following algorithm $\Omega = 0°; 90°; 45°; 135°; \otimes; \oplus$;

VII – block for digital registration of coordinate distributions of the intensity of polarization images of biological samples – a digital camera with $m \times n$ – the number of pixels of the photosensitive area;

VIII – block of analytical information processing – a personal computer and a package of applied programs that provide the calculation of the coordinate distributions of the parameters of the phase ($\delta_{0,90};\ \delta_{45,135};\ \delta_{\otimes,\otimes}$) and amplitude ($\Delta\mu_{0,90};\ \Delta\mu_{45,135};\ \Delta\mu_{\otimes,\otimes}$) anisotropy of partially depolarizing biological layers.

Optical probing of histological sections (polycrystalline films) of biological preparations was carried out using a beam of a gas He-Ne laser 1 formed by a collimator, parallel with a diameter of 2 mm, with a wavelength of λ = 0.6328 μm.

The formation of discrete states of polarization of the optical probe was carried out using phase-shifting (0.25λ) plates (manufacturer – Achromatic True Zero-Order Waveplate) and a dichroic polarizer 4 (manufacturer – B+W Kaesemann XS-ProPolarizer MRC Nano). The biological layer was sequentially probed with a laser beam with the following types of polarization: linear with azimuths of 0°, 90°, +45° and right-handed circulation (⊗). The formation of a series of linear states of polarization was carried out by orienting the axis of the highest velocity of the phase-shifting element 3 at an angle of ÷ 45° relative to the plane of polarization of laser radiation, followed by rotation of the plane of transmission of the polarizer at angles of 0°, 90°, +45°. A right circularly polarized wave was formed by introducing a phase-shifting quarter-waveplate with the axis of maximum velocity oriented at an angle of 0° relative to the plane of polarization of the laser beam +45°. Laser radiation intensity distributions in the plane of histological sections (polycrystalline films) of biological preparations were formed using a polarizing microlens (manufacturer – Nikon CFI Achromatic P, focal length – 30 mm, numerical aperture – 0.1, magnification – 4x) (The Imaging Source DMK 41AU02.AS, monochrome 1/2" CCD, Sony ICX205AL (progressive scan); resolution – 1280×960; size of the light-sensitive area – 7600×6200 μm; sensitivity – 0.05 lx; dynamic range of which are a contains m×n = 1280×960 pixels.

Polarization filtering of the coordinate distributions of the intensity of microscopic images of histological sections (polycrystalline films) of biological preparations was carried out using a linear polarizer (the transmission plane angle was the following discrete values $0°;\ 90°;\ 45°; 135°$) and a quarter-wave phase plate 8 (the orientation angle of the axis of maximum velocity was $45°; 135°$) [9, 10, 11].

The data obtained make it possible to determine expressions for calculating the optical anisotropy parameters characterizing the linear and circular:

- birefringence ($LB_{0.90};\ \ LB_{45.135};\ \ CB_{\otimes,\oplus}$):

$$\left.\begin{aligned}\langle m_{34}\rangle &= r^{-1}\,ln\left(\frac{f_{34}}{f_{43}}\right) = r^{-1}\,ln\left(\frac{S_3^{\otimes}-0.5(S_3^0+S_3^{90})}{S_4^{45}-0.5(S_4^0+S_4^{90})}\right)\\ \langle m_{34}\rangle &= r^{-1}\,ln\left(\frac{f_{43}}{f_{34}}\right) = r^{-1}\,ln\left(\frac{S_4^{45}-0.5(S_4^0+S_4^{90})}{S_3^{\otimes}-0.5(S_3^0+S_3^{90})}\right)\end{aligned}\right\} \Rightarrow LB_{0.90} \quad (1)$$

$$\left.\begin{aligned}\langle m_{42}\rangle &= r^{-1}\,ln\left(\frac{f_{42}}{f_{24}}\right) = r^{-1}\,ln\left(\frac{0.5(S_4^0-S_4^{90})}{S_2^{\otimes}-0.5(S_2^0+S_2^{90})}\right)\\ \langle m_{24}\rangle &= r^{-1}\,ln\left(\frac{f_{24}}{f_{42}}\right) = r^{-1}\,ln\left(\frac{S_2^{\otimes}-0{,}5(S_2^0+S_2^{90})}{0.5(S_4^0-S_4^{90})}\right)\end{aligned}\right\} \Rightarrow LB_{45.135} \quad (2)$$

$$\left.\begin{aligned}\langle m_{23}\rangle &= r^{-1}\,ln\left(\frac{f_{23}}{f_{32}}\right) = r^{-1}\,ln\left(\frac{S_2^{45}-0.5(S_2^0+S_2^{90})}{0.5(S_3^0-S_3^{90})}\right)\\ \langle m_{32}\rangle &= r^{-1}\,ln\left(\frac{f_{32}}{f_{23}}\right) = r^{-1}\,ln\left(\frac{0.5(S_3^0-S_3^{90})}{S_2^{45}-0.5(S_2^0+S_2^{90})}\right)\end{aligned}\right\} \Rightarrow CB_{\otimes,\oplus} \quad (3)$$

- dichroism ($LD_{0.90}\quad LD_{45.135}\quad CD_{\otimes,\oplus}$):

$$\langle m_{12}\rangle = \langle m_{21}\rangle = r^{-1}\,ln(f_{12}f_{21}) = $$
$$= r^{-1}\,ln\left(0.25(S_1^0 - S_1^{90})(S_2^0 + S_2^{90})\right) \Rightarrow LD_{0.90} \quad (4)$$

$$\langle m_{13}\rangle = \langle m_{31}\rangle = r^{-1}\,ln(f_{13}f_{31}) = $$
$$= r^{-1}\,ln\left(0.25\left(S_1^{45} - 0.5(S_1^0 + S_1^{90})\right)(S_3^0 + S_3^{90})\right) \Rightarrow$$
$$\Rightarrow LD_{45.135} \quad (5)$$

$$\langle m_{14}\rangle = \langle m_{41}\rangle = r^{-1}\,ln(f_{14}f_{41}) = $$
$$= r^{-1}\,ln\left(0.25\left(S_1^{\otimes} - 0.5(S_1^0 + S_1^{90})\right)(S_4^0 + S_4^{90})\right) \Rightarrow$$
$$\Rightarrow CD_{\otimes,\oplus}. \quad (6)$$

Here $S_{i=2;3;4}^{0;45;90;\otimes}$ – set of parameters of the Stokes vector at the points of a digital microscopic image of a sample of a partially depolarizing biological layer, experimentally determined for a series of linearly ($0^0;\ 45^0;\ 90^0$) and right-circular (⊗) polarized probing laser beams according to the following relations

$$S_{i=1}^{0;45;90;\otimes} = I_0^{0;45;90;\otimes} + I_{90}^{0;45;90;\otimes};$$
$$S_{i=2}^{0;45;90;\otimes} = I_0^{0;45;90;\otimes} - I_{90}^{0;45;90;\otimes};$$
$$S_{i=3}^{0;45;90;\otimes} = I_{45}^{0;45;90;\otimes} - I_{135}^{0;45;90;\otimes};$$
$$S_{i=4}^{0;45;90;\otimes} = I_{\otimes}^{0;45;90;\otimes} + I_{\oplus}^{0;45;90;\otimes} \quad (7)$$

Here $I_{0;45;90;135;\otimes;\oplus}$ – polarization-filtered intensities of laser radiation converted by a biological object. The filtering operation corresponds to the following experimental actions – the passage of an object beam through a linear polarizer 9 with the angles of rotation of the transmission axis Θ: $0^0;\ \ 45^0;\ \ 90^0;\ \ 135^0$, as well as through the phase filtering system „quarter-waveplate – polarizer", which separates the right – (⊗) and left – (⊕) circularly polarized components of the object laser radiation [2, 3, 10].

3. Algorithm for determining the prescription of the formation of damage to the internal organs of a person

The criterion for detecting the interval for determining the prescription of damage formation is the time interval (τ) of a continuous linear change in the magnitude of the statistical moments of the 1st – 4th moments ($Z_{i\,=\,1;2;3;4}$), characterizing the distribution of optical-anisotropic parameters (birefringence, LB) histological sections, which provides an analysis of the morphological structure of various biological tissues [4, 5, 10].

The scheme of algorithmic determination of the prescription of damage to internal organs is shown in Fig. 1.

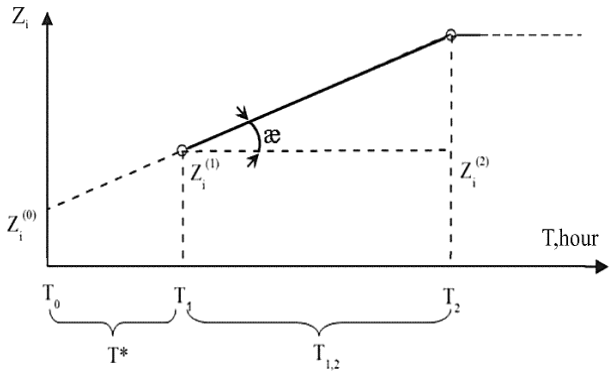

Fig. 1. Scheme of algorithmic determination of damage age: τ_1 – time of the beginning of measurements of the magnitude of statistical moments of the 1st – 4th orders $Z_i^{(1)}$; τ_2 – completion time of the linear change in the magnitude of statistical moments of the 1st – 4th orders $Z_i^{(2)}$; τ_0 – unknown time of occurrence of damage; ϰ – time dependence slope $Z_i^{(τ)}$

An analysis of the algorithmic scheme (Fig. 1) revealed the following relationships for determining the prescription (time τ^*) of damage to human internal organs with an accuracy $\Delta\tau^*$

$$\tau^* = \left(Z_i^{(1)} - Z_i^{(0)}\right)\frac{\tau_2-\tau_1}{Z_i^{(2)}-Z_i^{(1)}} \quad (8)$$

Here $Z_i^{(0)}$ is the value of the statistical moment calculated for the polarization-tomographic map of linear birefringence LB of the histological section of intact biological tissue [1, 8, 13].

4. Analysis and discussion of experimental data

4.1. Myocardium

The following groups were formed (control of those who died from coronary heart disease (CHD)) and experimental (with different duration of damage τ^*) samples of histological sections of the human myocardium and lung tissue – table 2.

Table 2. Characteristics of the objects of study

Groups									
Control	Experienced with different prescription damage, hours								
Died from CHD	1	6	12	18	24	48	72	96	120
(number of samples *n = 21*)	*n = 21*	*n = 21*	*n = 21*	*n = 21*	*n = 21*	*n = 21*	*n = 21*	*n = 21*	*n = 21*

Within each of the groups of histological sections:

- maps of linear birefringence were determined LB,
- statistical moments of the 1st – 4th orders ($Z_{i=1,2,3,4}$), characterizing the distribution of the quantity LB was calculated,
- was determined within the framework of the control and the totality of experimental groups, the average value and the error of the value of each of the statistical moments of 1–4 orders,
- algorithmically (formula (1)) the age of damage was calculated – τ^*.

Fig. 2 shows the coordinate distributions ((1) – (3)) of the magnitude of linear birefringence (LB) of histological sections of the myocardium of the dead from the control group (1), experimental groups with different duration of damage (6 hours – (2)) and (18 hours – (3)).

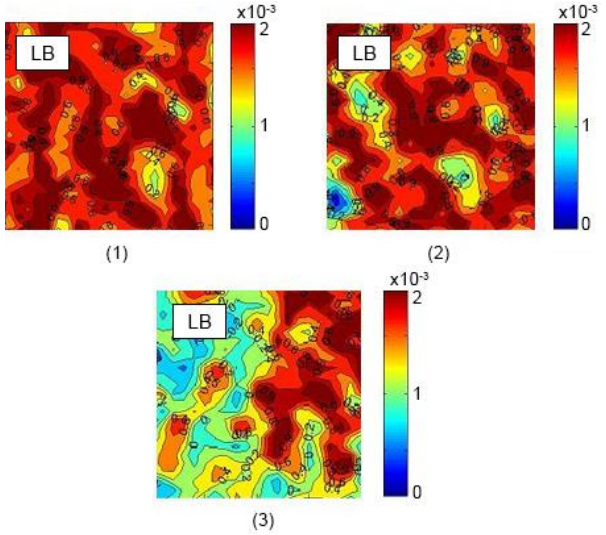

Fig. 2. Coordinate distributions ((1)–(3)) of the linear birefringence of histological sections of the myocardium of the dead from the control group ((1)), research groups with different damage duration (6 hours – (2)) and (18 hours – (3))

Table 3. Time dynamics of changes in statistical moments of 1–4 orders characterizing the distribution of the magnitude of linear birefringence (LB) of histological sections of the myocardium

***T*, hours**	**2**	**4**	**6**	**12**	**18**
$Z_1 \times 10^{-1}$	1.74±0.069	1.54±0.058	1.34±0.057	1.12±0.049	0.93±0.038
p	$p < 0.05$				
$Z_2 \times 10^{-1}$	1.29±0.055	0.97±0.039	0.64±0.028	0.41±0.019	0.38±0.018
p	$p < 0.05$				$p > 0.05$
Z_3	0.38±0.016	0.54±0.023	0.71±0.035	1.24±0.056	1.53±0.069
p	$p < 0.05$				
Z_4	0.25±0.011	0.49±0.022	0.73±0.034	1.21±0.056	1.69±0.069
p	$p < 0.05$				
***T*, hours**	**24**	**48**	**72**	**96**	**120**
$Z_1 \times 10^{-1}$	0.73±0.035	0.51±0.022	0.52±0.021	0.49±0,022	0.48±0.021
p	$p < 0.05$		$p > 0.05$		
$Z_2 \times 10^{-1}$	0.38±0.017	0.35±0.016	0.33±0.017	0.34±0,018	0.33±0.016
p	$p < 0.05$	$p > 0.05$			
Z_3	1.65±0.071	2.01±0.092	2.36±0.105	2.29±0,11	2.28±0.12
p	$p < 0.05$			$p > 0.05$	
Z_4	2.02±0.099	2.59±0.12	3.07±0.14	3.13±0.15	3.09±0.14
p	$p < 0.05$			$p > 0.05$	

From the analysis of the data obtained, it can be seen:

- histological sections of the myocardium of the dead from all the studied groups have linear birefringence – LB ≠ 0,
- with an increase in the time of damage, the average level and the root-mean-square spread of random values of the linear birefringence value decrease LB.

Table 2 illustrates the time dependences of the set of statistical moments of 1–4 orders characterizing the coordinate distributions of the LB value of histological sections of the myocardium of the dead.

Dynamic ranges were established, as well as diagnostic sensitivity to the prescription of myocardial damage of statistical moments of the 1st–4th orders ($Z_{i=1;2;3;4}$) with subsequent linear time intervals (highlighted in color – table 1; $\propto$ = const – Fig.1) and a statistically significant change ($p \leq 0.05$) of the Eigen values of the linear birefringence LB:

- 1st order statistical moment (average Z_1) – 48 hours and 1.23,
- 2nd order statistical moment (dispersionZ_2) – 24 hours and 0.91,
- 3rd order statistical moment (asymmetryZ_3) – 72 hours and 1.98,
- 4th order statistical moment (kurtosis Z_4) – 72 hours and 2.82.

4.2. Lung tissue

The results of a digital histological study of the degree of crystallization of lung tissue samples from the experimental (1) and two control (2), (3) groups are shown in Fig. 3.

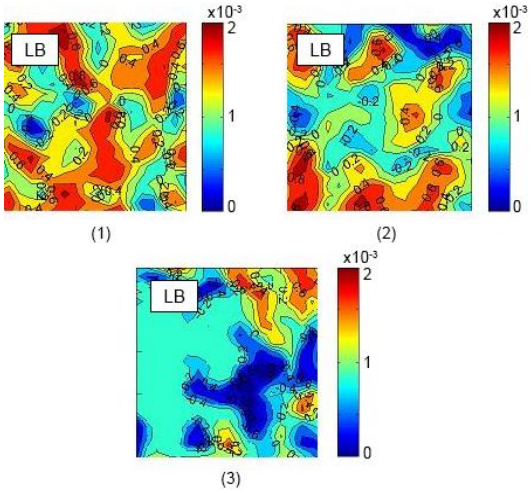

Fig. 3. Coordinate distributions ((1)–(3)) of the linear birefringence of histological sections of the lung tissue of the dead from the control group ((1)), research groups with different damage duration (6 hours – (2)) and (18 hours – (3))

As in the case of a polarization tomographic study of myocardial samples, for the obtained data on the optical anisotropy of lung tissue samples, one can see:

- histological sections of the lung tissue of the deceased from all the studied groups have linear birefringence – LB ≠ 0,
- the average level and spread of the LB value is 1.2 – 2 times less than the similar parameter of the optical anisotropy of the myocardium,
- with an increase in the time of damage, the average level and the root-mean-square spread of random values of the linear birefringence value decrease LB.

Table 4. Time dynamics of changes in statistical moments of 1–4 orders characterizing the distribution of the magnitude of linear birefringence (LB) of histological sections of the lung tissue

***T*, hours**	**2**	**4**	**6**	**12**	**18**
$Z_1 \times 10^{-1}$	0.58±0.024	0.53±0.021	0.48±0.029	0.38±0.017	0.28±0.015
p	p < 0.05				
$Z_2 \times 10^{-1}$	0.39±0.019	0.33±0.013	0.27±0.014	0.21±0.014	0.15±0.007
p	p < 0.05				
Z_3	1.43±0.065	1.64±0.077	1.83±0.081	2.11±0.099	2.44±0.11
p	p < 0,05				
Z_4	1.77±0.073	2.01±0.098	2.19±0.105	2.68±0.12	3.21±0.14
p	p < 0.05				
***T*, hours**	**24**	**48**	**72**	**96**	**120**
$Z_1 \times 10^{-1}$	0.18±0.008	0.13±0.006	0.12±0.007	0.13±0.008	0.12±0.007
p	p < 0.05		p > 0.05		
$Z_2 \times 10^{-1}$	0.12±0.005	0.15±0.008	0.13±0.007	0.14±0.008	0.13±0.007
p	p < 0.05	p > 0,05			
Z_3	2.82±0.13	3.19±0.15	3.57±0.16	3.45±0.16	3.49±0.17
p	p < 0.05			p > 0.05	
Z_4	3.63±0.17	4.06±0.19	4.78±0.21	4.66±0.21	4.77±0.21
p	p < 0.05			p > 0.05	

The revealed differences between the maps of linear birefringence of the myocardium and lung tissue can be attributed to the fact that the cardiac muscle is formed by spatially structured networks of myosin fibrils, which form a significantly higher level of structural anisotropy compared to the parenchyma structure of lung tissue.

Table 4 illustrates the time dependences of the value of the set of statistical moments of 1-4 orders, characterizing the distribution of the LB value of histological sections of the lung tissue of the dead.

From the analysis of data from digital polarization tomographic histology of lung tissue samples from the control group and experimental groups with different duration of damage, the following diagnostically relevant linear time intervals and ranges of changes in the magnitude of statistical moments of 1–4 orders of magnitude were established:

- 1st order statistical moment (average Z_1) – 48 hours and 0.45,
- 2nd order statistical moment (dispersion Z_2) – 24 hours and 0.27,
- 3rd order statistical moment (asymmetry Z_3) – 72 hours and 2.14,
- 4th order statistical moment (kurtosis Z_4) – 72 hours and 3.01.

5. Time intervals and accuracy of digital histological determination of damage age by polarization tomography

The time intervals and accuracy of determining the prescription of damage to the myocardium and lung tissue by the method of polarization tomography digital histology are presented in table 5.

Table 5. Time intervals and accuracy of the polarization mapping method for linear birefringence maps

Samples	Myocardium		Lung tissue	
Statistical moments	Interval, hours	Accuracy, min.	Interval, hours	Accuracy, min.
Average	1–48	35	1–48	45
Dispersion	1–24	35	1–24	45
Asymmetry	1–72	25	1–72	35
Kurtosis	1–72	25	1–72	35

6. Conclusions

1. The main interrelations between temporal changes in the statistical structure of topographic maps of the degree of crystallization of histological sections of the myocardium and lung tissue and variations in the magnitude of statistical moments of 1–4 orders that characterize them are revealed.
2. The time ranges of linear changes in the magnitude of statistical indicators of the tomography technique of digital histology and the accuracy of determining the age of damage were established:

- average, dispersion – 24–48 hours, accuracy 35 min. – 45 min.,
- asymmetry, kurtosis – 72 hours, accuracy 25 min. – 35 min.

References

[1] Avrunin, O. G. et al.: Possibilities of automated diagnostics of odontogenic sinusitis according to the computer tomography data. Sensors 21(4), 2021, 1–22.
[2] Blatter C. et al.: Dove prism based rotating dual beam bidirectional Doppler oct. Biomed. Opt. Express 4, 2013, 1188–1203.
[3] Hong Y.-J. et al.: Optically buffered Jones-matrix-based multifunctional optical coherence tomography with polarization mode dispersion correction. Biomed. Opt. Express 1, 2015, 225–243.
[4] Isaieva O. A. et al.: Features of image analysis under UV-video dermoscopy. Proc. of SPIE 11456, 2020, 114560H.
[5] Kovalova A. et al.: Possibilities of automated image processing at optical capillaroscopy. Proc. of SPIE 11456, 2020, 114560G.
[6] Macdonald C., Meglinski I.: Backscattering of circular polarized light from a disperse random medium influenced by optical clearing. Laser Phys. Lett. 8(4), 2011, 324–328.
[7] Park B. H., de Boer J. F.: Polarization sensitive optical coherence tomography. In: Drexler W., Fujimoto J. G. (Eds.): Optical Coherence Tomography: Technology and Applications, 2nd ed. Springer Reference, Science + Business Media, New York 2015, 1055–1101.
[8] Peyvasteh M., Tryfonyuk L. et al.: 3D Mueller-matrix-based azimuthal invariant tomography of polycrystalline structure within benign and malignant soft-tissue tumours. Laser Physics Letters 17(11), 2020, 115606.
[9] Rovira J. R. et al.: Methods and resources for imaging polarimetry. Proc. of SPIE 8698, 2012, 86980T.
[10] Ushenko V. A. et al.: 3D Mueller matrix mapping of layered distributions of depolarisation degree for analysis of prostate adenoma and carcinoma diffuse tissues. Scientific Reports 11(1), 2021, 5162.
[11] Ushenko V. A. et al.: Embossed topographic depolarisation maps of biological tissues with different morphological structures. Scientific Reports 11(1), 2021, 3871.
[12] Wang W. et al.: Roles of linear and circular polarization properties and effect of wavelength choice on differentiation between ex vivo normal and cancerous gastric samples. J. Biomed. Opt. 19(4), 2014, 046020.
[13] Wójcik W. et al.: Information Technology in Medical Diagnostics II. Taylor & Francis Group, CRC Press, Balkema book, London 2019.
[14] Yamanari M. et al.: Scleral birefringence as measured by polarizationsensitive optical coherence tomography and ocular biometric parameters of human eyes in vivo. Biomed. Opt. Express 5(5), 2014, 1391–1402.
[15] Yasuno Y. et al.: Jones Matrix based polarization sensitive optical coherence tomography. In: Drexler W., Fujimoto J. G. (Eds.): Optical Coherence Tomography: Technology and Applications, 2nd ed. Springer Reference, Science + Business Media, New York 2015, 1137–1162.

M.Sc. Olexandra Litvinenko
e-mail: sawasawa901@gmail.com

Postgraduate student at the Department of Forensic Medicine and Medical Law, Bukovina State Medical University, Ukraine. Research interests: digital and polarisation histology of biological tissues in the tasks of damage type and time detection.

http://orcid.org/0000-0003-3897-6765

D.Sc. Victor Paliy
e-mail: paliy@vnmu.edu.ua

Doctor of medical sciences, professor at the Department of General Surgery, National Pirogov Memorial University of Vinnytsia.
Scientific direction – research of antimicrobial efficacy of a medicines with prolonged antiseptic effect and their use for treatment of purulent wounds.

http://orcid.org/0000-0002-2289-1786

D.Sc. Olena Vysotska
e-mail: evisotska@ukr.net

Head of Department of Radio-electronic and Biomedical Computer-aided Means and Technologies National Aerospace University H.E. Zhukovsky "Kharkiv Aviation Institute", Ukraine.
Scientific direction – medical expert systems, modeling in medicine, proceeding of biomedical imaging and signals.

http://orcid.org/0000-0003-3723-9771

Ph.D. Inna Vishtak
e-mail: vishtakiv@vntu.edu.ua

Candidate of technical sciences, assistant professor. Assistant of the Department Safety of Life and Safety's Pedagogy, Deputy Director of the Institute of Doctoral and Postgraduate Studies, Vinnytsia National Technical University.
Scientific direction – mechatronics, mechanics, biomechanics and nanosructures, life safety, labor protection. Expert of the National Agency for Quality Assurance of Higher Education.

http://orcid.org/0000-0001-5646-4996

Ph.D. Saule Kumargazhanova
e-mail: SKumargazhanova@gmail.com

She is currently the Dean of the Department of Information Technologies and Intelligent Systems of D. Serikbayev East Kazakhstan Technical University. Author over 50 papers in journals and conference proceedings. Her professional interests are software engineering, data processing and analysis.

http://orcid.org/0000-0002-6744-4023

http://doi.org/10.35784/iapgos.3274 received: 13.11.2022 | revised: 8.12.2022 | accepted: 15.12.2022 | available online: 30.12.2022

ANALYSIS OF UPPER RESPIRATORY TRACT SEGMENTATION FEATURES TO DETERMINE NASAL CONDUCTANCE

Oleg Avrunin[1], Yana Nosova[1], Nataliia Shushliapina[2], Ibrahim Younouss Abdelhamid[1], Oleksandr Avrunin[1], Svetlana Kyrylashchuk[3], Olha Moskovchuk[4], Orken Mamyrbayev[5]

[1]Kharkiv National University of Radio Electronics, Kharkiv, Ukraine, [2]Kharkiv National Medical University, Kharkiv, Ukraine, [3]Vinnytsia National Technical University, Vinnytsia, Ukraine, [4]Vinnytsia Mykhailo Kotsiubynskyi State Pedagogical University, Vinnytsia, Ukraine, [5]Institute of Information and Computational Technologies of the Kazakh National Technical University named after K. I. Satbayev, Almaty, Kazakhstan

Abstract. *The paper examines the features of segmentation of the upper respiratory tract to determine nasal air conduction. 2D and 3D illustrations of the segmentation process and the obtained results are given. When forming an analytical model of the aerodynamics of the nasal cavity, the main indicator that characterizes the configuration of the nasal canal is the equivalent diameter, which is determined at each intersection of the nasal cavity. It is calculated based on the area and perimeter of the corresponding section of the nasal canal. When segmenting the nasal cavity, it is first necessary to eliminate air structures that do not affect the aerodynamics of the upper respiratory tract - these are, first of all, intact spaces of the paranasal sinuses, in which diffuse air exchange prevails. In the automatic mode, this is possible by performing the elimination of unconnected isolated areas and finding the difference coefficients of the areas connected by confluences with the nasal canal in the next step. High coefficients of difference of sections between intersections will indicate the presence of separated areas and contribute to their elimination. The complex configuration and high individual variability of the structures of the nasal cavity does not allow segmentation to be fully automated, but this approach contributes to the absence of interactive correction in 80% of tomographic datasets. The proposed method, which takes into account the intensity of the image elements close to the contour ones, allows to reduce the averaging error from tomographic reconstruction up to 2 times due to artificial sub-resolution. The perspective of the work is the development of methods for fully automatic segmentation of the structures of the nasal cavity, taking into account the individual anatomical variability of the upper respiratory tract.*

Keywords: aerodynamics of nasal breathing, nasal cavity, tomographic reconstruction, segmentation, upper respiratory tract, air conduction

ANALIZA CECH SEGMENTACJI GÓRNYCH DRÓG ODDECHOWYCH W CELU OKREŚLENIA PRZEWODNICTWA NOSOWEGO

Streszczenie*. W pracy przeanalizowano cechy segmentacji górnych dróg oddechowych w celu określenia powietrznego przewodnictwa nosowego. Przedstawiono zdjęcia 2D i 3D procesu segmentacji oraz uzyskanych wyników. Podczas formowania analitycznego modelu aerodynamiki jamy nosowej głównym wskaźnikiem charakteryzującym konfigurację kanału nosowego jest ekwiwalentna średnica, którą wyznacza się na każdym skrzyżowaniu jam nosowych. Jest ona obliczana na podstawie pola powierzchni i obwodu odpowiedniego odcinka kanału nosowego. Podczas segmentacji jamy nosowej w pierwszej kolejności należy wyeliminować struktury powietrzne, które nie wpływają na aerodynamikę górnych dróg oddechowych – są to przede wszystkim nienaruszone przestrzenie zatok przynosowych, w których dominuje rozproszona wymiana powietrza. W trybie automatycznym jest to możliwe dzięki eliminacji niepołączonych izolowanych obszarów i znalezieniu, w kolejnym kroku, współczynników różnicy obszarów połączonych konfluencjami z przewodem nosowym. Wysokie współczynniki różnic przekrojów pomiędzy skrzyżowaniami będą wskazywały na obecność wydzielonych obszarów i przyczynią się do ich eliminacji. Złożona konfiguracja i duża zmienność osobnicza struktur jamy nosowej nie pozwala na pełną automatyzację segmentacji, jednak takie podejście przyczynia się do braku konieczności interaktywnej korekcji w 80% zestawów danych tomograficznych. Zaproponowana metoda, uwzględniająca intensywność elementów obrazu znajdujących się blisko konturu, pozwala na nawet 2-krotne zmniejszenie błędu uśredniania z* rekonstrukcji tomograficznej, wynikającego ze sztucznej subrozdzielczości. *Perspektywą pracy jest opracowanie metod w pełni automatycznej segmentacji struktur jamy nosowej z uwzględnieniem indywidualnej zmienności anatomicznej górnych dróg oddechowych.*

Słowa kluczowe: aerodynamika oddychania przez nos, jama nosowa, rekonstrukcja tomograficzna, segmentacja, górne drogi oddechowe, przewodzenie powietrza

Introduction

Over the past 20 years, evidence-based medicine approaches have been established in the treatment and diagnostic procedures. Such evidentiary studies are based on the objectification of application based on quantitative instrumental methods and statistically reliable results. Thus, given the lack of hard standards for medical data, there are still many unsolved questions about the reliability of the obtained results, especially when conducting functional studies. One of the main tasks of modern medicine is to determine the dependence between the anatomical and functional properties of organs and their respective individual variability. In rhinology, such studies are conducted to analyze the functional indicators of nasal breathing and the architecture of the upper respiratory tract [13]. This is especially important when changing the configuration of intranasal structures during corrective surgical interventions to improve nasal air conduction in cases of nasal membrane distortions, chronic sinusitis, and other nosologies of functional rhinology [18]. At the same time, mathematical modeling allows predicting the results of operative interventions and carrying out their planning in virtual mode.

X-ray computed tomography and its modifications, such as spiral and cone-beam tomography [7, 18], are the main method of endoscopic diagnosis of the state of the upper respiratory tract. Taking into account the relatively small prevalence of the methods of functional testing of nasal breathing - rhinomanometry, the low repeatability of data and the absence of clear standards of some indicators in different conditions, types and methods of research, at this stage the task of adding functional information to the results of computed tomography examinations [17, 23, 31]. For this, it is necessary to clearly define the configuration of the airways of the nasal cavity and build an aerodynamic model of the air flow during breathing on its basis [10, 24]. The design of aerodynamic models for channels with a complex configuration always involves the precision determination of the geometric shape of their walls, in particular, this applies to biological objects with high anatomical variability. Therefore, an urgent task is to study the peculiarities of the segmentation of the upper respiratory tract sections according to computer tomography data.

The purpose of the work is to study the features of the segmentation of the upper respiratory tract to determine nasal conduction.

1. Analysis of literature

Well-known specialists in the field of rhinology [13, 24] are dedicated to research in the field of nasal aerodynamics in the diagnosis of diseases of the upper respiratory tract. The latest data were the study of the characteristics of the nasal cavity using CFD methods and the verification of modeling results with clinical signs, as well as the prediction of functional results in rhinosurgery [8, 9]. The planning approaches of functional operative rhinosurgical interventions are being improved [20, 27]. The influence of the anatomical structure and changes in the architecture of the nose on the aerodynamics of the nasal cavity [11, 28], odontogenic sinusitis [18, 21], and sleep apnea syndrome

[2, 15], is being investigated. The simulation of the nasal cavity and the corresponding study of the characteristics of the air flow during breathing are carried out [6, 22].

Many works [24] are also dedicated to the methods of functional testing of nasal breathing, in particular to the methods of front [10, 24] and rear active rhinomanometry, which allow obtaining data on the coefficient of aerodynamic nasal resistance in different breathing modes. The principles of construction of rhinomanometry equipment and features of its use are considered, in particular, errors in the measurement of respiratory parameters. Evidential studies of respiratory and olfactory function are being conducted [5, 12, 29]. The issues of acoustic rhinometry in the non-invasive determination of the configuration of the nasal cavity [8, 26, 30] and natural 3D modeling of the upper respiratory tract [4, 19] and intelligent analysis of geometric data [14] are also considered. These approaches make it possible to study the personalized functional capacity of the upper respiratory tract to pass air in certain breathing modes, as well as to conduct an analysis of the adequacy of therapy [8, 27].

In general, the vast majority of approaches to studying the aerodynamics of the upper respiratory tract are aimed at building CFD models and their virtual tests. For this, various methods are used to obtain the configuration of the nasal cavity, such as X-ray computed tomography (the most common) and other medical imaging methods, such as acoustic rhinometry. The latter is non-invasive (does not involve X-ray radiation), but in some cases, due to overprints, it causes a large error in determining the boundaries of the airways. In recent years, after the widespread introduction of 3D prototyping methods, the approach of printing personalized full-scale models of the nasal cavity and testing them on aerodynamic stands to determine the corresponding pressure losses has been adopted. But the high adequacy of full-scale modeling of the nasal cavity is possible only when printing models that fully imitate the properties of both the mucous membrane and the mobile structures of the external nose, which requires the use of different materials for printing and complicates the process of making such models. The authors propose a discrete mathematical model of one-dimensional air flow in the nasal cavity, which allows analytically and more visually to investigate the coefficient of aerodynamic nasal resistance in each cross-section according to its equivalent hydraulic diameter. The reliability of such simulations, both CFD and natural, depends on the correct definition of the configuration of the nasal cavity. However, the peculiarities of creating aerodynamic models of the upper respiratory tract, the construction of which directly depends on the accuracy of the presentation of the geometric configuration of the nasal cavity, remain unsolved issues [1, 3].

Therefore, it is appropriate to consider the features of the segmentation of the airways of the nasal cavity for the construction of aerodynamic models for determining nasal conductivity [28].

2. Materials and methods

X-ray spiral computed tomography SOMATOM + E-motion of SIEMENS firm (Germany) on the basis of the Otorhinolaryngology Department of the Kharkiv Regional Clinical Hospital was used for endoscopic studies. Scanning was performed parallel to the orbito-meatal line with a step of 1 mm between slices and a spatial resolution in the slice plane of 0.4 mm. The raw data were obtained in DICOM format with the image size of slices 512×512 elements. Next, multiplanar reconstructions were performed in the frontal plane with a step of 2 mm parallel to the sections that are perpendicular to the air flow throughout the nasal cavity during breathing. An analytical model of one-dimensional air flow in the nasal cavity was used to build the aerodynamic model.

The error of the tomographic reconstruction on the used equipment was 0.2 mm (half of the voxel size in the slice plane). This is approximately 2% of the typical linear size (10 mm) of nasal airway cross-sections on most slices. The error in the frontal reconstruction is 1 mm in the distance between the slices, the error in the vertical direction is 0.5 mm (approximately 5% of the measured characteristic size).

Analytical determination of the coefficient of aerodynamic resistance of the nasal cavity is based on the assumption that the airways of the nose are considered as two parallel channels. The total air flow is the sum of the flow through the left Q_L and right Q_R nasal passages, respectively.

$$Q_\Sigma = Q_L + Q_R \tag{1}$$

and the pressure drops are the same for the left Δp_L and right Δp_R nasal canals.

$$\Delta p = \Delta p_L = \Delta p_R \tag{2}$$

At the same time, the nasal cavity is divided into sections that are perpendicular to the air flow, and the total pressure losses along the length $\sum \Delta p_{l_L}$, $\sum \Delta p_{l_R}$ and local (r-regional) $\sum \Delta p_{r_L}$, $\sum \Delta p_{r_R}$ are the sums of these resistances in each section. Therefore, in accordance with expression (1), taking into account the quadratic dependence of the pressure drop Δp on the air flow rate Q in the turbulent flow regime under most breathing modes, the pressure drops through each nasal passage will be determined by the following formulas [6, 7]

$$\begin{aligned}\Delta p_L &= Q_L^2 A_L = \sum \Delta p_{l_L} + \sum \Delta p_{r_L} = \\ &= \sum \lambda_L \cdot \rho \frac{L_L}{d_{e_L}} \frac{Q_L^2}{2S_L^2} + \sum \xi_L \cdot \rho \frac{Q_L^2}{2S_L^2}\end{aligned} \tag{3}$$

$$\begin{aligned}\Delta p_R &= Q_R^2 A_R = \sum \Delta p_{l_R} + \sum \Delta p_{r_R} = \\ &= \sum \lambda_R \cdot \rho \frac{L_R}{d_{e_R}} \frac{Q_R^2}{2S_R^2} + \sum \xi_R \cdot \rho \frac{Q_R^2}{2S_R^2}\end{aligned} \tag{4}$$

where λ_L, λ_R are the Darcy coefficients (pressure loss along the length) for the left and right nasal passages, respectively;

ξ_L, ξ_R are local resistance coefficients for the left and right nasal passages, respectively;

L_L, L_R are the lengths of the left and right nasal passages, respectively;

Q_L, Q_R – air flow through the left and right nasal passages, respectively;

ρ – air density;

d_{e_L}, d_{e_R} are the equivalent diameters of the left and right nasal passages, respectively, which are expressed for each intersection of the left and right nasal canals with the planes S_L, S_R and P_L, P_R perimeters, respectively, according to the formula, where * is replaced by *L* and *R*

$$d_{e_*} = \frac{4S_*}{P_*} \tag{5}$$

A_L, A_R – coefficients of aerodynamic nasal resistance for the left and right nasal channels, which are determined from formulas (3), (4) and (5) as

$$A_L = \sum \lambda_L \cdot \rho \frac{L_L}{d_{e_L} \cdot 2S_L^2} + \sum \xi_L \cdot \rho \frac{1}{2S_L^2} \tag{6}$$

$$A_R = \sum \lambda_R \cdot \rho \frac{L_R}{d_{e_R} \cdot 2S_R^2} + \sum \xi_R \cdot \rho \frac{1}{2S_R^2} \tag{7}$$

Figure 1 shows typical segmented cross-sections of the airways of the nasal cavity with a location near the nose (Fig. 1a), in the central area (Fig. 1b) and at the exit to the nasopharynx (Fig. 1c).

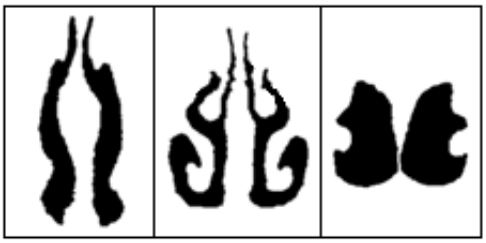

a) b) c)

Fig. 1. Typical segmented cross-sections of the airways of the nasal cavity with the location: a) near the crown; b) in the central area; c) when exiting the nasopharynx

Based on the fact that in the proposed model it is not possible to take into account the mutual influence of local resistances, only the largest of them is determined. The overall coefficient of aerodynamic nose drag was determined as with the parallel connection of two air ducts.

3. Results and discussion

From the above formulas (4)-(7) and taking into account the complexity of the configuration of the air channels of the nasal cavity in Fig. 1, it is obvious that the accuracy of determining the coefficients of aerodynamic nasal resistance depends on the accuracy of determining the parameters of the sections of the nasal passages, in particular the area and equivalent diameter. Therefore, special attention is paid to their definition when creating a mathematical model of the nasal cavity. Segmentation of the air regions of the upper respiratory tract on tomographic multiplanar reconstructive slices $B(\mathrm{x},\mathrm{y})$ is carried out according to the threshold level *T*, which corresponds to the air density in HU numbers, or directly according to the minimum level of brightness when setting the parameters of the soft tissue window of tomographic visualization.

$$F(\mathrm{x},\mathrm{y}) = \begin{cases} 1; & B(\mathrm{x},\mathrm{y}) \le \mathrm{T} \\ 0; & B(\mathrm{x},\mathrm{y}) > \mathrm{T} \end{cases} \tag{8}$$

where $F(\mathrm{x},\mathrm{y})$ is the binary characteristic function of air regions

An example of building a binary characteristic function of air regions for a tomographic section in figure 2a is given in figure 2b.

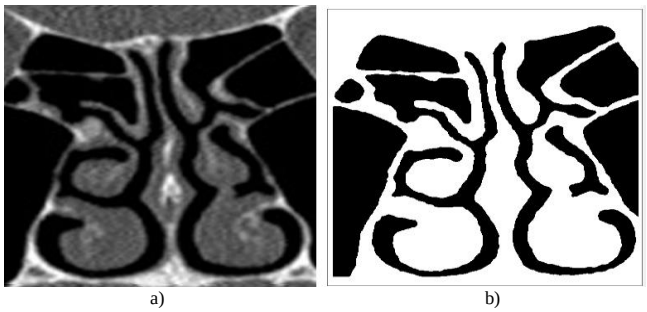

a) b)

Fig. 2. Illustration of the segmentation of the frontal section of the nasal cavity: a) input tomographic section; b) binary characteristic function of air regions

A three-dimensional visualization of the segmented airways of the nasal cavity is shown in figure 3. The original image clearly shows cavities containing air, but not all of them (for example, paranasal sinuses, conchobuloses) directly affect the aerodynamic processes in the upper respiratory tract and should be removed from the model, which will be discussed later. Determining contours of segmented structures is performed on already obtained binary images using differential operators

$$A_{px} = \begin{pmatrix} 1 & 0 \\ 0 & -1 \end{pmatrix};\ A_{py} = \begin{pmatrix} 0 & 1 \\ -1 & 0 \end{pmatrix} \tag{9}$$

or structured elements, or logical conditions of boundary features.

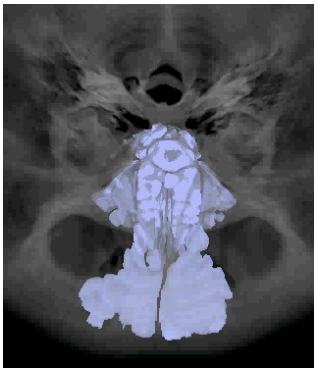

Fig. 3. Volumetric visualization of the segmented airways of the nasal cavity

A contour segmented image of the right half of the nasal cavity is shown in figure 4a. Figure 4b shows the corresponding contour image after thinning the border and removing unnecessary corner elements of the border according to the illustration in figure 5.

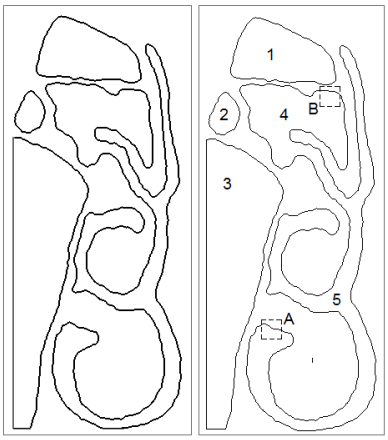

a) b)

Fig. 4. Illustration of the process of contour segmentation of the right half of the nasal cavity on the tomographic section from figure 2: a) input image after contour segmentation; b) the corresponding contour image after thinning the border and removing unnecessary corner elements of the border with designations of areas belonging to anatomical structures with designations (1, 2, 4 – cells of the clavicle, 3 – fragment of the maxillary sinus; 5 – nasal passage; A – designation of the area in lower nasal passage, B is the designation of the area in the cells of the ethmoid bone)

A contour model of nasal airway slices is shown in figure 6.

The algorithm for building a the contour model based on frontal multiplanar tomographic reconstructions is reduced to the following steps:

- segmentation of air cavities by intensity threshold;
- logical filtering of separate unconnected local disturbances of a small area and cavities that do not participate in aerodynamic processes, according to the method of determining the coefficients of difference of sections of segmented areas on different sections;
- processing of a segmented image by gradient operators;
- morphological post-processing to thin contours and eliminate discretization errors when determining the perimeter of the intersections.

As mentioned earlier, the main problem for fully automated segmentation of such data is that cavities that do not affect nasal aerodynamics remain in the output images. Their elimination can be carried out in the following sequential steps: perform multi-valued segmentation and eliminate unrelated objects (cells of the ethmoid bone with numbers 1, 2 and maxillary sinus 3) according to the example in figure 4b. But, if the obtained frontal tomographic section is located in the plane of the conjuncture of the parasinus (object 4 in Fig. 4b) and is directly connected to the airways of the nasal cavity (area 5 in Fig. 4b), then difficulties arise in its elimination.

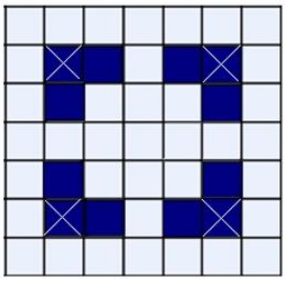

Fig. 5. Schematic illustration of the elimination of unnecessary corner elements of the border (indicated by hatching)

Performing successive operations of erosion and augmentation of areas to eliminate the co-mouth may not provide the required result with certain anatomical features and close values of the width of the co-mouth and the corresponding section of the nasal passage, as shown in the example from figures 2 and 4. Therefore, a differential technique is proposed at the next step, which takes into account the presence/absence of separate sections of objects at adjacent frontal intersections. At the same time, the coefficient of difference is calculated for each averaged section of the segmented upper respiratory tract for adjacent intersections with numbers *n* and *n-1*

$$k_n = M_n - M_{n-1} \tag{10}$$

where M_n and M_{n-1} are the averaged values of the characteristic function of image sections at adjacent intersections with numbers *n* and *n-1*, respectively. It is advisable to take the sizes of the plots as 3×3. Taking into account the absence of significant changes in the configuration of the nasal passages during the preliminary elimination of unrelated components of the paranasal sinuses on most sections, it is possible to deduce the empirical value of the difference coefficient threshold for areas that are absent on adjacent sections, which will be 0.25.

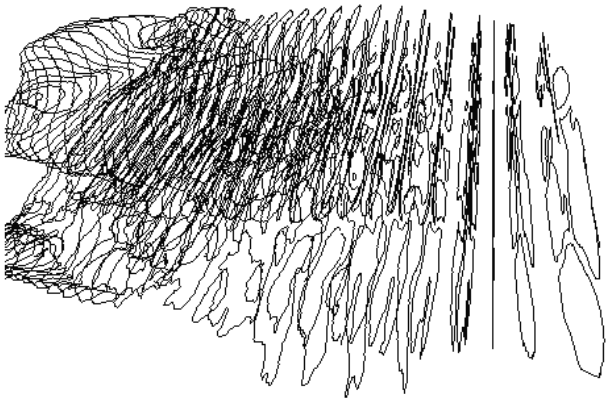

Fig. 6. Contour model of sections of the airways of the nasal cavity

An illustration of the values of the coefficient of difference k for sections A and B at the intersection with number n=24 is shown in figure 7. For the region of the lower nasal passage (A), the value of the coefficient of difference k is less than 0.25 and the section is correctly segmented; for the area of the accessory sinus of the ethmoid bone, the difference will be high (more than 0.9) due to the absence of the non-connected area of the sinus removed at the previous stage on the adjacent section. It is advisable to carry out the above calculations on the data of the binary characteristic function (Fig. 2b), the sections in Fig. 4b are shown for clarity. Based on the analysis of 110 tomographic datasets of the upper respiratory tract, manual actions during segmentation were performed in 23 cases, which was approximately 20%. At the same time, the main interactive operations were exclusion from the configuration of the model of various anatomical structures, in most cases – cells of the reticular labyrinth and correction of fine structures in the area of the upper nasal passage. With an average width of the nasal canal of about 10 mm, the spatial tomographic resolution is 0.4 mm, which immediately provides an error in determining diametrically opposite walls of about 8%.

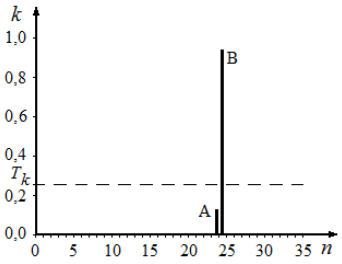

Fig. 7. Illustration of the values of the coefficient of difference k for sections A and B in figure 4, b (n – numbers of frontal intersections)

At the same time, it is expedient to use an algorithm that artificially increases the resolution by 2 times and performs manipulations on the image with the intensity of elements at sub-resolution according to the illustration in figure 8. According to this figure, at sub-resolution, an image element with intensity $B(x, y)$, which is in the border region to of a well-defined area with air, is divided into near $(x_n^{(s)}, y)$ and far $(x_f^{(s)}, y)$ elements during sub-resolution with the corresponding intensities $b(x_n^{(s)}, y)$ and $b(x_f^{(s)}, y)$.

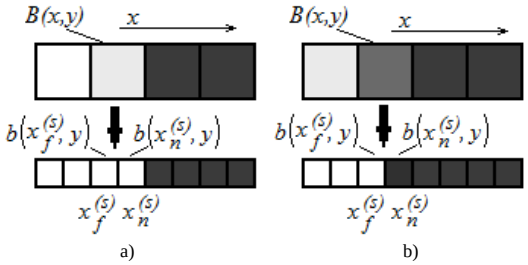

Fig. 8. Illustration of obtaining the intensity values of the contour elements of the image during the sub-resolution procedure ($B(x, y)$ input intensity of the input element of the image located in the boundary region to a clearly defined area with air; sub-resolution into near $(x_n^{(s)}, y)$ and $(x_f^{(s)}, y)$ far elements with corresponding intensities $b(x_n^{(s)}, y)$ and $b(x_f^{(s)}, y)$)

Moreover, the intensity of the subdistinct element close to the air section will be determined as

$$b(x_n^{(s)}, y) = \begin{cases} 1; & B(x, y) \le T_s \\ 0; & B(x, y) > T_s \end{cases} \tag{11}$$

where T_s is the threshold intensity value of the input element of the image, which can be about 18% of the maximum intensity in the image.

This approach makes it possible to eliminate the error from averaging during tomographic reconstruction of the image and increase the accuracy of determining the contour elements of the image up to 2 times (up to 4 percent). Areas *S* and perimeters *P* for each section of the nasal cavity are determined on the resulting segmented images for substitution in formulas (3) – (7). The area is defined as the sum of all values of the binary characteristic function at the intersection, and the perimeter taking into account linear n_l and diagonally n_d located contour elements according to the formula

$$P = n_l + \sqrt{2} \cdot n_d \tag{12}$$

This allows to reduce the error due to the separate consideration of the diagonal elements of the rectangular raster. When determining the area, the relative value of such elements will be insignificant and their individual contribution can be ignored. The resulting visualization of the contour at the intersection of the nasal canal after image processing in figures 2 and 4 is shown in figure 9, a. The initial surface visualization of both nasal channels is shown in figure 9b.

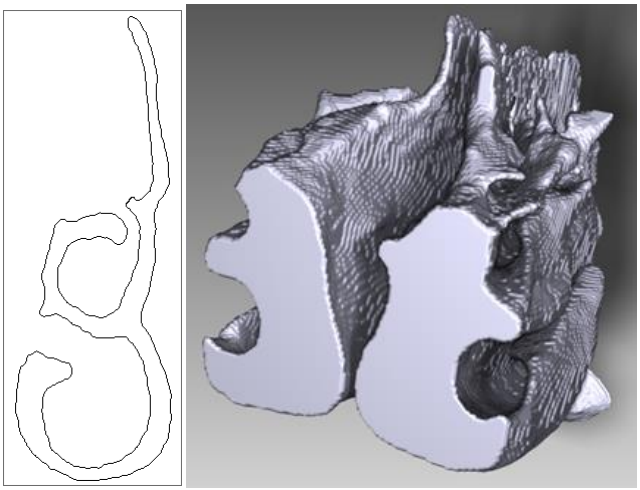

a) b)

Fig. 9. An example of the segmentation of the contours of the nasal canals: a) the resulting cross section of the nasal canal after image processing in figures 2 and 4; b) initial surface visualization of both nasal passages

4. Conclusions

When forming an analytical model of the aerodynamics of the nasal cavity, the main indicator that characterizes the configuration of the nasal canal is the equivalent diameter, which is determined at each intersection of the nasal cavity. It is calculated based on the area and perimeter of the corresponding section of the nasal canal. When segmenting the nasal cavity, it is first necessary to eliminate air structures that do not affect the aerodynamics of the upper respiratory tract – these are, first of all, intact spaces of the paranasal sinuses, in which diffuse air exchange prevails. In the automatic mode, this is possible by performing the elimination of disconnected isolated areas and finding the difference coefficients of the areas connected by mouths to the nasal canal in the next step. High coefficients of difference of sections between intersections will indicate the presence of separated areas and contribute to their elimination. The complex configuration and high individual variability of the structures of the nasal cavity does not allow segmentation to be fully automated, but this approach contributes to the absence of interactive correction in 80% of tomographic datasets. The proposed method, which takes into account the intensity of the image elements close to the contour ones, allows to reduce the averaging error from tomographic reconstruction up to 2 times due to artificial sub-resolution. The perspective of the work is the development of methods for fully automatic segmentation of the structures of the nasal cavity taking into account the individual anatomical variability of the upper respiratory tract.

References

[1] Aras A. et al.: Dimensional changes of the nasal cavity after transpalatal distraction using bone-borne distractor: an acoustic rhinometry and computed tomography evaluation. J. Oral Maxillofac. Surg. 68(7), 2010, 1487–1497.

[2] Avrunin O. G. et al.: Features of image segmentation of the upper respiratory tract for planning of rhinosurgical surgery. Paper presented at the 2019 IEEE 39th International Conference on Electronics and Nanotechnology, ELNANO 2019, 485–488.

[3] Avrunin O. G. et al.: Principles of computer planning in the functional nasal surgery. Przeglad Elektrotechniczny 93(3), 2017, 140–143 [http://doi.org/10.15199/48.2017.03.32].

[4] Avrunin O. G. et al.: Study of the air flow mode in the nasal cavity during a forced breath. Proc. of SPIE 10445, 2017 [http://doi.org/10.1117/12.2280941].

[5] Avrunin O. G. et al.: Possibilities of Automated Diagnostics of Odontogenic Sinusitis According to the Computer Tomography Data. Sensors 21, 1198, 2021 [http://doi.org/10.3390/s21041198].

[6] Berger M. et al.: Agreement between rhinomanometry and computed tomography-based computational fluid dynamics. International Journal of Computer Assisted Radiology and Surgery 16(4), 2021, 629–638 [http://doi.org/10.1007/s11548-021-02332-1].

[7] Cankurtaran M. et al.: Acoustic rhinometry in healthy humans: accuracy of area estimates and ability to quantify certain anatomic structures in the nasal cavity. Ann Otol. Rhinol. Laryngol. 116(12), 2007, 906–916.

[8] Churchill S. E. et al.: Morphological Variation and Airflow Dynamics in the Human Nose. Am. J. Of Hum. Biol. 16, 2004, 625–638.

[9] Cilluffo G., et al.: Assessing repeatability and reproducibility of anterior active rhinomanometry (AAR) in children. BMC Medical Research Methodology 20(1), 2020 [http://doi.org/10.1186/s12874-020-00969-1].

[10] Clement P. A.: Standardisation Committee on Objective Assessment of the Nasal Airway. Consensus report on 43, 2005, 169–179.

[11] Fyrmpas G. et al.: The value of bilateral simultaneous nasal spirometry in the assessment of patients undergoing. Rhinology 49(3), 2011, 297–303.

[12] Hsu Y. et al.: Role of rhinomanometry in the prediction of therapeutic positive airway pressure for obstructive sleep apnea. Respiratory Research 21, 2020, 115 [http://doi.org/10.1186/s12931-020-01382-4].

[13] Kang Y. J. et al.: The diagnostic value of detecting sudden smell loss among asymptomatic COVID-19 patients in early stage: The possible early sign of COVID-19. Auris Nasus Larynx 47(4), 2020, 565–573 [http://doi.org/10.1016/j.anl.2020.05.020].

[14] Kirichenko L. et al.: Machine learning in classification time series with fractal properties. Data 4(1), 2019, 5 [http://doi.org/10.3390/data4010005].

[15] Kuo C. J. et al.: Application of intelligent automatic segmentation and 3D reconstruction of inferior turbinate and maxillary sinus from computed tomography and analyze the relationship between volume and nasal lesion. Biomedical Signal Processing and Control 57, 2020, 101660 [http://doi.org/10.1016/j.bspc.2019.101660].

[16] Li C. et al.: Nasal structural and aerodynamic features that may benefit normal olfactory sensitivity. Chemical Senses 43(4), 2018, 229–237.

[17] Mlynski G. et al.: Correlation of nasal morphology and respiratory function. Rhinology 39(4), 2001, 197–201.

[18] Moghaddam M. G.et al.: Virtual septoplasty: A method to predict surgical outcomes for patients with nasal airway obstruction. International Journal of Computer Assisted Radiology and Surgery 15(4), 2020, 725–735 [http://doi.org/10.1007/s11548-020-02124-z].

[19] Ohlmeyer S. et al.: Cone beam CT imaging of the paranasal region with a multipurpose X-ray system-image quality and radiation exposure. Applied Sciences 10(17), 2020, 5876 [http://doi.org/10.3390/app10175876].

[20] Ott K.: Computed tomography of adult rhinosinusitis. Radiologic Technology 89(6), 2018, 571–593.

[21] Paul M. A. et al.: Assessment of functional rhinoplasty with spreader grafting using acoustic rhinomanometry and validated outcome measurements. Plastic and Reconstructive Surgery – Global Open. 6(3), 2018, p e1615 [http://doi.org/10.1097/GOX.0000000000001615].

[22] Pavlov S. V. et al.: Information Technology in Medical Diagnostics. CRC Press, 2017.

[23] Radulesco T. et al.: Correlations between computational fluid dynamics and clinical evaluation of nasal airway obstruction due to septal deviation: An observational study. Clinical Otolaryngology 44(4), 2019, 603–611 [http://doi.org/10.1111/coa.13344].

[24] Romanyuk S. et al.: Using lights in a volume-oriented rendering. Proc. of SPIE 10445, 2017, 104450U.

[25] Rovira J. R. et al.: Methods and resources for imaging polarimetry. Proc. of SPIE 8698, 2012, 86980T.

[26] Tang H. et al.: Dynamic Analysis of Airflow Features in a 3D Real-Anatomical Geometry of the Human Nasal Cavity. 15th Australasian Fluid Mechanics Conference, University of Sydney, Australia, 2004.

[27] Toriumi D.M.: Assessment of rhinoplasty techniques by overlay of before-and-after 3D images. Facial Plast Surg Clin North Am. 19(4), 2011, 711–723.

[28] Valtonen O. et al.: Three-dimensional printing of the nasal cavities for clinical experiments. Scientific Reports 10, 2020, 502 [http://doi.org/10.1038/s41598-020-57537-2].

[29] Vogt K., Jalowayski A. A.: 4-Phase-Rhinomanometry Basics and Practice. Rhinology 21, 2010, 1–50.

[30] Wójcik W., Pavlov S., Kalimoldayev M.: Information Technology in Medical Diagnostics II. London: Taylor & Francis Group, CRC Press, Balkema book, 2019.

[31] Zhang G. et al.: Correlation between subjective assessment and objective measurement of nasal obstruction. Zhonghua 43(7), 2008, 484–489.

D.Sc. Oleg Avrunin
e-mail: oleh.avrunin@nure.ua

Doctor of technical sciences, professor, Head of Biomedical Engineering Department, Kharkiv National University of Radio Electronics, Ukraine. Scientific supervisor of research work on research of theoretical and technical principles of diagnostics, assessment and correction of medical and social human conditions. Invited Professor in Gottfried Wilhelm Leibniz Universität Hannover (Germany) and Harbin Engineering University (China).

http://orcid.org/0000-0002-6312-687X

Oleksandr Avrunin
e-mail: oleksandr.avrunin@nure.ua

Student of the Department of Electronic Computers, Faculty of Computer Engineering, Kharkiv National University of Radio Electronics, Ukraine.
Research interests: information technologies in healthcare, signal processing and images, functional diagnostics of nasal breathing.

http://orcid.org/0000-0002-5202-0770

Ph.D. Yana Nosova
e-mail: yana.nosova@nure.ua

Ph.D., senior lecturer of the Department of Biomedical Engineering, Kharkiv National University of Radio Electronics, Ukraine. As part of the team of authors of the patent "Device for the testing of respiratory disorders of smell" was awarded the diploma of the winner of the All-Ukrainian contest "Invention of the Year – 2016" in the nomination "Best invention in Kharkiv region". Research Interests: biomedical signal processing and images.

http://orcid.org/0000-0003-4310-5833

Ph.D. Svetlana Kyrylashchuk
e-mail: ksa07750@gmail.com

Candidate of pedagogical sciences, Dean of the Faculty of Information Technologies and Computer Engineering, Associate Professor of the Higher Mathematics Department of the Vinnytsia National Technical University.
Scientific direction: methodology for the development of engineering thinking during the teaching of higher mathematics.

http://orcid.org/0000-0002-8972-3541

Ph.D. Nataliia Shushliapina
e-mail: schusha75@ukr.net

Ph.D., associate professor of Department of Otolaryngology, Kharkiv National Medical University.
Research interests: diagnostics of respiratory-olfactory disorders, functional chronology, connection of microcirculation with chronic diseases of the nasal cavity, computer planning of rhinosurgical interventions, intellectual training systems in otorhinolaryngology.

http://orcid.org/0000-0002-6347-3150

Ph.D. Olha Moskovchuk
e-mail: moskovchuk.olga11@gmail.com

Assistent, Ph.D., Vinnytsia Mykhailo Kotsiubynskyi State Pedagogical University, Department of Pedagogy, Professional Education and Management of Educational Institutions, Vinnitsa, Ukraine.
Research interests: information technology, methodology for the development of engineering thinking during the teaching of higher mathematics.

http://orcid.org/0000-0003-4568-1607

M.Sc. Ibrahim Younouss Abdelhamid
e-mail: ibrahim.younouss.abdelhamid@nure.ua

Ph.D. student, Department of Biomedical Engineering, Kharkiv National University of Radio Electronics. Research interests: biomedical signal processing and images, functional diagnostics of nasal breathing.

http://orcid.org/0000-0003-2611-2417

Ph.D. Orken Mamyrbayev
e-mail: morkenj@mail.ru

Deputy General Director in science and Head of the Laboratory of Computer Engineering of Intelligent Systems at the Institute of Information and Computational Technologies of the Kazakh National Technical University named after K. I. Satbayev and associate professor in 2019 at the Institute of Information and Computational Technologies.
Main research field: machine learning, deep learning, and speech technologies.

http://orcid.org/0000-0001-8318-3794

http://doi.org/10.35784/iapgos.3246 received: 6.11.2022 | revised: 11.12.2022 | accepted: 15.12.2022 | available online: 30.12.2022

THE USE OF Q-PREPARATION FOR AMPLITUDE FILTERING OF DISCRETED IMAGE

Leonid Timchenko[1], Natalia Kokriatskaia[1], Mykhailo Rozvodiuk[2], Volodymyr Tverdomed[1], Yuri Kutaev[1], Saule Smailova[3], Vladyslav Plisenko[1], Liudmyla Semenova[1], Dmytro Zhuk[1]

[1]State University of Infrastructure and Technology, Kyiv, Ukraine, [2]Vinnytsia National Technical University, Vinnytsia, Ukraine, [3]D.Serikbayev East Kazakhstan State Technical University, Ust-Kamenogorsk, Kazakhstan

Abstract. *The article was aimed at improving the amplitude filtering process of the sampled image through the use of generalized Q-preparation. The existing correlation algorithms for image preprocessing were analyzed and their advantages and disadvantages were identified. The process of amplitude filtering and the main methods of preprocessing with such filtering were considered. A method of amplitude filtering of images based on the generalized Q-transformation with the use of sum-difference preprocessing of images has been developed. The efficiency of this method was analyzed, and a variant of the scheme for the corresponding preprocessing of images was proposed. The efficiency of the method was confirmed by computer simulation.*

Keywords: amplitude filtering, generalized Q-preparation, correlation algorithms

ZASTOSOWANIE Q-PREPARACJI DO FILTROWANIA AMPLITUDOWEGO ZDYSKRETYZOWANEGO OBRAZU

Streszczenie. *Artykuł miał na celu usprawnienie procesu filtrowania amplitudy zdyskretyzowanego obrazu za pomocą uogólnionej Q-preparacji. Przeanalizowano istniejące algorytmy korelacji do wstępnego przetwarzania obrazu i określono ich wady i zalety. Omówiono proces filtracji amplitudowej oraz główne metody wstępnego przetwarzania z taką filtracją. Opracowano metodę filtrowania amplitudowego obrazów w oparciu o uogólnioną transformację Q z wykorzystaniem wstępnego przetwarzania obrazów na podstawie różnic sumy. Przeanalizowano skuteczność tej metody i zaproponowano wariant odpowiedniego schematu wstępnego przetwarzania obrazu. Skuteczność metody została potwierdzona symulacją komputerową.*

Słowa kluczowe: filtrowanie amplitudy, uogólniona Q-preparacja, algorytmy korelacji

Introduction

Pattern recognition is a relevant and promising area of information technologies, the scope of its application is expanding every year. In turn, recognition has separate tasks that must be solved in order to obtain the most accurate result. This includes the recognition [2, 11, 13] process itself, image preprocessing for detecting and eliminating interference, dividing image into segments, real-time recognition, etc. One of the urgent tasks in the field of pattern recognition is the task of creating correlation systems for automatic measurement of coordinates [5, 6]. In such systems, the functional of linking the current image and the reference image is calculated, as well as the coordinates of the extremum of this functional are determined. Among the advantages of such systems is the fact that they provide the ability to work in conditions of great uncertainty in the noise-signaling environment and provide resistance to the influence of decorrelating factors. Such factors can be: noise, uneven sensitivity, geometric distortions of the video sensor, errors in analog-to-digital conversion, etc [1, 7, 9].

Thus, the development and improvement of such systems makes it possible to recognize signals or images more accurately due to filtering under the influence of various environmental noises. The existing methods have their drawbacks, which can be eliminated using the method presented in the article, namely, using amplitude filtering using Q-preparation [3, 6, 8].

1. Analysis of literature data and problem statement

Modern image recognition systems are characterized by work in a difficult jamming environment. When designing such systems, can often encounter the problem of detecting signals in noise when their characteristics are not known in advance or are subject to changes. Signals in such systems are functions of two spatial coordinates and time and are called images. Correlation algorithms are very often used in such problems; the physical meaning of correlation processing in this case consists in combining images.

There are many correlation algorithms [1, 10, 17], the main ones are:

- optimal spatial filtration,
- background correlation,
- binary correlation,
- correlation of conversion factors,
- optical matched filter,
- three-dimensional correlation,
- combination of relative information vectors,
- combination of structural models.

With optimal spatial filtering, images are filtered to optimize registration. Optimal filters are constructed using typical images. The advantages of this method are the increased ratio of the main peak of the correlation function to the side lobes, the homogeneity of the side lobes, and the possibility of an analytical description. At the same time, the disadvantages of this method are that it is based on the knowledge of the gray level of the image, and the design of the filter requires the estimation of noise statistics [15].

Background correlation is a real correlation using the inverse Fourier transform of the mutual energy spectrum of the phase. The advantages of this correlation method are: sharp correlation peaks, implementation efficiency, and lack of sensitivity to narrowband noise. However, the method requires prediction of the gray level of the images and requires a broadband image plot [4, 16, 19].

For binary correlation, images are preliminarily converted into binary form. The method provides an efficient implementation and desensitization to errors in gray level prediction. In this case, the information content of the images decreases due to the transition to binary images, and there is a need to implement the prediction of the gray level of images.

The correlation of transform coefficients provides processing using the algorithm of the minimum absolute difference of the Hadamard coefficients of the reference and current images. Due to this, an increase in the sharpness of the peak and a decrease in sensitivity to noise are achieved. In this case, the method requires prediction of the gray level and gives an increase in the amount of computation [18].

An Optical Matched Filter is an analog matched filter using coherent light processing. The method provides almost instantaneous correction, has an extremely large amount of memory, and implements parallel processing of several reference images. The disadvantages are that it is based on gray level prediction, with the processing flexibility being limited by the hardware implementation [7, 20, 21].

Three-dimensional correlation combines a three-dimensional target model and active rangefinder data. No gray prediction is required here. The method can take into account all possible approaches to the approach and is insensitive to deliberate changes in target attributes. However, it requires a range sensor and a significant amount of computation.

The alignment of relative information vectors is based on maximizing the number of corresponding information-relative vectors. No gray prediction is required here. The method includes three-dimensional objects and is insensitive to contrast inversion. The disadvantage is that you need to implement feature extraction, the method is sensitive to noise, and the analytical description is difficult [6, 14].

When structural models are combined, feature models (lines, segments, tops, spots) are combined. The method does not require prediction of gray levels, is insensitive to contrast inversion, and has minimal memory requirements. However, it is necessary to implement feature extraction, the method is sensitive to noise, and the analytical description of the characteristics is difficult.

The classical algorithm for correlation image processing is understood as the calculation of a cross-correlation function or a convolution-type integral with the subsequent search for the maximum of this function. The disadvantage of the classical algorithm is a large amount of computation, since the calculation of the cross-correlation function is performed for all possible relative shifts of the processed images [1, 23]. Moreover, if the dimensions of the image are equal to M×M, N×N, then the number of points for which the correlation function is calculated is$(N - M + 1)^2$. This number is usually significant.

In the process of preprocessing a sampled image, the most important task is to filter the amplitude and geometric noise [1], which are the result of external and internal noise influences on the processes of formation, registration, transformation and transmission of sampled images.

Amplitude noise distorts the value of the samples in the image of an object, while geometric noise changes the number and location of the samples associated with this image, i.e. samples exceeding, for example, the general signal detection threshold [1]. For each of these types of noise, there are separate methods for preprocessing (filtering) images.

In a number of applied problems of the theory of pattern recognition, preprocessing methods are used based on the formation of a difference image with its subsequent threshold preprocessing: delta modulation [1, 13], generalized contour preparation, contouring [7, 12], etc. All of them lead to an increase in the noise level of the transformed Images.

There are also heuristic preprocessing methods, their essence lies in the summation of local groups of samples of the converted image. But there are problems with their implementation. The first is to combine the operations of nonlinear difference of image preprocessing and averaging of local groups of samples to reduce image noise. The second problem is the creation of a processor element with a universal structure for a homogeneous processor environment, which will be suitable for performing sum-difference preprocessing operations. The last problem is related to determining the optimal sizes$P_{opt} \times q_{opt}$ a local group of image samples, averaged according to heuristic-type smoothing algorithms [8, 9], or a preprocessing algorithm using the partial Q-summation method.

Thus, the analysis shows that the existing methods of correlation are processing and image preprocessing have a number of disadvantages. This article proposes a method for amplitude filtering images to help avoid them [10, 22].

2. The purpose and objectives of the study

The article is focused on the development of a method for amplitude filtering of images. The proposed method uses a generalized Q-preparation, previously passed the sum-difference preprocessing of the type H_C, H_L or H_C, H_G ($\sum Q\Delta$-processing and $\sum Q\nabla$-processing, respectively).

To achieve this goal, it is necessary to consider the process of amplitude filtering of images, existing preprocessing methods for amplitude filtering, select one of them and develop an appropriate filtering method using generalized Q-preparation.

3. Materials and research methods

Amplitude filtering of a sampled image is a transformation of the amplitude of the central sample of a local group of samples according to the sample mean value of the amplitude of the sample of this group.

In accordance with this, the following preprocessing methods are used:

- averaging over the neighborhood of the elements,
- differential preprocessing in the neighborhood of elements,
- sum-difference preprocessing in the neighborhood of elements.

3.1. Averaging over the neighborhood of the elements

Spatial decorrelation of noise makes it possible to use efficient, easy-to-implement algorithms for averaging over the local neighborhood of elements based on the convolution of the original image $G(m,n) = \{g_{m,n}\}$, where $m = 0, 1, \dots, M_1 = \overline{0, E_1}$ and $n = \overline{0, N_1}$ with array $H(a,c) = \{h_{a,c}\}$, where $|a| \le K_a > 0, |c| \le c > 0 \; and \; h_{a,c} > 0$

$$\tilde{g}_{m,n} = \frac{1}{N_h}\sum_a \sum_c g_{m+a,n+c} h_{a,c} \tag{1}$$

where $N_h = \sum_a \sum_c h_{a,c}$ is the normalizing divider to exclude the shift of the mean value of the samples $\tilde{g}_{m,n}$ of the transformed image $\tilde{G}(m,n) = \{g_{m,n}\}$.

Most commonly used masks $H(a,c)$[17]

$$\frac{1}{9}\begin{bmatrix}1 & 1 & 1\\ 1 & 1 & 1\\ 1 & 1 & 1\end{bmatrix}; \frac{1}{10}\begin{bmatrix}1 & 1 & 1\\ 1 & 2 & 1\\ 1 & 1 & 1\end{bmatrix}; \frac{1}{16}\begin{bmatrix}1 & 2 & 1\\ 2 & 4 & 2\\ 1 & 2 & 1\end{bmatrix} \tag{2}$$

The use of these masks reduces the variance of the additive normal noise by $9 \div 7$, respectively, however, complicates the practical implementation of the filter due to the inclusion in (1) of samples diagonally located to the sample to be smoothed, and also due to the inconvenience of dividing by 9 for mask (2) when using traditional binary or binary-decimal system of coding image samples. In addition, these masks do not provide suppression of local noise spikes.

Therefore, the smoothing algorithm includes the following procedure

$$\tilde{g}_{m,n} = \begin{cases} g_{m,n}, \left|g_{m,n} - \bar{g}_{m,n}\right| \le \varepsilon \\ \bar{g}_{m,n}, \left|g_{m,n} - \bar{g}_{m,n}\right| > \varepsilon \end{cases} \tag{3}$$

where:

$\bar{g}_{m,n} = \frac{1}{8}\sum_a \sum_c g_{m+a,n+c}(a,c) \neq (0,0)$, $\varepsilon > 0$ for example, ε does not exceed $\frac{1}{4}$ of the maximum possible value of $g_{m,n}$.

Given the above, it seems appropriate using simpler smoothing masks as follows kind:

$$\frac{1}{5}\begin{bmatrix}0 & 1 & 0\\ 1 & 1 & 1\\ 0 & 1 & 0\end{bmatrix}; \frac{1}{4}\begin{bmatrix}0 & 1 & 0\\ 1 & 0 & 1\\ 0 & 1 & 0\end{bmatrix} \tag{4}$$

In this case, along with the limiting simplification of practical implementation, the deterioration of smoothing to ~ 2.25 times (estimated by variance) in comparison with the previously considered masks can be compensated for by subsequent processing.

3.2. Difference preprocessing based on the neighborhood of elements

Fig. 1 shows the masks corresponding to some currently widespread types of local difference image preprocessing by neighborhood 3×3 element. In this case, the differences in direction, the Laplacian and the gradient for the masks (Fig. 1) are respectively defined as follows:

$$\Delta^{(0,1)}g_{m,n} = \left|\left(g_{m-1,n+1} + g_{m,n+1} + g_{m+1,n+1}\right) - \right.$$
$$\left. - \left(g_{m-1,n-1} + g_{m,n-1} + g_{m+1,n-1}\right)\right| \quad (5)$$

$$\Delta^{(1,0)}g_{m,n} = \left|\left(g_{m-1,n+1} + g_{m-1,n} + g_{m-1,n-1}\right) - \right.$$
$$\left. - \left(g_{m+1,n+1} + g_{m+1,n} + g_{m+1,n-1}\right)\right| \quad (6)$$

$$\Delta g_{m,n} = \frac{1}{8}\left(-\sum_a \sum_c g_{m+a,n+c} + 8g_{m,n}\right), (a,c) \neq (0,0) \quad (7)$$

$$\Delta g_{m,n} = \left(-\sum_a \sum_c g_{m+a,n+c} + 4g_{m,n}\right), (a,c) \neq (0,0) \quad (8)$$

$$\nabla g_{m,n} = \left|g_{m,n} - g_{m+1,n}\right| + \left|g_{m,n} - g_{m,n+1}\right| \quad (9)$$

$$\begin{matrix}\begin{bmatrix}0 & -1 & 0\\ -1 & 5 & -1\\ 0 & -1 & 0\end{bmatrix} & \begin{bmatrix}-1 & -1 & -1\\ -1 & 9 & -1\\ -1 & -1 & -1\end{bmatrix} & \begin{bmatrix}1 & -2 & 1\\ -2 & 5 & -2\\ 1 & -2 & 1\end{bmatrix}\\ a) & b) & c)\end{matrix}$$

$$\begin{matrix}\begin{bmatrix}0 & 0 & 0\\ 0 & 1 & 0\\ -1 & 0 & 0\end{bmatrix} & \begin{bmatrix}0 & 0 & 0\\ 0 & 1 & 0\\ 0 & -1 & 0\end{bmatrix} & \begin{bmatrix}0 & 0 & 0\\ 0 & 1 & 0\\ 0 & 0 & -1\end{bmatrix} & \begin{bmatrix}0 & 0 & 0\\ 0 & 1 & -1\\ 0 & 0 & 0\end{bmatrix}\\ d) & e) & f) & g)\end{matrix}$$

$$\begin{matrix}\begin{bmatrix}1 & 1 & 1\\ 0 & 0 & 0\\ -1 & -1 & -1\end{bmatrix} & \begin{bmatrix}1 & 0 & -1\\ 1 & 0 & -1\\ 1 & 0 & -1\end{bmatrix} & \frac{1}{8}\begin{bmatrix}-1 & -1 & -1\\ -1 & 8 & -1\\ -1 & -1 & -1\end{bmatrix}\\ h) & i) & j)\end{matrix}$$

$$\begin{matrix}\begin{bmatrix}0 & -1 & 0\\ -1 & 4 & -1\\ 0 & -1 & 0\end{bmatrix} & \begin{bmatrix}0 & -1 & 0\\ 0 & 2 & -1\\ 0 & 0 & 0\end{bmatrix} & \begin{bmatrix}0 & -1 & 0\\ -1 & 4 & -1\\ 0 & -1 & 0\end{bmatrix}\\ k) & l) & m)\end{matrix}$$

Fig. 1. Local differential processing masks

Note that the quasi-Laplacian masks used here and below (Fig. 1) differ from the corresponding masks (Fig. 1) of the mathematical definition of the Laplacian (11) by the presence of a factor $\frac{1}{N_h}$ (N_h equals 8 or 4) averaging the pairwise differences between the central sample and the samples corresponding to the coefficients –1 of the filter of the following masks:

$$\underset{H_{L8}}{\frac{1}{8}\begin{bmatrix}-1 & -1 & -1\\ -1 & 8 & -1\\ -1 & -1 & -1\end{bmatrix}};\ \underset{H_{L4P}}{\frac{1}{4}\begin{bmatrix}0 & -1 & 0\\ -1 & 4 & -1\\ 0 & -1 & 0\end{bmatrix}};\ \underset{H_{L4D}}{\frac{1}{4}\begin{bmatrix}-1 & 0 & -1\\ 0 & 4 & 0\\ -1 & 0 & -1\end{bmatrix}} \quad (10)$$

Calculation of the quasi-Laplacian according to the mask H_{L4P} is simpler than calculating it according to the masks H_{L8} and H_{L4D}. Masks H_{L8} and H_{L4P} insignificantly, no more than 1.25 times, increase the noise variance; therefore, their use is advisable for low-noise images. Similarly to the masks of the quasi-Placian, we introduce the masks of the quasi-gradient H_{G8}, H_{G4P} and H_{G4D}:

$$\underset{H_{G8}}{\frac{1}{4}\begin{bmatrix}1 & 1 & 1\\ 1 & 0 & -1\\ -1 & -1 & -1\end{bmatrix}};\ \underset{H_{G4P}}{\frac{1}{2}\begin{bmatrix}0 & 1 & 0\\ 1 & 0 & -1\\ 0 & -1 & 0\end{bmatrix}};\ \underset{H_{G4D}}{\frac{1}{2}\begin{bmatrix}1 & 0 & -1\\ 0 & 0 & 0\\ 0 & 0 & -1\end{bmatrix}} \quad (11)$$

Calculating the quasi-gradient according to the mask H_{G4P} is simpler than calculating it according to the masks H_{G8} and H_{G4D}.

3.3. Sum-difference preprocessing by the neighborhood of elements

For noisy images, before calculating the quasi-Placian or quasi-gradient, it is advisable to pre-smooth the noise with appropriate masks:

$$\underset{H_{C8}}{\frac{1}{8}\begin{bmatrix}1 & 1 & 1\\ 1 & 0 & 1\\ 1 & 1 & 1\end{bmatrix}};\ \underset{H_{C4P}}{\frac{1}{4}\begin{bmatrix}0 & 1 & 0\\ 1 & 0 & 1\\ 0 & 1 & 0\end{bmatrix}};\ \underset{H_{C4D}}{\frac{1}{4}\begin{bmatrix}1 & 0 & 1\\ 0 & 0 & 0\\ 1 & 0 & 1\end{bmatrix}} \quad (12)$$

Let us find a reduction in image noise by sequentially applying one of the smoothing masks (14) and one of the differential preprocessing masks (12) or (13). For this, consider the neighborhood 5× 5 elements *mn*-th image element, which corresponds to a set of readings $\{q_{m+a,n+c}\}$, $a = \overline{-2.2}$, $c = \overline{-2.2}$. As an example, consider the sequential application of masks H_{C8} and H_{L8}:

$$\tilde{q}_{m+a1,n+c1} = \sum_{a_2}\sum_{c_2} q_{m+a_1+a_2,n+c} \cdot h_{c_8,a_1+a_2,c_1+c_2},$$
$$a_2 = -\overline{1.1}, c_2 = -\overline{1.1} \quad (13)$$

The equivalent calculation mask according to (15) is shown in Fig. 2.

Equivalent computation masks for other possible combinations of smoothing masks and differential preprocessing masks are shown in Fig. 2 and Fig. 3, and the corresponding coefficients for reducing the noise variance in table 1 and 2.

To simplify the analysis, Fig. 2, 3 empty spaces are left in place of mask coefficients with zero values.

$$\begin{matrix}\frac{1}{64}\begin{bmatrix}-1 & -2 & -3 & -2 & -1\\ -2 & 6 & 4 & 6 & -2\\ -3 & 4 & -6 & 4 & -3\\ -2 & 6 & 4 & 6 & -2\\ -1 & -2 & -3 & -2 & -1\end{bmatrix} & \frac{1}{32}\begin{bmatrix} & -1 & -1 & -1 & \\ -1 & 2 & 2 & 2 & -1\\ -1 & 2 & -4 & 2 & -1\\ -1 & 2 & 2 & 2 & -1\\ & -1 & -1 & -1 & \end{bmatrix} & \frac{1}{32}\begin{bmatrix}-1 & -1 & -2 & -1 & -1\\ -1 & 4 & 2 & 4 & -1\\ -2 & 2 & -4 & 2 & -2\\ -1 & 4 & 2 & 4 & -1\\ -1 & -1 & -2 & -1 & -1\end{bmatrix}\\ a)\ (H_{C8}, H_{L8}) & b)\ (H_{C8}, H_{L4P}) & c)\ (H_{C8}, H_{L4D})\end{matrix}$$

$$\begin{matrix}\frac{1}{32}\begin{bmatrix} & -1 & -1 & -1 & \\ -1 & 2 & 6 & 2 & -1\\ -1 & 6 & -4 & 6 & -1\\ -1 & 2 & 6 & 2 & -1\\ & -1 & -1 & -1 & \end{bmatrix} & \frac{1}{16}\begin{bmatrix} & & -1 & & \\ & -2 & 4 & -2 & \\ -1 & 4 & -4 & 4 & -1\\ & -2 & 4 & -2 & \\ & & -1 & & \end{bmatrix} & \frac{1}{16}\begin{bmatrix} & -1 & & -1 & \\ -1 & 4 & 2 & 4 & -1\\ & 2 & & 2 & \\ -1 & 4 & 2 & 4 & -1\\ & -1 & & -1 & \end{bmatrix}\\ d)\ (H_{C4P}, H_{28}) & e)\ (H_{C4P}, H_{L4P}) & f)\ (H_{C4P}, H_{L4D})\end{matrix}$$

$$\begin{matrix}\frac{1}{32}\begin{bmatrix}-1 & -1 & -2 & -1 & -1\\ -1 & 8 & -2 & 8 & -1\\ -2 & -2 & -4 & -2 & -2\\ -1 & 8 & -2 & 8 & -1\\ -1 & -1 & -2 & -1 & -1\end{bmatrix} & \frac{1}{16}\begin{bmatrix} & -1 & & -1 & \\ -1 & & 2 & & -1\\ & 2 & & 2 & \\ -1 & & 2 & & -1\\ & -1 & & -1 & \end{bmatrix} & \frac{1}{16}\begin{bmatrix}-1 & & -2 & & -1\\ & 4 & & 4 & \\ -2 & & -4 & & -2\\ & 4 & & 4 & \\ -1 & & -2 & & -1\end{bmatrix}\\ g)\ (H_{C4D}, H_{L8}) & h)\ (H_{C4D}, H_{L4P}) & i)\ (H_{C4D}, H_{L4D})\end{matrix}$$

Fig. 2. Equivalent computation masks for possible combinations of smoothing masks and masks of differential preprocessing

Table 1. Combinations of masks and dispersion reduction factors

Combination of masks	H_{C8} H_{L8}	H_{C8} H_{L4P}	H_{C8} H_{L8D}	H_{C4P} H_{L8}	H_{C4P} H_{L4P}	H_{C4P} H_{L4D}	H_{C4D} H_{L8}	H_{C4D} H_{L4P}	H_{C4D} H_{L4D}
Dispersion reduction coefficient	11.91	11.07	8.26	5.45	2.56	2.91	8.26	10.67	2.56

$$\frac{1}{32}\begin{bmatrix}1&2&3&2&1\\2&2&2&&2\\3&&&&3\\2&&-2&-2&2\\1&2&3&2&1\end{bmatrix}\quad \frac{1}{16}\begin{bmatrix}&-1&1&1&\\1&2&&&-1\\1&&&&-1\\1&&&-2&-1\\&-1&-1&-1&\end{bmatrix}\quad \frac{1}{16}\begin{bmatrix}1&1&&-1&-1\\1&&&&-1\\2&2&&2&-2\\1&&&&-1\\1&1&&-1&-1\end{bmatrix}$$

$a)\ (H_{C8}, H_{G8})$ $b)\ (H_{C8}, H_{G4P})$ $c)\ (H_{C8}, H_{G4D})$

$$\frac{1}{32}\begin{bmatrix}&1&1&1&\\1&2&2&&1\\1&&&&-1\\-1&&-2&-2&-1\\&-1&-1&-1&\end{bmatrix}\quad \frac{1}{8}\begin{bmatrix}&&1&&\\&2&&&\\1&&&&-1\\&&&-2&\\&&-1&&\end{bmatrix}\quad \frac{1}{8}\begin{bmatrix}&1&&-1&\\1&2&&&-1\\&&&-2&\\1&&&&-1\\&1&&-1&\end{bmatrix}$$

$d)\ (H_{C4P}, H_{G8})$ $e)\ (H_{C4P}, H_{G4P})$ $f)\ (H_{C4P}, H_{G4D})$

$$\frac{1}{16}\begin{bmatrix}1&1&2&1&1\\1&&&&-1\\&&&&\\1&&&&-1\\-1&-1&-2&-1&-1\end{bmatrix}\quad \frac{1}{8}\begin{bmatrix}&1&&1&\\1&&&&-1\\&&&&\\1&&&&-1\\&-1&&-1&\end{bmatrix}\quad \frac{1}{8}\begin{bmatrix}1&&&&-1\\&&&&\\2&&&&-2\\&&&&\\1&&&&-1\end{bmatrix}$$

$g)\ (H_{C4D}, H_{G8})$ $h)\ (H_{C4D}, H_{G4P})$ $i)\ (H_{C4D}, H_{G4D})$

Fig. 3. Equivalent computation masks for possible combinations of smoothing masks and masks of differential preprocessing

Table 2. Combinations of masks and dispersion reduction factors

Combination of masks	H_{C8} H_{G8}	H_{C8} H_{G4P}	H_{C8} H_{G8D}	H_{C4P} H_{G8}	H_{C4P} H_{G4P}	H_{C4P} H_{G4D}	H_{C4D} H_{G8}	H_{C4D} H_{G4P}	H_{C4D} H_{G4D}
Dispersion reduction coefficient	11.64	12.8	9.14	9.14	5.33	4	12.8	8	5.33

From a comparison of the data table. 1 and 2, it follows that the combination of masks of local averaging and quasi-gradient gives, on average, a significantly greater noise reduction than the combination of masks of local averaging and quasi-gradient. It is important that the minimum value of the coefficient of variance reduction for table 2 is ≈1.6 times higher than its value for table 1 and not less than the value of this coefficient for a separate smoothing mask (8 – for H_{C8}, 4 - for H_{C4P} or H_{C4D}).

From the point of view of performing the total-difference processing of each type, according to table. 1 or 2, in a processor element with a universal structure, combinations of masks (H_{C8}, H_{L8}), (H_{C4P}, H_{G4P}), and (H_{C4D}, H_{G4D}) are attractive, while preprocessing for the last two combinations of masks is simpler in practical implementation.

3.4. Amplitude filtering of images using generalized Q-preparation

Of course, each of the images $G_l(m,n)$ be subjected to a generalized Q-preparation by the method of generalized Q-preparation (GQP) or partial Q-summation (PQS) [6], i.e. it does not take into account that this image was obtained as a result of sum-difference preprocessing.

However, taking into account the total-difference preprocessing when carrying out a generalized Q-transformation of an image, in particular, GQP, does not allow obtaining significant hardware savings without reducing the efficiency of subsequent processing of the prepared image, for example, when it is correlated-extreme comparison with the prepared reference image. In this case, taking into account the total-difference character of the GQP image converted by the method $G_l(m,n)$ Z ∈ *{l,g}* and using the concept of local difference threshold (LDT) (drop detection threshold), generalized Q-preparation is mathematically described as follows (Tab. 3):

$$\hat{g}_{zm,n} = \begin{cases} a^+, when\ g_{zm1n} \geq q \\ a^0, when\ \left|g_{Zm,n}\right| < q \\ a^-, when\ g_{zm1n} \leq -q \end{cases} \quad (14)$$

where $Z \in \{l, g\}, \hat{g}_{zm,n}$ is the readout of the generalized Q-preparation (GQP) $\hat{G}_{z(m,n)} = \{g_{zm,n}\}$ of the original image $\hat{G}_z(m_1 n)$.

The most compact is GQP, obtained as a result of rank signed delta modulation [11], for which the following takes place:

$$a^+ = a,\ a^0 = 0,\ a^- = -a \quad (15)$$

In this case, according to (19), signals with positive, zero and negative potential values, respectively, should correspond to the numbers a^+, a^0 and a^- in the medium for storing the GQP.

3.5. Research results

Let us consider the features of the representation of the elementary sections of the brightness surfaces by the GQP of the quasilaplacian and the quasi-gradient (Q_Δ and Q_∇, respectively), and it seems expedient to take areas of flat, cylindrical and spherical surfaces as reference surfaces. In this case, a flat surface is characterized by the constancy of derivatives along any two mutually orthogonal directions, a cylindrical surface is characterized by the constancy of an arbitrary one along one of two mutually orthogonal directions (which coincides with the direction of the generatrix of this surface), and a spherical surface is characterized by the variability of the derivative along any two mutually orthogonal directions.

Table 3.Values 00 of Q_∇ and Q_Δ of reference surfaces

Surface type / Countdown GQP	Sphere		Plane	Cylindrical	
	convex	concave		convex	concave
Q_∇	+, 0, - +	+, 0, - -	+, 0, - 0	+, 0, - +	+, 0, - -
Q_Δ	+	-	0	+	-

The division factor for the intensity of the fiber-optic switch 2 is 2. A variant of the circuit in Fig. 4 b is more preferable in terms of hardware costs and less complexity of connections between OPS.

These results were obtained from computer simulations of the obtained method of amplitude image filtering using generalized Q-preparation on the developed scheme (Fig. 4). The system was designed and the corresponding program was written in the C++ programming language. The program simulates the operation of the obtained method, using the sum-difference preprocessing in the vicinity of the elements. Various local difference thresholds were also used to check performance of the method. A set of reference images and images from the test

sample were used. Obtained earlier results were confirmed by simulation.

To check the effectiveness of the method, the reference and test images used in the simulation were processed by the main filtering methods discussed at the beginning of the paper. In comparison with the developed method, they provide less processing efficiency, namely, a larger amount of calculations, require more processing time, and have less system flexibility.

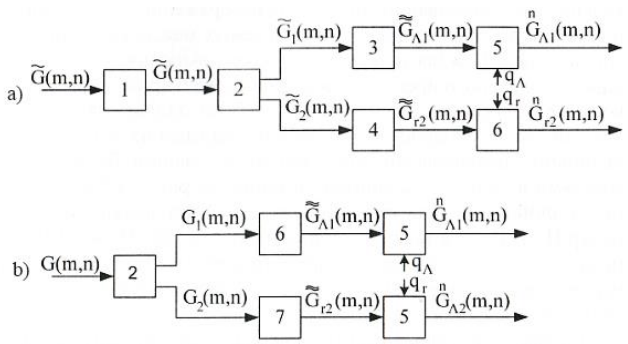

Fig. 4. Option of two-channel image preprocessing: 1, 3–7 – homogeneous processing environments for averaging, calculating Q_Δ and Q_∇ OQP, respectively; 2 – fiber optic switch

The use of other preprocessing methods for generalized Q-preparation of images was discussed above and confirms that the most effective for that purpose will be the sum-difference preprocessing using the local difference threshold.

The figure 5 shows an example of comparing two biomedical images over time using the proposed method.

Fig. 5. Comparing two biomedical images over time

3.6. Discussion of the results

The convenience of entering the characteristics Q_Δ and Q_∇ is explained by the properties of their local isotropy, that is, regardless of the direction when processing in a 3×3 window. Therefore, with GQP Q_Δ and Q_∇ in the learning process, there are no stages of optimization in terms of the magnitude and direction of the rank vector [1], which achieves a significant saving in time and hardware costs. At the same time, the adaptive properties of preprocessing to the information problem being solved remain high, both due to varying the value of LRS q, and due to the possibility of using the methods of generalized Q-transformation at the following levels of representation Q_Δ and Q_∇ the processed luminance image.

4. Conclusions

The article considered the recognition of sampled images in conditions of noise in the image. The analysis of the corresponding correlation preprocessing algorithms was carried out and their advantages and disadvantages were presented. Methods for filtering amplitude noise were considered and, accordingly, the goal and objectives of the study were set. The methods of preprocessing with amplitude filtering were considered. On their basis, using a generalized Q-preparation, an amplitude filtering method with a sum-difference image preprocessing was developed. Also was suggested the scheme of two-channel image preprocessing based on the developed method and was carried out computer simulation, which confirmed good performance and effectiveness of the method. The resulting method has a number of advantages. It provides significant savings in time and hardware costs due to the lack of optimization stages in terms of the magnitude and direction of the rank vector. Also, the high adaptive properties of preprocessing to the information problem being solved are preserved. Thus, the obtained method can be used for preprocessing discretized images when carrying out their amplitude filtering, while increasing the recognition efficiency.

The implementation of the Q-preparation principle is described in [15, 16, 19].

References

[1] Avrunin O. G., Nosova Y. V., Abdelhamid I. Y., Pavlov S. V., Shushliapina N. O., Bouhlal N. A., Harasim D.: Research active posterior rhinomanometry tomography method for nasal breathing determining violations. Sensors 21(24), 2021, 1–27.
[2] Bochkarev A. M.: Correlation-Navigation Navigation Systems. Foreign radio electronics 9, 1981, 12–16.
[3] Cai Y., Liu Z., Wang H., Sun X.: Saliency-Based Pedestrian Detection in Far Infrared Images. IEEE Access 5, 2017, 5013–5019.
[4] Dougherty E. R.: Digital Image Processing Methods. CRC Press, Boca Raton 2020.
[5] Gan W. S.: Signal Processing and Image Processing for Acoustical Imaging. Springer, Singapore 2020.
[6] Image correlation analysis system. Cipher "Cyber" – Research report. Vinnitsa Polytechnic Institute N01890065739, Vinnitsa 1991.
[7] Kutaev Y. F.: Systemic correlation-extreme measurement of coordinates with generalized Q-preparation of images. VNTU, Vinnitsa 1989
[8] Nosova Y. V., Tymkovych M. Y., et al.: Peculiarities of pre-processing of tomographic images for segmentation of paranasal sinuses. IEEE 39th International Conference on Electronics and Nanotechnology, ELNANO 2019, 489–492.
[9] Pavlov S. V., Vassilenko V. B., Saldan I. R., Vovkotrub D. V., Poplavskaya A. A., Kuzin O. O.: Methods of processing biomedical image of retinal macular region of the eye. Proc. of SPIE 9961, 2016, 99610X.
[10] Pogribnoi V. A.: Airborne signal processing systems. Kiev, Naukova Dumka 1984.
[11] Pratt W.: Digital image processing (T. 1 & 2). Wiley, New York 1982.
[12] Sacerdoti F.: Digital Image Processing. In: Sacerdoti, F., Giordano, A., Cavaliere, C. (eds): Advanced Imaging Techniques in Clinical Pathology. Current Clinical Pathology. Humana Press, New York 2016.
[13] Surabhi N., Unnithan S.: Image Compression Techniques: A Review. IJDER 5(1), 2017, 585–589.
[14] Timchenko L. I., Kokriatskaia N. I. et al.: Analysis of computational processes of pyramidal and parallel-hierarchical processing of information. Proc. of SPIE 10808, 2018, 1080822.
[15] Timchenko L. I., Kokryatskaya N. I., Melnikov V. V., Kosenko G. L.: Method of forecasting energy center positions of laser beam spot images using a parallel hierarchical network for optical communication systems. J. Optical Engineering 52(5), 2013, 055003.
[16] Trishch R., Nechuiviter O., Vasilevskyi O., Dyadyura K., Tsykhanovska I., Yakovlev M.: Qualimetric method of assessing risks of low quality products. MM Science Journal 2021(4), 2021, 4769–4774.
[17] Tulbure A., Tulbure A. A.: The use of image recognition systems in manufacturing processes. IEEE International Conference on Automation, Quality and Testing, Robotics. Cluj-Napoca 2018.
[18] Tymkovych M., Avrunin O. et al.: Ice crystals microscopic images segmentation based on active contours. IEEE 39th International Conference on Electronics and Nanotechnology, ELNANO 2019, 493–496.

[19] Vasilevskyi O., Koval M., Kravets S.: Indicators of reproducibility and suitability for assessing the quality of production services. Acta IMEKO 10(4), 2021, 54–61.
[20] Vasilevskyi O., Kulakov P., Kompanets D., Lysenko O. et al.: New approach to assessing the dynamic uncertainty of measuring devices. Proc. of SPIE 10808, 2018, 108082E.
[21] Vyatkin S. I., Romanyuk S. A. et al.: Using lights in a volume-oriented rendering. Proc. of SPIE 10445, 2017, 104450U.
[22] Wójcik W., Pavlov S., Kalimoldayev M.: Information Technology in Medical Diagnostics II. Taylor & Francis Group, CRC Press, Balkema book, London 2019.
[23] Zabolotna N. I., Pavlov S. V., Ushenko A. G., Karachevtsev A. O., Savich V. O. et al.: System of the phase tomography of optically anisotropic polycrystalline films of biological fluids. Proc. of SPIE 9166, 2014, 916616.

Prof. Leonid Timchenko
e-mail: tumchenko_li@gsuite.duit.edu.ua

Doctor of technical science, professor. State University of Infrastructure and Technology, Kyiv, Ukraine.
Sciettific directions: teaching, artificial intelligence, software engineering, data processing.
55 articles published in Scopus, 215 citations in 106 articles (h-index = 8).

http://orcid.org/0000-0001-5056-5913

Ph.D. Natalia Kokriatskaia
e-mail: nkokriatskaia@gmail.com

Ph.D., associate professor. State University of Infrastructure and Technology, Kyiv, Ukraine
Sciettific directions: teaching, artificial intelligence, software engineering, data processing.
34 articles published in Scopus, 109 citations in 77 articles (h-index = 6).

http://orcid.org/0000-0003-0090-3886

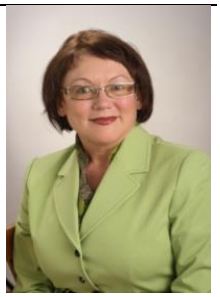

Ph.D. Mykhailo Rozvodiuk
e-mail: rozvodiukmp@gmail.com

Dean of the Faculty of Power Engineering and Electromechanics; scientific leader of the Center for Electronic Communications "InterCEC" of the VNTU.
International internship – University du Littoral Côte d'Opale (Dunkirk, France, 2004), University of West Bohemia (Pilsen, Czech Republic, 2019–2021).
The scientific direction of research is technical diagnostics of functional systems, information technologies, big data.

http://orcid.org/0000-0002-0916-1172

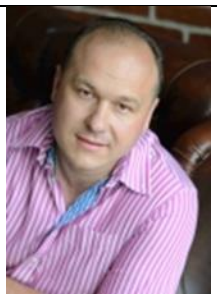

Ph.D. Volodymyr Tverdomed
e-mail: tverdomed@gsuite.duit.edu.ua

Ph.D., associate professor. State University of Infrastructure and Technology, Kyiv, Ukraine
Sciettific directions: teaching, artificial intelligence, software engineering, data processing.
13 articles published in Scopus, 13 citations in 16 articles (h-index = 3).

http://orcid.org/0000-0002-0695-1304

Ph.D. Yuri Kutaev
e-mail: kutaev@gmail.com

Ph.D., associate professor. State University of Infrastructure and Technology, Kyiv, Ukraine.
Sciettific directions: teaching, artificial intelligence, software engineering, data processing.
31 articles published in Scopus, 118 citations in 64 articles (h-index = 7).

http://orcid.org/0000-0001-8025-8172

Ph.D. Saule Smailova
e-mail: Saule_Smailova@mail.ru

A lecturer at the Department of Information Technology. D.Serikbayev East Kazakhstan State Technical University Ust-Kamenogorsk. Co-author over 60 papers in journals, book chapters, and confer ence proceedings. Member of Expert Group in the Computer Science specialization of IQAA.
Her professional interests are teaching, artificial intelligence, software engineering, data processing.

http://orcid.org/0000-0002-8411-3584

M.Sc. Vladyslav Plisenko
e-mail: plisenko_vo@gsuite.duit.edu.ua

Post-graduate student at State University of Infrastructure and Technology.
Sciettific directions: teaching, artificial intelligence, software engineering, data processing.

http://orcid.org/0000-0002-5970-2408

M.Sc. Liudmyla Semenova
e-mail: semenova_lm@gsuite.duit.edu.ua

Post-graduate student at State University of Infrastructure and Technology.

Sciettific directions: teaching, artificial intelligence, software engineering, data processing.

http://orcid.org/0000-0002-0904-3002

M.Sc. Dmytro Zhuk
e-mail: zhuk_do@ukr.net

Post-graduate student at State University of Infrastructure and Technology.
Sciettific directions: teaching, artificial intelligence, software engineering, data processing.

http://orcid.org/0000-0001-8951-5542

http://doi.org/10.35784/iapgos.3250 received: 6.11.2022 | revised: 11.12.2022 | accepted: 15.12.2022 | available online: 30.12.2022

INFORMATION MODEL OF THE ASSESSMENT OF TOURISM SECTOR COMPETITIVENESS IN THE CONTEXT OF EUROPEAN INTEGRATION POLICY

Iryna Prychepa[1], Oksana Adler[1], Liliia Ruda[1], Olexander Lesko[1], Zlata Bondarenko[1], Lee Yanan[1], Dinara Mussayeva[2]

[1]Vinnytsia National Technical University, Department of Economic Enterprise and Production Management, Vinnytsia, Ukraine, [2]Institute of Economics CS MES RK, Almaty, Kazakhstan

Abstract: *The aim of this paper is to identify the main problems and prospects of tourism growth in Ukraine including international experience in the context of deepening of the integration connections. The paper studied the main trends and characteristics of the tourism industry development in Ukraine in the context of European integration, describe the state, structure, dynamics of the relevant indices of the tourism sector in Ukraine, monitored the relationships and dependencies, determined the correlation factors. Main practical directions of the domestic tourism growth were determined. Determined the place of Ukraine in a highly competitive European tourism market. In addition, the paper made significant theoretical and practical contribution to overcome main problems associated with the characteristic feature of the tourist complex of Ukraine. The results of research identified the main problems of the development of the tourism sector of Ukraine, as well as highlighted the potential prospects for tourism development, taking into account the conditions of European integration.*

Keywords: tourism industry, growth, assignment, development, information model

MODEL INFORMACYJNY OCENY KONKURENCYJNOŚCI SEKTORA TURYSTYCZNEGO W KONTEKŚCIE POLITYKI INTEGRACJI EUROPEJSKIEJ

Streszczenie*: Celem pracy jest określenie głównych problemów i perspektyw rozwoju turystyki na Ukrainie z uwzględnieniem doświadczeń międzynarodowych w kontekście pogłębiania powiązań integracyjnych. W pracy zbadano główne trendy i cechy rozwoju branży turystycznej na Ukrainie w kontekście integracji europejskiej, opisano stan, strukturę, dynamikę istotnych wskaźników sektora turystycznego na Ukrainie, monitorowano związki i zależności, określono czynniki korelacji. Wyznaczono główne praktyczne kierunki rozwoju turystyki krajowej. Określono miejsce Ukrainy na wysoce konkurencyjnym europejskim rynku turystycznym. Ponadto, praca wniosła istotny wkład teoretyczny i praktyczny do przezwyciężenia głównych problemów związanych z cechami charakterystycznymi kompleksu turystycznego Ukrainy. Wyniki badań określiły główne problemy rozwoju sektora turystycznego Ukrainy, jak również podkreśliły potencjalne perspektywy rozwoju turystyki, biorąc pod uwagę warunki integracji europejskiej.*

Słowa kluczowe: branża turystyczna, wzrost, destynacja, rozwój, model informacyjny

Introduction and literature review

The socio-economic and cultural development of the country, the formation of its attractiveness and providing high competitiveness on the world stage is impossible without the development of the tourism industry, which is an integral part of the socio-economic and international policy of the country in modern conditions.

Nowadays, the tourism business is one of the most dynamic and a profitable sector of the world economy and it demonstrates rapid growth and provides high potential benefits for the country. The tourist sphere affects directly the general state and trends of the world economy, promotes acceleration of comprehensive development. According to the World Tourism Organization [19], the contribution of the tourism industry to the global gross domestic product is 10%. In addition, tourism contains 7% of world export of goods and services in general and 30% of world export of services in particular. In the service sector, which directly or indirectly relates to tourism, every tenth employee in the world is engaged [13].

Since tourism is connected with more than 50 industries, its development promotes employment growth, diversification of the national economy, development of cultural potential, preservation of the natural environment, increases the level of innovation of the national economy also promotes harmonization of relations between the different countries and peoples [9]. Accordingly, the development of tourism should become a strategic direction of the state policy of any country, the primary task of which is the introduction of economic and legal mechanisms for the successful conduct of tourism business and the development of appropriate infrastructure in the country.

The state, structure, dynamics of the relevant indices of the tourism sector in Ukraine and other regions are widely discussed the mean he scientific literature an did was investigated in works of Alekseeva N., Drin O. [1], Griko Y. [10], Kifyak V. [11], Mel'nyk A. [14], Stoyka S. [18], Feodinec N. [8], Shvedun V [15], Melnychenko O. [15], Baggio R. [4], Cabrini L. [6], Brandao F., Costa C., Buhalis D. [5], Korzhenko K. [12], Yurchenko O. [22] and others.

At the same time, the issue of the main problems of tourism development in Ukraine in the conditions of intensified competition in the international tourism business, and the prospects for growth of the tourism sector in Ukraine, with the allowance for requirements of international experience and deepening of integration connections is insufficiently studied and requires further research.

The aim of this study is to identify the main problems and prospects of tourism growth in Ukraine including international experience in the context of deepening of integration connections.

1. Materials and methods

The following scientific tasks were identified to achieve the goal:

1) analyze trends and determine the peculiarities of the development of the tourism industry in Ukraine under current conditions,
2) determine the place of Ukraine in a highly competitive European tourism market,
3) distinguish the main problems of tourism development in Ukraine in the conditions of intensified competition in the international tourism business,
4) outline the prospects for growth of the tourism sector in Ukraine, with the allowance for requirements of international experience and deepening of integration connections.

Such methods were used to solve the problems set in this paper: critical analysis and synthesis, induction and deduction, logical generalization, comparison, graphical and tabular analysis, etc.

The primary data for the analysis were statistical data of the Ukraine State Statistics Service, UNWTO data and Eurostat [7, 19].

After processing the statistical data and table's correlation, a qualitative analysis of the relevant indices was conducted. The collected and processed statistical material as a result of the analysis enabled to describe the state, structure, dynamics of the relevant indices of the tourism sector in Ukraine, monitoring the relationships and dependencies, the correlation with the factors, determining them.

The results of the statistical analysis allowed identifying the problem points, the positive aspects and disadvantages for outlining the perspective directions of the tourism sector growth in Ukraine.

2. Results and discussion

In the modern world, tourism is a multifaceted phenomenon, which is closely connected with economics, history, geography, architecture, medicine, culture, sports, and other spheres of human life. However, none of them can fully and exhaustively characterize it as an object of their own research, and none of the existing socio-economic institutions can solve these complex problems independently. There are many views on tourism both in the economy, as well as in the inter-industry complex or market, where a tourist enterprise produces a tourism product from various industries [11, 12].

Due to the specific character of its nature, the tourism service market has a direct economic impact on the development of the country as a whole, and significantly regulates the development of such interconnected sectors as transport and communications, construction, agriculture, production of consumer goods, estimated by significant multiplicative effect, acts as a catalyst for socio-economic development, improving the well-being of the population [12].

The United Nations General Assembly declared 2017 as the International Year of Sustainable Development of Tourism. The resolution emphasizes the promotion of better common understanding among peoples around the world, which implies raising awareness of the great heritage of different civilizations and ensuring a better understanding of the values inherent in different cultures, thereby contributing to the consolidation of peace throughout the world [19].

As a result, 2017 became quite successful for the development of the world tourism business, as evidenced by the growth of international tourist arrivals by almost 7% in comparison with the previous year, which is the highest index of growth since the 2009, the year of the global economic crisis and much higher than UNWTO growth indices (3.8% annually during the period of 2010-2020).

The most popular region in the world in 2017 was Europe, which was visited by slightly more than half (51%) of the 1.326 billion international tourists. Within eight years, the tourism industry in Europe has shown steady growth.

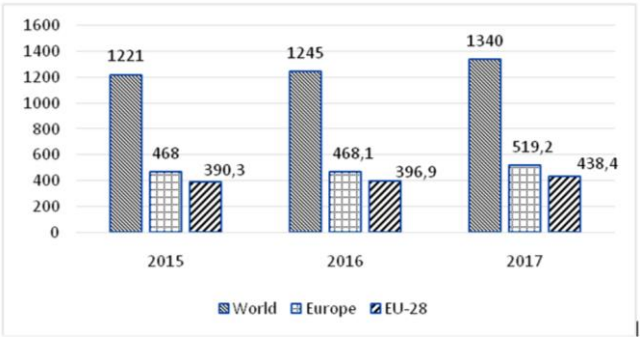

Fig. 1. International tourism revenues, $ billion

In 2017, the number of tourists arriving in Europe increased by 8%, which is 52 million more than in the previous year. Growth of the revenues from the tourism business also amounted to 8% ($ 519 billion – 39% of world income from tourism) [1, 2, 15] (Fig. 1).

Tourism in the European Union, which is one of the leading sectors of its economy and directly affects economic growth, employment and social development, makes up a significant share of the European tourist sector. EU policy is aimed at preserving the status of Europe as one of the leading tourist destinations, maximizing the contribution of tourism to the social and economic development of the region.

According to UNWTO, several European Union member states are among the world's leading tourist destinations. In 2017, France (86.9 million) had more tourists than any other country in the world, while Spain (the second place – 81.8 million, rising from third position in 2016), Italy (5th place – 58.3 million), the United Kingdom (7th place – 37.7 million), Turkey (8th place – 37.6 million) and Germany (9th place – 37.5 million) were also among the 10 best tourist countries in the world [7, 19].

The most popular tourist destination in the European Union was the Canary Islands in Spain – almost 103 million nights were spent in hotels. The Canary Islands also had the highest regional level of occupancy, and the second by the number of records – in Ilyis-Balears, also in Spain.

Ukraine is located in the center of Europe and has all the prerequisites for the proper development of tourism activities: convenient geographical location, favorable climate, diverse relief, and unique combination of natural and recreational resources, cultural and historical heritage, branching of sanatorium and resort base [1].

There are many unique architectural monuments on the territory of our state. A lot of spectacular places such as the Black and Azov seas, the Carpathians, the Dnieper, Podillya and Slobozhanshchyna, and more than 70,000 rivers, the largest of which are the Dnipro, the Dniester, the Southern Bug, the Seversky Donets, the Desna and the Danube, constituting the basis of Ukraine's tourist resources. Such places, however, are left out of attention both domestic and foreign tourists as well [17].

In spite of resource provision and unlimited potential tourism opportunities, the economic system of our country not enough attention is paid to tourism, it results in the fact that Ukraine still has no opportunity to compete with developed tourist countries, So domestic industry is significantly lagging behind the leading countries of the world in terms of development of tourist infrastructure and the quality of tourist services.

In addition, the financial and economic crisis and complicated political events in Ukraine led to the decrease of tourism flows, had a negative impact on the tourism structure and the implementation of tourism opportunities of the country on internal and external tourist markets.

As a result, in 2014, volumes of outbound tourism decreased by 5.6% in comparison with 2013. Even worse was the situation with inbound tourism, the volume of which in 2014 decreased more than twice (51.1%) [9, 16]. Such a critical situation was provoked by the crisis events of 2014, which threatened the tourism industry of Ukraine (Fig. 2).

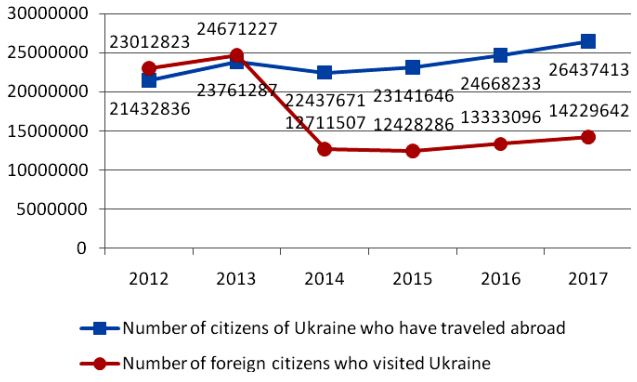

Fig. 2. Indices of the volume of inbound and outbound streams

Table 1. International Tourist Arrivals, thousand arrivals (UNWTO)

2010			2016			2017		
Position	Country	Arrivals, 1000	Position	Country	Arrival, 1000	Position	Country	Arrivals, 1000
1	France	77648	1	France	82700	1	France	86918
2	Spain	52677	2	Spain	75315	2	Spain	81786
3	Italy	43626	3	Italy	52372	3	Italy	58253
4	Turkey	31364	4	United Kingdom	35814	4	United Kingdom	37651
5	United Kingdom	28296	5	Germany	35595	5	Turkey	37601
6	Germany	26875	6	Turkey	30289	6	Germany	37452
7	RF	22281	7	Greece	24799	7	Greece	27194
8	Austria	22004	8	Austria	28121	8	Austria	29460
9	Ukraine	21203	9	RF	24571	9	RF	24390
10	Greece	15007	10	Portugal	18200	10	Portugal	21200
11	Poland	12470	11	Poland	17463	11	Poland	18400
12	Nether-lands	10883	12	Nether-lands	15828	12	Nether-lands	17924
13	Hungary	9510	13	Hungary	15256	13	Hungary	15785
14	Croatia	9111	14	Croatia	13809	14	Croatia	15593
15	Czech Republic	8629	15	Ukraine	13333	15	Ukraine	14230
In general, inEurope		487666	In general, in Europe		619492	In general, in Europe		671710
The share of Europe's leading tourist countries		0.7	The share of Europe's leading tourist countries		0.658	The share of Europe's leading tourist countries		0.657

Since 2015, we can observe a gradual increase of the amounts of Ukrainian citizens who had been travelling abroad, as well as foreign citizens who visited Ukraine. Despite a number of problems, already in 2016, the volumes of outbound Ukrainian citizens reached the values corresponding to the tourist flows in 2013, and in 2017, in comparison with 2016, they grew by 7.2%. A slightly different situation is observed with foreign citizens visiting Ukraine.

Thus, the dynamics are quite positive – the increase of foreign citizens' flows by 7.3% and 6.7% in 2016 and 2017, respectively, but to reach the index of 2013, when the rate growth of outbound and inbound tourists was almost equal, and failed. The main reason for this imbalance can be explained by restrictions on the entry of citizens of the certain countries.

Such a dynamic of indicators of foreign tourist arrivals was directly reflected on the position of Ukraine in the structure of the European tourism market (table 1).

It should be noted that by the results of 2010, Ukraine ranked 9th in the rating of popular European tourist destinations, having ranked among the top ten countries-leaders visited by 70% of tourists, ahead of such tourist-friendly countries as Greece, Poland, the Netherlands, Hungary, Croatia and the Czech Republic.

However, according to the results of 2016–2017, Ukraine ranked only 15th in the rating of European tourist countries (9 position remained in 2012–2013, 2014 – 12 positions, 2015 – 14th position, ahead of the Greece), despite the increase in flows of foreign citizens during this period in comparison with 2014–2015 – a period of deep decline in the tourist sector of the country [4].

Accordingly, the dynamics of amounts of inbound and outbound streams had a direct impact on the main indices of volumes of tourists in 2012–2017 years (Fig. 3).

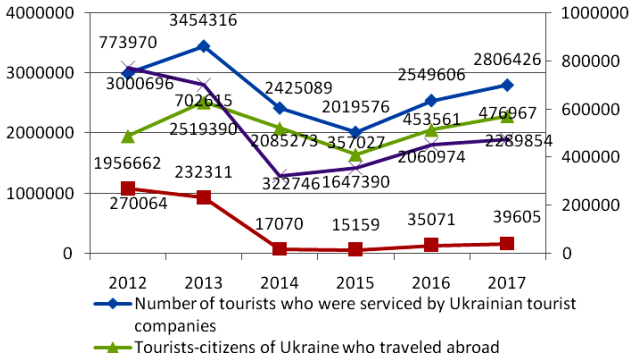

Fig. 3. The indices of tourism volumes

2013 was characterized by the increase in the volume of tourists served by tourists by 15%, and accordingly by tourists-citizens of Ukraine who traveled abroad by 28.7%. However, the volume of domestic tourism has decreased considerably – by 9.2% and foreign tourists – by 14.8%. This situation testifies that the main accents of tourism activity subjects of Ukraine in 2013 were aimed at outbound tourism, the main aspects of the tourist industry of Ukraine did not take into account their domestic tourism opportunities and potential [18–20].

According to above mentioned indices, 2014 and 2015 – the reduction of tourists served by tourist companies by 42.6% (16.9% in 2015 compared to 2014), the reduction of trips abroad in 2014 17.1% (by 21.2% in 2015), the catastrophic decline of foreign citizens is almost 14 times in 2014 [9]. Such a situation was caused primarily by certain political events and internal factors of Ukraine, and it didn't promote the development of the tourism industry [3, 21].

And since 2016, some revival of the positive dynamics of indicators of tourist volumes was observed. Particular attention should be paid again to outbound tourism, which in 2016 and 2017 increased by 26.9% and 5.1%, respectively. Slight positive trends are observed in the number of foreign and domestic tourists, which respectively increases the volume of tourists serviced by the subjects of tourism activity in Ukraine. But at the same time, none of the above indicators has ever revived to the 2013 level.

This situation requires careful research of the main factors, which create favorable c00ondition for the development of the tourism industry in Ukraine, and ways of improving them.

Particularly important indicator that determines the competitiveness of the tourism industry of the country and ensures its implementation and service is the number of available tourism activity companies and the number of employees involved in tourism. For the period of 2012–2015, the number of tourism activity companies has been constantly decreasing compared to each preceding year – by 5.4%, 30.5%, and 22.1%, respectively.

This situation was primarily caused by the low level of financing of the tourism industry, the high cost of servicing tourist activity, the lack of interest in the development and support of the domestic subject of tourism activity. Accordingly, in this period, employment in the tourism sector and decreased – if in 2012 in the sphere of tourism 15558 full-time employees were involved, then in 2015 – only 9588, it showed a decrease of this indicator by 62.3%. Despite the fact that the share of employment in the tourism sector is insignificant, the reduction of tourism subjects directly affects the unemployment rate in the country. Certain positive trends were observed in 2017, which was an increase in tourist activity in comparison with 2015 by 9%, and accordingly, by 3.4%, the number of full-time employees involved in tourism has increased.

Tourism industry of Ukraine has a great potential for development, but the main task at the state level should be creating favorable conditions for the development of the cultural level and improvement of the infrastructure of the country. In this regard, particular attention should be paid

to the development and increase of tourism resources that can attract a potential tourist. The actual decrease in the number of theaters in 17.7% in 2014, museums by 4.6% than in 2013 could not be unnoticed for the tourist industry in Ukraine. Besides, some positive trends are observed in the increase in the natural objects' capacity of Ukraine. It provides great opportunities for the development of sports and green tourism.

Over the past five years, the number of natural objects in Ukraine has increased by 2.3% (from 1565215.4 hectares in 2012 to 1600435 hectares in 2017).

Analyzing the import and export of tourist services in Ukraine, we can conclude that the priority task in this direction is the tourist's interest in a national tourist product. This is a rather difficult task, because attracting a European tourist and preserving one's own involves the creation of appropriate conditions that require significant investment. The total import share in the total tourist flow of Ukraine reached the lowest value in 2014 – 14%. For 2015–2017, the situation slightly improved – 18.4%, 19.2%, 18.4%, respectively. At the same time, exports of travel services in Ukraine reached 86% in 2013 and 81.6% in 2017. All exported tourist services are potential internal financial losses of the country.

The tourism industry is a specific branch of the economy, which forms not only the economic component of the state's development, but also social and cultural, and therefore it is also necessary to evaluate its economic efficiency over the analyzed period (Fig. 4).

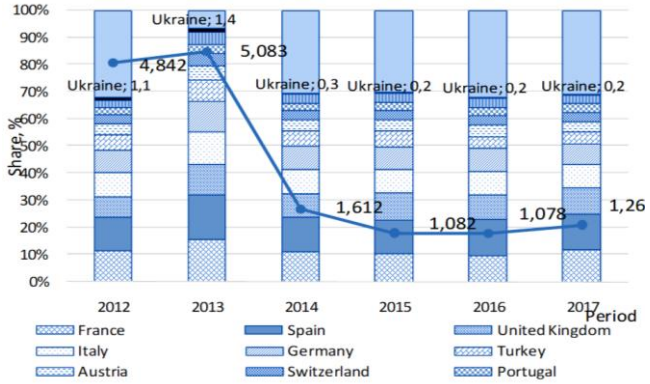

Fig. 4. Revenues from tourism activity in Europe

As it seen in figure 4, France, Spain, UK, Germany and Turkey have the greatest revenues from foreign tourism in Europe, and they also leaders in receiving foreign tourists (table 1) and relatively generate about 55% (in 2013, about 75%) of total revenues from servicing the European inbound tourism flows.

Ukraine had the highest revenues from providing tourist services in 2012-2013, when the incoming tourist arrivals in the country were the largest. Accordingly, in the structure of incomes of the European tourist market, Ukraine had the highest share: 1.1% and 1.4% in 2012–2013, respectively. It is obviously that a significant decrease in the volume of foreign tourists in 2014 (almost 93%) directly affected the income from the providing of tourist services: in 2014, the decline was 68.3%, had been caring on to 78.7% in 2015; in 2016 – 78.8%; 2017 – 75.2% compared to 2013, when incomes from providing tourist services in Ukraine were the highest during the analyzed period. Such a significant decrease of revenues directly affected the share of Ukraine in the revenues of the European tourist market: 2014 – 0.3%, 2013–2017 – 0.2%.

The decrease in revenues from the tourism services in Ukraine and the increase in operating expenses, which were observed in the period from 2012 to 2014, led to the decrease in the amount of taxes received from the tourism activity (in 2014 the amount of taxes on tourism decreased by almost 9 times in comparison with 2012). A substantial increase in tourism consumption in 2017 increased the revenue from the tourism services, and, accordingly, the volume of the taxes received in the budget of the country.

3. Experiment

For deepening the analysis, based on the statistical data, a regression and correlation analysis was conducted. Trends and econometric models of dependence of Ukraine tourism flows on various macroeconomic factors were constructed.

Trend models with the maximum determination coefficient among all considered trend lines are presented in table 2. It was revealed that the highest reliability of forecasting for statistical data is precisely the polynomial approximation used to describe the variables that are increasing and decreasing. Such tendencies are directly characteristic of the studied indicators of Ukraine tourism flows. It confirms the results of the analysis. Relative exception is the number of foreign tourists for whom the determination coefficient of the linear and polynomial approximation for the calculations performed is the same.

Table 2. The equation of trends of Ukraine tourism flows

index	graphic representation and trend equation
number of Ukraine citizens who have traveled abroad, persons	$Y = 40892X^2 - 69869X + 1E+07$ $R^2 = 0.923$
number of foreign citizens who visited Ukraine	$Y = -19278X^2 + 4E+06X + 1E+06$ $R^2 = 0.799$
number of tourists, serviced by subjects of tourist activity of Ukraine, persons	$Y = 10761X^2 - 17649X + 3E+06$ $R^2 = 0.116$
number of foreign tourists, persons	$Y = - 27244X + 50118$ $R^2 = 0.628$
tourists-citizens of Ukraine who traveled abroad, persons	$Y = 8704X^2 - 33501X + 30615$ $R^2 = 0.731$
number of domestic tourists, persons	$Y = -76662X + 2E+06$ $R^2 = 0.447$

According to the forecast, negative tendencies are expected for indicators of foreign citizens visiting Ukraine, including the number of foreign tourists, as well as decline in the rate of domestic tourists.

Therefore, there is a need to determine the main factors of influence on the indicators of Ukraine tourism flows, which allows analyzing linear correlation coefficients. It was summarized the results of calculations for the most significant factors of the influence in table 3.

The analysis shows that during the period of observation (2000-2017gg.), the factors identified have a rather close direct relationship with the indicators of the number of Ukrainian citizens traveling abroad, including travel for the purpose. It is worth noting that at the same time, internal tourist flows have an inverse relationship with the investigated factors of influence.

Table 3. Double linear coefficients of correlation for Ukraine tourism flows

index	factors of influence				
	GDP of Ukraine	average monthly salary in Ukraine	average resources per month for one Ukrainian household	GPD of the world	Europe an union GDP
number of Ukraine citizens who have traveled abroad, persons	0.939	0.939	0.931	0.874	0.596
number of foreign citizens who visited Ukraine	0.158	0.115	0.211	0.479	0.762
number of tourists, serviced by subjects of tourist activity of Ukraine, persons	0.353	0.349	0.373	0.441	0.449
number of foreign tourists, persons	-0.871	-0.864	-0.865	-0.810	-0.550
tourists-citizens of Ukraine who traveled abroad, persons	0.883	0.874	0.901	0.920	0.697
number of domestic tourists, persons	-0.728	-0.721	-0.740	0.7.27	-0.472

Number of foreign visitors of Ukraine does not depend on macroeconomic indicators at the host country level, but it is in close interconnection with the European Union's GDP and moderate interconnection with world's GDP. This is due to the fact that a significant part of foreign guests are residents of the EU.

According to the study, the multiple regression equation for the dependence of the number of Ukrainian tourists traveling abroad and the most significant factors of influence were identified:

$$У = – 1.33 \cdot X_1 – 237.967 \cdot X_2 + 1006.33 \cdot X_3 + 85566.08 \quad (1)$$

where X_1 – gross domestic product in Ukraine, UAH million; X_2 – average monthly salary per one full-time employee, UAH; X_3 – total resources on average per month for household, UAH.

The coefficient of multiple correlation for the constructed model is 0.92, which indicates a close relationship between the investigated factors. The coefficient of multiple determination is 0.85 and it indicates that the resultant variable depends on the selected factors by 85%, which is also quite high and enough to be reliable model.

At 5% level of significance and the number of degrees of freedom $k_1 = 3$, $k_2 = 14$, F_{cr} is 3.34. Since $F_r = 25.5$, the model is considered to be adequate.

To study the change in the indicator of foreign tourists in Ukraine, an appropriate model has been drawn up:

$$У = 555338.6 – 1.4E\text{-}08 \cdot X_1 + 3.53E\text{-}08 \cdot X_2 \quad (2)$$

where X_1 is the gross domestic product of the world, current US $; X_2 is the gross domestic product of the European Union, current US $.

For the constructed model, the coefficient of the multiple correlation is 0.88, which confirms the close relationship between the investigated factors. The coefficient of multiple determinations is 0.77 and indicates that the resultant variable depends on the selected factors by 77%, which is sufficient to consider the model to be reliable.

At 5% level of significance and the number of degrees of freedom $k_1 = 2$, $k_2 = 15$ F_{cr} is 3.68. Since $F_r = 25.59$, the model is considered adequate.

The constructed models correspond to reality and can be used in practice to predict tourist flows in Ukraine.

As the analysis shows, activating of state support for tourism business in Ukraine allows solving a significant part of existing problems in the industry. Accordingly, at the present stage, the development of Ukrainian national tourism requires the improvement of the state policy in this area – the introduction of effective organizational, legal, socio-economic and information mechanisms for the development of tourism in Ukraine as a highly profitable sector of the national economic system through the operation of the main regulatory mechanisms at all levels of governance: regulatory, organizational, controlling, corrective, social and stimulating.

It is worth noting that Ukraine already has a number of positive developments in the direction of the development of national tourism, which is the result of increased attention from the state to this problem, the implementation of various projects, programs and strategies that distinguish tourism industry of Ukraine as an industry that is the basis for the development of entrepreneurship, contributes to raising the level of employment of the population, is a guarantee of social and cultural development of the country.

One of the steps towards promoting the issue of tourism in Ukraine is that Ukraine joined the initiative of the UN General Assembly, proclaiming 2017 as the year of tourism in Ukraine, hoping to intensify the development of tourism in Ukraine.

It is recognized that the only solution to systemic problems in the field of tourism and resorts is a strategically oriented state policy at the national level [22]. In accordance with this, the Government of Ukraine has developed a "Strategy for the Development of Tourism and Resorts for the Period up to 2026", which defines tourism as one of the main priorities of the state and declares the need for the introduction of economic and legal mechanisms for the successful conduct of tourism business, investment mechanisms for the development of tourism infrastructure, information and marketing measures on the formation of the tourist image of Ukraine in the world [7, 9].

4. Conclusions

Tourism is a quite specific branch of the economy, which can significantly affect the socio-economic development of the state through diversified ties with other sectors of the economy as a whole. Taking into account the specifics of tourism, strict international competition and relevant national interests in Ukraine, there is a need for enhanced participation of the state in the management of the tourism industry of the country.

One of the main advantages and opportunities of Ukraine is that its tourist destinations are incredibly diverse: there are mountains, seas, various sanatoriums, castles and monuments of architecture. A positive feature is that virtually all areas, even where there are no mountains and seas, new tourist products were appeared.

However, the level of development of the national tourism infrastructure and the quality of tourist services in most cases do not meet the requirements of the international market, which requires the formation and promotion of a competitive national tourism product, which is impossible without a well-considered and responsible state policy at the national and regional levels.

The general conclusion is that the state policy of Ukraine of the regional complex development should be formed taking into account the satisfaction of human needs, ensuring the social efficiency of its functioning and effective nature use; to focus on the practical realization of the priorities of the personal principle as the basis of the welfare of society; on ecologization of management, including on a reasonable policy of resource consumption; production of consumer goods and services, which promote the comfort life and job intellectualization of the population; to focus on the practical development of spheres promoting awareness and creative activity of the individual and increase its social status. Therefore, an important task for the Ukrainian government should be the formation of a positive image of Ukraine on the world market as an attractive tourism destination, which is strategically important on the way to ensuring further stabilization and socio-economic growth of the country in the long run.

References

[1] Alekseeva N., Drin O.: Research of tourist streams in Ukraine. Proc. of conf. Actual scientific achievements, Czech Republic, 2014.
[2] Azarova A., Zhytkevych O.: Mathematical methods of identification of ukrainian enterprises competitiveness level by fuzzy logic using. Economic Annals-XXI 9-10(2), 2013, 59–62.
[3] Azarova A. O. et al.: Information technologies for assessing the quality of IT-specialties graduates' training of university by means of fuzzy logic and neural networks. International Journal of Electronics and Telecommunications 66(3), 2020, 411–416.
[4] Baggio R.: Symptoms of complexity in a tourism system. Tourism Analysis 13(1), 2017.
[5] Brandao F. et al.: Tourism Networks: A Regional Approach. European Journal of Tourism Studies 18, 2018, 33–56.
[6] Cabrini L.: Conclusions of the UNWTO Conf. "Impact of the European Union Enlargement on tourism development in Europe". Vilnius, Lithuania, 2017.
[7] Eurostat Regional Yearbook 2018, https://ec.europa.eu/eurostat/statistics-explained/index.php/Eurostat_regional_yearbook (available 20.01.2019).
[8] Feodinec N.: Organizational aspects of the activity of domestic tourism enterprises in the conditions of crisis. The series is economical 50, 2018, 182–186.
[9] Government portal. Resolution of the CMU On approval of the Tourism Development and Resorts Development Strategy for the period up to 2026, https://www.kmu.gov.ua/ua/npas/249826501 (available 20.01.2019).
[10] Griko Y.: Influence of international tourism on the development of countries of the world. Student Scientific Herald of Lutsk National Technical University 4, 2017, 67–73.
[11] Kifyak V.: Organization of tourism activity in Ukraine. Books XXI, Chernivtsi 2017.
[12] Korzhenko K.: Major strategic perspective of national tourism in Ukraine under the social and economic instability. Sustainable development of economy 1, 2018, 6–10.
[13] Kotler P. et al.: Marketing for hospitality tourism. Pearson Academic, 2017.
[14] Melnyk A.: Foreign experience of hospitality and especially its use in Ukraine. http://www.nbuv.gov.ua/portal/Soc_gum/aprer/2008_4_2/94.pdf (available 20.01.2019).
[15] Shvedun V., Melnychenko O.: Features of development industry of tourism in Ukraine. NUTZU, Kharkiv 2018.
[16] Shyian A. A. et al.: Modeling communication between the public and the authorities while implementing innovative projects in the context of e-democracy and public administration. Science and Innovation 16(6), 2021, 18–27.
[17] State Statistics Service of Ukraine. http://www.ukrstat.gov.ua (last accessed 20.01.2019).
[18] Stoyka S.: Problems and prospects for development of Ukrainian tourism business in the conditions of economic instability. Investments: practice and experience 21, 2018, 86–91.
[19] UNWTO, Tourism Highlights, http://www2.unwto.org (2013–2018).
[20] Yaremko S. et al.: Using artificial intelligence technologies for forecasting business processes. Computer-integrated technologies: education, science, production 23, 2021, 230–234.
[21] Yarmolenko V. et al.: Practice Analysis of Effectiveness Components for the System Functioning Process: Energy Aspect. Lecture Notes on Data Engineering and Communications Technologies 77, 2022, 282–296.
[22] Yurchenko O.: Innovations in the hotel business at the present stage. Visnyk of Lviv National University. International Relations 34, 2017, 292–300.

Ph.D. Iryna Prychepa
e-mail: prychepa.iryna@gmail.com

Ph.D., associate professor, Vinnytsia National Technical University, Vinnytsia.
Scientific direction: problems of innovative development and formation of competitive advantages of domestic enterprises under the conditions of globalization of economic relations, intellectualization of economic relations and processes at different levels of management and improvement of their management efficiency.

http://orcid.org/0000-0002-0805-2732

Ph.D. Oksana Adler
e-mail:oksana_adler1983@ukr.net

Ph.D., associate professor, Vinnytsia National Technical University, Vinnytsia.
Scientific direction: progressive methods of diagnosis and increasing the competitiveness of modern enterprises in the conditions of a market economy. Management of innovations of a modern enterprise.

http://orcid.org/0000-0002-4673-366X

Ph.D. Liliia Ruda
e-mail:rudalist_ok@ukr.net

Ph.D., associate professor, Vinnytsia National Technical University, Vinnytsia.
Scientific direction: financial and economic performance indicators of economic entities.

http://orcid.org/0000-0002-1598-8301

Ph.D. Olexander Lesko
e-mail:epvm@ukr.net

Ph.D., associate professor, Vinnytsia National Technical University, Vinnytsia.
Scientific direction: personnel management, modern methods of efficient organization of production, development of leading branches of the economy of Ukraine.

http://orcid.org/0000-0002-5687-4052

Ph.D., Zlata Bondarenko
e–mail: bondarenko@vntu.edu.ua

Associate professor of the Department of Higher Mathematics, Vinnytsia National Technical University.
Scientific direction: innovative technologies for training future specialists in technical specialties.

http://orcid.org/0000-0003-3339-0570

M.Sc. Lee Yanan
e-mail: amaodemao@gmail.com

Ph.D. student, Vinnytsia National Technical University, Vinnytsia.
Scientific direction: personnel management, modern methods of efficient organization of production, development of leading branches of the economy.

http://orcid.org/0000-0002-6652-4953

M.Sc. Dinara Mussayeva
e-mail: d_i_n_mus@mail.ru

Scientific Secretary and Research Associate of the Institute of Economics CS MES RK, Almaty, Kazakhstan.
She is a master of Al-Farabi Kazakh National University, Ph.D. student of the Institute of Economics of the CS MES RK, specialty – „World Economy".
As a responsible executive, he actively participates in conducting fundamental and applied research in priority areas for the state, such as digitalization of the economy, knowledge-based economy, etc.

http://orcid.org/0000-0002-8349-213X

http://doi.org/10.35784/iapgos.3249 *received: 6.11.2022 | revised: 3.12.2022 | accepted: 15.12.2022 | available online: 30.12.2022*

FORECASTING BUSINESS PROCESSES IN THE MANAGEMENT SYSTEM OF THE CORPORATION

Svitlana A. Yaremko[1], Elena M. Kuzmina[1], Nataliia B. Savina[2], Iryna Yu. Yepifanova[3], Halyna B. Gordiichuk[4], Dinara Mussayeva[5]

[1]Vinnitsa Institute of Trade and Economics State University of Trade and Economics, Vinnytsia, Ukraine, [2]National University of Water and Environmental Engineering, Rivne, Ukraine, [3]Vinnytsia National Technical Uneversity, Vinnytsia, Ukraine, [4]Vinnytsia Mykhailo Kotsiubynskyi State Pedagogical University, Vinnytsia, Ukraine, [5]Institute of Economics CS MES RK, Almaty, Kazakhstan

Abstract. *One of the key issues in corporate management is business process management. That is why the greatest interest for company analysts is the issue of effective forecasting of business processes. In today's digitalization of the economy, integration and automation of business processes have become the main priorities for achieving efficiency and effectiveness of companies, and especially for effective management decisions. This problem can be solved with the help of integrated systems, which are tools for effective management decisions, modeling and optimization of business processes. The article provides an analytical review of known forecasting methods and identifies the features of their application, analyzes the advantages and disadvantages that will take them into account in modeling the company and promote economic development, competitiveness and optimize business processes.*

Keywords: corporation, management, forecasting, business process, integrated system, making effective management decisions

PROGNOZOWANIE PROCESÓW BIZNESOWYCH W SYSTEMIE ZARZĄDZANIA KORPORACJĄ

Streszczenie. *Jednym z kluczowych zagadnień w zarządzaniu przedsiębiorstwem jest zarządzanie procesami biznesowymi. Dlatego też największym zainteresowaniem analityków firmowych jest kwestia skutecznego prognozowania procesów biznesowych. W dobie dzisiejszej cyfryzacji gospodarki integracja i automatyzacja procesów biznesowych stały się głównymi priorytetami dla osiągnięcia sprawności i efektywności przedsiębiorstw, a przede wszystkim dla skutecznych decyzji zarządczych. Problem ten można rozwiązać za pomocą systemów zintegrowanych, które są narzędziami do podejmowania skutecznych decyzji zarządczych, modelowania i optymalizacji procesów biznesowych. W artykule dokonano analitycznego przeglądu znanych metod prognozowania i wskazano cechy ich zastosowania, przeanalizowano zalety i wady, które pozwolą uwzględnić je w modelowaniu przedsiębiorstwa i wspierać rozwój gospodarczy, konkurencyjność oraz optymalizować procesy biznesowe.*

Słowa kluczowe: korporacja, zarządzanie, prognozowanie, proces biznesowy, zintegrowany system, podejmowanie efektywnych decyzji zarządczych

Introduction

The mechanism of effective corporate governance will expand the opportunities for investing in business, increase the productivity and competitiveness of companies. The course of the world economy (including the Ukrainian one) on digitalization will help to rethink traditional ways in organizing business and allow realizing the advantages of modern information technologies. Today's functioning of companies is due to the special attention given to management processes. And one of the main warehouse management processes is business processes. For this very reason, the greatest interest for analyst companies is to become the basis for effective management of business processes, based on their forecasts. In addition, in the business environment, there is an increase in the role of victory and the promotion of modern methods to improve these business processes.

Nutrition for the development of corporate governance in the rest of the world is widely discussed in the international and domestic business environment. Researched nutrition, which is related to corporate governance and system optimization [4, 6–8], dedicated their scientific practice to such universities, as Ross S., Westerfield R., Jordan B., Van Horne D., Ihnatyeva I. A., Hafonova O. I., Mostenska T. L., Novak V. O. [14, 21, 25, 28] etc. Previous methods of forecasting in management companies were used by the following scientists: Vanderput N., Wilson J., Meskon M., Hanke J., Mitelhammer R., Bakanov M. I., Fisenko M. A. and insh [13, 20]. This practice is the basis for the development and implementation of new direct and flexible methods for modeling the economic activity of companies based on effective forecasting methods [5, 12, 16, 24].

Creating an effective and efficient corporate governance system is a multifaceted management system, which consists of operating in a reliable legal field, development of investment processes, implementation of corporate governance standards, use of positive experience of the world, their concepts and technologies, implementation of integrated management systems and others.

1. Formulation of the problem

One of the key problems in corporate management is business process management, where forecasting is an integral part [11, 13]. In today's economy, forecasting the financial performance of companies is a rather complex process. At the same time, the experience of countries with developed economies shows the need for financial planning in companies and corporations, as the effectiveness of economic activity depends primarily on management strategy. A well-designed strategy avoids significant miscalculations and associated costs. This is achieved by being able not only to assess the current financial and economic condition of the company, but also to predict the future taking into account the state of the market, business activity of partners, competition and more.

Every business leader wants to make their company more efficient and profitable. A manager who thinks about the future will strive to improve his business. And modeling and forecasting business processes is one of the effective tools to improve the business management system and its indicators.

A company's business process is a set of related actions and functions that are necessary to produce a certain result that has value for external or internal consumers. The approach of business process modeling is the basis of process management of the company, when all the tasks and activities of the organization are presented in the form of a set of different processes, related and interacting with each other [13, 31]. Many experts consider this approach to be the most effective in organizing the company's activities. When we single out individual processes in the company's activities, we can achieve more efficient performance of work, as we can appoint a person responsible for the work of this process, we can plan the result and monitor the entire path to its achievement. We can also, based on this, build the most optimal system of motivation for employees working on a particular process, and thus achieve greater productivity.

The study of this problem has shown that insufficient attention is paid to the question of reasonable choice of the most optimal methods of forecasting the company's activities, which requires further research.

The purpose of the article is to study and substantiate the choice of the most optimal method for forecasting the company's activities.

2. Theoretical research

In the classical approach, all business processes can be divided into three types: basic (operational), management and supporting (or auxiliary). The main processes are those that directly bring the company a profit. These are the functions that are aimed at creating products or services of the company. Auxiliary or supportive are those that support the main business processes, make it possible to implement them. Business management processes are functions that are responsible for the management and development of the entire organization, and this includes, first of all, strategic management. Also, in order to highlight the company's business processes, you need to know that they can be of several levels, regardless of type. This is usually the upper level and lower. Top-level processes – the company's activities are described as a „top view", without going into detail. A more detailed description of the activity takes place at the lower level. The description of business processes at the first stage should be carried out on a „as is" basis. And only then, after analyzing the „bottlenecks" and identifying all the problems, apply the principle of „as it should be" or „as it should be" to the described business processes. Each dedicated business process must have the result and the input resources needed to obtain that result. Each process has its own supplier and consumer who is interested in obtaining (exit the business process). In addition, each business process has its own manager or owner – a manager who has the authority to optimize, change the business process and others. Implementing a process approach in a company can make business more transparent and predictable, manageable, controlled. When the company's processes are formalized and prescribed, the influence of the human factor decreases. Formalization and engineering of business processes form a systematic approach to process management in terms of their maximum efficiency [7, 15, 26].

A classic corporation is three levels of management, a hierarchy of decisions, regulations and procedures, accounting cycles, basic functions – accounting and control, analytics – a fact plan.

Digital corporation is a flat structure, decentralization of decisions, flexible business processes, real-time situational management, basic functions – analysis based on data (dynamic planning, sliding forecasting). The transition in corporate business process management to integrated systems is the first step towards digitalization of the company. If we consider digitalization in full, we are talking about the introduction of artificial intelligence technologies, digital money, blockchain, smart spaces, cloud technologies and others [14, 21, 27]. In the future, digital management technologies will be developed as hybrid solutions in which artificial intelligence does not replace humans, but is a partner system to reduce uncertainty and increase the effectiveness of decisions. Functions of corporate governance with components of artificial intelligence (shown in Fig. 1). Implementing forecasting tools in an integrated corporate governance system can make business more predictable, manageable and controlled.

Business Process Management – allows companies to model, forecast, automate, execute, control, measure and optimize business activities. Integrated systems of companies that allow modeling, forecasting and optimizing business processes are a tool for making effective management decisions. That is why the issues of effective management in the company are closely related to integrated management systems.

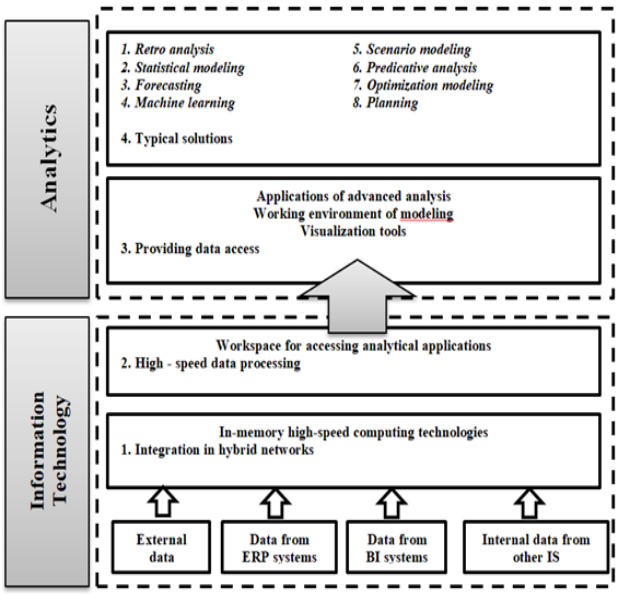

Fig. 1. Corporate governance functions with artificial intelligence components [9]

Forecasting is a necessary component of analytical modeling of business processes. In many cases, the forecasting of economic activity of the company occurs in conditions of uncertainty or chance. Therefore, to increase the efficiency of forecasting, management should identify (at the preparatory stage) those forecasting methods, the use of which is most appropriate under the given conditions. In this regard, it is important to study the known methods of forecasting, identify their advantages and disadvantages, as well as the features of application to solve a range of problems.

Forecasting the economic activity of the company is a process of scientific substantiation of possible quantitative and qualitative changes in its state in the future, as well as alternative ways to achieve the expected state [6, 14, 21, 23]. The main principles on which the forecast is based are shown in Fig. 2.

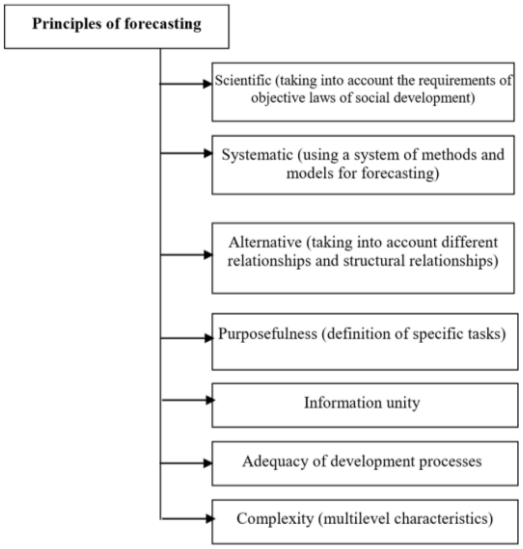

Fig. 2. Basic principles of forecasting

According to these principles, forecasts of the future state of the corporation are formed.

In practice, modern companies use different types of forecasting, the most common of which are [11, 13, 17]:

- forecasting, which is based on creative prediction of the future, using intuition,
- search forecasting, which is based on existing information and can be an extrapolation of the past into the future or one

of the alternative development options taking into account changes in the environment,
- normative-target, focused on specific goals using quality research methods.

Depending on the tasks, forecasting can be short, medium and long-term (by term), factual or heuristic (depending on available sources of information), exploratory, normative (on the topic of forecasts), passive and active (possibly influencing the future activities of the enterprise) [13, 16, 20, 29].

Consider forecasting methods to determine the features of their application in the process of modeling the economic activity of the company.

Factual methods allow you to make a detailed forecast of changes in time of individual features of the object under study or all of these features. Factual methods include extrapolation, functions, correlation and regression models (Fig. 2) [11, 13, 17].

The method of extrapolation is one of the main methods of predicting the development of complex production systems; it is based on the assumption of invariance of the factors that determine the development of the object of study. The essence of the method of extrapolation is to extend the patterns of development of the object in the past to its future [6, 13].

The method of functions refers to statistical forecasting methods based on the use of autocorrelation functions (autocorrelation – the expression of the relationship between neighboring members of the time series). The process of forecasting using autocorrelation functions is to formulate the forecasting task, determine the criteria for its solution and reflect the process of development of production system parameters over time based on time series, which allows to determine the forecast value for the long term while minimizing predictive errors [13].

Prediction using correlation models (methods) is to find mathematical formulas that characterize the statistical relationship of one indicator with another (pairwise correlation) or with a group of others (multiple correlation). A prerequisite for the possibility and feasibility of such methods is to establish the degree of reliability of correlation formulas based on logical analysis of a sufficient statistical sample [11, 13, 17, 20, 23].

Heuristic forecasting methods involve the implementation of forecasting developments using logical techniques and methodological rules of theoretical research. Specific forecasting methods for this group include two subgroups – intuitive and analytical. Among the main methods of the first group are methods of expert evaluation and „brainstorming", and the second – methods of morphological analysis, construction of „goal tree", information modeling, optimization [12, 17, 25].

In the absence of sufficient statistical information or in its unsuitability for forecasting certain phenomena, it is necessary to use the method of expert assessments. It is based on a method of collecting the necessary information, mainly through questionnaires. The expert questionnaire should be compiled in such a way that it is possible to obtain [23]:
- quantitatively unambiguous answers to the questions offered to the expert,
- formalized information on the nature of the sources of argumentation, the degree of influence of each of the sources on the expert,
- quantified by the expert assessment of the level of his knowledge of the subject proposed for analysis and conclusions.

When using the method of expert assessments, two approaches to forecasting are used: individual and group assessments. Individual assessments are that each expert gives an independent assessment in the form of an interview or an analytical note. Group assessments are based on the collective work of experts and obtaining a summary assessment from the entire group of experts involved in the forecast assessment of specific economic processes.

The „brainstorming" method is a kind of group expert assessment and consists in the creative cooperation of a certain group of experts to solve the task by way of discussion („brainstorming"). Participants in such a discussion must follow two rules of conduct [17, 20, 24]:
- do not allow criticism and negative comments on the views of opponents,
- not to deny new ideas, no matter how absurd they may seem in terms of its possible practical implementation.

The method of building a „goal tree" is used in forecasting in order to divide the main tasks into subtasks and create a system of „balanced" according to expert assessments of relationships. Interaction matrices and graph theory are widely used to select factors for the prognostic model and to construct a system of relationships [24].

A specific method of forecasting is the method of information modeling. It is based on the fact that the characteristics of mass flows of information create conditions for forecasting the development of specific objects on the basis of analysis of the maximum possible number of factors related to production and financial and economic indicators and take into account the degree of their interaction [11, 16, 24].

Causal modeling is the most complex in terms of mathematics. It is used in cases where there is more than one variable. Causal modeling is an attempt to predict what happens in similar situations by studying the statistical relationship between the factor and other variables [21, 22, 26].

For businesses, when certain circumstances do not allow the use of complex models, it is advisable to use methods of naive forecasting, which do not require significant costs and are easy to apply. Thus, in particular, in cases where it is necessary to take into account shifts in the data structure during certain periods, use the method of „moving average", which is calculated as the average of a number of elements in expression (1) [13, 20, 31]:

$$\hat{Y}_{t+1} = \frac{(Y_t + Y_{t-1} + Y_{t-2} + ... + Y_{t-k+1})}{k} \tag{1}$$

where $\hat{Y}_{t+1}$ – the average value of the elements $Y_t + Y_{t-1} + Y_{t-2} + ... + Y_{t-k+1}$ for k – periods of time.

In cases where the data have a trend (α), it is advisable to use exponential Holt smoothing (2) [13, 26]:

$$L_i = \alpha Y_i + (1-\alpha)(L_{i-1} - T_{i-1}) \tag{2}$$

where L_i – exponentially smoothed rows (level estimation).

Forecasting for p periods ahead is carried out by expression (3) [26]:

$$\hat{Y}_{i+p} = L_i + pT_i \tag{3}$$

If the data are seasonal, it is advisable to use the Winters model (4) [13, 26]:

$$L_i = \alpha \frac{Y_i}{S_{i-s}} + (1-\alpha)(L_{i-1} - T_{i-1}) \tag{4}$$

The assessment of seasonality is carried out by expression (5) [6, 17]:

$$\hat{Y}_{i+p} = (L_i + pT_i)S_{i-s+p} \tag{5}$$

In addition, these methods are effective when it is necessary to make short-term forecasts for a large number of product names, or when there is no information about previous sales volumes.

Although small and medium-sized enterprises with relatively simple business can be guided by naive forecasting methods, large firms and firms with complex business structures are forced to use regression analysis to study the relationship between several variables based on estimating the multidimensional regression function (6) [20, 23, 24]:

$$f\{Y\} = \beta_0 + \sum_{i=1}^{n} \beta_i x_i + \sum_{\substack{i;l=1 \\ i<l}}^{n} \beta_{il} x_i x_l \tag{6}$$

where $f\{Y\}$ – target function that characterizes the integrated performance of the corporation, β_i, $i=1,2,...,l$ – unknown coefficients of influence, x_i, $i=1,2,...,l$ – influencing factors, n – the total number of studies of influencing factors.

Estimation of theoretical coefficients β_i, β_{il} carried out on the basis of sample coefficients of influence b_i, b_{il}. To do this, first select the intervals of variation for each of the factors. Under the interval of variation according to the theory of statistical modeling [20] understand the number (characteristic of each factor), which as a result of addition to the zero level, gives the upper, and as a result of subtraction – the lower level of the factor. In the first stage (when obtaining a linear model), the factors always change only on two levels. The interval of variation cannot be less than the error with which the factor level is fixed, otherwise the upper and lower levels will be the same. In addition, the lower and upper levels must be within the scope of the factors [20, 23].

If the number of factors is known, then to vary the factors at two levels in the linear model, the number of observations of factors can be determined by the formula (7):

$$n = 2^k \tag{7}$$

where n – number of factor studies, k – number of factors.

To simplify the planning and processing of results, it is recommended to convert measured controlled factors into dimensionless normalized $z_i = (x_i - x_{i0}) / \Delta x_i$, which makes it easier to write the planning matrix, as the upper and lower levels of variation and in relative units are equal to +1 and -1 regardless of the physical nature of the factors and the values of the main intervals of variation of factors [20, 22, 26].

The process of finding a mathematical model for [17] has the following sequence: planning and conducting research on factors; verification of reproduction (homogeneity of sample variances); obtaining a mathematical model of the object of study with verification of the statistical significance of sample regression coefficients and verification of the adequacy of the mathematical description.

Mathematical planning for the determination of influential factors involves the construction of a matrix according to the following requirements [1, 20, 23]:

1. Each i-th row of the matrix must contain a set of coordinates of the point at which the study of the g-th factor.

2. Because of variables take values only +1 and -1, all interactions $z_i, z_l (i; l = 1,2,3; i \neq l)$ can only take the same values.

3. In the first line (i = 1) all controlled factors are selected at the lower level, ie = -1. The following i-th variants of variation in the compilation of the planning matrix are selected so that in the sequential search of all options, the frequency of change of the sign of the factors for each subsequent factor was twice less than the previous one.

4. After conducting research, it is necessary to test the hypothesis of equality of general variances $\sigma^2\{Y_1\} = \sigma^2\{Y_2\} = ... = \sigma^2\{Y_n\}$ according to the formula (8) [3, 4, 16]:

$$s^2{}_j = s^2_{VIDT} = \frac{1}{l-1}\sum_{g=1}^{k}(Y_{gj} - \bar{Y}_j)^2 \tag{8}$$

Since all estimates of variances are obtained from samples of the same number of parallel studies, the number of degrees of freedom for all will be:

To test the hypothesis of homogeneity of estimates variances it is necessary to use the Cochren test [16], which is based on the law of distribution of the ratio of the maximum estimate of variance to the sum of all compared estimates of variance as reflected in the expression (9):

$$G = \max\{s_j^2\} / \sum_{g=1}^{k} s_j^2\{Y\} \tag{9}$$

Independent estimates must be determined to obtain a mathematical description of the response function b_0, b_i, b_{il} corresponding coefficients $\beta_0, \beta_i, \beta_{il}$, scilicet $b_0 \to \beta_0, b_1 \to \beta_1, b_2 \to \beta_2, b_3 \to \beta_3$. These estimates are in terms of expressions (10–12) [20, 23, 24]:

$$b_0 = \frac{1}{n}\sum_{i=1}^{n} z_0 \bar{Y}_j \tag{10}$$

$$b_i = \sum_{i=1}^{n} \bar{Y}_j z_{ij} / n,\ j = 0,1,2,...,m, i = 1,2,...,n \tag{11}$$

$$b_{il} = \frac{1}{n}\sum_{i=1}^{n} z_{ij} z_{lj} \bar{Y}_{j,} (i; l = 1,2,...n; i \neq l) \tag{12}$$

After determining the estimates of the b regression coefficients, it is necessary to test the hypotheses about their significance, ie to test the corresponding null hypotheses β = 0. The hypothesis of the significance of the coefficients is tested using the Student's test (13) [23, 24, 32]:

$$t = |b| / s\{b\} \tag{13}$$

$$s^2\{b\} = \frac{1}{nm} s^2_{VIDT}\{Y\} \tag{14}$$

where $s^2\{b\}$ – variance of the coefficient estimation b; n – number of observations, m – number of parallel observations.

According to the requirements of significance, if the calculated value of *tri* for the corresponding coefficient b exceeds the value *tκ*, found from the Student's t-distribution table, the null hypothesis H_0:β = 0 rejected and the corresponding assessment of the coefficient is considered significant. Otherwise, the null hypothesis does not reject the assessment bi considered statistically insignificant, ie β = 0.

Checking the adequacy of the mathematical description of the response functions is to estimate the deviation of the predicted by the obtained regression equation of the magnitude of the response $\hat{Y}_j$ from research results $\bar{Y}_j$ at the same points of the factor space. The scattering of the results of observations near the regression equation estimating the true response function is determined by the variance of adequacy (15) [18, 23, 24]:

$$s^2_{AD} = \frac{m}{n-d}\sum_{i=1}^{n}(\bar{Y}_j - \hat{Y}_j)^2 \tag{15}$$

where d – the number of members of the approximating polynomial.

In order to check the adequacy of the model, it is necessary to calculate the relationship between the variance of adequacy s^2_{AD} and estimating the variance of response reproducibility . If these estimates of variance are homogeneous, then the mathematical description adequately reproduces the results of research, otherwise the description is considered inadequate. Using Fisher's F-test allows us to test the hypothesis of homogeneity of two sample variances s^2_{AD} and $s^2_{VIDT}\{Y\}$.

In case $s^2_{AD} > s^2_{VIDT}\{Y\}$, F-criterion is characterized by the ratio (16) [2, 20, 23]:

$$F = s^2_{AD} / s^2_{VIDT}\{Y\} \tag{16}$$

Next is the Fischer F-distribution table with significance level q for degrees of freedom $v_{1AD} = n-d, v_{2AD} = n(m-1)$ is the value *Fkp*. If the value of Fisher's F-test calculated for (16) is less than *Fkp*, the adequacy hypothesis is not rejected and the mathematical description is considered adequate. Otherwise, the obtained mathematical description is considered inadequate and requires additional research [19, 30].

Thus, the constructed mathematical model makes it possible to investigate and determine the coefficient of influence of each of the predetermined influencing factors on the type of objective

function, which is an integral indicator of the financial institution and apply appropriate measures to optimize this impact.

The multidimensional regression function is used to study different market segments to determine which variables actually affect market share, frequency of purchases, product availability, commitment to a particular product or brand, and many other factors [33].

With the help of regression analysis, HR managers investigate the relationship between the level of wages and geographical location of companies, the unemployment rate in the region, the growth rate of industry and more.

Financial analysts identify the reasons for rising stock prices by analyzing dividends, earnings per share, stock splitting, expected interest rates, savings, inflation, and more.

Thus, regression analysis provides managers with a powerful and flexible tool for studying the relationship between dependent and multiple independent variables.

When the amount of information is insufficient or management does not understand the complex method, qualitative forecasting models can be used [3, 23, 24]. In this case, forecasting the future is carried out by experts who seek help. The most common among high-quality forecasting methods are „jury opinion", „collective view of sellers", „consumer expectation model".

Forecasting by the „jury opinion" method is to combine and average the opinions of experts in relevant fields. A variant of this method is „brainstorming", during which participants first try to generate as many ideas as possible. Only after the process of generating ideas are evaluated. This method can be time consuming, but gives useful results, especially when the company needs a lot of new ideas and alternatives [8, 23, 24].

The method of „aggregate view of sellers" is based on the fact that experienced sales agents can very well predict future demand. They are well acquainted with consumer demand and can take it into account faster than they can build a quantitative model.

The „consumer expectation model" is a forecast based on the results of customer surveys of the organization. They are asked to assess their own future needs as well as new needs. Having collected all the data obtained in this way, the manager, taking into account his own experience, can better predict future demand [12, 23, 24].

Therefore, based on the considered methods and models of forecasting, it is possible to determine the features of their application depending on the tasks, lead time, availability of input information and so on.

The results of the analytical review are presented in table 1.

The data presented in table 1 indicate that in cases where it is necessary to make a detailed forecast of changes in the studied factor (eg demand) and there is information for previous periods, it is advisable to use factual, causal methods. And in cases where there is no information for previous periods and you need to get alternative solutions and new ideas, it is more appropriate to use heuristic and high-quality methods [9, 10, 18].

Table1. Features of forecasting methods in the process of modeling the economic activity of the company

Characteristic features	Forecasting methods			
	Factual	Heuristic	Causal	Qualitative
Features of application	To make a detailed forecast combination	For forecasting developments	For a large number of variables	For more information
Advantages	Detailed forecast	Independence from data for past periods	Establishing closeness between studied factors	Getting a lot of new ideas and alternatives
Disadvantages	The need for information from previous periods	Dependence on the human factor	The need for input information	It takes a lot of time

Thus, based on the analytical review of known forecasting methods, the features of their application were identified and the advantages and disadvantages were analyzed, which will take them into account in the process of modeling the company and promote economic development, competitiveness and optimize business processes.

3. Experimental research

Currently, there are a large number of software tools for forecasting using regression analysis methods. Thus, in particular, the analytical platform Deductor Studio allows, using the built-in tools of linear regression and neural network learning, to predict the values of the target function for future periods.

We present a generalized algorithm for determining the correlation between variables and the response function; the importance of the influence of these variables on the response function and the construction of a regression model based on important influencing factors. When developing the block diagram of the algorithm, we will use the existing standards.

As input data for building a regression model, we will use the corporation's data on the sale of its goods for past periods, denoted by *Xi* and the response function under the influence of these parameters – *Y*. Then, according to the correlation-regression analysis method, we will use blocks of procedures to determine the correlation coefficients between the input variables and the response function and estimates of the significance of determining these coefficients.

To check whether the coefficient is significant, we will use a conditional block. If the condition $tri > t\kappa$ is fulfilled, then procedure blocks are used to include this variable in the regression model. Next, the procedure for building a regression model is implemented. After that, a conditional block is used to check the adequacy of the constructed model. If the model is adequate, its parameters are derived and graphically visualized, if not, the model building procedure is used again. The algorithm for automating the construction of a correlation-regression model is presented in Fig. 3.

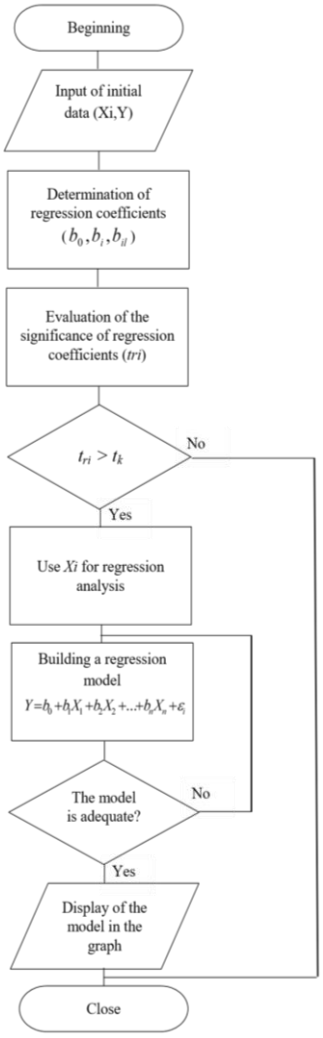

Fig. 3. Block diagram of automation of regression analysis

Here is an example of the use of regression analysis tools in Deductor Studio, where based on the actual input data of the corporation, reflecting the sales of its products for 2019–2021 (Fig. 4, 5) forecasting sales for 2022 (Fig. 6, 7).

In the first stage, Deductor Studio imported initial data on the sale of goods by the corporation, which is presented in the form of a graph to improve visualization. We see that they have a lot of noise and need partial processing to remove anomalous values (Fig. 4).

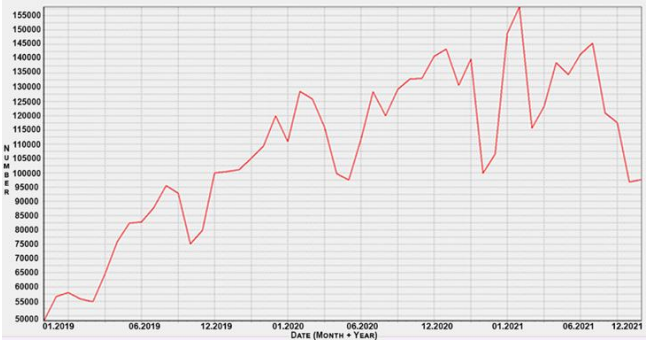

Fig. 4. Initial sales data imported into Deductor Studio as a chart

After applying the partial processing tool in Deductor Studio, it can be seen that the graph got a smoother shape as a result of eliminating values that differed significantly from the total data set (Fig. 5).

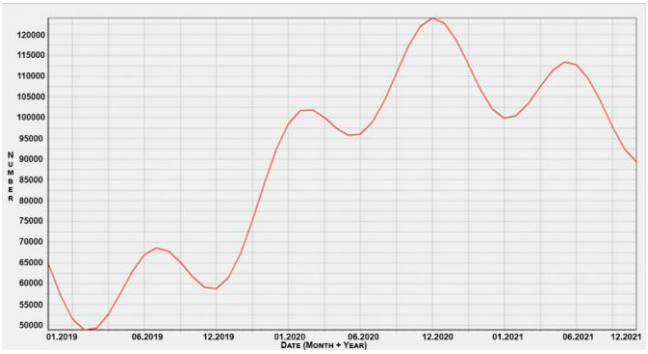

Fig. 5. Initial sales data after partial processing

Then the parameters for forecasting sales indicators for future periods (3 months) were adjusted and the forecasting process was performed using the mathematical apparatus of regression analysis (expressions (6) – (16)) and neural network tools (Fig. 6).

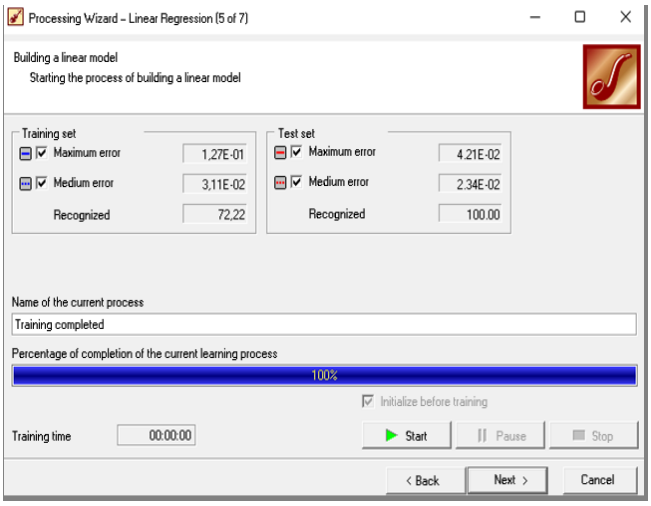

Fig. 6. Forecasting settings based on regression analysis and neural network

As a result of the use of forecasting tools in Deductor Studio on the basis of actual data for 2019–2021, the estimated sales of goods for the first three months of 2022 were obtained, which are marked in blue on the chart (Fig. 7).

As can be seen from the graph presented in figure 5, compared to the actual data on sales of goods by the corporation for 2019–2021 (marked in red) in early 2022, a downward trend is forecast, and then there will be significant growth by the end of the first quarter of 2022. This can be explained by the projected growth in demand in the first half of the year, as it happened in the corresponding previous periods in 2019–2021.

Thus, based on the results obtained, it is possible to get an idea of both the sales of certain goods for the forecast periods, and see the general trend of sales of goods in the future, which indicates the effectiveness of these forecasting methods.

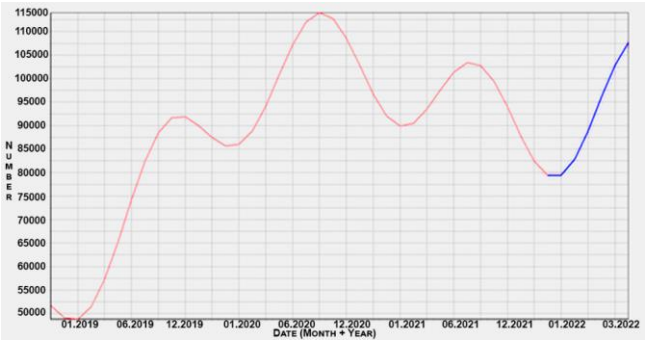

Fig. 7. Projected sales data for the coming months

4. Conclusions

Strategically important processes of companies were the analysis of the market and consumer needs, the study of changes in their needs and behavior, which determine all future policies for product creation, production, delivery to the consumer and profit. Only integrated systems can provide an adequate rapid response to rapid changes and growing variability of the business environment in the corporate governance system. The process approach is the consideration of all the activities of the corporation as a set of interacting processes that take place within the organizational structure and realize the purpose of its existence. That is why the need to apply a process approach to their management comes to the fore in the functioning of companies. The main object of the process approach to management is a business process, which is a planned algorithm of interrelated actions or workflows, which is subject to systematic change under the influence of external and internal factors, which involves all company resources to meet consumer demand and profit maximization. If the profit exceeds the cost of business processes, then the company's activities can be considered effective. Therefore, to provide the company with stable profits and reduce costs, it becomes necessary to carry out competent business process management. A necessary component of analytical modeling of business processes is forecasting to determine the future prospects of the company. That is why the greatest interest for company analysts is the issue of effective forecasting of business processes. Business process forecasting will allow modeling and optimizing business activities in the future. Implementing forecasting tools in an integrated corporate governance system can make business more predictable, manageable and controlled.

Given the development of information technology and analytical systems with components of artificial intelligence, it is necessary to understand that digital technologies will evolve as hybrid solutions. Thus, the sooner a corporation embarks on the path of digitalization, the more effective corporate governance will be.

The mechanism of effective corporate governance significantly expands the opportunities to attract investment in business, promotes productivity and competitiveness of companies.

References

[1] Azarova A.: Information Technologies and Neural Network Means for Building the Complex Goal Program "Improving the Management of Intellectual Capital". Lecture Notes on Data Engineering and Communications Technologies 77, 2022, 534–547.
[2] Azarova A., Zhytkevych O.: Mathematical methods of identification of ukrainian enterprises competitiveness level by fuzzy logic using. Economic Annals-XXI 9–10(2), 2013, 59–62.
[3] Azarova A.O. et al.: Information technologies for assessing the quality of IT-specialties graduates' training of university by means of fuzzy logic and neural networks. International Journal of Electronics and Telecommunications, 66(3), 2020, 411–416.
[4] Berk J. et al.: Fundamentals of Corporate Finance, Global Edition. Pearson Available, 2022.
[5] Box G. et al.: Time Series Analysis: Forecasting and Control. Wiley, 2015.
[6] Brealey R. et al.: ISE Fundamentals of Corporate Finance. Irwin McGraw-Hill Publishing Co. Ltd., 2022.
[7] Brigham E., Houston J.: Fundamentals of Financial Management. Learning EMEA, 2021.
[8] Bruskin S. N. et al.: Business performance management models based on the digital corporation's paradigm. European Research Studies Journal. EU. 20(4A), 2017, 264–274.
[9] Clayman M. et al.: Corporate Finance: A Practical Approach. Wiley, 2012.
[10] Ehrhardt M. et al.: Financial Management EMEA: Theory and Practice. Cengage Learning EMEA, 2019.
[11] Evans M. K.: Practical Business Forecasting. Wiley, 2008.
[12] Garg P.K.: Forecasting Management: Futurism on Management. Global India Publications, 2009.
[13] Hanke J. E., Wichern D. W., Reitsch A. G.: Business Forecasting. Prentice Hall, 2001.
[14] Ihnatyeva I. A., Harafonova O. I.: Korporatyvne upravlinnya: Pidruchnyk. Tsentr uchbovoyi literatury, Kyiv 2013.
[15] Kuzmina E. et al.: Methods and techniques for evaluating effectiveness of information technology implementation into business processes. Proc. of SPIE. 10808, 2018, 108081N.
[16] Lawrence K. D. et al.: Advances in Business and Management Forecasting. Emerald Publishing Ltd., 2018.
[17] Makridakis S. et al.: Forecasting methods and applications. Wiley India Pvt. Ltd., 2008.
[18] Melicher R. et al.: Introduction to Finance: Markets, Investments, and Financial Management. Wiley, 2013.
[19] Mescon M. H. et al.: The Fundamentals of Management. Williams, 2019.
[20] Mittelhammer R. C.: Mathematical Statistics for Economics and Business. Springer, 2013.
[21] Mostenska T. L. et al.: Korporatyvne upravlinnya. Karavela, Kyiv 2015.
[22] Shyian A. A. et al.: Modeling communication between the public and the authorities while implementing innovative projects in the context of e-democracy and public administration. Science and Inn. 16(6), 2021, 18–27.
[23] Shmueli G. et al.: Data Mining for Business Analytics: Concepts, Techniques, and Applications in R. Wiley, 2017.
[24] Vandeput N.: Data Science for Supply Chain Forecasting. Business & Economics, 2021.
[25] Van Horne J. et al.: Fundamentals of financial management. Pearson Ed. Ltd., 2009.
[26] Voynarenko M. P. et al.: Managing the development of innovation business processes with automated information systems. Marketing and innovation management 4, 2017, 133–148.
[27] Wade D. et al.: Corporate Performance Management. Routledge, 2001.
[28] Westerfield R. et al.: Fundamentals of Corporate Finance. Irwin McGraw-Hill Publishing Co. Ltd., 2019.
[29] Wilson H. et al.: Business Forecasting with Forecastx. McGraw-Hill Ed. 2009.
[30] Yaremko S. A. et al.: Intelligent system in the context of business process modeling. International Journal of Electronics and Telecommunications 67(2), 2021, 163–168.
[31] Yaremko S. et al.: Using artificial intelligence technologies for forecasting business processes. Computer-integrated technologies: education, science, production 23, 2021, 230–234.
[32] Yarmolenko V. et al.: Practice Analysis of Effectiveness Components for the System Functioning Process: Energy Aspect, Lecture Notes on Data Engineering and Communications Technologies 77, 2022, 282–296.
[33] Zanda G.: Corporate Management in a Knowledge-Based Economy. Palgrave MacMillan, 2012.

Ph.D. Svitlana A. Yaremko
e-mail: s.yaremko@vtei.edu.ua

Ph.D., associate professor of the Department of Economic Cybernetics and Information Systems, Vinnitsa Institute of Trade and Economics State University of Trade and Economics. Author of more than 200 publications, including 2 monographs, 2 collective monographs, 2 textbooks, 1 patent for inventions of Ukraine, and more than 50 scientific articles in professional journals, of which 7 are in scientometric databases Scopus and WoS.

http://orcid.org/0000-0002-0605-9324

Ph.D. Elena M. Kuzmina
e-mail: o.kuzmina@vtei.edu.ua

Ph.D., associate professor of the Department of Economic Cybernetics and Information Systems, Vinnitsa Institute of Trade and Economics State University of Trade and Economics.
Author of more than 200 publications, including 4 monographs, 2 collective monographs, 4 textbooks, 3 patents for inventions of Ukraine, and more than 60 scientific articles in professional journals, of which 7 are in scientometric databases Scopus and WoS.

http://orcid.org/0000-0002-0061-9933

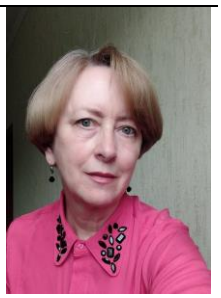

Prof. Nataliia B. Savina
e-mail: n.b.savina@nuwm.edu.ua

Doctor of science in economics, professor, Vice-Rector for Research and International Relations in National University of Water and Environmental Engineering.
Scientific directions are evaluation and forecasting of the efficiency of investments in entrepreneurial projects, in logistics and economic systems of various levels, in human capital. Deals with financial instruments of international scientific and technical cooperation, modeling of the marketing business-processes under the industrial enterprise's competitiveness reflexive control, and modeling of the dialogue „human-computer" for ergonomic support of e-learning.

http://orcid.org/0000-0001-8339-1219

Prof. Iryna Yu. Yepifanova
e-mail: yepifanova@vntu.edu.ua

Doctor of economic sciences, professor, acting dean of the Faculty of Management and Information Security of Vinnytsia National Technical Uneversity, academician of the Academy of Economic Sciences of Ukraine.
Scientific interests – financial support of innovative activities of domestic enterprises, enterprise potential, competitiveness, personnel management, digital economy, energy saving

http://orcid.org/0000-0002-0391-9026

Ph.D. Halyna B. Gordiichuk
e-mail: ggord@bigmir.net

Candidate of pedagogical sciences, associate professor of the Department of Innovative and Information Technologies in Education, Vinnytsia Mykhailo Kotsiubynskyi State Pedagogical University.
Research Interests: professional pedagogy, formation of information and communication competence, professional education in the field of digital technologies

http://orcid.org/0000-0001-6400-5300

M.Sc. Dinara Mussayeva
e-mail: d_i_n_mus@mail.ru

Scientific Secretary and Research Associate of the Institute of Economics CS MES RK, Almaty, Kazakhstan.
She is a master of Al-Farabi Kazakh National University, Ph.D. student of the Institute of Economics of the CS MES RK, specialty – „World Economy".
As a responsible executive, he actively participates in conducting fundamental and applied research in priority areas for the state, such as digitalization of the economy, knowledge-based economy, etc.

http://orcid.org/0000-0002-8349-213X

http://doi.org/10.35784/iapgos.3248 received: 6.11.2022 | revised: 26.11.2022 | accepted: 15.12.2022 | available online: 30.12.2022

ELABORATION AND RESEARCH OF A MODEL OF OPTIMAL PRODUCTION AND DEVELOPMENT OF INDUSTRIAL SYSTEMS TAKING INTO ACCOUNT THE USE OF THE EXTERNAL RESOURCES

Dmytro Hryshyn[1], Taisa Borovska[1], Aliya Kalizhanova[2]
[1]Vinnytsia National Technical University, Vinnytsia, Ukraine, [2]University of Power Engineering and Telecommunications; Institute of Information and Computational Technologies MES CS RK, Almaty, Kazakhstan

Abstract. *The problem of optimization of investment projects related to the development of modern production systems is considered. The tasks of managing of operation and development of production systems considering external resources – the synthesis and analysis of optimal credit strategies – are posed and solved. An analysis of analogs – solutions of the variational problem of optimal development, the disadvantage of which is the difficulty of obtaining information about the state of production and the external environment, was carried out. The new solution is based on the resource approach, when external resources are taken into account in the cost of production resources. A generalized model of optimal development is used, in which the planned period of the investment project is divided into intervals. At the beginning of each interval, the optimal development strategy is adjusted taking into account the clarification of information about the future state of the active environment: actions of competitors, consumers, world markets. To determine the optimal amount and optimal distribution of credits between subsystems, the maxima of the criterion – the parameterized function of the system's efficiency – are determined at each interval. A new model has been developed based on the model of optimal development, which takes into account the use of external resources, such as loans. The method of including an external resource in the development function and the production function is considered. Examples of modeling are given.*

Keywords: optimal aggregation, production function, development function, external resource, simulation modeling

OPRACOWANIE I BADANIE MODELU OPTYMALNEJ PRODUKCJI I ROZWOJU SYSTEMÓW PRZEMYSŁOWYCH Z UWZGLĘDNIENIEM WYKORZYSTANIA ZASOBÓW ZEWNĘTRZNYCH

Streszczenie*. Rozpatrywany jest problem optymalizacji przedsięwzięć inwestycyjnych związanych z rozwojem nowoczesnych systemów produkcyjnych. Postawiono i rozwiązano zadania zarządzania funkcjonowaniem i rozwojem systemów produkcyjnych z uwzględnieniem zasobów zewnętrznych – synteza i analiza optymalnych strategii kredytowych. Przeprowadzono analizę analogów – rozwiązań wariacyjnego problemu optymalnego rozwoju, którego wadą jest trudność uzyskania informacji o stanie produkcji i otoczeniu zewnętrznym. Nowe rozwiązanie oparte jest na podejściu zasobowym, kiedy to zasoby zewnętrzne są uwzględniane w kosztach zasobów produkcyjnych. Wykorzystano uogólniony model optymalnego rozwoju, w którym planowany okres realizacji projektu inwestycyjnego podzielono na przedziały. Na początku każdego interwału optymalna strategia rozwoju jest korygowana z uwzględnieniem doprecyzowania informacji o przyszłym stanie otoczenia aktywnego: działań konkurentów, konsumentów, rynków światowych. W celu określenia optymalnej ilości i optymalnej dystrybucji kredytów pomiędzy podsystemami, w każdym interwale wyznaczane są maksima kryterium – sparametryzowanej funkcji efektywności systemu. Na podstawie modelu optymalnego rozwoju opracowano nowy model, który uwzględnia wykorzystanie zasobów zewnętrznych, takich jak kredyty. Rozpatrzono metodę uwzględniania zasobu zewnętrznego w funkcji rozwoju i funkcji produkcji. Podano przykłady modelowania.*

Słowa kluczowe: optymalna agregacja, funkcja produkcji, funkcja rozwoju, zasób zewnętrzny, modelowanie symulacyjne

Introduction

Globalization, a steady trend of increasing the efficiency of production and services, growth of the impact of uncertainty and disturbances, taken together, have led to the parametric and structural changes in production as an object of management [18].

Main problems in the field of practice and theory of optimal management and development of production are: novelty, dynamism and significant nonlinearity; natural non-stationarity of the processes of functioning and development of the modern production system; lack of effective optimal control methods for high-dimensional problems [7, 21, 30, 31]. Works with fundamental theoretical solutions of variational problems are known [2, 3, 14, 15]. The general feature of these tasks is an object nothigher than of the third order, significant restrictions on the type of functions [4, 5, 32]. To manage large-scale systems – energy systems, economic segments, market systems, „open control" („fair play"), „artificial social systems" is used [9, 19]. In these methods, the global problem of a large production system is solved by each „participant" taking into account their own goals. Such methods allowed to obtain a large number of fundamental and useful results for practice. We conducted modeling of optimal control algorithms proposed by Opoitsev [23]. With the introduction of non-smooth and non-convex „production functions" into the model, it was not possible to ensure the convergence of algorithms for finding the optimal state of equilibrium. This was the primary reason for developing a searchless method of optimal aggregation [6, 9]. A large number of studies have been conducted on the attraction and use of external resources. In [14, 33], two variants of the Hamilton function were proposed: in the form of the term „credit function" and in the form of a multiplier with a variable „cost" in the function of production development. The development of the optimal aggregation operator for the „production, development" structure [7, 10] made it possible to modify and generalize the task of crediting the processes of optimal functioning and development of the production system.

This paper presents the solution of one of the tasks of creating a generalized mathematical model of optimal development. Section 2 of this article presents the results of research and development of the first stage, on which the development of a new model is based [11, 15, 20].

The aim of the research is to develop a new approach to optimization of the credit strategy of an enterprise in the active environment of competitors and consumers. Tasks of the research:

- formulation and solution of the optimization and development problem of structures „innovation, development, production, accumulation", taking into account external resources,
- decomposition of the planning period into intervals to improve efficiency in the conditions of close forecasting horizons,
- development of software modules for optimization of use of external resource based on the „embedding" of loans in the functions of production and development,
- on the basis of developed modules, perform modeling of optimal development processes using an external resource.

1. Optimal aggregation methodology

The theoretical basis for the development is the optimal aggregation methodology [8], which: sets the rational structure for the production system; allows any loosely monotonous production functions; requires the identification of all significant resource relationships; provides a reconfiguration of the production system in case of failures in the subsystems [11, 24];

provides the adaptability of optimal control to changes in prices and technological parameters [1, 11, 23].

Working models for optimal production and development process are developed using Mathcad software, which gives us an instrument for running simulations of optimal processes of real production systems.

2. Analysis of the analogs of production and development of the production systems

We analyzed (with texts, graphics, and formulas) basic analogues in the field of objects and methods of modern production systems management, and assessed the existing state of this field.

Figure 1 shows the complex processes in the system „manufacturers, products of manufacturing process" of a particular production segment [8]. This is concept analysis of „globalization, a steady trend of increasing the efficiency of production and services, and the growing influence of uncertainty and disturbances, led together". Fig. 1a shows two implementations of a random process of functioning and development of manufacturers system on the market of one product. The mathematical model of the system is assembled on the basis of classical models of microeconomics; 3D graph – a sequence of rank distributions of the producers. The dependencies of the total demand and supply on time, as well as the dynamics of the ranks of the selected manufacturer „amid" the entire system state, are located in the same phase space. Otherwise, it is „the dynamics of the element of the system of producers in the active environment of competitors and consumers". Fig. 1b presents two implementations of random process for a multi-product system. Besides the ranked processes, unranked processes are also presented. Simulation scenario: at the beginning of the process, manufacturers are ranked, the first half of high-rated manufacturers use classical management methods, the second half of low-rated manufacturers use innovative – risky management methods. Risky management gives a manufacturer with a low rating non-zero probability to increase significantly the rating. In the upper graph of Fig. 1b the outsider has become a leader; in the lower graph of Fig. 1b outsider remains an outsider.

We analyzed existing models of production systems considering credits.

The closest analog [6, 12, 13] researches the problem of optimal credit policy for the manufacturer to minimize total production cost. Developed model takes into account credits and reliability of produced items.

However, it does not take into account internal resource distribution between subsystems such as „development", „production", „innovations".

Satisfactory models of attracting and using external resources to solve the problem of „development of production systems in an active environment" have not been found. Based on the results of developments [8, 16, 25], the structure of the management system based on simulation models of the system of producers of a certain production segment with the involvement of external resources such as lending was proposed (Fig. 2). The basis of the scheme is a predictor model and a real-time model. In the center are two examples. Above is the empirical frequency distribution of income of some enterprise of the „3 products, 4 manufacturers" system. The diagram displays the „loans" subsystem and the corresponding resource and financial ties.

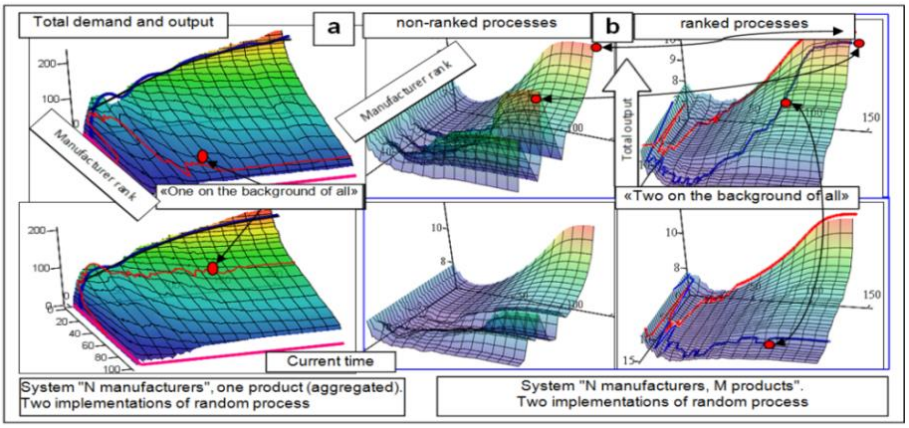

Fig. 1. Modeling of manufactures system dynamics

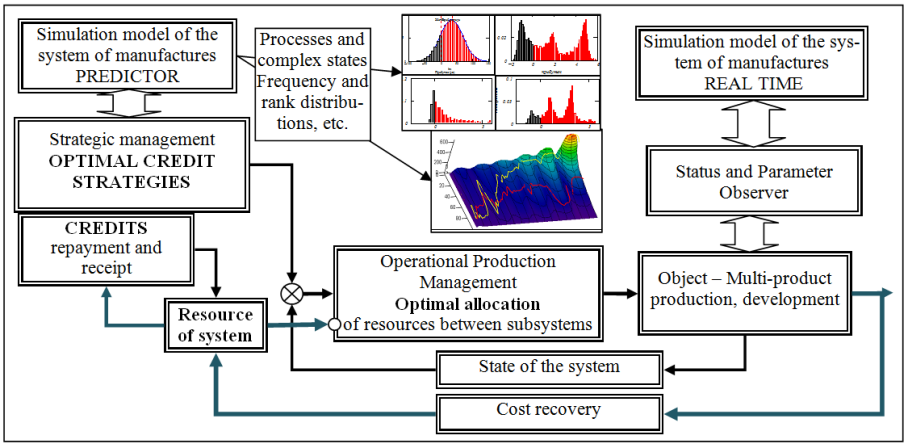

Fig. 2. Diagram of ASUP based on a simulation model of the class „one against the background of all"

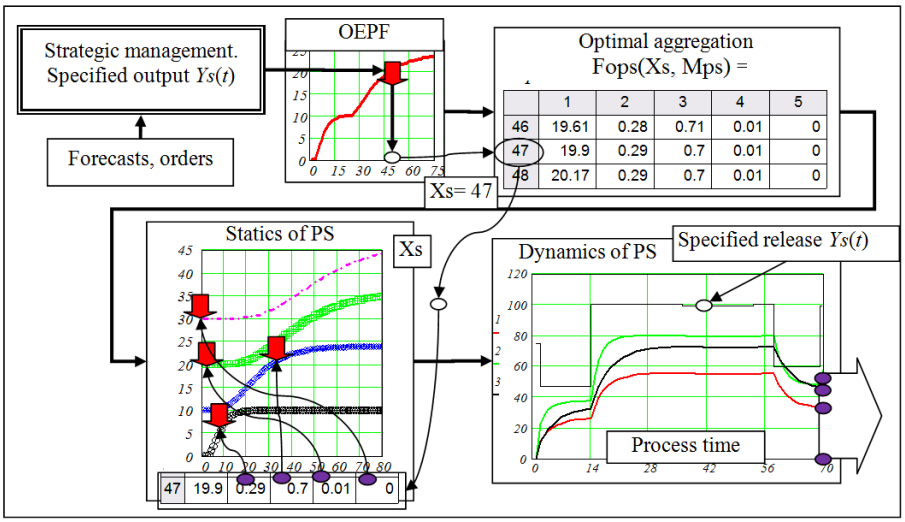

Fig. 3. Operational production management based on optimal aggregation

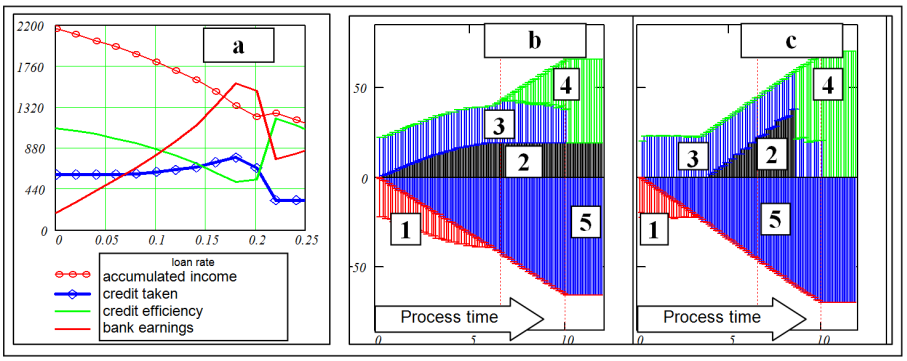

Fig. 4. Credit Policy Analysis Examples

The characteristic feature of the control system in Fig. 2 – availability of a system of specialized models of the system of manufacturers and a production system: real-time simulation models and a predictor model; state and parameter observer. These models create information support for the subsystems of strategic and operational management. The diagram highlighted the subsystem „credits", which is element of the external resource in this article.

Fig. 3 gives a visual representation of production management based on optimal aggregation methods. The „dynamics" block contains transients in subsystems for a given input effect of the production system. The „strategic management" block determines a specified output, for which the module „optimal aggregation" calculates the minimum of the total costs Xs, and their distribution over the elements of the system. The „static" block represents the definition of subsystem outputs for a specified resource distribution. The block „dynamics" represents the rate of the output in the subsystems.

Analysis and selection of optimal use of external resources. We analyzed analogs of the model of the optimal development of the enterprise, taking into account lending [12, 17]. The area of these model's adequacy is „passive" external environment, independent of the actions of producers and consumers. The novelty of this research is the development of adequate enterprise management, taking into account the active environment of competitors and consumers.

Fig. 4 presents an example of a comparative analysis of credit strategies. Fig. 4a – dependences on the credit rate of the following indicators: „accumulated income of the manufacturer", „took loans", „effectiveness of loans", „bank income". Let us analyze the dependence of the indicator „took loans" from the rate: from zero to 6% – a slight drop, the more expensive the loans, the less we take. The interval is from 6 to 18% – the higher the rate, the more we take loans, the reason – it is necessary to overcome the „inefficiency threshold" of production. The interval from 18 to 25%: expensive loans are not covered – less credits are taken. Let us compare the dependencies of „bank income" and „credit efficiency" (for production): the complete opposite. Relevant for the manufacturer indicator: „accumulated income" monotonously decreases with the increase of the loans rate.

Figs. 4b and 4c show two alternative strategies of optimal development (description: 1 – credits strategy; 2 – credit return strategy; 3 – development spending; 4 – accumulation rate – criterion increment; 5 – production rate). Processes have different credit recovery strategies. In Fig. 4c it is: „all profits (3) go to the return of debt on credits". In practice, the strategy of „deferred payments" is used. These credit recovery strategies are part of a set of models and programs [12, 21, 26]. Regarding the use of working models, presented in Fig. 3, it should be noted that they are adequate to the reality only for an „autonomous" enterprise with an unlimited market, independent on the actions of competitors and the „whims" of the consumers.

The given examples of the solution of variational development problems, taking into account the use of external resources [9, 22, 27] – is a small part of the research and development in the field of optimal development of the systems. The possibilities of obtaining new scientific and practical results are not exhausted within the framework of the developed models of optimal development and new information technologies of designing new models for new tasks. This should be an operational optimal decision on the allocation of loans: which subsystem, in what time interval, in what volume and taking into account the state of the system and the external environment. Further the development of credit strategies of manufacturers in the active environment of competitors and consumers is presented. This development is the approximation to the requirements.

3. Statement and solution of the problem of optimal aggregation taking into account loans

Development of a model for attracting external resources based on aggregation „production, development".

We used the methodology of optimal aggregation, the main point of which is the possibility of equivalent replacement of a rational production system by an optimal equivalent element with a production function: $Ys = Fops(Xs, Mps)$, where Xs, Ys – total costs and output of the system; $Fops$ – optimal equivalent production function (OEPF); $Mps = augment(vpp, vpr, vpc, vpkr)$ – parameters matrix, OEPF, composed of appropriate vectors. Here: vpp, vpr – vectors of parameters of production and development functions, vpc – vector of price parameters and $vpkr$ – vector of credit parameters.

The input data for the optimal aggregation problem are the production functions of the elements of the system, which are given in a discrete form, in the form of a table of the relationship between the spent resource and produced value. The result is the optimal equivalent production function, which is also provided in a discrete form, and shows the optimal distribution of resources between the elements of the system at each step of the process. The paper uses a „resource" approach, in which inputs and outputs are measured in abstract units.

We choose the following alternatives to return credits: from the incomes of production and the strategies of credits return, which are presented in Fig. 4.

We modified the production and development functions taking into account credits as a specific „borrowed resource" and displayed it in the parameters of operators of optimal aggregation of parallel structures and structures „production, development". No close analogues of this approach were found, therefore at the first stage of development we use structural and logical methods of applied system analysis [7, 8, 16].

Fig. 5 presents the analysis of the credit impact of subsystems „production" and „development". We assume that the return of loans is related to the costs of production at the level of the production system on the whole. In this paper, we consider the tasks at the resource level, and the prices are included as parameters. Models of the markets where prices are formed are described in work of Borovska [9, 11]. On the left graph of Fig. 5 three functions of production are presented: excluding and taking into account the cost of debts repayment. The situation when loans supplement own resources is considered. We see that the output at constant total costs may differ significantly. On the right graph of Fig. 5 four functions of production are presented: the initial, after the cost of a loan for development and two functions, taking into account the cost of paying debts. We see that the output at constant production costs may differ.

The model in Fig. 5 allows to identify the specific features of production processes development. „Short" loans should be taken in case when maximum return in the form of products, production facilities is expected. It is advisable to return credits with a deferred payment. In a multi-product system, it is possible and desirable to form the chains of „production, development" processes in different phases of implementation [27, 28, 29].

General conclusions regarding the analysis of credits: credits should be spent on improving the efficiency of the production system on the levels of „production", „development", and „innovation".

4. Mathematical model of optimal development taking into account the external resources. Embedding credits in production and development functions

Based on the materials, proposed above, we solve the problem of optimal aggregation for the structure of „production, development", taking into account external resources. Optimal aggregation of a binary structure is the solution of one-dimensional problem of non-linear programming for a pair of elements of the „costs, output" class. The solution is found for the entire interval of determining the variable „costs", and the result of the aggregation is the „optimal equivalent production function" (OEPF) of a given binary structure. Optimal aggregation operations could be made associative. This enables you to create the „algebra of production functions", similar to the algebra of transfer functions in Automatic control theory [16].

Binary operators and operands of optimal aggregation algebra. The binary operator can be represented by a mathematical model, and then by the appropriate computer program or immediately – a „working model". The development of the binary operator of optimal aggregation is the main intellectual component of optimal aggregation methods. The result of the development is a multidimensional nonlinear programming problem, which is decomposed into a system of one-dimensional problems, solved by the searchless method. The form of solving the problem of optimal aggregation is: a function of the total resource, as well as of the parameters. Parameters could be numbers, vectors, matrices, and subroutines.

Mathematical model of structure with parametric resource connection „production, development". Substantial background: modern high-tech, innovative productions are integrated with the subsystems of development and maintenance of production units, subsystems of management, control and testing. Organizational integration makes management and financial integration desirable and possible. These transformations generate a new class of optimization problems and corresponding mathematical models. We considered the basic model of the integrated system „production, development" [11, 35]. In this paper, we modify this model to account the use of credits.

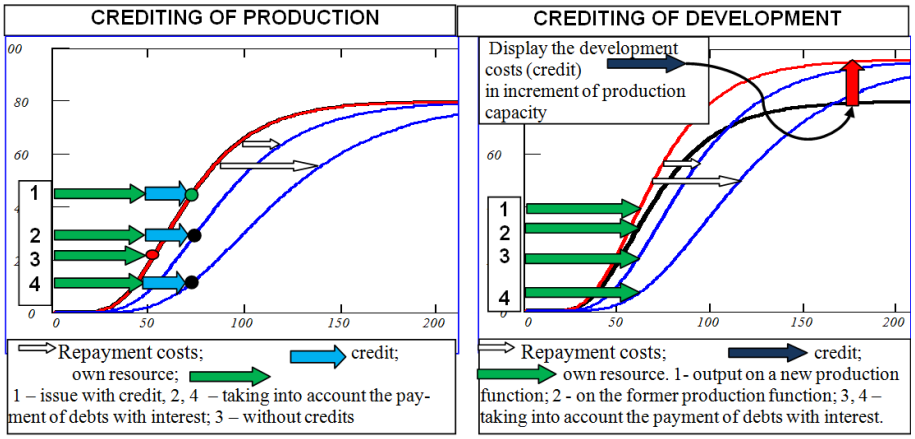

Fig. 5. Resource schemes of credits for the production and development

We write down the functions of production (PF) and development (DF):

$$fp(xp) = fpp(xp, vPp(xr, vPp0)); \; fr(xr) = fc(xr, v\Pr) \quad (1)$$

where *xp*, *xr* – production and development resources, *vPp0* – the initial value of the vector of parameters of the production function (PF), *vPr* – vector of development function parameters (DF).

We consider in details the parametric coupling function of the production function (PF) with the development function (DF):

$$vPp(xr, vPp0) \Rightarrow vPp = VP2(\alpha, \Delta xs, vPp0, v\Pr) \quad (2)$$

where *VP2*() – a function that characterizes the transformation of the costs of the „development" subsystem into a change in the parameters of the production function (PF) – increase of the efficiency and production capacity, decrease of service costs, $\Delta xs \cdot \alpha$, $0 \le \alpha \le 1$ – quantum of system resource and the proportion of its distribution between development and production. The initial state of the system is set: *xp*0 – production rate: *vPp*0 – parameter vector of the production function (PF); *vPr* – vector of development function parameters (DF).

We write the equation of state of the system „production, development" after using a quantum of resource:

$$xp = xp0 + \alpha \cdot \Delta xs; \; xr = (1-\alpha) \cdot \Delta xs \quad (3)$$

Authors display development costs in the changes in production capacity $yr = fr(xr, v\Pr)$, taking into account (3) and obtain $yr = fr((1-\alpha) \cdot \Delta xs, v\Pr)$. We use three-parameter models of the production function (PF) and development functions (DF), we assemble into the user vector function: the dependencies of the parameters of the production function model (PF) for specific segments of production and technologies:

$$vPp = VP2(\alpha, \Delta xs, vPp0, v\Pr) \quad (4)$$

After using the resource quantum for the development and production, taking into account (3) and (4), rate of production will have following form:

$$yp = fp(xp, vPp) = fp((xp0 + \alpha \cdot \Delta xs), (vPp0 + \delta vPp)) \quad (5)$$

Taking into consideration (4), (5), we form the function of the user – „new rate of release":

$$yp(\Delta xs, \alpha) = fp((xp0 + \alpha \cdot \Delta xs), VP2(\alpha, \Delta xs, vPp0, v\Pr)) \quad (6)$$

and user function „output increment":

$$\delta yp(\Delta xs, \alpha) = yp(\Delta xs, \alpha) - yp0 = yp(\Delta xs, \alpha) - fp(xp0, vP0) \quad (7)$$

Expression (7) is the optimization criterion in the basic problem of optimal aggregation of the integrated system „production, development". Modification of the binary operator „production, development" to account he credits. Fig. 6 presents an example of the development of a transition operator between development process intervals.

The unpacking of the user function $Foppt(MP1, MP2)$ – OEPF test system is performed. The details and logic of the transition between the matrices of parameters of the integrated system „production, development" are presented. In the upper part – the initial data; in the middle part – the dependencies between the elements of the parameter matrices; in the lower part – the transition between the states of the matrix of parameters of the optimally aggregated production system, which has a parametric resource connection between the subsystems „production" and „development", for two points in time. In the right part of Fig. 6 the results of calculations for the three steps of „working out" „quanta" of the resource are shown.

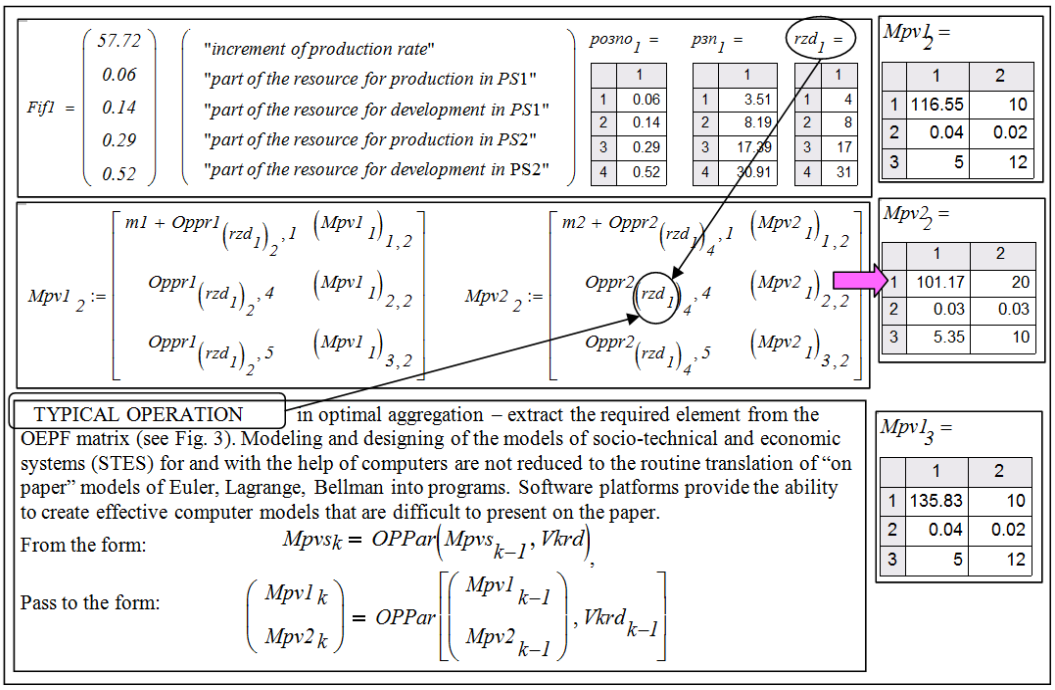

Fig. 6. Obtaining of the operator of the transition between the development process intervals

5. Testing of modules of optimal development and analysis of the structure of the complex models

All elements of the developed complex models have been tested. On a set of models, testing was performed to reproduce the available empirical data, to match the results obtained on alternative models. Fig. 7 shows an example of testing a key component – the operator of the transition between intervals.

Fig. 7a – testing of the „response" of the system to the dynamics of the magnitude of the resource quanta: with increasing and decreasing. Results are represented by graphs, numbers, vectors *Ra*, *Rb*. Fig. 7b – construction of optimal equivalent efficiency functions for three development intervals, and the results (outputs and resource distributions) of resource quantum development with and without credits are derived. Also areas of maximum efficiency loans are highlighted.

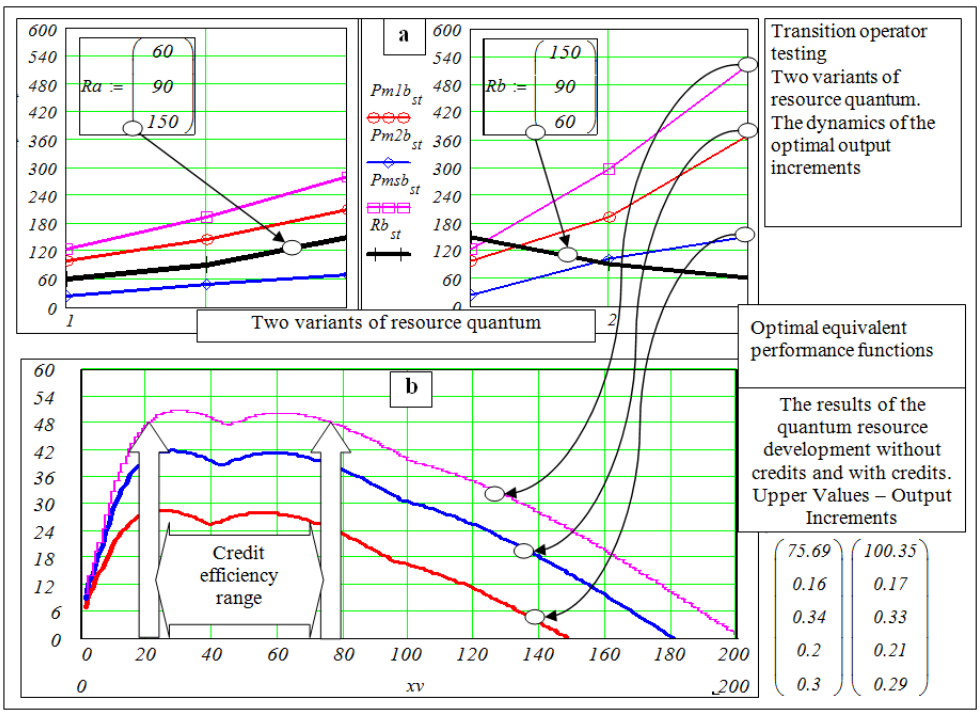

Fig. 7. Testing of the transition operator between the intervals of the development process – the optimal development of a quantum of resource. Example

6. Conclusions

Analysis of analogues and prototypes showed the constant relevance of optimal development problems for production systems of all the levels. Fundamental mathematical models for the simplified problems and objects of nothigher than the third order are obtained. The solutions obtained for variational problems were not generalized. There were no adequate and effective mathematical development models using external resources.

The goal of generalizing the problem of optimal development of production systems based on the optimal aggregation methodology is set so that the changes in the control system during the transition to the new object – with new technologies, new production products, are reduced to parametric tuning.

The search and analysis of direct analogues was performed. New tasks have been set to achieve the goal. The development base is the classical formulation of a variation development problem and its solution by the maximum principle method and the optimal aggregation methodology. Scientific novelty:

- new task of optimal aggregation of structures with parametric connections „innovation, development, production, accumulation" has been solved. The result of aggregation is the optimal distribution of the system resource between development subsystems and production subsystems;
- decomposition of the planning period into intervals to improve efficiency in the conditions of close forecasting horizons is performed. At the beginning of each interval, the optimal development strategy is calculated for the remainder of the planned period;
- software optimization of use of external resource based on the „embedding" of loans in the functions of production and development is proposed and implemented.

The software system has been developed, modeling of optimal development processes using an external resource has been performed.

Practical significance. Research and development allow for any moment of the process the optimum volume of credits depending on the current pace of production and demand forecasts. Optimal rapid allocation of own resources between production reduces the need for loans. Prospects. The next stage for this development is the creation of mathematical models and software module „virtual reality" statistics based on Predictor models. This will take into account the risks in the optimal management of the production and development. The results are used for further research to develop optimal adaptive control system of modern enterprise.

References

[1] Avrunin O. et al.: Classification of CT-brain slices based on local histograms. Proc. of SPIE 9816, 2015, 98161J.
[2] Azarova A.: Information Technologies and Neural Network Means for Building the Complex Goal Program „Improving the Management of Intellectual Capital". Lecture Notes on Data Engineering and Communications Technologies 77, 2022, 534–547.
[3] Bellman R. E. et al.: Certain problems of mathematical control theory. Publishing House of Foreign Literature, Moscow 1963.
[4] Bellman R. E., Kalaba R. E.: Dynamic programming and modern control theory. Academic, New York 1965.
[5] Bertsekas D. P.: Dynamic programming and Optical Control. Athena Scientific, 2017.
[6] Borovska T, Hryshyn D.: Comparative Analysis of Methods for Optimizing Production Systems based on Hamiltonian and the Method of Optimal Aggregation. IEEE 16th International Conference on Computer Sciences and Information Technologies (CSIT), 1, 2021, 345–348 [http://doi.org/10.1109/CSIT52700.2021.9648626].
[7] Borovska T. et al.: Searchless Intelligent System of Modern Production Control. IEEE 15th International Conference on Computer Sciences and Information Technologies (CSIT), Zbarazh, Ukraine, 2020, 291–296 [http://doi.org/10.1109/CSIT49958.2020.9321842].
[8] Borovska T.: Generalized model of optimal development, based on the integration of production and development subsystems. XII International Scientific and Technical Conference „Computer science and information technologies" CSIT'2017, Lviv, Ukraine, 2017, 446–449, 17353622 [http://doi.org/10.1109/STC-CSIT.2017.8098826].
[9] Borovska T. et al.: Intelligent System of Modern Production Control Based on the Methodology of Optimal Aggregation, 2021, 291–296 [http://doi.org/10.1109/CSIT49958.2020.9321842].

[10] Borovska T. et al: Adaptive production control system based on optimal aggregation methods. Proc. of SPIE 10808, 2018, 108086O [http://doi.org/10.1117/12.2501520].
[11] Borovska T. et al.: Mathematical models of production systems development based on optimal aggregation methodology. Proc. of SPIE 10445, 2017, 104452P [http://doi.org/10.1117/12.2281222].
[12] Chertovskoy V., Tsehanovsky V.: Optimal model of manufacturing control system. Journal of Physics Conference Series 1864(1), 2021, 012096 [http://doi.org/10.1088/1742-6596/1864/1/012096].
[13] Das S. et al.: A production inventory model with partial trade credit policy and reliability. Alexandria Engineering Journal 60(1), 2021, 1325–1338 [http://doi.org/10.1016/j.aej.2020.10.054].
[14] Denardo E. V.: Dynamic Programming: Models and applications. Dover Publications 2003.
[15] Fagin R., Kumar R., Sivakumar D.: Efficient similarity search and classification via rank aggregation. ACM SIGMOD International Conference on Management of Data, SIGMOD 2003 [http://doi.org/10.1145/872794.872795].
[16] Forrester J.: Fundamentals of cybernetics of the enterprise (Industrial dynamics). Progress, Moscow 1971.
[17] Koulouris A. et al.: Applications of process and digital twin models for production simulation and scheduling in the manufacturing of food ingredients and products. Food and Bioproducts Processing 126, 2021, 317–333.
[18] Leggatt T. W.: The evolution of Industrial Systems. Croom Helm, London 1985.
[19] Leontiev V.: Theoretical assumptions and nonobservable facts. Economy, ideology, politics 9, 1972, 15.
[20] Mesarovic M., Takahara Y.: General systems theory: mathematical foundations. Academic Press, New York, San Francisco, London 1975.
[21] Mukha Ap. A.: Control of the process of complex engineering systems and processes development. Characteristic features of FMEA-analysis application. Mathematical machine and systems 2, 2012, 168–176.
[22] Murayama T., Devis P.: Optimal aggregation of noisy observations. Journal of Physics: Conference Series 233(1), 2003, 301–312 [http://doi.org/10.1145/872794.872795].
[23] Opoitsev V. I.: Equilibrium and stability in models of collective behavior. Mir, Moscow 1977.
[24] Raymo M. et al.: A New Method for Food Production Analysis and Optimization Applied to Citrus Industry. Computer Aided Chemical Engineering 48, 2020, 2005–2010.
[25] Romanyuk N. et al.: Microfacet distribution function for physically based bidirectional reflectance distribution functions. Proc. of SPIE 8698, 2012, 86980L [http://doi.org/10.1117/12.2019338].
[26] Romanyuk O. et al.: Method of anti-aliasing with the use of the new pixel model. Proc. of SPIE 9816, 2015, 981617 [http://doi.org/10.1117/12.2229013].
[27] Romanyuk S. et al.: New method to control color intensity for antialiasing. International Siberian Conference Control and Comm. – SIBCON, 2015 [http://doi.org/10.1109/SIBCON.2015.7147194].
[28] Rüttimann B., Stockli M.: Going beyond triviality: The Toyota production system-lean manufacturing beyond Muda and Kaizen. J. Serv. Sci. Manag. 9, 2016, 140–149 [http://doi.org/10.4236/jssm.2016.92018].
[29] Rüttimann B.: Introduction to Modern Manufacturing Theory. Springer International Publishing AG 2018 [http://doi.org/10.1007/978-3-319-58601-4].
[30] Skrynkovskyy R. et al.: Improvement of the express diagnostics of the production activity of the enterprise taking into account the method of determining the optimal production programs in the operational management system. Technology Audit and Production Reserves 6(44), 2018, 4–10 [http://doi.org/10.15587/2312-8372.2018.147968].
[31] Skrynkovskyy R. et al.: Improvement of the model of the innovative development of the production system of industrial enterprises. Reports on Research Projects 1/4(45), 2019, 53.
[32] Taylor C.: Dynamic programming and the curses of dimensionality. Applications of dynamic programming to agricultural decision problems. CRC Press, 2019.
[33] Tsybakov B.: Optimal Rates of Aggregation, Statistical Learning Theory and Stochastic Optimization. In: Saint-Flour E. D. et al.: Statistical learning theory and stochastic optimization: École d'eté de probabilités de Saint-Flour XXXI – 2001. 2004, 54–69.
[34] Weijia D., Ginger Z., Jungmin L.: Optimal Aggregation of Consumer Ratings. NBER Working Paper No. 18567, 12–23.
[35] Xinxin L.: Self-Selection and Information Role of Online Product Reviews. Information Systems Research 19(4), 2012, 56–64.

M.Sc. Dmytro Hryshyn
e-mail: dmitriygrishin2@gmail.com

Ph.D. student of Computer Control Systems Department, Vinnytsia National Technical University. He has published 14scientificpapers. The main direction of his scientific activity is research of optimal development and production processes.

http://orcid.org/0000-0001-5397-3592

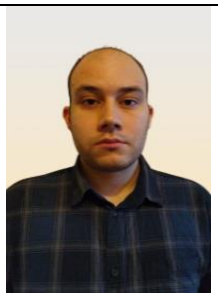

D.Sc. Eng. Taisa Borovska
e-mail: taisaborovska@gmail.com

Professor with Computer Control Systems Department, Vinnytsia National Technical University. Author of more than 220 scientific works. Main works are devoted to the theory of modeling and optimization of distributed production systems based on decomposition methods and the theory of meta models, solution of the problems of „import substitution", „optimal control of region development", „structure of the regional work places management".

http://orcid.org/0000-0002-5308-4872

Ph.D. Aliya Kalizhanova
e-mail: kalizhanova_aliya@mail.ru

Candidate of physical and mathematical sciences, professor, University of Power Engineering and Telecommunications, the Chief Researcher of the Institute of Information and Computational Technologies of the Ministry of Education and Science CS of the Republic of Kazakhstan.
Scientific interests: mathematical modeling of systems, models of transport systems network analysis, optimization methods, technologies for developing sensor systems for signals receive – transmit, mathematical modeling of Bragg fiber gratings.

http://orcid.org/0000-0002-5979-9756

http://doi.org/10.35784/iapgos.3272 received: 11.11.2022 | revised: 26.11.2022 | accepted: 15.12.2022 | available online: 30.12.2022

MODELING THE DEVELOPMENT PROCESS OF INCLUSIVE EDUCATION IN UKRAINE

Mariana M. Kovtoniuk[1], Olena P. Kosovets[1], Olena M. Soia[1], Olga Yu. Pinaieva[2], Vira G. Ovcharuk[3], Kuralay Mukhsina[4]

[1]Vinnytsia Mykhailo Kotsiubynskyi State Pedagogical University, Faculty of Mathematics, Physics and Computer Sciences, Vinnytsia, Ukraine, [2]Vinnytsia Mykhailo Kotsiubynskyi State Pedagogical University, Educational and Scientific Institute of Pedagogy, Psychology, Training of Highly Qualified Specialists, Vinnytsia, Ukraine, [3]Vinnytsia National Technical University, Physical Education Department, Vinnytsia, Ukraine, [4]Institute of Information and Computing Technologies of the CS MES RK, Almaty, Kazakhstan

Abstract. *The article presents the results of research on the implementation of the principles of inclusive education in Ukraine, substantiates its relevance in the development of a democratic society and European integration policy. The principles of the state policy in the field of inclusive education, its normative-legal support and international practice of providing educational services to citizens with special needs are described. Advanced experience of inclusion introduction in the educational process of preschool, general secondary, vocational and higher education institutions is analyzed. Official statistics on the total number of people with disabilities in Ukraine; availability of special secondary education institutions (boarding schools) and their contingent; the number of children with disabilities in preschool education institutions, students with disabilities in full-time secondary education institutions, persons with disabilities in vocational education institutions, persons with disabilities among students of higher education institutions etc., have been handled. The importance and expediency of the scientific development of the principles of inclusive education, its practical implementation and study of socio-economic effect are substantiated. Graphic visualization of the correlation between the employed persons with disabilities and persons without disabilities, number of children, pupils, students with special educational needs in education establishments of Ukraine is presented.*

Key words: inclusive education, inclusive environment

MODELOWANIE PROCESU ROZWOJU EDUKACJI WŁĄCZAJĄCEJ NA UKRAINIE

Streszczenie*. W artykule przedstawiono wyniki badań nad procesem wdrażania zasad edukacji włączającej na Ukrainie, uzasadniono ich znaczenie w warunkach rozwoju społeczeństwa demokratycznego i europejskiej polityki integracyjnej państwa. Opisano zasady krajowej polityki państwa w zakresie edukacji włączającej, jej wsparcie regulacyjne i prawne oraz międzynarodową praktykę świadczenia usług edukacyjnych obywatelom ze specjalnymi potrzebami. Przeanalizowano najlepsze doświadczenia z wdrażania integracji w procesie edukacyjnym placówek przedszkolnych, ogólnokształcących, zawodowych i wyższych. Opracowano oficjalne dane statystyczne dla Ukrainy dotyczące całkowitej liczby osób niepełnosprawnych; dostępność specjalnych szkół średnich (internatów) i ich zespołów; liczby dzieci niepełnosprawnych w placówkach wychowania przedszkolnego, uczniów niepełnosprawnych w dziennych placówkach ogólnokształcących, osób niepełnosprawnych w placówkach kształcenia zawodowego (zawodowego i technicznego), osób niepełnosprawnych wśród studentów szkół wyższych itp. Uzasadniono wagę i celowość naukowego opracowania zasad edukacji włączającej, jej praktyczne zastosowanie oraz badanie efektu społeczno-ekonomicznego. Zaprezentowano graficzną wizualizację stosunku zatrudnionych osób z niepełnosprawnościami do osób sprawnych, liczby dzieci, uczniów i studentów ze specjalnymi potrzebami edukacyjnymi w instytucjach edukacyjnych Ukrainy.*

Słowa kluczowe: edukacja włączająca, środowisko włączające

Introduction

At the present stage of development of a democratic society in Ukraine and in the conditions of the realization of social and legal processes of European integration policy, conducted by the state, the problem of ensuring social protection of citizens in general and people with special educational needs in particular is of great importance. The urgency of the introduction and formation of the sphere of inclusive education is due to the fact that the number of people with special needs who require quality educational services and provision the conditions for adapting the educational space to their individual characteristics is constantly growing. A prudent policy strategy of many countries in the field of inclusion is a scientifically sound and proven statement that "it is economically feasible to invest in human capital wherever possible, instead of direct investment in social services" [10].

The issue of inclusive education in Ukraine in the context of the development of a democratic society and European integration policy is of great importance both for the Ukrainian state and for the European community as a whole. Therefore, research on this topic should be considered important from both a theoretical and a practical point of view. We used the priorities of the concept of sustainable world development as a basis for further research in the field of inclusive education.

The analysis of scientific and pedagogical research shows the relevance of improving inclusive education in Ukraine. Researcher O. Batsman [3] described the peculiarities of training future social workers to work with students with functional health limitations in institutions of higher education (2021), I. Kalinovska [8] considered the methodological foundations of training future practical psychologists to work in conditions of inclusive education students of general secondary education institutions (2020), O. Kasyanenko [9] investigated the readiness of future educators to work with preschool children in conditions of inclusion (2018), and O. Kosovets [11] developed a methodology for teaching informatics to students of vocational education institutions in conditions of inclusion (2015).

The purpose of the article is to investigate and model the process of development of inclusive education in Ukraine in the context of the development of a democratic society and European integration policy.

1. Formulation of the problem

International human rights standards are based on the idea of the participation of every individual in public life on the basis of equality and without discrimination. The spread of the process of inclusive education of children with physical and (or) mental health problems in Ukraine is not only a reflection of time, but also represents another step towards ensuring the full realization of the rights of children with special educational needs to quality education [31].

The legal field of providing educational services in the sphere of inclusive education is regulated by the current legislation [4, 5, 15, 17, 18 etc.] and international documents [21–23 etc.]. The Constitution of Ukraine (Article 43) states: "Everyone has the right to work, which includes the opportunity to earn a living by work which he freely chooses or agrees to freely" [5]. Additional guarantees for employment of persons with disabilities are provided by the Law of Ukraine as amended on February 13, 2020 under No 5067-VI "On Employment" [17].

Analyzing the experience of inclusion in the educational process, we note that of particular interest are the works of scientists D. Deppler, T. Lorman, F. Armstrong, B. Barber, G. Becker, P. Bourdieu, J. Davis, K. Jenks, X. Kerbo, M. Crozier, F. Crosby, who made a significant contribution to the

development of theoretical and methodological foundations of inclusive education. M. Andreeva, Y. Boginskaya, V. Tserklevych, T. Grebenyuk, T. Komar, V. Skrypnik, M. Tomchuk studied the problems of social and psychological adaptation of students with health problems to the study at universities. S. Bogdanov, G. Gavryushenko, N. Naida, N. Sofiy, I. Yarmoschuk, etc., dedicate their works to the study of the problem of involving people with special needs the study in education establishments, their rehabilitation and socialization to social norms [1, 10, 12–14, 16, 27, 28, 31 etc.]

The problem of inclusive education is closely connected with the new paradigm of education, which is based on the transition to new educational technologies. Thus, Canadian and American Researchers M. Forest, M. Giangreco, E. Lusthaus, J. Pearpoint, J. Putnam and others proposed to use the following innovative technologies: MAPS (Making Action Plans, from the English – "systematic production of action plans"); PATH (Planning Alternative Tomorrows with Hope); COACH (Choosing Options Accommodations for Children) [1].

As of the beginning of the 2020/2021 academic year, the number of special schools was 319 units with a contingent of 36,461 students (out of the total number of special schools with boarding department – 264 units (29,634 students)). Number of children with disabilities in preschool institutions – 8544 people. The number of students with disabilities in full-time secondary schools (at the beginning of the school year) is 74,354. Number of persons with disabilities in vocational education institutions (at the end of the year) – 4648 people. The number of people with disabilities among students of higher education institutions (at the beginning of the 2019/2020 academic year) is 12,959 applicants, for the 2020/2021 academic year there is no information [26].

However, according to experts, the number of children with physical and (or) mental disabilities is much higher [31]. And there is no complete statistical state registration of children with mental and physical disabilities in Ukraine today. The lack of a single transparent and reliable system of registration of children with disabilities and children with disabilities hinders adequate assessment of the real scale of the problem and the development of a clear strategy for the implementation of inclusive education in Ukraine [12].

2. Theoretical research

Over the last ten years, Ukraine has been developing the legal framework for the introduction and development of inclusive education for children with special educational needs. In this aspect, it is worth noting the following changes in the regulatory framework that allow for the effective development of inclusive education at different levels of public administration:

- adoption of a social approach to understanding disability and special educational needs as a basis for overcoming various barriers in the field of education, including through the implementation of inclusive education;
- enshrining in the field of education international principles in terms of ensuring the rights of persons with special educational needs and persons with disabilities, among which are the principles of non-discrimination, equality of opportunity, accessibility, respect for the development of abilities and individuality;
- definition of guarantees of the right of children with special educational needs and children with disabilities to access quality education, including inclusive education in general secondary education institutions at the place of residence, legal regulation of the rights and freedoms of this category of children in education; to create special conditions for such education;
- definition of competence and division of responsibilities of state bodies that carry out administration in the field of education to create a set of special conditions for children with special educational needs and children with disabilities, including their education in inclusive education etc. [14].

At the same time, pronounced deviations from the norm of development – the basis for the provision of special services to the child during his schooling, which until recently was not within the competence of general secondary education [16]. However, with regard to persons with disabilities in Ukraine, the principles of accessibility for every citizen of all forms and types of educational services provided by the state are also violated; equality of conditions of each person for full realization of his abilities, talent, comprehensive development, humanism, democracy etc. [31].

Currently, higher education institutions are actively involved in creating the necessary conditions for education and living of people with special needs, as their integration into the general education space of Ukraine is one of the areas of humanization of the entire education system. In particular, the professional activity of the teaching staff of Vinnytsia Mykhailo Kotsyubynsky State Pedagogical University is aimed at the development and formation of personality, ensuring socio-psychological and labor adaptation of people with special educational needs, education of universal values, civic position. In the conditions of an inclusive institution of higher education, "the activities carried out at the university are focused on solving the following tasks: appropriate conditions have been created for teaching and education in accordance with the current legal framework; an advisory group on inclusive education of persons with special educational needs was organized; created conditions and involved specialists for psychological and pedagogical diagnostics and forms of support aimed at developing individual curricula; the office of psychological unloading is equipped with the needed facilities; compliance with hygienic standards aimed at protecting and promoting health, harmonious development and improvement of the functional capabilities of the body of persons with disabilities is provided; the office of inclusive training in which the thematic literature, the corresponding educational and methodical materials is stored is organized; university monitoring is carried out to determine the level of knowledge and skills of people with special educational needs" [22].

The curricula for training specialists of Vinnytsia Mykhailo Kotsyubynsky State Pedagogical University include relevant disciplines, in particular: "Psychology of people with special needs", "Psychological support in an inclusive environment", "Assistance in an inclusive environment", "Special pedagogy with history", "Fundamentals of inclusive education", "Pedagogical technologies of inclusive education", "Differentiated teaching and standardized assessment in an inclusive classroom", "Speech therapy", "Logopsychology", "Theory and methods of raising children with speech disorders", "Methods of inclusive education in computer science" etc. [22].

Building an effective system of inclusive education in Ukraine is possible on the basis of the interaction of various factors, primarily strengthening funding for education, improving its regulatory support, improving the methodological and staffing of inclusive education. O. Zayavnyuk [31] identified the most significant in his opinion organizational and economic levers of micro-, meso- and macro-levels that can enhance the development of inclusive education in Ukraine (table 1).

Thus, it is extremely important to develop and improve inclusive education in educational institutions. The creation of an appropriate educational infrastructure, the provision of decent living conditions and the development of progressive training programs for people with special needs is an indicator of the development of a social and legal society.

Table 1. Organizational and economic levers of influence on the intensification of inclusive education in Ukraine

Macro level	
Organizational levers	Economic levers
1. Introduction of the Amendments to the laws of Ukraine „On Education", „On Preschool Education", „On General Secondary Education", „On Extracurricular Education". 2. Development of a training system for working with children with special educational needs. 3. Cultivating a positive opinion in society about inclusive education by involving the media in this matter. 4. Development of barrier-free social infrastructure. 5. Inclusion of a course on the practice of implementing inclusive education in Ukraine in the teacher training program. 6. Reduction of the number of children in classes where children with special educational needs study.	1. Increase funding for the development of the material base of educational institutions in order to turn them into an accessible learning environment. 2. The use of economic incentives to encourage teachers to develop special literature, methodological support for working with children with special educational needs; make them available to the general public.
Meso level	
Organizational levers	Economic levers
1. Usage of socio-psychological incentives for teachers and heads of educational institutions that successfully conduct inclusive education. 2. Conducting psychological training for teachers to reduce fears and rejection of changes in educational institutions that will be associated with the introduction of inclusion.	Use of financial and economic incentives to encourage educational institutions to implement inclusive education.
Micro level	
Organizational levers	Economic levers
1. Application of the latest learning technologies for children with special educational needs. 2. Inform the staff of the educational institution about the successes of its employees in the process of implementing inclusive education.	Using the possibilities of collective labour contract regulation of social and labor relations in order to create material incentives for teachers who work with children with special needs.

The use of a competency-based approach in inclusive education implies an adequate assessment of the level of formation of the relevant competencies. According to M. Malyar and A. Shtymak, the diagnosis of the formation of professional competence is the most problematic and requires the development of assessment methods that allow assessing the real level of students' competence [15].

In the context of incompleteness and inaccuracy of information in the process of inclusive education, obtaining unambiguous results is problematic and contradictory, therefore, methods using fuzzy logic, which are based on expert assessments and allow obtaining results as close to reality as possible, are promising.

Accordingly, the procedure for such assessment of the levels of professional competencies formed by students consists of three main stages:

- fuzzification: transformation of crisp input variables into fuzzy ones. As initial data, the results of individual assessment by the teacher using the 100-point ECTS scale are used, which takes into account the results of creative and research work over a certain period (semester). We turn the input data into fuzzy values. At the same time, the level of professional competence Q will be given by a set of four linguistic terms: K_1 – „low level", K_2 – „satisfactory level", K_3 – „sufficient level", K_4 – „high level" (in accordance with the levels of educational achievements of students of institutions of higher education). That is, $Q = \{K_i,\ i = 1...4\}$ and, moreover, each of the designated terms is a fuzzy set. To translate the input data, we use the membership function defined in the study [15]:

$$\mu_{K_i}(x) = \begin{cases} 0, x \le NG \\ \dfrac{x-(NG-1)}{RG}, RG \le x \prec VG \\ 1, x \ge VG \end{cases}$$

where NG is the lower limit of the gradation, VG is the upper limit of the gradation, RG is the range of the gradation.

That is, given the above, we will have:

a) the linguistic term K_1 is "low level", the corresponding values are in the range [0…59] and the membership function

$$\mu_{K_i}(x) = \begin{cases} 0, x \le 0 \\ \dfrac{x}{60}, 0 \le x \prec 60 \\ 1, x \ge 60 \end{cases}$$

b) the linguistic term K_2 – „satisfactory level", the corresponding values are in the range [60 ... 74] and the membership function

$$\mu_{K_i}(x) = \begin{cases} 0, x \le 60 \\ \dfrac{x-59}{15}, 60 \le x \prec 75 \\ 1, x \ge 75 \end{cases}$$

c) the linguistic term K_3 is "sufficient level", the corresponding values are in the range [75…89] and the membership function

$$\mu_{K_i}(x) = \begin{cases} 0, x \le 75 \\ \dfrac{x-74}{15}, 75 \le x \prec 90 \\ 1, x \ge 90 \end{cases}$$

d) the linguistic term K_4 – "high level", the corresponding values are in the range [90…100] and the membership function

$$\mu_{K_i}(x) = \begin{cases} 0, x \le 90 \\ \dfrac{x-89}{11}, 90 \le x \prec 100 \\ 1, x = 100 \end{cases}$$

According to the above formulas, we turn the obtained values of the levels of formation of theoretical, practical and personal-motivational criteria into fuzzy values;

- block of rules: establishment of rules, according to which the level of formation of professional competence is determined based on the use of the Tsukamoto fuzzy algorithm;
- defuzzification: transformation of a fuzzy initial value into a clear value of the level of the initial value, which is determined as a weighted average.

3. Results of investigations

Today, there are 2,724.1 thousand people with disabilities in Ukraine, it means that a significant percentage of the country's population - every eighteenth - has a disability, and the number of such people is growing, especially in connection with the military conflict. As of December 31, 2020, 41,397 people with disabilities worked at 90,331 enterprises, which is a lower figure compared with 2017 – 666.8 thousand people. Whereas in 2015 the number of working people with disabilities was 742.6 thousand people. At the same time, International Labor Organization standards require that at least half of the total number of persons with disabilities living in the country be employed.

In the graph of the Fig. 1 percent of employed people with disabilities in Ukraine is shown in light color. This chart shows that in Ukraine the largest percentage of employed persons with disabilities (about 20–24%) is in the age group of 30–34 years (i. e. in the most able-bodied age). But even in this case, their share is much smaller than employed people without disabilities (3.5 times). The largest gap (5 times) occurs before the age of 40, and the smallest – at retirement age (2 times).

Analyzing the sphere of employment of certain categories of citizens, we find that in modern society there are problems with insufficient quotas for places for people with special needs; in the underdeveloped area of remote work for people with a high degree of disability; in the reluctance of government and commercial organizations to hire „special" people [1].

The development and implementation of inclusive education in educational institutions of Ukraine will partially help to solve the existing problem of employment of persons with disabilities.

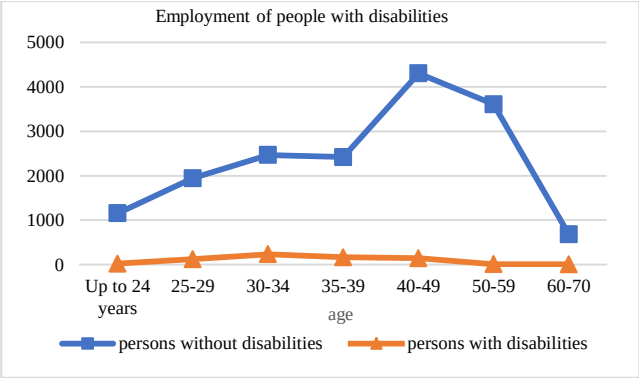

Fig. 1. Ratio of employed persons with disabilities and persons without disabilities

The head of the institution informs the body in the sphere of management of which the educational institution is located about the need to open an inclusive classroom and create an inclusive educational environment. Before the start of the new school year, the headmaster issues an order to enroll the child in school and forms an inclusive classroom [24].

The resolution „On the organization of inclusive education in general secondary education" clearly states that the head of the institution on the basis of the application of parents with the support of the relevant education body creates an inclusive educational environment taking into account the requirements of universal design for education of people with special educational needs. bring the territory of the institution, buildings and premises in accordance with the requirements of state building codes for accessibility; to provide the necessary educational and methodical and visual-didactic manuals and teaching aids in accordance with the needs of students; to equip resource rooms; to provide the educational process with the necessary employees in accordance with the needs of students with special educational needs [18].

A separate state fund provides a subvention to local budgets for the organization of an inclusive environment at school. About 20 thousand hryvnias are allocated for a calendar year. The list of expenses for which the specified subvention can be directed, is defined in item 4 of provision No 88, namely:

- conducting (providing) additional correctional and developmental classes (services), which are determined by the individual development program for students of inclusive classes and the working curriculum (individual student curriculum) for students of special classes;
- acquisition of special means of correction of psychophysical development, which allow the child to master the curriculum (35% of the subvention amount can be allocated for the purchase of equipment) [19].
- According to the Resolution the Cabinet of Ministers.

Resolution No 635 "On approval of the Order of inclusive education organization in higher education establishments" the organization of the educational process of students with special educational needs in higher education institutions provides for:

- creating an inclusive educational environment;
- application of the principles of universal design in the educational process;
- bringing the territory of the institution of higher education, buildings, structures and premises in accordance with the requirements of state construction norms, standards and rules. If the existing buildings, structures and premises of higher education institutions cannot be fully adapted to the needs of persons with disabilities, their reasonable adaptation is carried out taking into account the universal design;
- providing students with special educational needs of higher educational institutions of state and communal ownership with the necessary special means of correction of psychophysical development in accordance with the standard list approved by the Ministry of Education and Science of Ukraine;
- providing the necessary educational and methodical materials and information and communication technologies for the organization of the educational process;
- providing, if necessary, a reasonable adaptation;
- application in the educational process of the most acceptable for students with special educational needs methods and ways of communication, including Ukrainian sign language, relief-dot font (Braille) with the involvement of relevant specialists and teachers;
- ensuring the availability of information in various formats (Braille, enlarged font, electronic format, etc.) [20].

Given that the opportunities for access to higher education for people with special educational needs and normative citizens differ, the legislation of Ukraine provides for such entrants a number of benefits for admission to a higher education institution, namely:

- enrollment of persons with special educational needs who have I or II group of disability, children with disabilities under 18 years of age, who are not contraindicated to study in the chosen field (specialty) out of competition when submitting certificates of the Ukrainian Center for Educational Quality Assessment. tests not below the established level);
- persons with special educational needs who, according to the decision of the regulatory commission at the regional center for quality assessment of education, was denied registration for participation in external independent assessment due to the impossibility of creating special (special) conditions;
- in accordance with the conditions of admission on the recommendation of health and social protection bodies, the admissions committee should consider enrollment in excess of the state order based on the results of the interview with the right to study at the place of residence of applicants with special educational needs who are unable to attend. and is also obliged to create conditions for their training in external or distance forms;
- the right to transfer to vacant budget places have persons with disabilities of groups I, II and children with disabilities under the age of 18, who are not contraindicated to study in the chosen specialty [21].

The main problems of access to higher education for people with special educational needs or disabilities (primarily inclusive education), their integration into the educational and social environment, which also have different scales and nature, are:

- insufficient development of the legal framework for the education of persons with disabilities;
- insufficient level of quality of general secondary education of disabled people, which creates obstacles for their admission to higher education institutions;
- lack of conditions for combining professional training of students with special educational needs and their medical rehabilitation;
- lack of barrier-free architectural environment for the training of people with disabilities in colleges;
- low level of provision of students with disabilities with adaptive technical means of education (various surdo- , blind aids and other adaptive equipment);
- insufficient level of provision of students with special educational needs with educational and methodical literature adapted to their psychophysiological needs;
- low level of public awareness of understanding the problems and needs of people with disabilities;
- inactive consolidation of efforts of persons with disabilities (due to both subjective and objective circumstances) in terms of defending their rights, including the right to education [13].

Therefore, in order to ensure the inclusive education of students with special educational needs, it is necessary to form an external environment that affects the organization of an inclusive educational environment, and to adapt the internal educational and methodological environment of higher education institution (Fig. 2).

Main factors of social exclusion of persons with disabilities from the field of education are the insufficient number of educational places, limited by the quota for admission of such persons to higher education institutions; imperfection of legislation in the field of education, which leads to the lack of mechanisms for the development and financing of inclusive education; insufficient material and technical and staffing of educational institutions (lack of special auxiliary educational equipment, specially developed teaching methods, lack of material incentives for teachers and lecturers – developers of appropriate educational and methodological support; lack of special training for teachers to work with students and students with disabilities); unsuitability of educational buildings for unimpeded access to them by pupils and students with various diseases and pathologies. Thus, 27.4% of higher education institutions and only 8.4% of vocational education institutions are equipped with ramps for unimpeded access to the premises of students with disabilities [31].

Table 2 shows the number of children, pupils and students with special educational needs who study in inclusive classes of educational institutions of Ukraine. According to statistics, the number of children with special educational needs in preschools has been growing steadily over the past five years. This initial link is important for the further development and education of students with special educational needs in general secondary education.

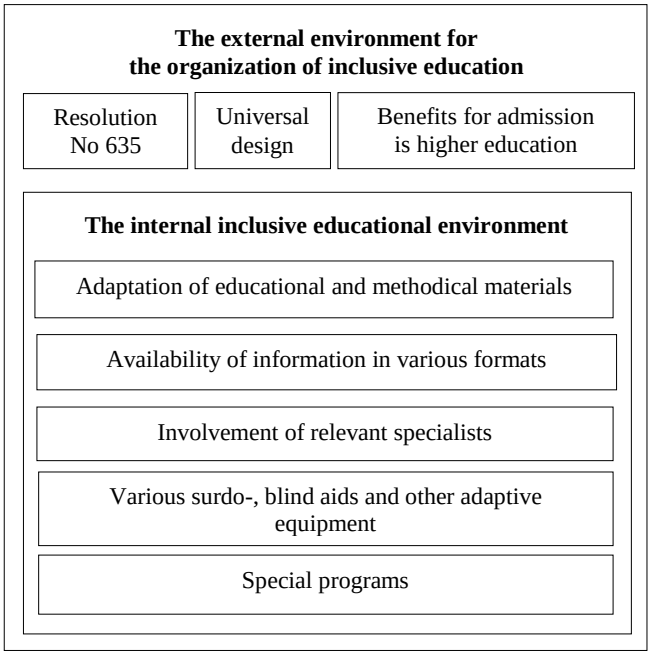

Fig. 2. Organizational principles of inclusive education in higher education institutions

Table 2. Number of children, pupils and students with special educational needs in educational institutions of Ukraine

Year	Number of children, pupils and students with special educational needs			
	in preschool education institutions	in general secondary education institutions	in vocational education institutions	education in higher education institutions
2015	8357	62075	5368	16090
2016	8892	65603	4988	14752
2017	9447	68714	4828	13216
2018	9014	73161	4617	12788
2019	9157	74452	4825	12959
2020	8544	74354	4648	…

The data on the number of children, pupils and students with special educational needs in educational institutions of Ukraine are prepared according to the Ministry of Education and Science of Ukraine and the State Information System of Education, provided by the State Scientific Institution „Institute of Educational Analytics" [26].

Fig. 3 shows a positive trend of increasing the number of students with special educational needs in general secondary education in Ukraine, which gives grounds to draw conclusions about the feasibility and necessity of further development of inclusive education.

At the same time, there is an obvious demand among people with disabilities for higher education. In Fig. 3 the number of students with special educational needs who study in higher education institutions is much higher than the number of students with special educational needs who study in vocational education institutions [2, 3, 23].

Modern education is characterized by the search for new pedagogical opportunities, which is primarily related to the idea of the integrity of the pedagogical process as a system. At the same time, all aspirations are based on the theory of universal human values, cultural growth and humanization of society. It has been experimentally proven that the implementation of the goals and objectives of high-quality training of specialists in the field of inclusive education stipulates the necessity of searching for innovative approaches to the formation of the readiness of future educators to work with the preschool children in the conditions of inclusion [9, 25], training of future practical psychologists to work in the conditions of inclusive education of the students of general educational institutions [8, 30], methods of teaching informatics of the students of vocational and technical educational institutions in conditions of inclusion [11], training of future social workers to work with students with functional health limitations in institutions of higher education [3] etc.

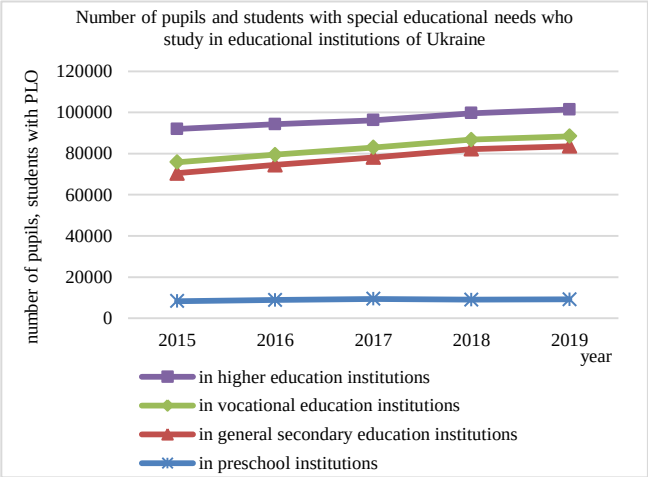

Fig. 3. Ratio of the number of children, pupils and students with special educational needs in educational institutions of Ukraine

The general picture of the results of the dissertation studies indicates the presence of the positive changes in the training of specialists in the field of inclusive education. We will check the validity of the proposed hypothesis using the method of mathematical statistics.

To check the heterogeneity of unrelated samples in the experimental and control groups in studies [3, 8, 9, 11], we will use the Student's t-test for unequal samples $n_1 \neq n_2$, the statistics of which has the form [23]:

$$t_{emp} = \frac{|\bar{X}_1 - \bar{X}_2|}{\sqrt{\frac{(n_1-1)\cdot s_1^2+(n_2-1)\cdot s_2^2}{n_1+n_2-2}\left(\frac{1}{n_1}+\frac{1}{n_2}\right)}}$$

where $\bar{X}_1$ i $\bar{X}_2$, s_1^2 i s_2^2, n_1 i n_2 are the average, variances and volumes of the first and second samples, respectively.

According to the Student's t-test, the null hypothesis H_0: $\mu_1 - \mu_2 = 0$ (μ_1 does not differ from μ_2) is that the

difference between the average values of the two samples is (statistically) equal to zero, that is, there are no differences. The alternative hypothesis H_1: $\mu_1 - \mu_2 \neq 0$ (μ_1 differs from μ_2) indicates that the difference is different from zero, that is, the matter is the significance of the differences, which is assessed by the level of significance – the probability that the differences are considered significant.

The critical value of the criterion t_{cr} for a given level of significance α and the number of degrees of freedom $df = n_1 + n_2 - 2$ can be obtained from Student's distribution tables. If $t_{emp} > t_{cr}$, then the hypothesis of homogeneity H_0 (about the absence of divergence) is rejected and the alternative hypothesis H_1 is accepted. If $|t_{emp}| \leq |t_{cr}|$, then the difference of averages is invalid.

Table 3 shows empirical data for experimental and control groups are taken from primary sources [3, 8, 9, 11].

Therefore, according to the Student's t-test for the independent samples, we have $t_{emp} > t_{0.05}$ everywhere. That is why, the training of specialists who will provide educational services to persons with special educational needs at various levels of education is relevant and requires special attention and appropriate financial support from the state.

4. Conclusion

Inclusion has a significant impact on policy, research and practice and has many meanings, ranging from simply enrolling students with special educational needs in regular classes to transforming the philosophy, values and practical approaches of entire education systems [1].

Table 3. Empirical data for experimental and control groups

Testing of statistical hypotheses by Student's t-test for independent samples for the level of significance α = 0.05; $t_{cr} = t_{0.05}$	
according to O. Kasyanenko 's empirical data [9] – preschool education	
$t_{emp} \gtrless t_{0.05}$	10.39 > 1.99
according to the empirical data of I. Kalinovska [8] – higher education and general secondary education	
$t_{emp} \gtrless t_{0.05}$	7.05 > 1.97
according to empirical data of O. Kosovets [11] – vocational and technical education	
$t_{emp} \gtrless t_{0.05}$	3.7 > 2.2
according to empirical data of O. Batsman [3] – higher education	
$t_{emp} \gtrless t_{0.05}$	5.25 > 1.97

The concept of independent living should be a key priority in the realization of the right of persons with special educational needs to the quality and accessibility of higher education. Educators together with the Government should develop measures to increase the involvement of such students in higher education, include indicators of their education in the rating system of higher education institutions; to strengthen control over the implementation of requirements for the creation of an inclusive environment in vocational and higher education institutions, to develop a network of transport services for students who have vision problems, problems with the musculoskeletal system; to promote employment and analyze the career growth of graduates with special educational needs; prevent and eliminate elements of discrimination and bullying; to involve the media to create a positive image of higher education for people who need an individual approach [1].

Education of people with disabilities is one of the most important tasks for the country. This leads to the creation of a truly inclusive environment where everyone can feel the importance of their existence. Society has a duty to enable everyone, regardless of their needs, to reach their full potential, to benefit society and to become its full-fledged member.

References

[1] Artyukhova O.: Inclusive education as a projection of the development of social and legal society. Current issues of humanitarian sciences: interuniversity collection of scientific works of young scientists of Ivan Franko Drohobytsk State Pedagogical University 28(1), 2020, 108–115.

[2] Azarova A.: Information Technologies and Neural Network Means for Building the Complex Goal Program "Improving the Management of Intellectual Capital". Lecture Notes on Data Engineering and Communications Technologies 77, 2022, 534–547.

[3] Batsman O. S.: Preparation of future social workers to work with students with functional health limitations in institutions of higher education: dissertation. Poltava National Pedagogical University named after V. G. Korolenko. Poltava, 2021.

[4] Convention on the Rights of Persons with Disabilities dated July 6, 2016, No. 995_g71 [http://zakon.rada.gov.ua/laws/show/995_g71].

[5] Constitution of Ukraine: Law of Ukraine dated 01/01/2020 No. 254k/96-BP/VRU [https://zakon.rada.gov.ua/laws/show/254%D0%BA/96-D0%B2%D1%80].

[6] Education 2030: Incheon Declaration and Framework for Action for the implementation of Sustainable Development Goal 4: Ensure inclusive and equitable quality education and promote life long learning – Document code: ED–2016/WS/28, 2016 [https: //unesdoc.unesco.org/ark:/48223/pf0000245656].

[7] Empowering children with disabilities for the enjoyment of their human rights, including through inclusive education. Report, submitted pursuant to Human Rights Council resolution 37/20, the United Nations High Commissioner for Human Rights. 2019 [https://www.inclusive-education-in-action.org/resources/empowering-children-disabilities-enjoyment-their-human-rights-including-through-inclusive].

[8] Kalinovska I. S.: Preparation of future practical psychologists to work in the conditions of inclusive education of students of general educational institutions. Uman State Pedagogical University named after Pavlo Tychyna. Uman, 2020.

[9] Kasyanenko O. M.: Formation of readiness of future educators to work with preschool children in conditions of inclusion. Volodymyr Hnatyuk Ternopil National Pedagogical University, Ternopil 2018.

[10] Kornienko S.: Inclusive education as a priority direction of the state policy of Ukraine in the field of education of children with disabilities. Bulletin of the National Academy of Public Administration under the President of Ukraine 2, 2012, 226–231.

[11] Kosovets O. P.: Methodology of teaching informatics to students of vocational and technical educational institutions in conditions of inclusion. Vinnytsia National Technical University, Vinnytsia 2015.

[12] Kushnir I. I., Popovych O. M., Cherepanya N. I.: Problems of teaching children with disabilities in a general educational institution. International scientific journal „Education and Science" 1(26), 2019, 129–131.

[13] Litvynova O. N., Stadnytska I. R.: Inclusive education in higher educational institutions of I-II levels of accreditation as a way to self-realization. Nursing 4, 2018, 41–43.

[14] Lys O. G.: State policy in the sphere of inclusive education in preschool education institutions through the prism of effective administrative practices. Legal scientific electronic journal 4, 2021, 670–673 [https://doi.org/10.32782/2524-0374/2021-4/166].

[15] Malyar M. M., Shtymak A. Yu.: A model for determining the level of graduate competence using fuzzy sets. Management of the development of complex systems 22 (1), 2015, 151–157.

[16] Mishchyk L. I.: Inclusive education as a condition for the socialization of disabled children in the learning process [http://www.nbuv.gov.ua/portal/soc_gum/Znpkhist/2012_5/12mliupn.pdf].

[17] On employment of the population: Law of Ukraine dated May 29, 2020 No. 5067-VI. Verkhovna Rada of Ukraine [https://zakon.rada.gov.ua/laws/show/5067-17].

[18] On making changes to the Procedure for organizing inclusive education in general educational institutions: Resolution of the CMU dated August 9, 2017 No. 588 [https://zakon.rada.gov.ua/laws/show/588-2017-%D0%BF#Text].

[19] On the approval of the Procedure and conditions for providing subventions from the state budget to local budgets for providing state support to persons with special educational needs: Resolution of the CMU dated February 14, 2017, No. 88 [https://zakon.rada.gov.ua/laws/show/88-2017-%D0%BF#Text].

[20] On the approval of the Procedure for the organization of inclusive education in institutions of higher education: Resolution of the CMU dated July 10, 2019, No. 635 [https://zakon.rada.gov.ua/laws/show/635-2019-%D0%BF#Text].

[21] Regarding informational materials about documents of entrants. Letter of the Ministry of Education and Science of Ukraine dated June 14, 2021 No. 1/9-311 [https://mon.gov.ua/ua/osvita/visha-osvita/vstupna-kapaniya-2021/informaciya-shodo-pilg-2021].

[22] Report of the rector of Vinnytsia State Pedagogical University named after Mykhailo Kotsyubynsky, Doctor of Ped. Sciences, Prof. N. I. Lazarenko on the results of fulfilling the terms of the contract for 2020 [http://www.vspu.edu.ua/content/img/education/rector_2020.pdf].

[23] Rudenko V. M.: Mathematical statistics: study guide. Center of educational literature, Kyiv 2012.
[24] Semko O.: Participation of parents in the organization of inclusive education [https://courses.ed-era.com/asset-v1:EdEra-SmartOsvita+Par+1+type@asset+block@books_inclusia-batky_KIS.pdf].
[25] Shyian A. A., Azarova A. A., Nikiforova L. O., Tkachuk L. M., Azarova V. V.: Modeling communication between the public and the authorities while implementing innovative projects in the context of e-democracy and public administration. Science and Innovation 16(6), 2021, 18–27.
[26] Social protection of the population of Ukraine in 2020: statistical collection. Rep. for the release of I. V. Senyk, Kyiv 2021.
[27] Tchaikovsky M. E.: Social-pedagogical work with youth with special needs in an inclusive educational space: monograph. „Ukraine" University, Kyiv 2015.
[28] Udych Z. I.: Basics of inclusive education: educational and methodological manual. Print Office, Ternopil 2015.
[29] UNESCO. 2020. Global Education Monitoring Report 2020: Inclusion and education: Allmeansall. Paris, UNESCO [https://en.unesco.org/gem-report/report/2020/inclusion].
[30] Yarmolenko V., Burennikova N., Pavlov S., Havrysh K., Pinaieva O.: Practice Analysis of Effectiveness Components for the System Functioning Process: Energy Aspect. Lecture Notes on Data Engineering and Communications Technologies 77, 2022, 282–296.
[31] Zayarnyuk O. V.: Inclusive education in Ukraine: problems and ways to solve them. Scientific Bulletin of the International Humanitarian University. Series: Economics and management 11, 2015, 190–193.

Prof. Mariana M. Kovtoniuk
e-mail: kovtonyukmm@vspu.edu.ua

Doctor of sciences (pedagogy), professor, Head of the Department of Mathematics and Computer Science Vinnytsia Mykhailo Kotsiubynskyi State Pedagogical University.
Research Interests: professional pedagogy, formation of information and communication competence, professional education in the field of digital technologies.

http://orcid.org/0000-0002-7444-1234

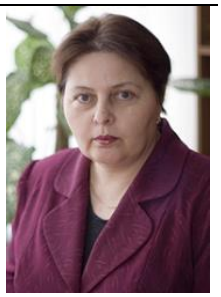

Ph.D. Olena P. Kosovets
e-mail: helen.kosovets@gmail.com

Candidate of sciences (pedagogy), senior lecturer of the Department of Mathematics and Computer Science Vinnytsia Mykhailo Kotsiubynskyi State Pedagogical University.
Research Interests: professional pedagogy, formation of information and communication competence, professional education in the field of digital technologies.

http://orcid.org/0000-0001-8577-3042

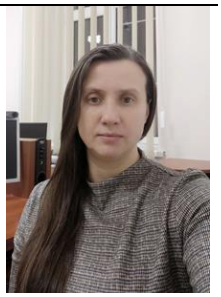

Ph.D. Olena M. Soia
e-mail: soia.om@vspu.edu.ua

Candidate of sciences (pedagogy), senior lecturer of the Department of Mathematics and Computer Science Vinnytsia Mykhailo Kotsiubynskyi State Pedagogical University.
Research Interests: professional pedagogy, formation of information and communication competence, professional education in the field of digital technologies.

http://orcid.org/0000-0002-0937-299X

Ph.D. Olga Yu. Pinaieva
e-mail: pinolga00@gmail.com

Candidate of science (pedagogy), associate professor of the Department of Pedagogy, Vocational Education and Management of Educational Institutions Vinnytsia Mykhailo Kotsiubynskyi State Pedagogical University.
Research Interests: professional pedagogy, formation of information and communication competence, professional education in the field of digital technologies.

http://orcid.org/0000-0002-8829-1388

M.Sc. Vira G. Ovcharuk
e-mail: ovcharukvira@vntu.edu.ua

Senior lector of Physical Education Department, Vinnytsia National Technical University.
Specialty „Pedagogy and methods of secondary education. Physical culture" and obtained the qualifications of a physical culture teacher, head of sports sections of school and extracurricular institutions.

http://orcid.org/0000-0002-0648-7994

Ph.D. Kuralay Mukhsina
e-mail: kuka_ai@mail.ru

Ph.D., senior researcher of the Institute of Information and Computing Technologies of the CS MES RK. Graduated from the Faculty of Physics and Mathematics of the Abai Almaty State University. Master of NARXOZ University. She defended her dissertation for the degree of Doctor of Philosophy in the specialty 6D07400 – Computer engineering and software on the topic „Development of a system for analyzing multilingual text information based on machine learning".

http://orcid.org/0000-0002-8627-1949

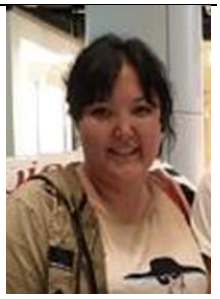

http://doi.org/10.35784/iapgos.3258 *received: 8.11.2022 | revised: 9.12.2022 | accepted: 15.12.2022 | available online: 30.12.2022*

FREQUENCY-TO-CODE CONVERTER WITH DIRECT DATA TRANSMISSION

Piotr Warda
Lublin University of Technology, Faculty of Electrical Engineering and Computer Science, Department of Automation and Metrology, Lublin, Poland

Abstract. *Signal frequency is one of the most popular information carriers in measurement technology. A circuit called a frequency-to-code converter is used to convert frequency into numerical values. Frequency-to-code converters usually operate in the mode of a recorder of a certain number of periods of the signal under test. Often it is a microcontroller-based circuit that uses built-in memory to collect measurement data. The size of the memory limits the measurement capabilities of the transmitter. The paper presents the development of a frequency-to-code converter that sends measurement data directly to the host computer without collecting the results in the RAM of the converter. The working algorithm of the transmitter is presented. The results of measurement experiments carried out for sample signals of constant and variable frequency are presented.. The metrological analysis of the results is presented.*

Keywords: frequency, digital period measurement, frequency-to-code converter, microcontroller

PRZETWORNIK CZĘSTOTLIWOŚĆ-KOD Z BEZPOŚREDNIĄ TRANSMISJĄ DANYCH

Streszczenie. *Częstotliwość sygnału jest w technice pomiarowej jednym z popularniejszych nośników informacji. Do konwersji częstotliwości w wartości liczbowe używa się układu zwanego przetwornikiem częstotliwość-kod. Przetworniki częstotliwość-kod zwykle pracują w trybie rejestratora określonej liczby okresów badanego sygnału. Często jest to układ oparty o mikrokontroler wykorzystujący wbudowaną pamięć do gromadzenia danych pomiarowych. Rozmiar pamięci ogranicza możliwości pomiarowe przetwornika. W artykule zaprezentowano opracowanie przetwornika częstotliwość-kod przesyłającego bezpośrednio dane pomiarowe do komputera nadrzędnego bez gromadzenia wyników w pamięci RAM przetwornika. Zaprezentowano algorytm pracy przetwornika. Przedstawiono wyniki przeprowadzonych eksperymentów pomiarowych dla przykładowych przebiegów o stałej i zmiennej częstotliwości. Przedstawiono analizę metrologiczną wyników.*

Słowa kluczowe: częstotliwość, cyfrowy pomiar okresu, przetwornik częstotliwości na kod, mikrokontroler

Introduction

Converting a physical quantity into frequency is one of the more common ways of converting information [4, 13]. A variable frequency signal is seen as an attractive transmission medium. It allows the transmission of information in an environment of increased electromagnetic interference [11]. In addition, due to its high resistance to signal amplitude attenuation, compared to a voltage signal, it allows information to be transmitted more easily over longer distances [10]. In the remainder of this paper, a signal in which information is transmitted by the value of its frequency will be referred to as a frequency signal.

Decoding the information transmitted by the frequency of the signal can be carried out by various methods. One of them is to apply a frequency-to-voltage converter [3, 7] and further transform the voltage signal using a standard measurement card containing an analog-to-digital converter (ADC). The result is a standardized data set obtained at uniform intervals, which can be analyzed using standard digital signal processing methods. However, the use of a data transmission channel with frequency carrier of information with intermediate additional processing with an ADC has some features that may be disadvantageous in some cases. The first is the need to verify that the introduced additional processing error will not have too great an influence on the total information processing error in the measurement system. The second feature is the increased complexity of the system structure. A larger number of components requires an increased amount of time to get the system up and running, and creates an additional risk of faults in the introduced intermediate data processing module.

One alternative to indirect conversion into voltage is to process the frequency of a signal by digitally measuring consecutive, information-carrying periods of the signal. Digital processing of period values [8] is widely known in the metrology literature. Correctly carried out measurement allows to obtain a very accurate result [14]. The attractiveness of the period measurement is also increased by the fact that the cost of the created system for direct analysis of the frequency signal is not high. The elements required to implement the measurement (counter, edge detection circuit, stable reference signal generator [1]) are contained in most microcontrollers, which are often used in control and measurement applications. Of course, it is not always possible to use any simple microcontroller for a particular purpose. What is important are the microcontrollers resources, its data transmission capabilities and the value of frequency of the microcontrollers clock signal.

1. Principle of measurement

The periods of a frequency signal are usually determined successively.

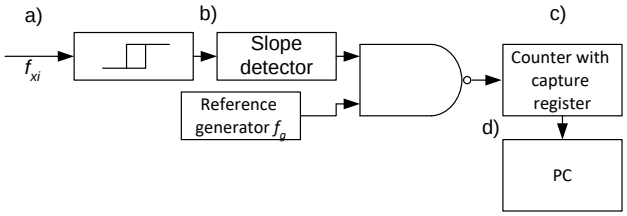

Fig. 1. An exemplary structure showing the processing of successive signal periods

Each period measurement is treated as a single, completely independent of the previous measurement [10]. Typically, the frequency signal, before being processed in the digital circuit, is formed in the Schmitt trigger [6] in order to adapt the signal amplitude to the requirements of the counter circuit used. The second reason for using a flip-flop is the need to form a square wave [5], allowing for precise detection of the boundaries of the processed period [3, 10].

An exemplary structure presenting the method of digital processing of the signal period is shown in figure 1. The waveforms showing the operation of the structure at more important points are shown in figure 2. The formed variable frequency waveform is fed to the signal edge detection circuit (Fig. 1b and Fig. 2b). At the selected edge (rising or falling), this system generates information about the end of the current period and the beginning of the next T_{xi} period of the frequency signal. In the defined limiting time moments (Fig. 1c and Fig. 2c), readings are made of the register of the counter continuously summing up the pulses from the reference signal generator. The difference between the successive read readings N_i of the counter is proportional to the length of a given period (Fig. 1d and Fig. 2d). The value of the difference is calculated from the dependence:

$$N_{xi} = N_{i+1} - N_i + C_m \cdot C_{Ov} \tag{1}$$

where: C_m – maximum number of pulses that can be registered by the frequency-to-code converter counter and C_{Ov} – number of registered overflows of the counter.

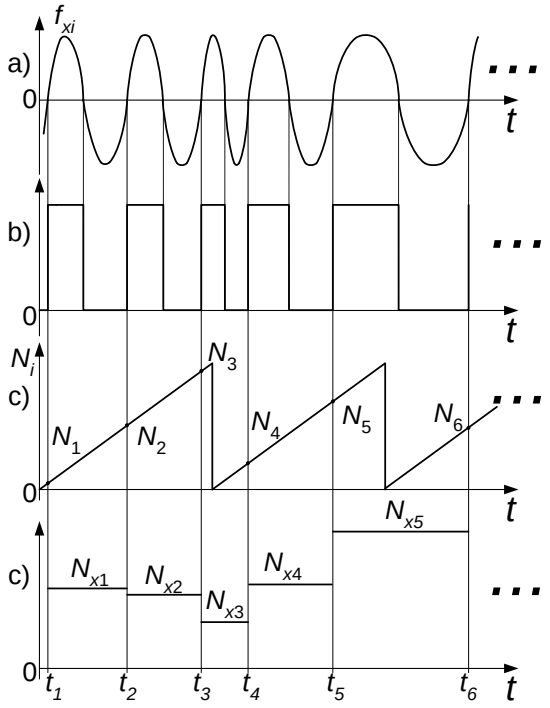

Fig. 2. Waveforms at selected points in the processing structure of successive periods of the signal

The period value is calculated as the product of the clock generator period T_g and the calculated difference of states for a given period T_{xi}:

$$T_{xi} = N_{xi} \cdot T_g \tag{2}$$

The system converting the signal frequency into numerical values is called the frequency-to-code converter [9] and marked with the symbol *f*/*N*.

2. The problem to be solved

During digital conversion of a period into numerical values, there is a problem of where to save large-volume measurement data. As it has already been written, microcontrollers [1] are often used for the construction of the *f*/*N* converter, which usually contain RAM memory in their structure. The advantage of the built-in memory chip is its direct accessibility and high speed of operation. Unfortunately, this memory is usually not very large, so it allows you to save only small sets of numerical data. Some microcontrollers allow you to add external memory. Unfortunately, also in this case the possibilities are small compared to the needs of using a possible longer measurement time. Much greater possibilities of data recording are offered by personal computers, usually controlling the measurement process.

The article presents an example of a frequency-to-code converter design using a personal computer for data storage.

3. Assumptions adopted for the transducer project being implemented

It was assumed that the developed *f*/*N* converter will be implemented with the use of the AVR family microcontroller. A standard UART module included in the microcontroller will be used for data transmission. The data will be received by a personal computer (PC) via the USB interface. A dedicated converter circuit will be used for the USB / RS232 conversion. It is obvious that the *f*/*N* converter system should not be burdened with unnecessary calculations that will slow down the measurement procedure. For this reason, instead of setting the measurement time, it was assumed that the number of T_{xi} period measurements to be performed by the *f*/*N* converter would be declared. It was assumed that the information about the number of measurements to be performed would be provided by the user via a PC.

4. Implementation

The ATmega32 microcontroller was chosen for the practical implementation of the *f*/*N* converter, which sends data to the computer via the FT232RL converter [16]. The integrated circuit 74LS132 [17] was selected to form the processed waveform of variable frequency into a rectangular shape with voltage levels adjusted to the requirements of the microcontroller. It was assumed that the test frequency signal would be produced in the Agilent 3322A generator [15]. The structure of the stand for the experimental verification of the developed frequency-to-code converter is shown in figure 3.

Fig. 3. The structure of the system for the implementation of the measurement experiment

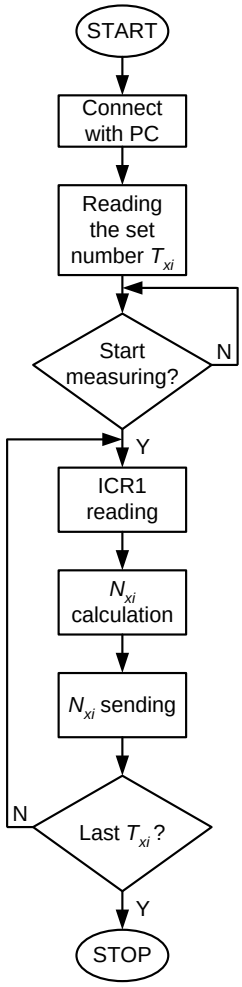

Fig. 4. The f/N converter work algorithm

The software of the *f*/*N* converter was created in the C language with the use of the AVR-GCC compiler [2]. The application work algorithm is shown in Fig. 4. After communicating with a PC, the transducer program waits for the determination of the required number of T_{xi} measurements. It then goes into a state of waiting for a frequency signal processing command. After receiving the expected command, the configuration of the T1 counter takes place, forcing the operation in the mode of capturing the instantaneous value of the totalizing register of the counter. The read states are stored

in the ICR1 register at the moments of the rising edge of the frequency signal (Fig. 2a and Fig. 2b). After the configuration, the counter is started and subsequent readings of the T1 counter are registered. The stored numerical values are then used to compute numerical values N_{xi} (1) representing successive periods T_{xi}. The N_{xi} numbers are sent to a PC to be stored in a file with measurement data for further processing and analysis.

5. Results of experiments

The data obtained in the experiment was analyzed with the use of proprietary software developed in the LabVIEW [12] programming environment of the National Instruments company. It was assumed that for the initial evaluation of the *f*/*N* converter operation, the software will present the evaluation in a way depending on the nature of the signal. For a fixed frequency waveform, a histogram of the measured frequencies will be presented. For a variable frequency waveform, a portion of the stored waveform will be presented and an error curve showing the relationship between the two errors. The first error is the value obtained by theoretical considerations [10]:

$$\delta_{\Sigma} = \frac{T_g}{T_{xi}} + 0.5\left(1 - \frac{\sin \pi F_x T_{xi}}{\pi F_x T_{xi}}\right) \tag{3}$$

where: F_x – frequency of the frequency signal value change.

The second error is the value obtained from the experiment. It is the difference between the set frequency signal and the reconstructed frequency signal [12]:

$$\delta_F = 0.5\left|\sin 2\pi F_x t - \sin 2\pi F t\right| \tag{4}$$

where: F – frequency of the change in the value of the frequency signal reconstructed from the measurement data.

The lower range of frequencies processed by the *f*/*N* converter working in the basic operating mode limits the capacity of the counter of the frequency-to-code converter.

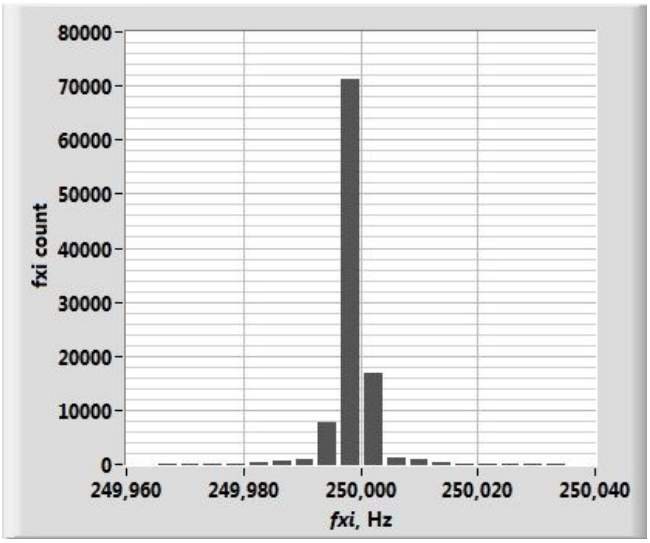

Fig. 5. Histogram of 100,000 frequency measurements of the frequency signal for a test signal with a frequency of 250 Hz

The discussed converter uses a 16-bit counter, and consequently the highest readable state is the number 65535. The period of the clock generator for the 16 MHz clock signal is 62.5 ns. As a result, the minimum measurable frequency, being the reciprocal of the product of the maximum counter state and the period of the clock generator, is approximately 244.144 Hz. To check the operation of the counter in the lower frequency range, a test signal with a frequency of 250 Hz was used. Figure 5 shows a histogram of the counter states after recording 100,000 periods of a frequency signal with a constant frequency of 250 Hz. The histogram shows that the read frequencies are very close to the set value in the test signal. The relative error of frequency measurement is within ± 0.014%.

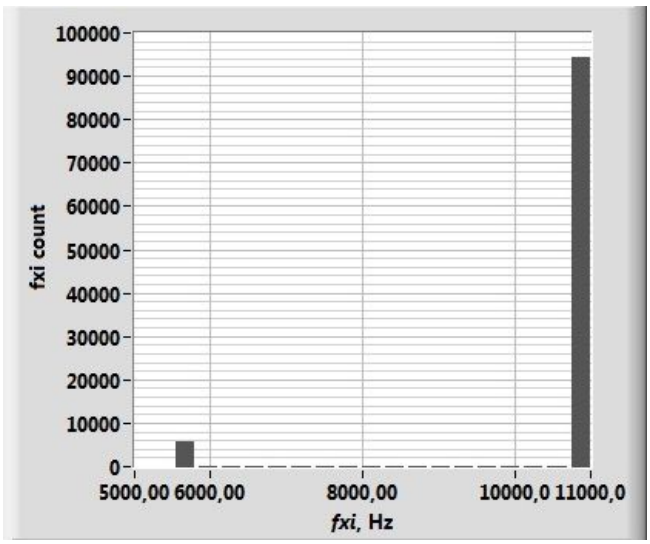

Fig. 6. Histogram of 100,000 frequency measurements of the frequency signal for a test signal with a frequency of 11 kHz

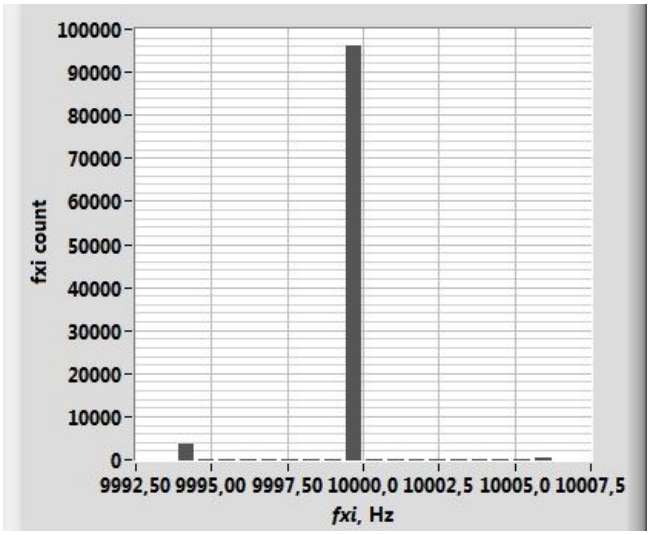

Fig. 7. Histogram of 100,000 frequency measurements of the frequency signal for a test signal with a frequency of 10 kHz

The frequency range for the top measuring range is limited by the calculation speed of the *f*/*N* converter and the data transmission baudrate through the interface. The histogram of the measurement of 100 thousand periods T_{xi} of the signal with the frequency of 11 kHz is shown in Figure 6. It can be seen that apart from the frequency of 11 kHz there is a frequency which is half of the set frequency. This is the effect of ineffective edge detection and recording of successive N_i states in the converter. Due to inefficiency problems some of the numbers N_{xi} read are actually the sum of two N_{xi}. The calculated frequency is then twice lower than the set frequency. Figure 7 shows a histogram of 100,000 period measurements of a 10 kHz signal. It can be seen that in this case the relative measurement error is ± 0.06%. The ability to process a variable frequency signal was also tested. Figure 8 shows a fragment of 1 million periods of a variable frequency test signal, the frequency of which varied according to the relationship:

$$\delta_F = 5250Hz + 5000Hz\left(\sin \pi F_x t\right) \tag{5}$$

Frequency F was set to 1 Hz. As can be seen, the reconstructed information allowed for the reconstruction of the given sinusoidal waveform with the parameters given in relation (5).

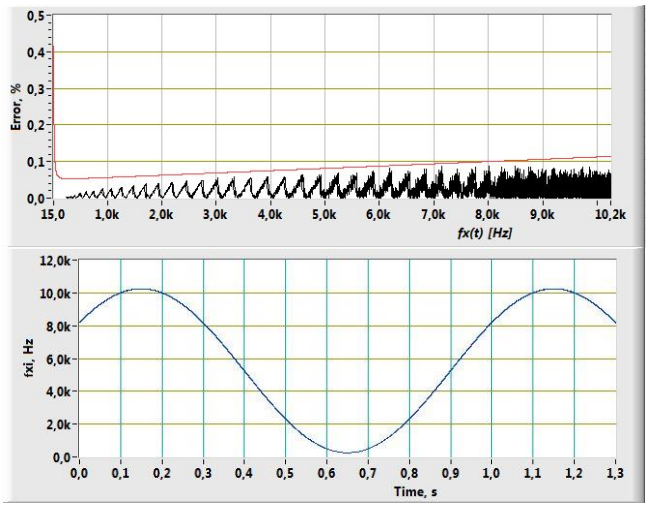

Fig. 8. The reconstructed fragment of the waveform with variable frequency (upper graph) and the error curve obtained experimentally for the processed frequency range (lower graph)

The graph of the theoretical information processing error curve in the *f*/*N* converter (3) with the generator error of 0.05% [15] is shown in red line. The course of the information processing error in the frequency-to-code converter obtained experimentally is shown in black line. As you can see, the real error introduced by the converter did not exceed the theoretical error curve at any point. It can be concluded that the developed *f*/*N* converter works properly.

6. Conclusions

The developed frequency-to-code converter allowed to confirm that there is a possibility of effective and useful direct data transmission from the digital signal period processing system to a personal computer. In the case of such a method of data archiving, microprocessor systems allowing for fast data transmission should be used. It is very important to develop an efficient data processing algorithm. As can be seen in the examples given, there are limitations in the speed of data processing in the microcontroller and they have a significant impact on the result of the processing. Of course, it is possible to increase the speed of code work, e.g. by the use of procedures created in assembler or the use of a microcontroller with higher performance. The developed device has demonstrated the ability to process a variable frequency signal in the range from 250 Hz to 10250 Hz.

References

[1] Barrett S. F., Pack D. J: Atmel avr microcontroller primer: Programming and interfacing. In Synthesis Lectures on Digital Circuits and Systems. Morgan & Claypool Publishers, Williston 2012.
[2] Francuz T.: Język C dla mikrokontrolerów AVR. Helion, 2011.
[3] Goswami J. C., Hoefel A. E.: Algorithms for estimating instantaneous frequency. Signal Process. 84, 2004, 1423–1427.
[4] Kirianaki N. V., Yurish S. Y., Shpak N. O., Deynega V. P.: Data Acquisition and Signal Processing for Smart Sensors. John Wiley & Sons, Chichester 2001.
[5] Murillo C. A., López B. C., Celma S.: Voltage-to-Frequency Converters: CMOS Design and Implementation. Springer, New York 2013.
[6] Pawłowski E., Świsulski D.: Problems with microprocessor voltage-to-frequency and frequency-to-voltage converters implementation. Przegląd Elektrotechniczny 91, 2015, 46–49.
[7] Pereira J. M., Postolache O. A., Girao P. S.: Analog to Digital Conversion Methods for Smart Sensing Systems. In: Sharma M. K. (Ed.): Advances in Measurement Systems. InTech Open, Rijeka 2010.
[8] Singh H. K., Bezboruah T.: Micro controller-based frequency to digital converter for interfacing frequency output sensors. International Conference on Electronic Design, Computer Networks & Automated Verification, 2015, 34–37.
[9] Swisulski D., Pawlowski E., Dorozhovets M.: Digital Processing of Frequency–Pulse Signal in Measurement System. Analysis and Simulation of Electrical and Computer Systems. Springer, Cham 2018.
[10] Warda P.: Adaptive correction of the quantization error in the frequency-to-code converter. 22nd International Conference on Methods and Models in Automation and Robotics (MMAR), 2017, 226–231.
[11] Warda P.: Measurement Data Transmission in the Presence of Electromagnetic Field. Proceedings of the International Conference on Electromagnetic Devices and Processes in Environment Protection with Seminar Applications of Superconductors (ELMECO &AoS), 2017.
[12] Warda P.: Simulation of an Adaptive Method of Improving the Accuracy and Extending the Range of Frequency Signal Processing in a Frequency-to-Code Converter. Applied Sciences 11(21), 2021, 1–19 [http://doi.org/10.3390/app112110341].
[13] Yurish S. Y.: Sensors and transducers: Frequency output versus voltage output. Sens. Transducers 49, 2004, 302–305.
[14] Yurish S. Y., Reverter F., Pallàs-Areny R.: Measurement error analysis and uncertainty reduction for period-and time-interval-to-digital converters based on microcontrollers. Meas. Sci. Technol. 16, 2005, 1660.
[15] Agilent 33220A20 MHz Function /Arbitrary Waveform Generator, User's Guide, 2007 Agilent Technologies, Inc.
[16] FT232R USB UART IC Datasheet,Version 2.16
[17] SN54132, SN54LS132, SN54S132, SN74132, SN74LS132, SN74S132 Quadruple 2-input positive-nand Schmitt triggers, 2022, Texas Instruments Incorporated

Ph.D. Eng. Piotr Warda
e-mail: p.warda@pollub.pl

Graduate of the Faculty of Electrical Engineering, Lublin University of Technology (1995). Since 2000, a research and teaching employee of the Department of Automation and Metrology at Lublin University of Technology. He defended his doctoral dissertation in 2008. His areas of interest include digital metrology and measurement signal processing.

http://orcid.org/0000-0002-7525-4668

http://doi.org/10.35784/iapgos.3255 *received: 8.11.2022 | revised: 8.12.2022 | accepted: 15.12.2022 | available online: 30.12.2022*

DIGITAL APPROACH TO THERMIONIC EMISSION CURRENT TO VOLTAGE CONVERSION FOR HIGH-VOLTAGE SOURCES OF ELECTRONS

Bartosz Kania
Lublin University of Technology, Department of Automatics and Metrology, Lublin, Poland

Abstract. *The thermionic emission current is used in many vacuum devices such as evaporators, rare gas excimers, or electron beam objects for high-energy physics. The stability of the thermionic emission current is a very important requirement for the accuracy of those devices. Hence, there is a number of control systems that use a feedback signal directly proportional to the emission current in order to stabilize the thermionic emission current. Most of them use feedback from a high-voltage anode circuit to a low-voltage cathode circuit. However, there is a novel solution that uses linear cathode current distribution and processing of two cathode circuit voltage signals for converting the emission current to voltage. However, it is based on old-fashioned analog technology. This paper shows the thermionic emission current to voltage conversion method with the use of a digital control system. A digital realization of a multiplicative-additive algorithm is presented and proper work in closed-loop mode is confirmed.*

Keywords: electron emission, electron sources, control system synthesis, digital control

CYFROWE PODEJŚCIE DO METODY KONWERSJI NATĘŻENIA PRĄDU TERMOEMISJI ELEKTRONOWEJ NA NAPIĘCIE DLA WYSOKONAPIĘCIOWYCH ŹRÓDEŁ ELEKTRONÓW

Streszczenie. *Prąd termoemisji elektronowej jest wykorzystywany w wielu przyrządach próżniowych takich jak ewaporatory, ekscymery gazów rzadkich czy w fizyce wysokich energii. Stabilność natężenia prądu termoemisji elektronowej jest ważnym wymaganiem w kontekście dokładności tych przyrządów. Istnieje wiele układów regulacji natężenia prądu termoemisji elektronowej, które używają sygnału sprzężenia zwrotnego wprost proporcjonalnego do natężenia prądu termoemisji elektronowej w celu jego stabilizacji. Większość z nich wykorzystuje sprzężenie od wysokonapięciowego obwodu anody do niskonapięciowego obwodu katody. Istnieje nowe rozwiązanie, które wykorzystuje liniowy rozkład prądu katody oraz przetwarzanie dwóch sygnałów z obwodu katody w celu konwersji natężenia prądu termoemisji na napięcie. Niestety metoda ta bazuje na przestarzałej technologii analogowej. W niniejszej pracy pokazana została konwersja natężenia prądu termoemisji elektronowej na napięcie z użyciem cyfrowego układu automatycznej regulacji. Cyfrowa realizacja algorytmu multiplikatywno-addytywnego została zaprezentowana, a poprawna praca w zamkniętej pętli sprzężenia zwrotnego potwierdzona.*

Słowa kluczowe: emisja elektronów, źródła elektronów, synteza systemu sterowania, sterowanie cyfrowe

Introduction

There are many vacuum devices that use thermionic electron sources operating under temperature or space charge limited mode, such as electron beam objects for high energy physics [17], water radiolysis [21], [23] integrated circuit manufacturing process monitors [16], X-ray photoelectron spectroscopes [22], devices producing rare gas excimers [3] or evaporators [15]. The stability of the electron emission current is one of the most important requirements for electron sources. Most thermionic emission current stabilizers use negative feedback loop control systems where thermionic emission current is measured in a high-voltage anode supply circuit [1, 4–10, 12, 14, 15, 18, 19] and transferred to a low-voltage cathode supply circuit. For relatively low values of electron accelerating voltage both, the cathode and the anode circuits, can be at a common electric potential. However, for higher values of electron accelerating voltage, some modifications are needed due to the limited breakdown voltage of semiconductor components, such as optical isolation [15], [8], in order to safe signal transfer between the anode and the cathode circuit.

An impediment to transferring feedback signal in high-voltage electron sources was a ground for a novel solution using cathode circuit currents measurements to convert emission current into voltage [13]. This solution offers relatively high conversion accuracy for low values of the electron work function of the cathode material. However, it bases on old-fashioned analog technology. This paper shows the thermionic emission current to voltage conversion method with the use of a digital control system. An implementation of a digital algorithm is presented, and proper work in closed-loop mode is confirmed.

1. Hardware design

A block diagram of control system hardware is presented in Fig. 1. The control system hardware consists of several main hardware components:

- a PC with the Windows operating system and LabVIEW scientific and engineering software from National Instruments,
- NI USB-6251 data acquisition card from National Instruments,
- the main electronic system processing measurement and control signals,
- controlled system – a hot cathode electron source.

A PC is a platform for control algorithms implemented in the LabVIEW environment. The algorithm's more detailed description is in the next section below. The data acquisition card [24] offers 8 differential inputs or 16 inputs operating in the common potential mode with a resolution of 16 bits. The maximum sampling rate is 1.25 MS/s for single-channel operation or 1 MS/s for multi-channel operation. In addition, the card offers 2 analog outputs with a resolution of 16 bits and a sampling frequency of 2.86 MS/s for single-channel operation and 2 MS/s for two-channel operation. The analog inputs of measuring amplifiers of the data acquisition card were used in the differential configuration ensuring the reduction of the common signal at the outputs.

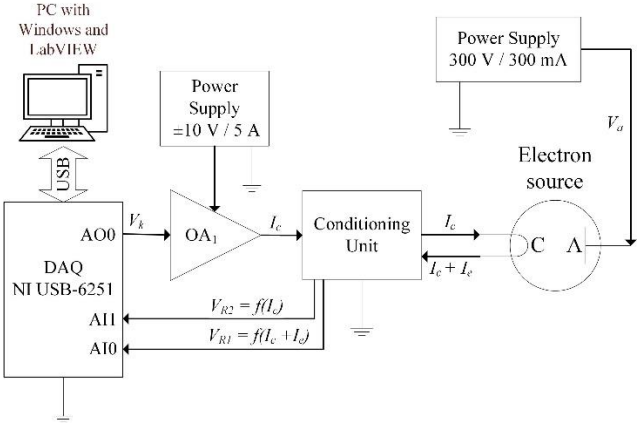

Fig. 1. A block diagram of control system hardware. OA_1 is the high-current operational amplifier OPA 549, V_a is the anode supply voltage, V_k is the cathode circuit supply voltage, V_{R1} and V_{R2} are voltage drops across sensing resistors R_1 and R_2 in the cathode circuit, respectively, I_e is a process value of the electron emission current, I_c is the cathode heating current, C means the cathode, A means the anode

The center of the test stand is an electronic system designed to process measurement and control signals. There are 2 circuits: cathodes one and anodes one.

Fig. 2 shows a schematic diagram of the electronic system. The cathode power supply voltage V_k is fed to the cathode through the operational power amplifier OA_1 (OPA549, Texas Instruments) with a voltage gain of 1.2 V/V. The current in the cathode circuit also flows through the sensing resistors R_1 and R_2. The signal V_a fed from power supply unit constitutes the control voltage of the anode. The emission current flows through the anode, the cathode, and the resistor R_1 to the ground of the system.

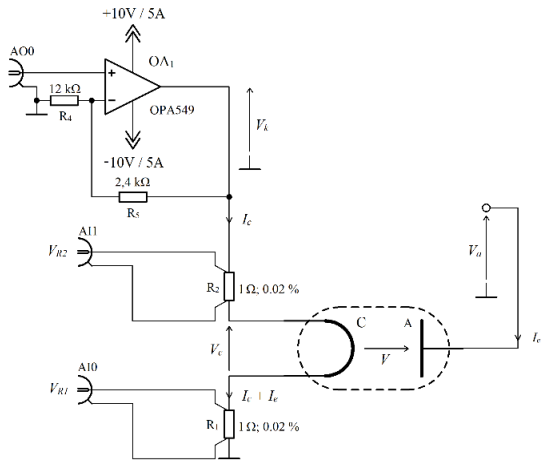

Fig. 2. Detailed control system hardware diagram. Controlling signals: V_k is the cathode power supply voltage, V_c is the cathode voltage, V_a is the anode supply voltage; V_{R1} and V_{R2} are voltage drops across sensing resistors R_1 and R_2, respectively; AI0 and AI1 are analog inputs of the data acquisition card, AO0 is analog output of the data acquisition card

The system uses two sensing resistors VPR221 (Vishay Foil Resistors) [25] with a resistance of 1 Ω, tolerance ± 0.02%, maximum temperature coefficient of ±5 ppm/°C, and power of 8 W each. They are connected in series in the cathode circuit: the resistor R_2 between the control voltage source V_k and the cathode terminal; the resistor R_1 between the other cathode terminal and the common reference potential – the ground of the system. According to the analysis presented in [13], the potential drop across the resistor R_2 is directly proportional to the cathode heating current I_c

$$V_{R2} = R_2 I_c \tag{1}$$

while the potential drop across the resistor R_1 is directly proportional to the sum of the currents flowing through the resistor.

$$V_{R1} = R_1(I_c + I_e) \tag{2}$$

Voltage signals from the terminals of the resistors are fed to the inputs of the data acquisition card, where they are subjected to analog-to-digital conversion. A high-voltage power supply in the anode circuit supplies energy to the anode.

2. Algorithm

Data acquisition, analysis, and control algorithm are implemented with the use of a PC with Windows operating system and LabVIEW (National Instruments) environment. The algorithm is presented in Fig. 3.

The algorithm begins with the initialization of the data acquisition card. Moreover, the following properties are configured: the source of the clock signal (internal clock signal), the type of measurement (differential), the range of input values (0 – 2 V or 0 – 10 V), and the sampling frequency (250 kSPS). The next part of the process is reading the input signals. The collected measurement data contains a noise signal. Therefore, as part of digital processing, the data is averaged over the iteration period of the algorithm, and then transformed according to assumption R = R_1 = R_2 and formula (3).

$$\mathrm{I_e} = \frac{V_{R1} - V_{R2}}{R} \tag{3}$$

The iteration period of the algorithm was determined as – Fig. 3.

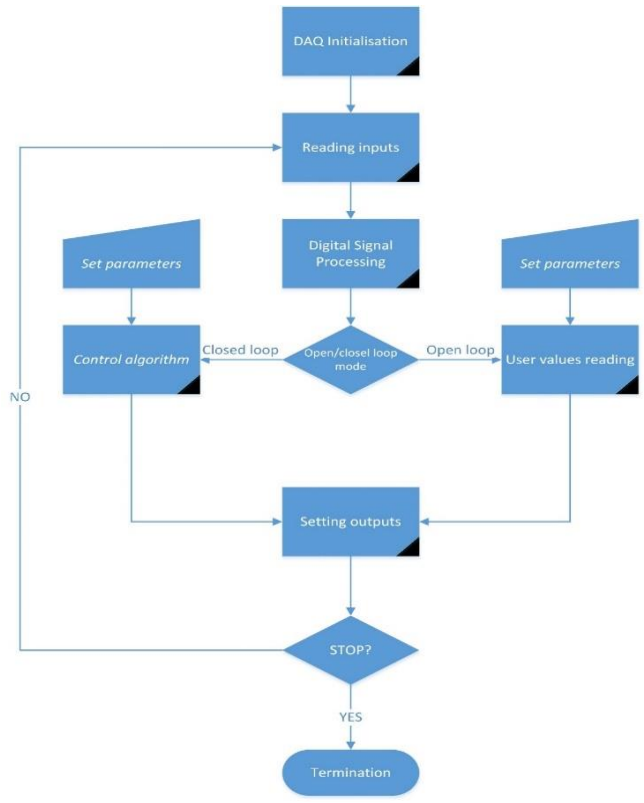

Fig. 3. The algorithm diagram

$$T_s \cong \frac{1}{12} T_{95} \cong 100 \text{ ms} \tag{4}$$

where T_s is the iteration period of the control algorithm, and T_{95} is the settling time (until the step response reaches 95% of the set value). Then, depending on the active mode, the value of the control signal is calculated with the use of given parameters (closed feedback loop) or the data, such as the cathode circuit supply voltage V_k', is taken from an user (open feedback loop). In the case of the closed-loop operation, the user has to determine the reference value of the electron emission current I_{eref}'. Next, the output signals of the data acquisition card are updated. At this point, the control process can be completed, or the cycle starts again, i.e. reading the input signals.

A block diagram of the developed of the electron emission current control system is presented in Fig. 4.

As one can see, the controlled system covers two input signals and three output signals. The thermionic electron source has a higher-order inertia nature [20], [11]. Taking into account small signal transconductance *G(s)* [13]

$$G(s) = \frac{G_0}{T_c s + 1} e^{-sT_0} \tag{5}$$

where G_0 is the DC transconductance, T_c is the time constant, T_0 is the delay time, s is the Laplace operator, and the equation derived in [13], which describes electron accelerating voltage V

$$V = V_a - \frac{1}{3} R_c I_e - \frac{1}{2} R_c I_c \tag{6}$$

where R_c is the resistance of the cathode; the controlled system transfer function **H(s)** (see Figure 4) can be described as a series of two transfer functions, $\mathbf{H_1(s)}$ and $\mathbf{H_2}$:

$$\begin{bmatrix} I_e \\ I_c \end{bmatrix} = \underbrace{\begin{bmatrix} \frac{G_0}{T_c s + 1} e^{-sT_0} \\ \frac{1}{R_2 + R_k + R_1} \end{bmatrix}}_{\mathbf{H_1}(s)} [V_k] \tag{7}$$

$$[V] = \underbrace{\begin{bmatrix} 1 & -\frac{1}{3} R_c + R_1 & -\frac{1}{2} R_c + R_2 \end{bmatrix}}_{\mathbf{H_2}} \begin{bmatrix} V_a \\ I_e \\ I_c \end{bmatrix} \tag{8}$$

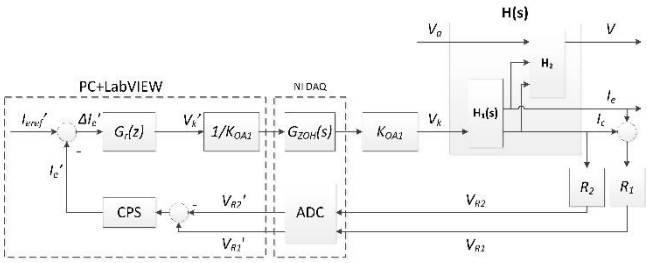

Fig. 4. A block diagram of the electron emission current control system; I_{eref}' is the digital set value of the electron emission current, I_e is the process value of the electron emission current, I_e' is a digital value of the electron emission current, ΔI_e' is a digital value of an electron emission current error, V_a is the anode supply voltage, V is the accelerating voltage, V_k' is the digital value of the cathode circuit supply voltage, V_k is the cathode circuit supply voltage, I_c is the cathode heating current, $G_r(z)$, H(s) and $G_{ZOH}(s)$ are transfer functions of the controller, the electron source, and digital to analog converters respectively. K_{OA1} is gain of the operational amplifiers OA_1. V_{R1} and V_{R2} are the voltage drops across the measurement resistors R_1 and R_2 in the cathode circuit, respectively, V_{R1}' and V_{R2}' are digital values of the voltage drops V_{R1} and V_{R2}, block ADC is an analog to digital converter, block DSP is digital signal processing

3. Results

The controlled system is a hot cathode electron source. A vacuum diode, 1B3-GT type [2], was used for the tests due to the favorable ratio of the thermionic emission current to the heating current. The rated value of the cathode current is 200 mA, at which the value of the thermal emission current is equal to 3.9 mA (the electron accelerating voltage is equal to 60 V). The cathode has the form of a filament and has a length of 6 mm and a diameter of 0.482 mm. The measurements of the emission current and the cathode voltage were made using HP 34461A multimeters. Type B relative standard uncertainty values of voltage V_c and current I_e are less than 0.0028% and 0.03%, respectively. Fig. 5a shows the static characteristic of the investigated electron source, that is thermionic emission current I_e as a function of the cathode voltage V_c for different values of the anode supply voltage V_a and Figure 5b presents the thermionic emission current I_e vs. the anode supply voltage V_a for different values of the cathode current I_c.

The measurements were performed at open-loop control mode, for heating current I_c up to 200 mA, the anode supply voltage V_a up to 65 V, measurements resistors R_1 and R_2 were shortened ($R_1 = R_2 = 0\ \Omega$). As one can see in Fig. 5a and Fig. 5b the thermionic emission current is dependent on the cathode voltage V_c and the anode supply voltage V_a. However, for relatively low values of the anode supply voltage ($V_a < 10$ V) and the cathode voltage more than 0.85 V, the electron source operates in the space charge range. Then the thermionic emission current remains approximately constant with the increase of the cathode voltage V_c. For higher values of the anode voltage, the space charge range is more exiguous, and the emission current saturation range is wider.

Fig. 6 presents the difference of voltage drops V_{R1} and V_{R2} across measurement resistors R_1 and R_2 measured by data acquisition card as a function of thermionic emission current I_e and also linear fitting. The linear function can be expressed by the equation

$$V_{R1} - V_{R2} = 0.9993 \cdot I_e - 0.0035 \qquad (9)$$

and a correlation coefficient is 0.99998. Relative nonlinearity for emission current higher than 1 mA is lower than 0,01 %.

Fig. 7 shows the 20-minutes relative standard deviation of the thermionic emission current for the closed-loop mode operation of the thermionic emission current control system. The anode voltage is set to 60 V to ensure that the electron source operates outside the space charge area. The average value of all relative standard deviation points is 0.18 % which confirms the satisfactory stabilization of the thermionic emission current and proper work of the control system using I_e-V conversion method in the cathode supply circuit.

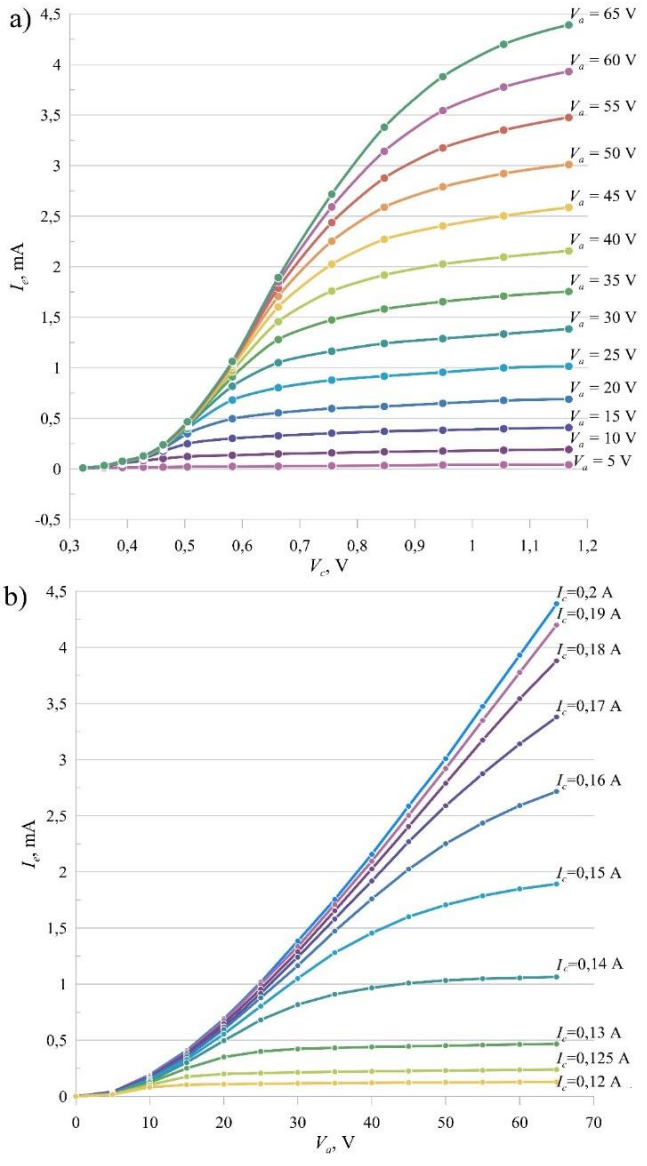

Fig. 5. a) The thermionic emission current I_e vs. the cathode voltage V_c for different values of the anode supply voltage V_a, b) the thermionic emission current I_e vs. the anode supply voltage V_a for different values of the cathode current I_c.

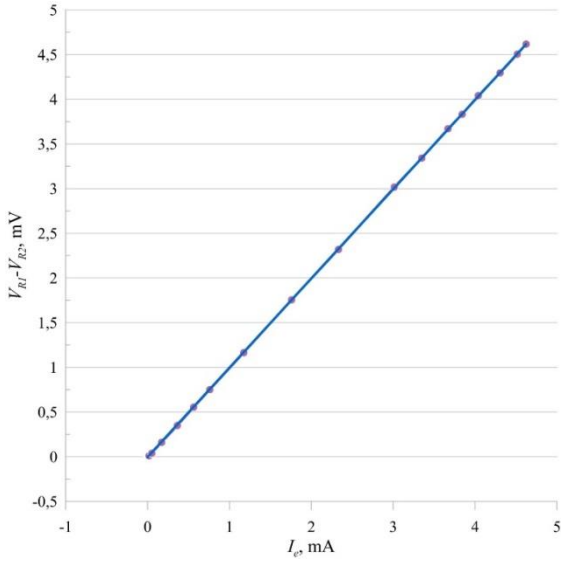

Fig. 6. Difference of voltage drops V_{R1} and V_{R2} across measurement resistors R_1 and R_2 measured by data acquisition card vs. thermionic emission current I_e (dots) and linear fitting (line)

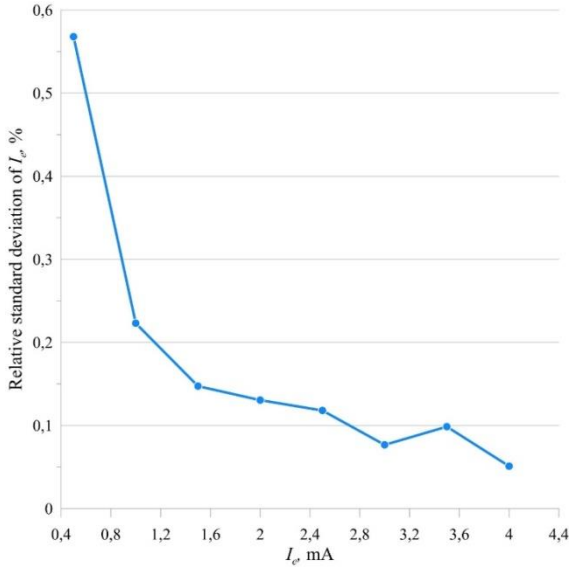

Fig. 7. The 20-minute relative standard deviation of the thermionic emission current I_e for the closed-loop mode operation. The average value of the relative standard deviation is 0.18 %. The anode voltage is 60 V

4. Conclusions

The implementation of the electron emission current to the voltage conversion method in the digital control system was presented. Moreover, the conversion of the emission current to voltage with the use of vacuum diode and sensing resistors in the cathode power supply circuit was successfully tested. The results of experiments with the use of the data acquisition card and digital signal processing of measurement signals confirm high linearity of conversion for more than 1 mA of the thermionic emission current. A relatively high value of the thermionic emission current to the cathode heating current ratio contributes to satisfactory stabilization of the thermionic emission current control system. Moreover, the digital controller is easily tuneable and offers system management or monitoring.

Funding: This research was funded by Lublin University of Technology, Lublin, Science Fund No. FD-20/EE-2/101.
Acknowledgments: The author is thankful to Professor Jarosław Sikora for lots of helpful advices.

References

[1] Ahn J. et al.: Microprocessor-controlled Electron Impact Ion Source Operated at Constant Discharge Current and Voltage. Review of Scientific Instruments 57(3), 1986, 325–328 [http://doi.org/10.1063/1.1138939].
[2] Angiolillo P.: On Thermionic Emission and the Use of Vacuum Tubes in the Advanced Physics Laboratory. American Journal of Physics - Amer J Phys 77, 2009, 1102–1106 [http://doi.org/10.1119/1.3212463].
[3] Barcellan L. et al.: A Battery-Operated, Stabilized, High-Energy Pulsed Electron Gun for the Production of Rare Gas Excimers. Review of Scientific Instruments 82(8), 2011, 095103 [http://doi.org/10.1063/1.3636078].
[4] Chapman R.: Versatile Wide Range Electron Current Regulator. Review of Scientific Instruments 43(10), 1972, 1536–1538 [http://doi.org/10.1063/1.1685484].
[5] Close K. J., Yarwood J.: A Precision Electron Emission Regulator. Vacuum 22(2), 1972, 45–46 [http://doi.org/10.1016/0042-207X(72)90001-2].
[6] DAQ M Series Manual. National Instruments, 2016.
[7] Donkov N., Knapp W.: Control of Hot-Filament Ionization Gauge Emission Current: Mathematical Model and Model-Based Controller. Measurement Science and Technology 8(7), 1997, 798–803 [http://doi.org/10.1088/0957-0233/8/7/016].
[8] Durakiewicz T.: Electron Emission Controller with Pulsed Heating of Filament. International Journal of Mass Spectrometry and Ion Processes 156(1), 1996, 31–40 [http://doi.org/10.1016/S0168-1176(96)04417-5].
[9] Flaxer E.: Programmable Smart Electron Emission Controller for Hot Filament. Review of Scientific Instruments 82(2), 2011, 025111 [http://doi.org/10.1063/1.3555340].
[10] Foil Resistors VPR220 & VPR221. Vishay Precision Group, 2014, http://www.vishaypg.com/foil-resistors/list/product-63012/
[11] Halas S., Sikora J.: Electron Emission Stabiliser with Double Negative Feedback Loop. Measurement Science and Technology 1(9), 1990, 980–982 [http://doi.org/10.1088/0957-0233/1/9/023].
[12] Herbert B. K.: A Circuit for Stabilizing the Electron Current to the Anode of a Hot-Filament Device. Vacuum 26(9), 1976, 363–369 [http://doi.org/10.1016/S0042-207X(76)80225-4].
[13] Kania B., Sikora J.: System Identification of a Hot Cathode Electron Source: Time Domain Approach. AIP Advances 8(10), 2018, 105107 [http://doi.org/10.1063/1.5044258].
[14] Kania B., Sikora J.: Thermionic emission controller with PID algorithm. 23rd International Conference "Mixed Design of Integrated Circuits and Systems" MIXDES 2016, 480–83 [http://doi.org/10.1109/MIXDES.2016.7529790].
[15] Kuś D. et al.: Conversion Method of Thermionic Emission Current to Voltage for High-Voltage Sources of Electrons. Electronics 10(22), 2021, 2844 [http://doi.org/10.3390/electronics10222844].
[16] Lin X. W. et al.: A Miniature Electron-beam Evaporator for an Ultrahigh-vacuum Atom-probe Field-ion Microscope. Review of Scientific Instruments 61(12), 1990, 3745–3749 [http://doi.org/10.1063/1.1141547].
[17] Meyer zu Heringdorf F. J., Belton A.C.: Flexible Microprocessor-Based Evaporation Controller. Review of Scientific Instruments 75(12), 2004, 5288–5292 [http://doi.org/10.1063/1.1818911].
[18] Oberai A., Jiann-Shiun Y.: Smart E-Beam for Defect Identification & Analysis in the Nanoscale Technology Nodes: Technical Perspectives. Electronics 6(4), 2017, 87 [http://doi.org/10.3390/electronics6040087].
[19] Pepitone K. et al.: Operation of a High-Current Drive Beam Electron Gun Prototype for the Compact Linear Collider. Review of Scientific Instruments 91(9), 2020, 093302 [http://doi.org/10.1063/5.0013144].
[20] Shaw S. Y., Juh T. L.: An Integrated Circuit Based Vacuum Ionisation Gauge Meter. Journal of Physics E: Scientific Instruments 13(11), 1980, 1150–1153 [http://doi.org/10.1088/0022-3735/13/11/003].
[21] Sikora J.: Dual Application of a Biasing System to an Electron Source with a Hot Cathode. Measurement Science and Technology 15(1), 2003, N10–14 [http://doi.org/10.1088/0957-0233/15/1/N03].
[22] Sikora J. et al.: Thermionic Electron Beam Current and Accelerating Voltage Controller for Gas Ion Sources. Sensors 21(8), 2021, 2878 [http://doi.org/10.3390/s21082878].
[23] Siwek M., Edgecock T.: Application of Electron Beam Water Radiolysis for Sewage Sludge Treatment, a Review. Env. Science and Pollution Research 27(34), 2020, 42424–42448 [http://doi.org/10.1007/s11356-020-10643-0].
[24] Stevie F. A., Carrie L. D.: Introduction to X-Ray Photoelectron Spectroscopy. Journal of Vacuum Science & Technology A 38(6), 2020, 063204 [http://doi.org/10.1116/6.0000412].
[25] Zimek Z.: Wytyczne do budowy radiacyjnej instalacji obróbki wód balastowych przy użyciu wiązki elektronów. Raporty IChTJ. Seria B nr 2/2020.

M.Sc. Eng Bartosz Kania
e-mail: b.kania@pollub.pl

He is a graduate of the Faculty of Electrical Engineering and Computer Science of the Lublin University of Technology. In 2013, he began doctoral studies at the Faculty of Electrical Engineering and Computer Science of the Lublin University of Technology in the discipline of Electrical Engineering. He is also a research and lecturer at the Department of Automatics and Metrology of the Lublin University of Technology. Scientific work focuses on the implementation of control algorithms and processing of digital measurement signals.

http://orcid.org/0000-0001-8429-6360

http://doi.org/10.35784/iapgos.3217 *received: 31.10.2022 | revised: 10.12.2022 | accepted: 15.12.2022 | available online: 30.12.2022*

SYSTEM SOFTWARE AT LABORATORY STAND „LIGHTS CONTROL ON THE BASIS OF PROGRAMMABLE LOGIC CONROLLER”

Laura Yesmakhanova, Raushan Dzhanuzakova, Bauyrzhan Myrkalykov
Taraz Regional University named after Dulati M.K., Taraz, Kazakhstan

Abstract. *The article is concerned with the issues of practical utilization of controllers for automation in various technical fields as example Mitsubishi controllers of MELSEC FX1N and FX3U series. Any task, which requires the utilization of electrical control devices, is easy to solve by means of usage of programmable logic controllers. By using software with controllers programming package GX Developer, user has the possibility to program the controller or input changes into existing program. The Laboratory Stand was developed for effective learning of controller programming in LD language.*

Keywords: controller, program, control, relay

OPROGRAMOWANIE SYSTEMOWE NA STANOWISKU LABORATORYJNYM „STEROWANIE OŚWIETLENIEM W OPARCIU O PROGRAMOWALNY STEROWNIK LOGICZNY”

Streszczenie. *Artykuł dotyczy zagadnień praktycznego wykorzystania sterowników do automatyzacji w różnych dziedzinach technicznych, na przykład sterowników Mitsubishi serii MELSEC FX1N i FX3U. Każde zadanie, które wymaga wykorzystania elektrycznych urządzeń sterujących, można łatwo rozwiązać za pomocą programowalnych sterowników logicznych. Korzystając z oprogramowania z pakietem programowania sterowników GX Developer, użytkownik ma możliwość zaprogramowania sterownika lub wprowadzenia zmian do istniejącego programu. Stanowisko laboratoryjne zostało opracowane z myślą o efektywnej nauce programowania sterowników w języku LD.*

Słowa kluczowe: sterownik, program, sterowanie, przekaźnik

Introduction

The contemporary production is based on high technologies that are designed to provide speed, scale, reliability, safety and high quality of task performance. Long-standing need for flexible process control, efficient use of production capacity, remote control in real time determined the need to move from bulky Ladder Diagram to reprogrammable logic controllers. Contemporary controllers swiftly process data and automatically control the processes. The ability to change the program allows quickly change the technological process depending on the current task.

Programmable logic controller (PLC) is a specialized microprocessor device with embedded hardware and software that is utilized to perform the functions of controlling process equipment. PLC is a device accessible for programming by a non-specialist in IT and designed to control sequential logical processes in an industrial environment in real time. The PLC repeatedly scans the inputs to which switches, sensors, etc. are connected, and depending on their state (”on” – 1, ”off” – 0), turns the outputs on and off, and hence the actuators connected to the outputs. The functional diagram of the control system (CS) based on the controller is shown in Figure 1. By utilizing the software, the user has possibility to program the controller or input changes to an existing program [1].

The programmable logic controller mainly consists of a central processing unit (CPU), a memory area, and I/O signal processing functions (i.e., inputs and outputs). Contingently, such a controller can be called the essential or base unit (module). It can be considered the PLC as hundreds or thousands of individual relays, counters, timers, and memory. All these counters, timers are simulated by the CPU and carry out the logic of work, according to the embedded program. The block diagram of the controller is shown in the figure 2.

- INPUTS provide communication with external devices. Physically exist and receive signals from switches, sensors, etc. There are analog and digital inputs designed to work with analog and digital signals, respectively.
- The CPU is the ”brain” of the PLC, carrying out the logic of the system. This is a processor that processes program commands and controls all internal elements of the controller: inputs, outputs, counters, timers, internal relays, registers, etc. In figure 2, the counters, timers, and internal relays are not shown separately; they are part of the CPU chip. I.e. each controller has a fixed set of such elements, which are given in the specification.
- INTERNAL RELAYS (MARKERS) are designed to ensure the operation of the program, because are a kind of information storage units. Along with ordinary markers, there are also service markers that carry a special semantic and functional load (for example, setting an enable flag to start high-speed counters). The purpose of each specific service marker is given in the documentation for the controller.

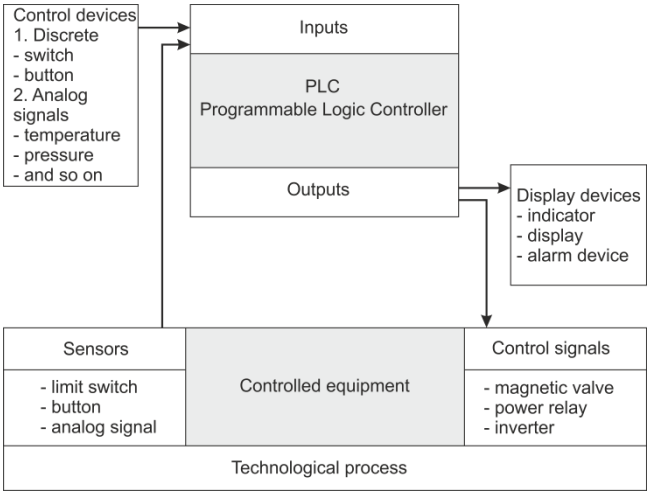

Fig. 1. Functional diagram CS on PLC base

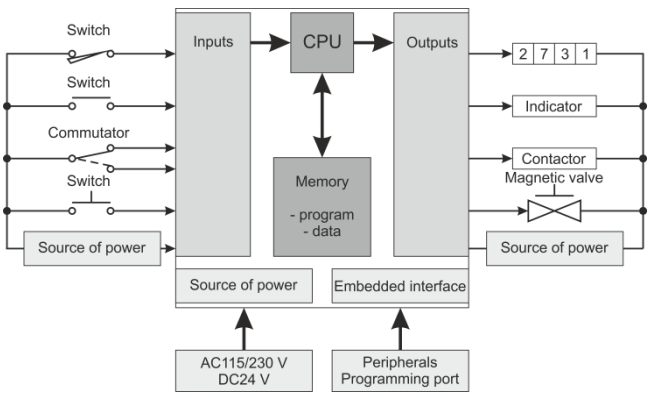

Fig. 2. Block diagram of the controller

- COUNTERS are designed for various types of counting. Separately allocate high-speed counters. Usually, there are restrictions on the count rate and the value to which the count is kept, for which it is necessary to refer to the documentation of a particular controller.
- TIMERS are designed, as a rule, to set the on / off delay time, etc. They differ mainly in the accuracy of timing and, as a result, in their purpose.
- MEMORY – the controller has a certain amount of memory, which may have a different organization in different controllers. Most commonly, memory is divided into a work area (RAM), where the program is loaded directly during the operation of the controller, and a data area (EEPROM, MMC, etc.), where the program and various data are stored. Often the size of the work area is measured in kilobytes, and the size of the data area is measured in the number of program steps.
- BUILT-IN INTERFACE provides connection of the PLC to a computer or programmer for data exchange, including for reprogramming the controller. Basically, these are RS-232C (COM-port), RS-422, RS-485, etc.
- OUTPUTS provide communication with external devices, i.e. provide switching on/off of actuators. There are two versions: relay, semiconductor (transistor and triac). There are analog and digital outputs designed to work with digital and analog signals, respectively.
- POWER SUPPLY is designed to ensure the operation of the controller. External power supplies can be used, both DC +12/24 V and AC – ~110/220 V. Many controllers have built-in service power supplies (usually +12/24V) that are used to power sensors or other devices connected to the controller to simplify input and output circuits [1].

1. Conditions and methods of research

Recently, there has been a tendency to expand the functionality of controllers via the implementation of built-in PID controllers, real-time clocks, networking controllers and using the ability to connect expansion units. In any case, the structure of the controller remains unchanged, and the choice of model is determined only by the requirements of the process, and a wide range of models allows you to choose a controller with an optimal price / performance ratio.

To understand the operation of the controller, figure 3 shows the algorithm of its operation.

During operation, the PLC continuously scans the current state of the inputs X1, X2…Xn and, in accordance with the requirements of the production process, changes the state of the outputs Y1, Y2…Yn (on/off). This cycle can be divided into four main steps.

The first step is to initialize the system. It must be remembered that in the event of a power failure or when the controller is turned off, the system must return to its original state. The importance of this part of the program code should not be underestimated; otherwise it can lead to failures and equipment breakdowns.

The second step is to check the current state of the inputs. The PLC checks the current state of the inputs and, depending on their state (”on” or ”off”), performs sequential actions specified in the program. The state of any of the inputs is stored in memory (in the data area) and can later be used when processing the third step of the program [3].

The third step is execution of the program. We will assume that during the process, the input (X1) switched from ”off” to ”on”, and in accordance with the process, we need to change the current state of the output (Y1) from ”off” to ”on”. Since the CPU scanned the current state of all inputs and stores their current state in memory, the choice of the next action is determined only by operation process.

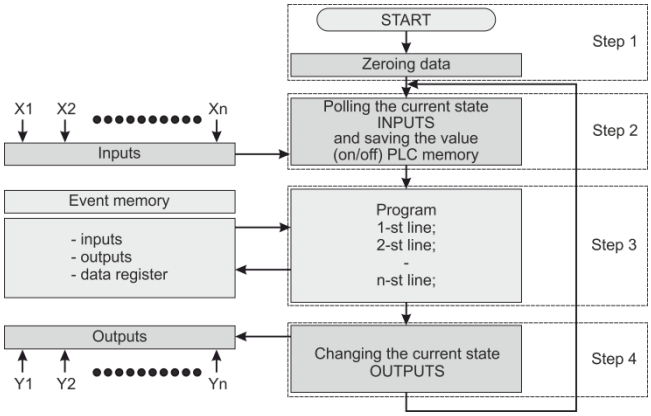

Fig. 3. Algorithmic diagram of controller operation

Step four is to change the current state of the output. The PLC changes the current state of the outputs depending on which inputs are disabled and which are enabled, based on the algorithm of the program stored in the memory, which was processed in the third step. I.e., the controller physically switched the output (Y1) and the actuators turned on: a light bulb, an engine, etc. This is followed by a return to the second step.

While using a DC power supply, it is necessary to connect the ”+” terminal of the power supply to the ”+” terminal of the controller, and the ”-” terminal of the power supply to the ”-” terminal of the controller. No other connection is allowed.

When using AC power supply:

- the phase line must be connected to the L terminal and the 0 line to the N terminal. To avoid electric shock, do not connect the L phase line to the N terminal,
- ground connection is required. Ground resistance must be R < 100 Ω.

An example of connecting a power supply is shown in Fig. 4.

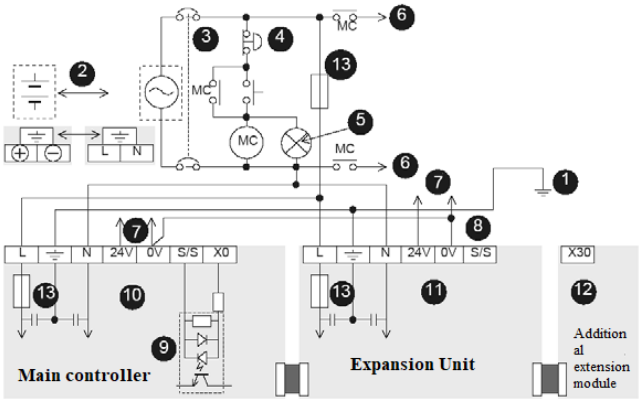

Fig. 4. Example of connecting a power supply to PLC: 1 – grounding: class 3; 2 – power supply; 3 – protective device; 4 – emergency stop; 5 – power indicator; 6 – load supply; 7 – built-in power supply; 8 – switch for the type of input switching; 9 – optocoupler; 10 – base block; 11 – extension block; 12 – extension module (ex. analog input); 13 – fuse (3 A)

If the system uses the built-in power supply of both the base unit and the expansion unit, then the ”0” terminals must be connected. At the same time, DO NOT CONNECT the ”24 V” terminals of the base unit and the expansion unit to each other; NEVER connect an external power supply to the ”24V” terminals.

2. Launch GX Developer, shell program overview

After installing the GX Developer programming environment on your computer, launch it by double-clicking the button in the START menu > Programs > MELSEC Application > GX Developer.

After launching GX Developed, the user software interface appears.

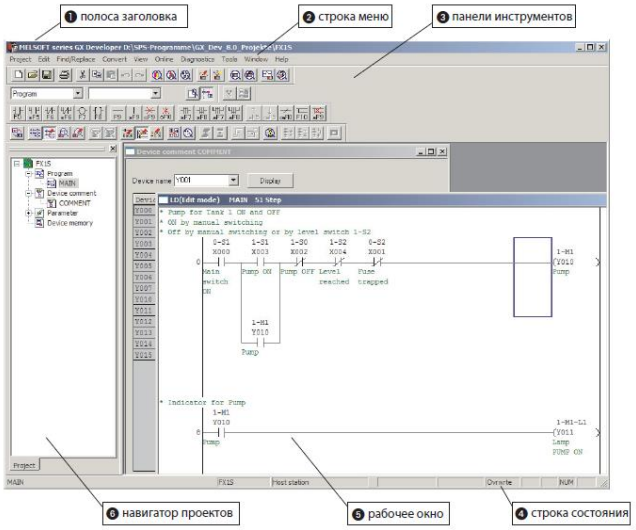

On this figure, for better visibility, the project is already open. After launching GX Developer, you only need to open an existing project or create a new project.

The MELSEC controllers of the FX family can only process one program (default name: MAIN).

To rename the MAIN program, click MAIN and press the right mouse button. Then select the action you want to take.

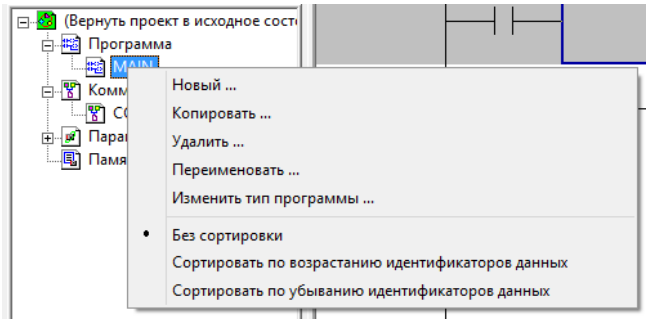

Comments can be added to each controller operand (inputs, outputs, markers, etc.), which can be seen on the screen in the program.

By opening a file with an operand comment in the project navigator, you can enter or edit comments. But input of comments is also possible directly during programming.

Double-clicking **PLC Parameters** opens a dialog where you can set all the parameters necessary for the controller operation. Controller parameters are transferred to the CPU along with the program [4].

In file in the directory **Device Memory**, you can already enter a value for any data register (D) of the CPU during programming. After loading this file into the controller together with the program, these initial values are taken into account already at the first start of the program.

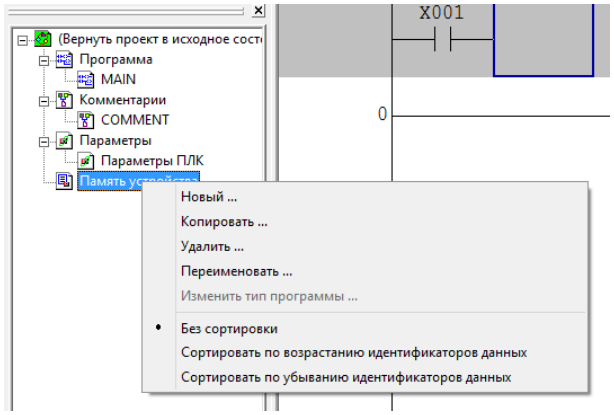

To do this, click on **Device Memory** and press the right mouse button. Then click on **New**... and name the file.

There are volatile and non-volatile (fixed) areas in the memory of operands of the central processor. If the data must be saved even when the controller is powered off until it is turned on again, they must be entered in fixed areas.

To create a new project, click on the menu Project on the line New project or click on the toolbar on this screen button  .

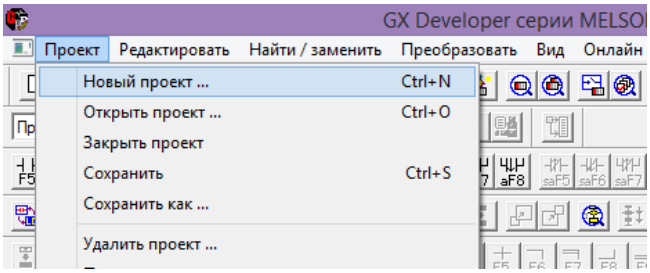

After that, the following dialog box appears:

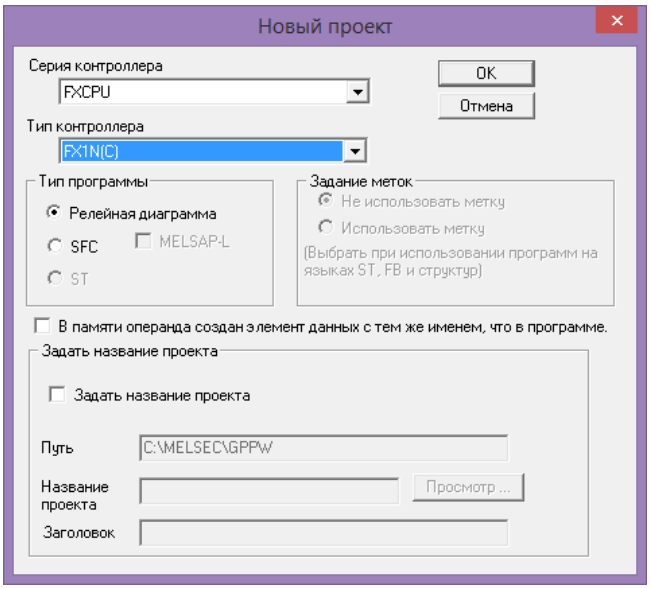

The **Controller series** entry field in the GX Developer FX software is pre-populated with the FXCPU series, since only MELSEC controllers of the FX family can be programmed with this software.

The base unit type is selected in the **Controller Type** field. Click the arrow at the right edge of the input field. A selection of all available types of processors of the FX family appears. If you click on the controller symbol, this selection is confirmed in the input field. For laboratory stand, choose FX1N(C) or FX3U(C). Next, select the type of program **Ladder Diagram** or **SFC**, set the name of the project.

After clicking OK, a new, as yet empty, MAIN program appears in the GX Developer work window.

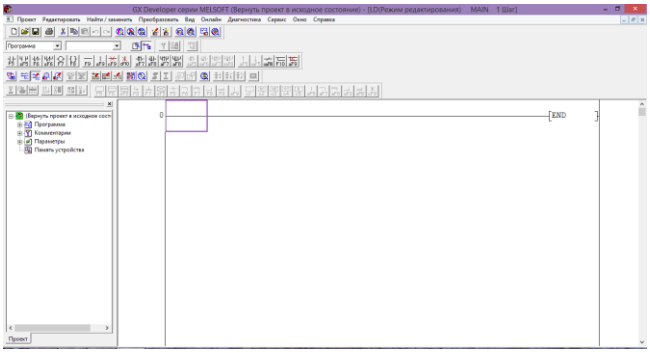

The stand ”Lighting control based on a programmable logic controller” consists of a differential automatic switch, a voltage and current relay; 24V power supply; PLC FX3U 24MR; control buttons; signal lamps.

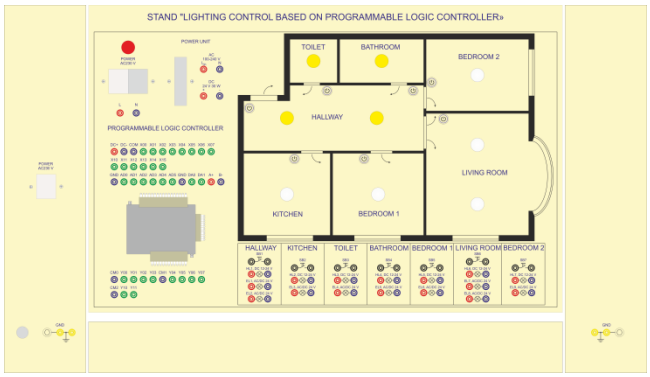

Fig. 5. General view of Stand ”Lighting control based on a programmable logic controller”

The front panel and body of the stand contain: – an AC power source, which includes a two-pole circuit breaker, a differential current circuit breaker of the AVDT32 series and a voltage relay; – a power source – UNO-PS / 1AC / 24DC / 24W; – control buttons; – programmable logic controller FX3U 24MRMitsubishi; – contact sockets. The stand also includes a set of connecting wires.

The GX Developer FX program is required to work with the stand. Connection to the PLC is made using an RS232 cable.

To create a control circuit for lighting operation using control buttons on the stand ”Lighting control based on a programmable logic controller”, assemble a control circuit with status indicators for PLC inputs and outputs, buttons that set lighting control signals.

The following must be done to write and run the program: 1. Create a new project, specifying the type of PLC on which the work will be performed. 2. Create a ladder diagram for this task. 3. Convert ladder diagram. 4. Establish communication with the PLC FX3U24MR at the stand ”Lighting control based on a programmable logic controller”. For that reason connect the RS-232 cable with driver installation, set transmission parameters. 5. Write the diagram to the PLC. 6. Collect the diagram at the stand. 7. Enable monitor mode in GX Developer FX. 8. Put the PLC in ”RUN” mode.

3. Example

On the example of the program ”Lighting control based on a programmable logic controller” let's consider the first main elements of the toolbar. Switching on will be done using the SB1 button, and switching off using the SB2 button. Light bulb EL1 will be an indicator of work.

The ladder diagram of this circuit is shown in figure 6.

On the diagram X000 – controller input from the SB1 button; X001 – controller input from the SB2 button; Y000 – controller output to the EL1 light bulb.

This ladder diagram utilizes a make and break contact, a coil, a shunt contact. The principle of operation is based on closing and opening the circuit.

Further you need to collect the following diagram on the stand – Fig. 7.

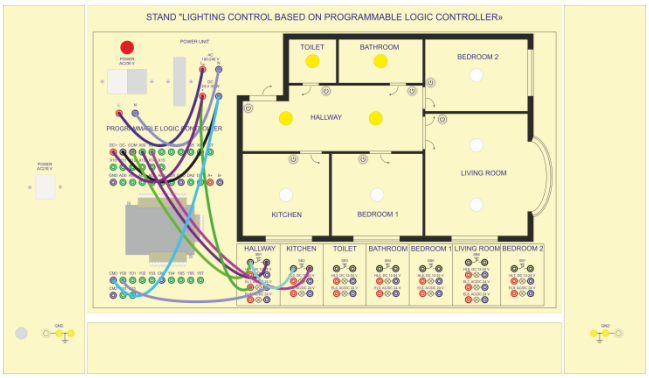

Fig. 7. Connecting patterns for ladder diagram at figure 6

The corridor lamps are turned on and off according to the following algorithm. One press of the SB1 button (input X000) turns on the output Y000 (lamp EL1), the next press turns off the output Y000 (lamp EL1). Double pressing the button SB1, turns on the output Y001 (lamp EL2), the next press turns off the output Y001 (lamp EL2). The algorithm also contains the function of simultaneously switching off two outputs Y000 and Y001. For that reason, press and hold the SB1 button for 3 seconds.

Lamp EL1 is connected to output Y000, and EL2 is connected to output Y001.

SB1 HL1 button light is directly connected to DC24V power supply.

The ladder diagram of this circuit is shown at figure 8.

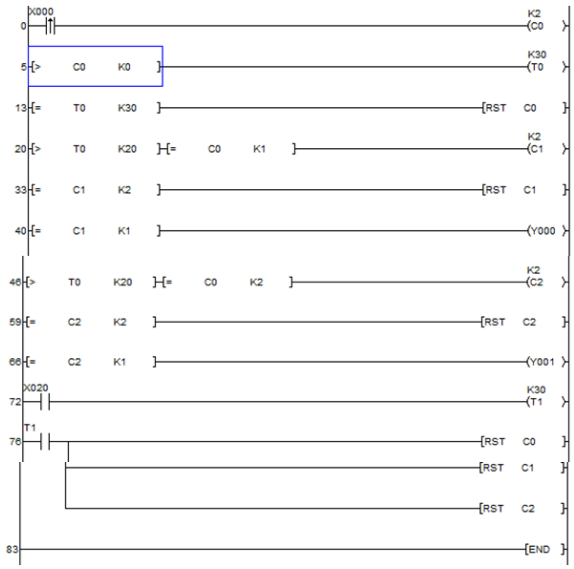

Fig. 8. Ladder diagram for corridor lighting control with one button

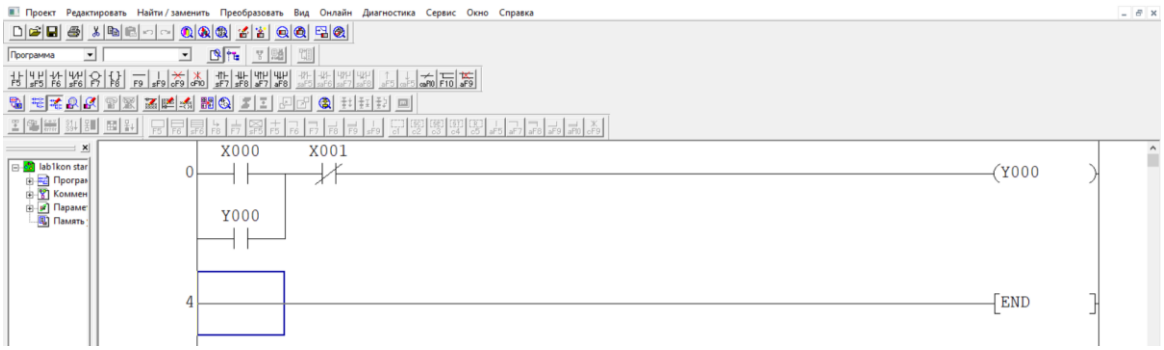

Fig. 6. The ladder diagram of program „Lighting control based on a programmable logic controller”

On the diagram X000 – input to the controller from the button SB1; Y000 – output from the controller to the bulb EL1; Y001 – output from the controller to the bulb EL2.

This ladder diagram utilizes 3 counters, 2 timers, LDP command (rising edge control), comparison functions, etc.

Further you need to collect the following diagram on the stand – Fig. 9.

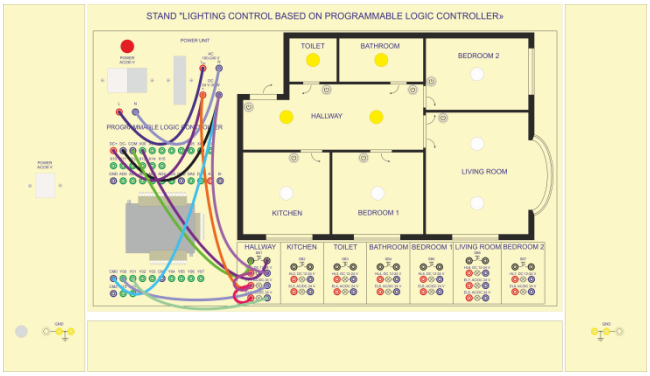

Fig. 9. Connecting patterns for ladder diagram at figure 8

The PLC specifications give typical operating cycle times. While measuring the user program must contain 1K (1024) simple logic instructions (in the IEC 1131-3 instruction list (IL) language). PLCs today have typical runtimes measured in units of milliseconds or less. Events that require a quick response are allocated to separate tasks, the priority and execution period of which can be changed.

4. Summary

So this work considers the issues of practical use of controllers for automation in various fields of technology on the example of Mitsubishi controllers of the MELSEC FX1N and FX3U series, as typical representatives of low-priced and widely used controllers.

Reference

[1] Introduction to PLC: What is a Programmable Logic Controller https://www.compel.ru/lib/95591
[2] Mitsubishi Melsec https://ru.wikipedia.org/wiki/Mitsubishi_Melsec
[3] Programmable Controller MELSEC https://ru3a.mitsubishielectric.com/fa/ru/products/cnt/plc/
[4] Programmable Logic Controllers Mitsubishi Electric. http://esspb.ru/dev.html
[5] GX Developer FX. Programming and Documentation System: Beginner's Guide. 2007. http://www.mitsubishi-automation.ru
[6] MELSEC FX Family. Programmable Controllers. Analog Input Modules, Analog Output Modules, Combined Analog I/O Modules, Temperature Recording Modules: Instruction Manual. 2012. http://www.mitsubishi-automation.ru

Ph.D. Laura Yesmakhanova
e-mail: laura060780@mail.ru

Graduate of the doctoral program of the Lublin University of Technology. Currently, he works as an associate professor at Taraz Regional University at the Department of Automation and Telecommunications. He is the author and co-author of several scientific publications in the field of the use of optoelectronic components in automated control systems and fiber-optic communication lines.

http://orcid.org/0000-0002-3308-9676

Ph.D. Raushan Dzhanuzakova
e-mail: rdd-taraz@mail.ru

Candidate of technical sciences in the Republic of Kazakhstan. He has copyrights for inventions, an innovative patent „Electromagnetic method for measuring stresses in ferromagnetic products"; copyrights for inventions, an innovative patent „Atopological method for measuring stresses in elements of products". He is the author and co-author of several scientific publications in the field of the use of optoelectronic components in automated control systems and fiber-optic communication lines.

http://orcid.org/0000-0001-7168-2676

Ph.D. Bauyrzhan Myrkalykov
e-mail: Baur-phd@mail.ru

Associate Director office of the Registra. He completed scientific internships at Lazar University in Warsaw (Poland) and at the University of Food Technologies in Plovdiv (Bulgaria). He is the author of several scientific publications in the field of innovative technologies. Studies the functions related to the organization of the process of high-quality and timely formation and effective use of the fund of modern control and measuring materials, based on the continuous improvement of methods and technologies of their development and expertise.

http://orcid.org/0000-0001-7224-4168

http://doi.org/10.35784/iapgos.3393 received: 14.12.2022 | revised: 23.12.2022 | accepted: 23.12.2022 | available online: 30.12.2022

FLAME ANALYSIS BY SELECTED METHODS IN THE FREQUENCY DOMAIN

Żaklin Grądz[1], Jacek Klimek[1], Czesław Kozak[2]
[1]Lublin University of Technology, Department of Electronics and Information Technology, Lublin, Poland, [2] Lublin University of Technology, Department of Electrical Equipment and High Voltage Technology Lublin, Poland

Abstract. *Diagnostics of pulverized coal combustion can be carried out in the field of process monitoring and analysis of measurement data. The information about changes in the flame is presented in the form of time series, which can be analyzed in the time and frequency domain. The paper presents an analysis of signals of changes in the intensity of the flame glow during pulverized coal combustion using power spectral density. On the basis of the periodograms determined using the Welch method, it was possible to determine the frequency components present in the signal.*

Keywords: flame luminosity, combustion process, power spectral density

ANALIZA PŁOMIENIA WYBRANYMI METODAMI W DZIEDZINIE CZĘSTOTLIWOŚCI

Streszczenie. *Diagnostyka spalania pyłu węglowego może być przeprowadzana w zakresie monitorowania przebiegu procesu oraz analizy danych pomiarowych. Informacje o zmianach zachodzących w płomieniu przedstawione są w postaci szeregów czasowych, które mogą być analizowane w dziedzinie czasu i czestotliwości. W artykule przedstaiono analize sygnałów zmian intesnywności świecenia płomenia podczas spalania pyłu węglowego przy użyciu gęstości widmowej mocy. Na podstawie periodogramów wyznaczonych z zastosowaniem metody Welcha możliwe było określenie składowych czestotliwościowych występujących w sygnale.*

Słowa kluczowe: intensywność świecenia płomiania, proces spalania, widmowa gęstość mocy

Introduction

Over the years, the complexity of industrial processes has increased, which has directly influenced the improvement of methods for diagnosis, detection, localization and identification of defects in various industrial fields [2, 3, 10, 12, 13]. In terms of generating electricity or heat using coal, the most important part of the process is the power boiler. The combustion process occurring in it must meet high parameters in technological, environmental and economic terms. Meeting all these conditions, despite the use of components characterized by high reliability, is a major challenge requiring various diagnostic methods.

In the diagnosis of combustion processes in the field of flame study, spectral analysis methods are used [1, 4, 14, 15]. Zhang W. at al [16] used power spectral density (PSD) to study the flame front wrinkling showing a common trend for different operating conditions. PSD has also been used to evaluate the performance of models at different frequencies during flame surface density studies [6]. In addition, the Welch method [8] is used in the analysis of laminar and turbulent flames in the frequency domain.

The article presents measured data on changes in flame intensity for two variants: stable flame and disturbance flame. In the combustion process, small changes in the flame intensity can result from actions carried out to carry out the process, for example: by activating the coal feeder. On the other hand, when disruptions occur, it is particularly important for process stability to detect and diagnose them quickly. In this paper, the analysis of measurement data was carried out in the frequency domain using power spectral density. Periodograms were determined for both flame variants using the Welch method.

1. Power spectral density

For discrete signals, the power spectral density (PSD) is a parameter that defines how power is distributed over the full frequency range in a signal. The PSD is considered a fundamental method for describing random data in the frequency domain [9]. It is determined using the following formula [5, 7]:

$$S_{xx}(\omega) = \sum_{m=-\infty}^{\infty} R_{xx}(m) e^{-j\omega m} \tag{1}$$

where: S_{xx} – power spectral density, $R_{xx}(m)$ – autocorrelation function, $\omega = 2\pi f/f_s$ – pulsation, f_s – sampling frequency of the signal.

Determination of the power spectral density using a periodogram is based on the Fourier transform of the fundamental signal x(n) and is expressed by the following equation [5, 7]:

$$S_{xx}(f) = \frac{|X(f)|^2}{N}, \tag{2}$$

where: $X(f)$ – Fourier transform.

2. Time series analysis of flame luminosity

The measurement data obtained from the combustion process comes from direct observation of the flame using a diagnostic system. The flame monitoring system allows the acquisition of information about the process in a non-invasive manner. The measurement data are one-dimensional time series representing changes in the intensity of the flame glow. The study was carried out during the combustion of pulverized coal at constant process parameters such as thermal power – 400 kW and excess air ratio λ = 0.75. More than 1.8 million observations were recorded. Two selected waveforms of changes in flame luminosity, which are characterized by an equal number of samples, were adopted for analysis. The first, variant I, corresponds to the stable flame (figure 1) and the second, variant II, is a flame with recorded disturbances (figure 2). Due to the large size of the analyzed time series, the measurement data was divided into 5 areas A-E of 363092 samples each.

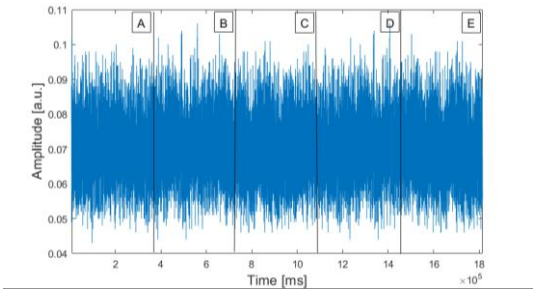

Fig. 1. Change of flame luminosity in stable flame, divided into areas A-E

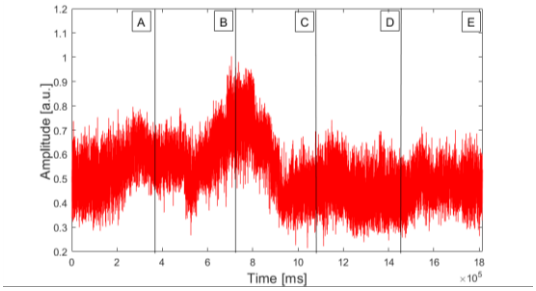

Fig. 2. Change of flame luminosity with disturbances, divided into areas A-E

Analysis of measured data in the frequency domain using power spectral density was carried out. The main purpose of using this method was to determine the spectral density estimate from the flame time series for variants I and II. PSD was determined using periodograms with the Welch method. With this approach, the input signal $x(t)$ is divided into smaller segments, and a Fourier transform is calculated for each segment using a Hamming window [11]. The result was then averaged.

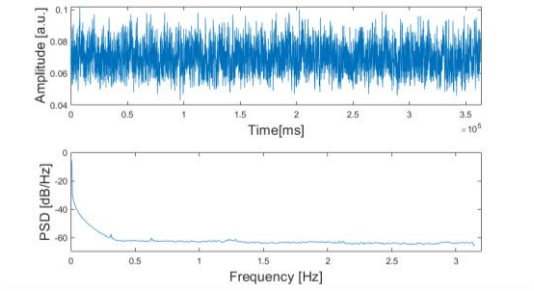

Fig. 3. Periodogram of changes in flame luminosity for stable flame in area A

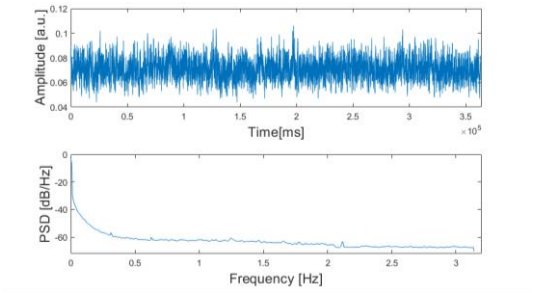

Fig. 4. Periodogram of changes in flame luminosity for stable flame in area B

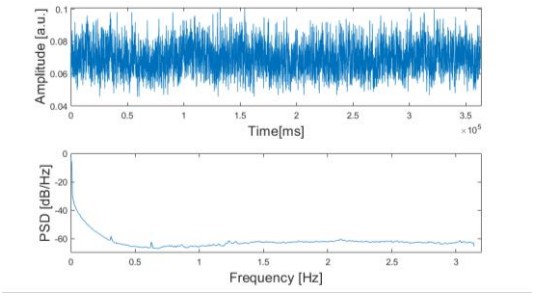

Fig. 5. Periodogram of changes in flame luminosity for stable flame in area C

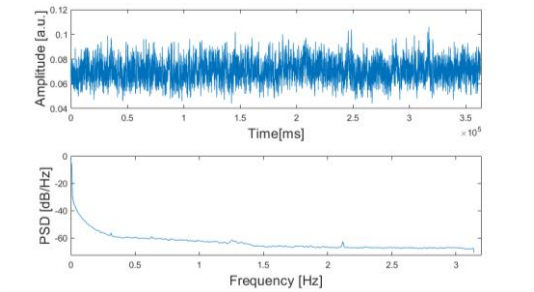

Fig. 6. Periodogram of changes in flame luminosity for stable flame in area D

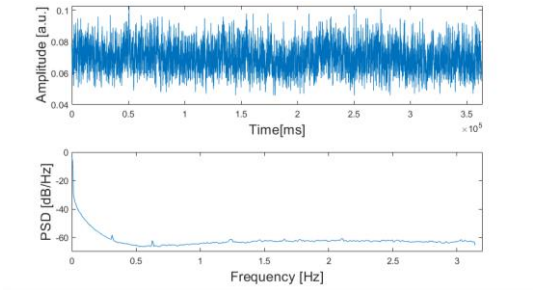

Fig. 7. Periodogram of changes in flame luminosity for stable flame in area E

Figures 3 – 7 show periodograms of changes in luminous intensity for the stable flame in areas A – E. It is observed that for the stable flame (variant I) in all areas A – E the largest frequency changes occur for low frequencies in the range from 0 to 0.5 Hz.

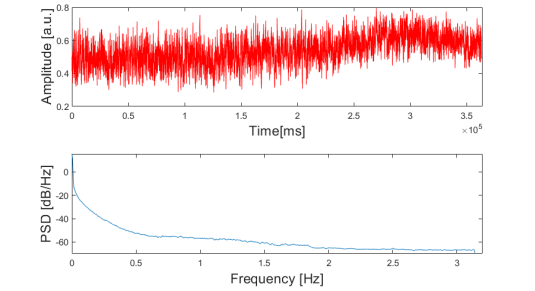

Fig. 8. Power spectral density for measured data from variant II in area A

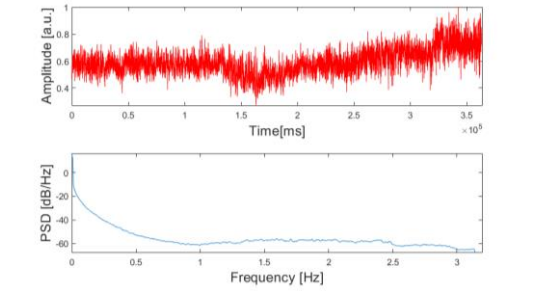

Fig. 9. Power spectral density for measured data from variant II in area B

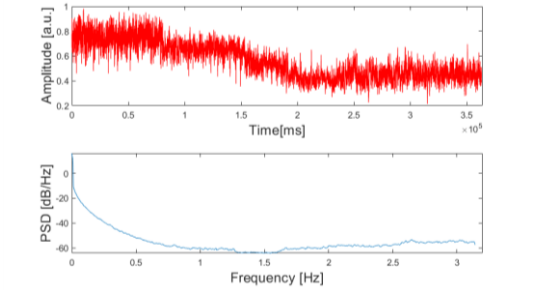

Fig. 10. Power spectral density for measured data from variant II in area C

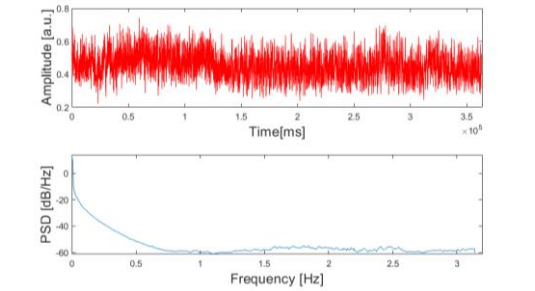

Fig. 11. Power spectral density for measured data from variant II in area D

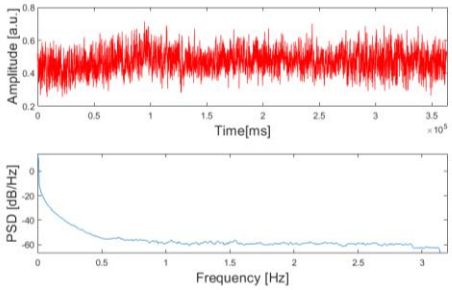

Fig. 12. Power spectral density for measured data from variant II in area E

The characteristics in figures 7 – 10 show the determined power spectral density estimates for the unstable flame (variant II) in all areas A – E. Analysis of the test results using the measurement data from variant II showed that different results were obtained for each area. The largest frequency changes were obtained in areas: A from 0 to 2 Hz and C from 0 to 1.5 Hz. In contrast, the following ranges were achieved for the other areas: B – 0–1 Hz, D – 0–1.25 Hz and E – 0–1 Hz.

The results of the power spectral density for the two flame variants in all areas A – E, indicated that in the case of a stable flame, it is possible to divide the time series into smaller areas. The division for variant I allows a detailed assessment of the changes occurring in the combustion process. In contrast, based on the periodograms for the unstable flame, it should be concluded that the division into areas is not effective. In the case of measurement data from variant II, larger time series should be adopted, which will allow a more in-depth evaluation of the process.

3. Conclusions

The acquisition of measurement data from the flame is carried out using specialized monitoring systems. They record information from the flame using a fiber-optic probe placed in the combustion chamber. The optical signals are then transferred to an optoelectronic block where they are converted to electrical form for further analysis. There are many methods for conducting analysis and diagnostics of the pulverized coal combustion process.

Time series from flame tests in the combustion process, among other things, can be analyzed in the time and frequency domains. The measurement data presented in the article for stable and unstable flame were subjected to spectral analysis of the signals. The time series for both flame variants were divided into areas A – E. The power spectral density was determined for each of them. It was estimated that for variant I of the flame, the largest frequency changes occur in the 0–0.5 Hz range. On the other hand, in the case of variant II – unstable flame – it was noted that for a full evaluation of the process, it is not necessary to divide into small areas; instead, larger time series should be used. In the unstable flame, the largest changes in frequency values were determined in area A in the range from 0–2 Hz. The use of periodograms enabled to study signals in the frequency domain.

References

[1] Æsøy E., Indlekofer T., Gant F., Cuquel A., Bothien M. R., Dawson J. R.: The effect of hydrogen enrichment, flame-flame interaction, confinement, and asymmetry on the acoustic response of a model can combustor. Combustion and Flame 242, 2022, 112176.
[2] Komada P.: Analiza procesu termicznej przeróbki biomasy. Monografie –Polska Akademia Nauk. Komitet Inżynierii Środowiska, Warszawa 2019.
[3] Korbicz J., Kościelny J.M., Kowalczuk Z., Cholewa W.: Diagnostyka procesów, Modele, Metody sztucznej inteligencji, Zastosowania. Wydawnictwo Naukowo-Techniczne, Warszawa 2002.
[4] Kotyra A., Wójcik W.: Wykorzystanie deksryptorów Fouriera w diagnostyce procesu spalania. Pomiary Automatyka Kontrola 10, 2010, 57–60.
[5] Matlab: Signal processing toolbox – User's Guide, Natick 2018.
[6] Panek P., Brouzet D., Talei M., Gordon R. L.: A priori assessment of flame surface density modelling for large-eddy simulation of sound generation by turbulent premixed flames. Combustion and Flame 241, 2022, 112143.
[7] Pilek B.: Analiza przydatności optoelektronicznych sygnałów pomiarowych płomienia do diagnostyki procesu spalania. Wydawnictwo Politechniki Lubelskiej, Lublin 2014.
[8] Rising C. J., Goodwin G. B., Johnson R. F., Kessler D. A., Sosa J., Thornton M., Ahmed K. A.: Numerical investigation of turbulent flame-vortex interaction in premixed cavity stabilized flames. Aerospace Science and Technology 129, 2022, 107805.
[9] Slavič J., Mršnik M., Česnik M., Javh J., Boltežar M.: Chapter 2 – Signal processing. Vibration Fatigue by Spectral Methods. Elsevier, 2021, 51–74.
[10] Smolarz A., Kotyra A., Wójcik W., Ballester J.: Advanced diagnostics of industrial pulverized coal burner using optical methods and artificial intelligence. Experimental Thermal And Fluid Science 43, 2012, 82–89.
[11] Welch P.: The use of fast Fourier transform for the estimation of power spectra: a method based on time averaging over short, modified periodograms. IEEE Trans. Audio Electroacoust. 15(2), 1967, 70–73.
[12] Wójcik W.: Application of fibre-optic flame monitoring systems to diagnostics of combustion process in power boilers. Bulletin of the Polish Academyof Sciences –Technical Sciences 56(2), 2008, 177–195.
[13] Wójcik W., Gromaszek K., Shegebayeva Z., Suleimenov B., Burlibay A.: Optimal control for combustion process. Przegląd Elektrotechniczny 90(4), 2014, 157–160.
[14] Wójcik W., Cięszczyk S., Kisała P., Komada P.: Flame emission spectrum analysis as an inverse problem in indirect measurements. Pomiary Automatyka Kontrola 55(2), 2009, 121–125.
[15] Wójcik W., Kotyra A., Golec T., Ławicki T.: Assessment of pulverized coal combustion using Fourier descriptors. Przegląd Elektrotechniczny 86(7), 2010, 241–243.
[16] Zhang W., Morsy M. E., Ling Z., Yang J.: Characterization of flame front wrinkling in a highly pressure-charged spark ignition engine. Experimental Thermal and Fluid Science 132, 2022, 110534.

M.Sc. Żaklin Grądz
e-mail: z.gradz@pollub.pl

In 2015, Ż.Grądz graduated from Lublin University of Technology with master's degree in Electrical Engineering. From 2015 she is a Ph.D. student at Electrical Engineering and Computer Science Faculty. She has been working as an assistant in Department of Electronics and Information Technology of Lublin University of Technology since 2016. She is an author of 8 articles, 20 chapters in monographs. Scientific research area: monitoring and diagnostics of combustion process, wavelet analysis, recursive neural networks.

http://orcid.org/0000-0003-1902-4953

Ph.D. Jacek Klimek
e-mail: j.klimek@pollub.pl

Jacek Klimek – assistant at the Faculty of Electrical Engineering and Computer Science of the Lublin University of Technology, author of many publications on fibre optics. He obtained his Ph.D. in 2021. His research focuses on the fabrication and study of optical periodic structures called Bragg gratings. Current research interests focus on issues related to complex periodic structures.

http://orcid.org/0000-0001-8141-6136

Ph.D. Czesław Kozak
e-mail: c.kozak@pollub.pl

Czeslaw Kozak, Ph.D. Eng. graduated with a master's degree in 1992 from the Faculty of Electrical Engineering and Computer Science of Lublin University of Technology. After graduation, he joined the Department of Electrical Equipment and High Voltage Technology, where he has worked as a research and teaching assistant professor. He received his doctoral degree in 2004, his work concerned the properties of copper contacts of electrical connectors coated by single-beam dynamic ion mixing. He is currently working on spectrophotometric studies of arc temperature in the interstice gap.

http://orcid.org/0000-0001-7642-4449

LIST OF REVIEWERS COOPERATING WITH THE JOURNAL IN 2022

LISTA RECENZENTÓW WSPÓŁPRACUJĄCYCH Z CZASOPISMEM W ROKU 2022

Prof.	Androshchuk	Iryna M.	Maria Grzegorzewska University (Warsaw, Poland)
Prof.	Avrunin	Oleg	Kharkiv National University of Radio Electronics (Kharkiv, Ukraine)
Ph.D.	Babyuk	Natalya	Vinnytsia National Technical University (Vinnytsia, Ukraine)
Ph.D.	Bober	Dariusz	University of Rzeszow (Rzeszow, Poland)
Ph.D.	Bojarczuk	Piotr	Kazimierz Pulaski University of Technology and Humanities in Radom (Radom, Poland)
Prof.	Borecki	Michał	Warsaw University of Technology (Warsaw, Poland)
Ph.D.	Boryczko	Krzysztof	Rzeszów University of Technology (Rzeszów, Poland)
Prof.	Boyko	Oksana	Danylo Halytsky Lviv National Medical University (Lviv, Ukraine)
Ph.D.	Buczaj	Agnieszka	University of Life Sciences in Lublin (Lublin, Poland)
Ph.D.	Buczaj	Marcin	Lublin University of Technology (Lublin, Poland)
Prof.	Chodakowska	Ewa	Bialystok University of Technology (Bialystok, Poland)
Prof.	Cięszczyk	Sławomir	Lublin University of Technology (Lublin, Poland)
Prof.	Droździel	Paweł	Lublin University of Technology (Lublin, Poland)
Prof.	Dubolazov	Olexander	Yuriy Fedkovych Chernivtsi National University (Chernivtsi, Ukraine)
Ph.D.	Fedotova	Natali	Sumy State University (Sumy, Ukraine)
Prof.	Fiala	Pavel	Brno University of Technology (Brno, Czech Republic)
Prof.	Goleman	Ryszard	Lublin University of Technology (Lublin, Poland)
Prof.	Gromaszek	Konrad	Lublin University of Technology (Lublin, Poland)
Prof.	Grudzień	Krzysztof	Lodz University of Technology (Lodz, Poland)
Ph.D.	Guzan	Milan	Technical University of Košice (Košice, Slovakia)
Ph.D.	Holuk	Mariusz	University College of Applied Sciences in Chełm (Chelm, Poland)
Prof.	Jackowska-Strumiłło	Lidia	Lodz University of Technology (Lodz, Poland)
Prof.	Junisbekov	Mukhtar	M. Kh. Dulaty Taraz State University (Taraz, Kazakhstan)
Ph.D.	Kalizhanova	Aliya	Institute of Information and Computational Technologies SR MES RK (Almaty, Kazakhstan), Al-Farabi Kazakh National University (Almaty, Kazakhstan)
Ph.D.	Klepacki	Dariusz	Rzeszów University of Technology (Rzeszów, Poland)
Ph.D.	Kłosowski	Grzegorz	Lublin University of Technology (Lublin, Poland)
Prof.	Kotyra	Andrzej	Lublin University of Technology (Lublin, Poland)
Ph.D.	Kovalchuk	Nadiia	Lutsk National Technical University (Lutsk, Ukraine)
Prof.	Krak	Iurii	Taras Shevchenko National University of Kyiv (Kyiv, Ukraine)
Prof.	Kryvonosov	Valery	National University "Odessa Maritime Academy" (Odessa, Ukraine)
Ph.D.	Kulisz	Józef	Silesian University of Technology (Gliwice, Poland)
Prof.	Kusznier	Jacek	Bialystok University of Technology (Bialystok, Poland)
Ph.D.	Kwedlo	Wojciech	Bialystok University of Technology (Bialystok, Poland)
Prof.	Lytvynenko	Volodymyr	Kherson National Technical University (Kherson, Ukraine)
Ph.D.	Maciaszczyk	Magdalena	Lublin University of Technology (Lublin, Poland)
Ph.D.	Mamyrbayev	Orken	Institute of Information and Computational Technologies SR MES RK (Almaty, Kazakhstan)
Prof.	Miaskowski	Arkadiusz	University of Life Sciences in Lublin (Lublin, Poland)
Ph.D.	Naumchuk	Oleksandr	National University of Water and Environmental Engineering (Rivne, Ukraine)
Prof.	Nazarenko	Ivan	Kyiv National University of Construction and Architecture (Kyiv, Ukraine)
Prof.	Nykyforova	Larysa	National University of Life and Environmental Sciences of Ukraine (Kyiv, Ukraine)
Prof.	Omiotek	Zbigniew	Lublin University of Technology (Lublin, Poland)
Ph.D.	Paśnikowska-Łukaszuk	Magdalena	Lublin University of Technology (Lublin, Poland)
Prof.	Pavlov	Sergey	Vinnytsia National Technical University (Vinnytsia, Ukraine)
Prof.	Prokopovych	Ihor	Odessa National Polytechnic University (Odessa, Ukraine)
Ph.D.	Przyłucki	Sławomir	Lublin University of Technology (Lublin, Poland)
Prof.	Różyło	Renata	University of Life Sciences in Lublin (Lublin, Poland)
Prof.	Rudyk	Andrii	National University of Water and Environmental Engineering (Rivne, Ukraine)
Prof.	Rymarczyk	Tomasz	Research & Development Centre Netrix S.A. (Lublin, Poland), WSEI University (Lublin, Poland)
Ph.D.	Sapon	Serhii	Chernihiv Polytechnic National University (Chernihiv, Ukraine)
Prof.	Savina	Natalia	National University of Water and Environmental Engineering (Rivne, Ukraine)
Prof.	Semenov	Andriy	Vinnytsia National Technical University (Vinnytsia, Ukraine)
Prof.	Sikora	Jan	Research & Development Centre Netrix S.A. (Lublin, Poland), WSEI University (Lublin, Poland)
Ph.D.	Smailova	Saule	D. Serikbayev East Kazakhstan State Technical University (Ust-Kamenogorsk, Kazakhstan)
Prof.	Smolarz	Andrzej	Lublin University of Technology (Lublin, Poland)
Ph.D.	Stelmakh	Nataliia	National Technical University of Ukraine „Kyiv Polytechnic Institute" (Kyiv, Ukraine)
Prof.	Sulemenov	Batyrbek	Kazakh National Research Technical University after K.I.Satpayev (Almaty, Kazakhstan)
Ph.D.	Susik	Robert	Lodz University of Technology (Lodz, Poland)
Ph.D.	Ścibisz	Marek	University of Life Sciences in Lublin (Lublin, Poland)
Prof.	Świsulski	Dariusz	Gdansk University of Technology (Gdańsk, Poland)
Prof.	Timchenko	Leonid	State University of Infrastructure and Technologies (Kyiv, Ukraine)
Prof.	Titova	Nataliia	Odessa National Polytechnic University (Odessa, Ukraine)
Prof.	Trishch	Roman	Ukrainian State Engineering Pedagogical Academy (Kharkiv, Ukraine)
Prof.	Ushenko	Alexander G.	Yuriy Fedkovych Chernivtsi National University (Chernivtsi, Ukraine)
Ph.D.	Wlaź	Paweł	Lublin University of Technology (Lublin, Poland)
Prof.	Yashchyshyn	Yevhen	Warsaw University of Technology (Warsaw, Poland)
Ph.D.	Yesmakhanova	Laura	M. Kh. Dulaty Taraz State University (Taraz, Kazakhstan)